

A SURVEY OF UNITED STATES AND TOTAL WORLD PRODUCTION,
PROVED RESERVES AND REMAINING RECOVERABLE
RESOURCES OF FOSSIL FUELS AND URANIUM
AS OF DECEMBER 31, 1976

by

Joseph D. Parent
J. Glenn Seay
Institute of Gas Technology
3424 South State Street
Chicago, Illinois 60616

Henry R. Linden
Gas Research Institute
10 West 35th Street
Chicago, Illinois 60616

In this report, current estimates are presented for U.S. and world nonrenewable energy sources. The data are presented in summary form due to space limitations. The full paper, available on request from the authors, presents full details of the resource estimates. U.S. fossil fuel resources are reported as of December, 1977. However, for the summary world resource tables, 1976 U.S. data were used to be consistent with the latest estimates available for other world areas.

U.S. Nonrenewable Energy Sources

The following tables present estimates for the remaining recoverable U.S. fossil-fuel resources. Table 1 summarizes the estimates for natural gas made over the past several years by recognized agencies: the American Gas Association (A.G.A.), the Potential Gas Agency, the U.S. Geological Survey (U.S.G.S.), the National Academy of Sciences (NAS), IGT, and some oil and gas producing companies. Table 2 summarizes recent crude oil estimates made by the American Petroleum Institute (A.P.I.), U.S.G.S., NAS, and others. In view of the considerable disagreement among the published data, a high degree of accuracy cannot be claimed despite the unquestionable expertise of the agencies involved.

Remaining recoverable resources as of year-end 1977 are given in Table 3 for the various fossil fuels based on the publications of the above agencies, and the U.S. Bureau of Mines. As in Tables 1 and 2, resources are reported both for the portions qualifying as proved reserves and for the estimated total remaining economically recoverable resources. In both cases recovery is to be economical with current technology. Because of uncertainties, ranges of total remaining recoverable resources have been used for most of the fossil fuels.

U.S. Life Expectancy

Table 4 shows the life expectancy of U.S. fossil fuels in the aggregate (including shale oil and bitumens), with consumption based solely on domestic production and increasing at various fixed annual rates of growth - 2%, 3%, and 4%. It is also based on reducing the resources to a 10-year forward reserve at the annual production rate ultimately reached. For example, if the demand for fossil fuels were to grow at 3%/year, the listed total remaining recoverable fossil fuels would last another 85 years under the conditions stipulated. If restricted to the reserves currently proved, the life expectancy would drop to 32 years. However, if the total remaining recoverable resources could be augmented to twice the present estimated level

Table 1. Estimates of Remaining Recoverable U.S. Natural Gas Resources at Year-End

Year End	Source	Potential Supply		Proved Reserves	Total
		Old Fields	New Fields	A.G.A.	
		trillion cubic feet			
1977	American Gas Association	--	--	209	--
1976	Potential Gas Committee	215	733 (708-758)	216	1164
	Exxon	111 (56-321)	287 (127-657)		635 (420-1215)
	U.S. Geological Survey (Miller, Thomsen, et al)	201.6	484 (322-655)		923 (761-1094)
1974	National Academy of Sciences	118.6 (calcd)	530	237	886
	Moody	65	485		787
	Average, some major oil cos. (Garrett)	100	500		837
1973	Mobil Oil Corp. (Moody and Geiger)	65	443	250	758
	U.S. Geological Survey (McKelvey)	130-250	1000-2000	266	1396-2516
1972	Potential Gas Committee	266	880		1412
	IGT (Linden)		634 (old and new fields)		900
	U.S. Geological Survey	130 (calcd)	361		770
1971	(Hubbert)			279	
	IGT (Linden)		575-704 (old and new fields)		854-983

Table 2. Estimates of Remaining Recoverable U.S. Crude Oil Resources at Year-End

Year End	Source	Potential Supply		Proved Reserves	Total
		Old Fields	New Fields	A.P.I.	
		Billion bbl			
1977	American Petroleum Institute	--	--	33.7	--
1976	American Petroleum Institute	--	--	35.2	--
	Exxon, rev.	59	63	41	163
	Exxon	57 (36-90)	55 (20-129)	34.25	146 (90-253)
	U.S. Geological Survey	23.1	50-127	38.9	112-189
1974	(Miller, Thomsen, et al.)				
	National Academy of Sciences, Incl. natural gas liquids	22.7 (calcd)	105-120	45.3	173-188
1973	Mobil Oil Corp. (Moody and Geiger)	11 (calcd)	88	40.4	139
1972	U.S. Geological Survey, Incl. natural gas liquids (McKelvey)	24-45	200-400	48.3	272-493
1971	U.S. Geological Survey (Hubbert)	18 (calcd)	55	43.0	116
	U.S. Geological Survey, Incl. natural gas liquids (Theobald, et al.)		450 (old and new fields)	52.1	502
1970	National Petroleum Council	--	--	--	339

in some way (i.e., imports), they would last 108 years. Some recent forecasts suggest that the growth rate of consumption might decrease to 2.5% or less. Hence, there should be adequate lead time to develop synthetic fuels from coal, oil shale, and bitumens, and allow use of the quantities of these materials suggested in Table 3.

Table 3. U.S. Fossil Fuel Resources as of December 31, 1977

	Proved and Currently Recoverable		Estimated Remaining Recoverable	
Dry Natural Gas				
Trillion CF	209		760-1170	
Quintillion (10^{18}) Btu		0.21		0.78-1.19
Natural Gas Liquids				
Billion bbl	6.0		21-33	
Quintillion Btu		0.02		0.09-0.13
Crude Oil				
Billion bbl	29.5		144-371	
Quintillion Btu		0.17		0.84-2.15
Coal				
Billion short tons	214		1036-1788	
Quintillion Btu		4.72		20.71-35.75
Shale Oil				
Billion bbl	74		1026	
Quintillion Btu		0.43		5.95
Bitumens				
Billion bbl	2.5		15	
Quintillion Btu		0.01		0.09
Total, Quintillion Btu		5.56		28.46-45.26

4. Life of U.S. Fossil Fuel Resources
At Various Demand Growth Rates
(Based on 1977 Year-End Estimates)

Annual Growth Rate, %	Date When Remaining Reserve/Consumption Ratio Drops to 10 Years		
	A	B	C
4	2004	2046	2063
3	2009	2062	2085
2	2015	2090	2123

A Proved reserves (5.56×10^{18} Btu)

B Total remaining recoverable resources (36.9×10^{18} Btu).

C Effective doubling of B resources.

World Nonrenewable Energy Sources

Proved recoverable and total remaining recoverable resource data for the world are shown in Table 5 in conventional units and in the common energy units Btu and metric tons of coal equivalent (tce).

World totals for proved recoverable and total remaining recoverable resource data for the world on a regional basis are shown in Table 2 in conventional units. The total remaining recoverable resources include proved reserves. Natural gas and crude oil proved reserves for the various regions are based primarily on the annual estimates for the component countries published by World Oil and by Oil & Gas Journal. Natural gas and crude oil remaining recoverable resources over and above proved resources are based on published estimates by a number of authorities.

Table 5. Nonrenewable World Energy Total Resources
(December 31, 1976)

	<u>Proved and Currently Recoverable</u>	<u>Estimated Total Remaining Recoverable</u>
Natural Gas		
Trillion (10 ¹²) CF	2118-2450	9090-9490
Billion (10 ⁹) tce	79-91	337-352
Quintillion (10 ¹⁸) Btu	2.18-2.52	9.36-9.78
Natural Gas Liquids		
Billion bbl	56-65 (Est.)	241-251 (Est.)
Billion tce	8.3-9.6	36-37
Quintillion Btu	0.23-0.27	0.99-1.03
Crude Oil		
Billion bbl	538-606	1500-1840
Billion tce	112-127	313-384
Quintillion Btu	3.12-3.52	8.70-10.67
Synchrude From Oil Shale and Bitumen		
Billion bbl	270	2415 (17,500)*
Billion tce	56	504 (3654)*
Quintillion Btu	1.57	14.01 (101.5)*
Coal		
Billion short tons	662	5367-6119
Billion tce	492	3864-4406
Quintillion Btu	13.67	107.34-122.38
Total Fossil Fuel Energy		
Trillion tce	0.748-0.776	5.054-5.683
Quintillion Btu	20.8-21.5	140.4-157.9
Uranium Oxide at <\$30/lb		
Thousand short tons	2443	6624
Burner Reactors		
Trillion tce	0.035	0.093
Quintillion Btu	0.977	2.570
Breeder Reactors		
Trillion tce	2.64	6.94
Quintillion Btu	73.28	192.7
Total Fossil Fissile Energy		
Burner Reactor		
Trillion tce	0.783-0.811	5.147-5.776
Quintillion Btu	21.7-22.5	143.0-160.4
Breeder Reactors		
Trillion tce	3.386-3.414	11.992-12.621
Quintillion Btu	94.0-94.8	333.1-350.6

* See footnote (++) in Table 6.

Note: In the conversion from conventional to energy units the assumed energy equivalents are:

1031 Btu/CF of natural gas
 5.8×10^6 Btu/bbl of crude oil or syncrude
 4.1×10^6 Btu/bbl of natural gas liquids
 20×10^6 Btu/short ton of coal (mixture of types), except for U.S. proved reserves where 22×10^6 Btu/short ton was used
 400×10^9 Btu/short ton of U_3O_8 in burner reactors
 30×10^{12} Btu/short ton of U_3O_8 in breeder reactors
 No plutonium recycle is assumed for burner reactors.
 $1 \text{ tce} = 27.778 \times 10^6$ Btu.

Table 6. Nonrenewable World Energy Resources By Region
 (December 31, 1976)

	<u>Proved and Currently Recoverable</u>	<u>Estimated Total Remaining Recoverable</u>
	Billion (10^9) Units	
United States		
Natural Gas, 1000 CF	216	790-1160
Natural Gas Liquids, bbl	6.4	21-31
Crude Oil, bbl	30.9	148-374
Shale Oil, bbl	74	1026 (2000) ⁺⁺
Bitumens, bbl	2.5	15
Coal, short tons	215	1036-1788
Uranium Oxide*		
short tons at <\$15/lb	410	1675
short tons at <\$30/lb	680	3370
Western Hemisphere (Incl. U.S.A.)		
Natural Gas, 1000 CF	352-382	2546-2946
Natural Gas Liquids, bbl	9.3-10.1	67-78
Crude Oil, bbl	66-71	320-420
Shale Oil, bbl	130	1500 (5000)
Bitumens, bbl	80	500
Coal, short tons	224	1114-1866
Uranium Oxide*		
short tons at <\$15/lb	628	2345
short tons at <\$30/lb	955	4331
Europe (Excl. U.S.S.R.)		
Natural Gas, 1000 CF	152-173	484
Natural Gas Liquids, bbl	4.0-4.6	13
Crude Oil, bbl	19-26	39-79
Shale Oil, bbl	15 ⁺	150 (1400)
Bitumens, bbl	N.A. ⁺	N.A.
Coal, short tons	141	356
Uranium Oxide*		
short tons at <\$15/lb	76	129
short tons at <\$30/lb	621	914

Table 6. Nonrenewable World Energy Resources By Region (cont.)
(December 31, 1976)

	<u>Proved and Currently Recoverable</u>	<u>Estimated Total Remaining Recoverable</u>
	Billion (10 ⁹)	Units
Asia -- Pacific (Incl. European U.S.S.R.)		
Natural Gas, 1000 CF	1415-1672	5064
Natural Gas Liquids, bbl	37.5-44.3	134
Crude Oil, bbl	402-445	1005-1175
Shale Oil, bbl	35	115 (6500)
Bitumens, bbl	N.A.	N.A.
Coal, short tons	280	3865
Uranium Oxide*		
short tons at <\$15/lb	322	427
short tons at <\$30/lb	367	501
Africa		
Natural Gas, 1000 CF	199-223	996
Natural Gas Liquids, bbl	5.3-5.9	26
Crude Oil, bbl	50-63	136-166
Shale Oil, bbl	10	100 (4100)
Bitumens, bbl	N.A.	N.A.
Coal, short tons	17	32
Uranium Oxide*		
short tons at <\$15/lb	370	423
short tons at <\$30/lb	500	677

* Thousands of units

† Not available

‡ Values in parenthesis include estimates of undiscovered or unappraised resources in the 25-100 gal/ton yield range according to Duncan and Swanson, "Organic-Rich Shale of the United States and World Land Areas," U.S. Geol. Surv. Circ. 523.

Coal resource data are those of the World Energy Conference 1974 Survey of Energy Resources, except for the United States, where U.S. Bureau of Mines data are used. Allowance has been made for recent production; a mining loss of 50% is assumed.

Uranium oxide (U₃O₈) resources are expressed in terms of the U₃O₈ content of ores and forward cost rather than the actual market price, which has been rising rapidly. No allowance is made in forward cost for amortization of capital, financing cost, or profit. The U.S. data, from ERDA, are as of year-end 1976; all other data, reported jointly by the European Nuclear Energy Agency and the International Atomic Energy Agency, are as of year-end 1974. The communist countries' resources are excluded due to the lack of suitable data.

Both 1976 production and cumulated production of natural gas, petroleum, coal, and uranium oxide are shown in Table 7. Cumulated production data for the United States come from the U.S.G.S. and ERDA and have been updated by the use of recent production data.

Estimates of life expectancy of world fossil resources based on the quantities given in Table 1 and on the current production rate increasing at selected fixed annual growth rates are shown in Table 8. Fortunately, the life expectancy of

remaining recoverable world fossil fuel resources, as now estimated, is of the order of 100 years at a reasonable growth rate of 2% to 3%/yr.

Table 7. Nonrenewable Energy Sources Current and Cumulated Production

	Natural Gas Trillion CF	Petroleum,* Billion bbl	Coal, Billion short tons	U ₃ O ₈ , 1000 short tons
World				
1976	54-55	21.1	4.2	[26] [†]
Cumulated	888-913	359-366	154	572
United States				
1976	19.8	2.97	0.671	12.7
Cumulated	519	112.0	44.2	295

* Gross minus reinjection.
[†] Estimate.

Table 8. Life of World Fossil Fuel Resources
 At Various Fixed Demand Growth Rates
 (Based on 1976 Year-End Estimates)

Annual Growth Rate, %	Year When Remaining Reserve/Consumption Ratio Drops to 10 Years		
	A	B	C
4	2005	2050	2067
3	2010	2067	2090
2	2017	2097	2130
1	2029	2164	2226

A: Proved reserves: 0.748 to 0.776×10^{12} tce; mean = 0.762×10^{12} tce.

B: Total remaining recoverable resources: 5.054 to 5.683×10^{12} tce; mean = 5.369×10^{12} tce.

C: Doubling of estimated B resources.

Note: Calculations are based on growth at fixed selected annual increases of 1% to 4% from the 1976 world annual production of 8.695×10^9 tce, as estimated by the U.N.

Peat Resources

Although peat has been used as a fuel for centuries, it is not included in conventional resource estimates because of the general lack of information on the extent of the reserves and the potential contribution to world energy supply. Some incomplete data on world peat resources is shown in Table 9. Based on available data peat lands occupy an estimated 408.8 million acres of land in the world. These data show that the Soviet Union has 228 million acres, about 56% of the total world peat resource area-wise. The Soviet Union annually produces some 205 million tons, about 95% of the world's annual production. Total acreage of peat land in the U.S. is 52.6 million acres. Finland ranks third in total extent of peat lands and Canada fourth. It is to be noted that the resources listed for Canada exclude the Arctic regions. If these were included it is likely that the Canadian resources would be much higher than shown, and Canada would probably rank second to Russia in total

peat resources.

Currently, only Russia, Ireland and Finland use large quantities of peat for fuel, mostly for generation of electric power. Research underway to convert peat to gaseous and liquid fuels could result in an accelerated development of this somewhat neglected energy source.

The basic problem with estimation of peat resources is that while the areal extent of peat deposits is fairly well known, data on the thickness of such deposits is sparse. Therefore, estimates in terms of energy content are difficult to make.

Table 9. World Peat Resources and Annual Production (1)

Country	Acres (millions)	Annual Production	
		(%)	(million tons)
U.S.S.R.	228.0	95.70	205.0
U.S.A.	52.6	0.30	0.6
Finland	35.6	0.36	0.7
Canada	34.0	0.25	0.5
(Excluding Arctic)			
E-W Germany	13.1	1.00	2.0
Great Britain and Ireland	13.1	2.00	4.2
Sweden	12.7	0.15	0.3
Poland	8.6	--	--
Indonesia	3.3	--	--
Norway	2.6	--	--
All others	<u>5.2</u>	<u>0.4</u>	<u>1.2</u>
TOTALS	408.8	100.0	214.5

General Comments on Reserve Changes and the
Future Role of Economically Marginal Resources

The crude oil reserve estimates shown in Table 6 do not include the most recent upward revision in Mexico. The proven reserves of January 1976, amounting to 6.3 billion barrels have been increased to 20.24 billion barrels as of July 31, 1978. In addition, probable reserves are estimated at an additional 37 billion barrels and potential reserves, including the proven and probable volumes, may be on the order of 200-300 billion barrels. Further exploration and development may place Mexico in the same rank as Saudia Arabia in terms of oil resources.

The oil reserves of mainland China could also be much larger than current estimates based on available information. One recent estimate places proved, probable and possible recoverable reserves at 100 billion barrels. Major exploration and development efforts will be necessary to confirm or amend this figure.

A recent assessment of giant oil fields and world oil resources, not included in the base data used for reporting world oil reserves, has been made by the Rand Corporation² for the Central Intelligence Agency. The author concludes that, as of the end of 1975, proved and probable recoverable world crude oil reserves were 676 billion bbl, compared with the 538-606 billion bbl shown in Table 5. However, the Rand figure includes some probable reserves in addition to the generally accepted data for proved and currently recoverable reserves. It is pointed out that the difference between the Rand estimate and those made by other authorities is probably

due to a) the definitions of probable reserves used in various estimates, b) the extent to which reserves and recent discoveries are included and c) the differences in various estimates of known total recovery in the Soviet Union. The Rand estimate of ultimate conventional world crude oil resources is in the range of 1,700 - 2,300 billion barrels. If the estimated prior production of 335 billion bbl is subtracted, the total remaining recoverable reserves would be in the range of 1,450 - 1,950 billion bbl, which corresponds very closely to the IGT estimate of 1,500 - 1,840 billion bbl.

A major unknown in estimates of oil reserves is the extent of heavy oil resources which may become exploitable at higher prices. For example, the Orinoco oil sands in Venezuela, with a resource base of 4 trillion barrels, may extend from the eastern slopes of the Andes to Argentina, Bolivia, Peru and Brazil. The resource base for heavy crudes in place in this area may exceed those estimated for Venezuela alone. The extent to which these resources are economically recoverable with current technology is not known, but is probably rather low.

The estimates of world gas reserves presented herein do not include the so-called "non-conventional" sources of natural gas, because such sources cannot be estimated within the framework of the conventional procedures used for reserve evaluation. However, they could become a very important source of future energy supplies as remaining conventional resources decline. In general, such resources are not recoverable under current or near-term economic conditions. The sources are shales of the Mississippian and Devonian age, tight gas formations, coal seams, geopressed aquifers, and gas hydrates. The data base for even preliminary evaluation of these resources is very scanty. However, due to the recent shortage of conventional gas supplies in the United States, these resources are being evaluated by the U.S. government agencies for potential future gas supply. As a result, most of the available data are applicable only to the U.S. situation.

The resource base of gas existing in the Devonian and Mississippian shales in the eastern U.S. is estimated to be on the order of 600 trillion cubic feet. There has been a small amount of production from these shales in the Appalachian area for many years. Major efforts are underway to more rigorously define the resource and to develop means of substantially increasing production rates from wells.

Large areas of gas-containing formations which are relatively impermeable to gas flow exist in the western U.S. (and also in western Canada). The resource base in the U.S. is estimated at 600 trillion cubic feet. Application of advanced fracturing techniques could result in recovery of substantial quantities of this gas.

Many coal seams in the world contain appreciable amounts of natural gas which may be recoverable by specialized drilling and drainage techniques. For the U.S., the resource based of methane associated with coal is estimated at 2,500 trillion cubic feet.

A belt of geopressed aquifers in the gulf coast region of the United States contains brine saturated with natural gas at pressure higher than the hydrostatic head from the surface to the formation. The lack of information on the extent and producibility of the aquifers has resulted in a very wide range for the methane resource estimate - 3,000 to 100,000 trillion cubic feet. Major experimental efforts are underway to more rigorously define the

resource base and to devise methods of producing the resource in an economic and environmentally acceptable manner.

The least well-defined and most speculative natural gas resource is gas hydrates. A gas hydrate is a solid compound of methane and related hydrocarbon and water which exists at a relatively low temperature and relatively high pressure. Deposits of gas hydrates have been discovered in Siberia and there is indirect but rather compelling evidence that gas hydrates exist in the North American Arctic regions and in the deep ocean bottom. Some Russian scientists³ have estimated that the world resource base of submarine gas hydrates is on the order of 1×10^{18} cubic meters. To date, no definitive progress has been made in further assessing the extent of this resource or the development of methods for recovery.

Although these unconventional gas resources have been discussed primarily in the context of U.S. experience there is every reason to believe that similar resources exist on a worldwide basis. Of the various sources, the resource base of natural gas associated with coal is probably the most amenable to estimation. Insufficient data are available on the remaining sources although tight sands, shales comparable to the eastern U.S. sources and high pressure zones encountered during oil drilling in other parts of the world lend credence to the belief that similar conditions exist outside the U.S. Only a very small fraction of these resources is producible under current economic conditions. However, as the decline of more conventional supplies of oil and gas forces the price up, the unconventional sources may provide an expanding source of future gas supply.

Another very large potential source of fossil energy is the lower grade oil shales. Recent experimental work by the Institute of Gas Technology has demonstrated that yields of oil from shales of 10-15 gal. oil per ton (by Fischer Assay), using a hydroretorting technique, gives energy recovery equivalent to the conventional retort yield from richer western U.S. shales. The estimated resources in four U.S. eastern states recoverable by above-ground hydroretorting are equivalent to 414 billion bbl oil. A similar resource base is very likely to exist in other parts of the world.

The combined effect of future higher energy prices and advanced technology could permit eventual massive exploitation of non-conventional gas supplies, low grade oil shale, peat, currently unmineable coal deposits and other currently economically marginal or uneconomic fossil energy supplies. In view of the potential size of the resource base, the rationale of doubling the current estimated remaining recoverable resources (Tables 4 and 8) to estimate U.S. and world possible extended fossil fuel resource life seems justified.

REFERENCES

- (1) Farnham, Rouse S. (Coordinator) Energy From Peat, Subcommittee 8 Report to the Minnesota Energy Agency, January, 1978.
- (2) Nehring, Richard, Giant Oil Fields and World Oil Resources Prepared for the Central Intelligence Agency, Rand Report No. R-2284-CIA, June, 1978, Rand Corporation, Santa Monica, Ca., 90406.
- (3) Trofimuk, A. A., Chersky, N. V. and Tsaryov, V. P., Conference Proceedings; The Future Supply of Nature - Made Petroleum and Gas, Schloss Laxenburg, Austria, 5-16 July, 1976, Pergamon Press, 1977.

WORLD ENERGY SUPPLY AS A PRICE DEPENDENT VARIABLE

Dr. Jay B. Kopelman

SRI International,* 333 Ravenswood Avenue, Menlo Park, Ca. 94025

Introduction

In the area of energy resource management, more uncertainties have developed in the last five years than in the previous twenty. In Figure 1, the posted price (real and current) of world crude oil is shown from 1960 through 1978. After a long period of relative stability, this price rose from \$2.59 per barrel to \$11.65 per barrel in one year (1973). A strong cartel (OPEC) developed that now asserts control over a large fraction of petroleum traded in international markets. This development has substantially affected the price outlook for other fuels as well. International energy markets and other segments of world economies have been changing rapidly in the past five years in a still emerging response to the formation of the cartel.

A common perception of the future^(1,2) is that there will be increasing disparity between growing demand and dwindling non-OPEC supplies and ever rising energy prices. In this view, the United States and other major industrial nations are confronted with the likelihood of a growing need for oil imports and greater dependence on foreign supplies. The resulting political and economic problems impel government and business planners to consider alternative responses.

In a recently completed two-year study of world energy supply and demand at SRI International, a somewhat different picture of the likely developments in future world energy balances has been obtained.

Summary

The principal conclusion of our analysis of world energy supply and demand is that there are adequate opportunities for increasing conventional supplies of hydrocarbon resources on a worldwide basis, diversifying the sources of supply, and substituting among fuels to allow an orderly development of alternatives through the remainder of this century and for some time into the next without large price increases. This conclusion is based on the following series of observations and estimates:

- The conventional techniques used to make estimates of resource availability in terms of a single number representing reserves are not adequate information to determine future supply/demand balances. Resource availability should be discussed in terms of recovery costs and market prices.
- There is no long-term condition of imbalance in supply and demand where "gaps" occur. In the absence of artificial price controlling regulations, prices respond well in advance of this impending situation to prevent just such a possibility.
- International energy supply and demand price elasticities have been broadly underestimated.
- Current estimates of proven oil reserves do not accurately reflect the long-range impact of higher petroleum prices. Higher oil prices are encouraging exploration and the application of advanced recovery techniques so that future additions to proven reserves will be greater than they would have been at lower oil prices.

- The opportunities for fuel substitution are greater than has generally been recognized.
- There will be an expansion of the class of major oil exporting nations to include some new members in the next few years (Mexico, the United Kingdom, Norway, China, etc.). The disparity of national interests will cause highly varied responses to changing supply/demand situations in the world markets. Those who join OPEC will increase the diversity of cartel membership and the complexity of production allocation and pricing decisions to be settled.

This view of world energy availability has not been the consensus. As mentioned earlier, many other analyses anticipate serious supply/demand imbalances in the 1980s. These different viewpoints arise principally from certain features of the present analysis described below that are not usually considered in this kind of study. These features do not eliminate the substantial uncertainties inherent in this kind of analysis from unanticipated political, social, or technological developments (e.g., wars, embargoes, a major depression, or a breakthrough in photovoltaic cell economics, etc.), but they do provide a powerful tool for evaluating the potential sensitivity of the results to these changes.

The Analytical Structure

It has been customary for energy analysts to hypothesize a "scenario" price or set of prices for some reference energy source, usually Middle East oil, and then try to determine how the demand for oil will grow and what supplies will be produced at this price. In that approach, demand is growing exponentially and supplies are relatively static. It is not surprising then that at some point demand exceeds the supply, creating an "energy gap."

The procedure outlined above simplifies the analysis by ignoring the feedback among energy supply, demand, and prices, and the effects of prices on interfuel substitution. That approach is not complete, however, because it ignores the dynamics of energy pricing through time.

Energy prices respond not only to the instantaneous supply/demand balance but also to producers' and consumers' perception of the future. If a producer perceives that his resource is growing scarce because of depletion of the reserves, he will demand higher prices now for incremental production. How much he can raise his price depends upon a variety of time dependent variables including:

- The rate at which the resource is being depleted now and what rate might be expected in the future
- That producer's potential loss of market share to other producers of the same resource or to competing substitutes or to declining demand
- The impact that higher prices would have on the stimulation of new technology to replace future demand for the product
- The individual producer's preference for present income versus deferred, perhaps higher, income at some future time.

Therefore, at any given time in energy markets, a variety of individual decisions are being made by producers and consumers that rebalances the supply/demand equations.

The quantitative analysis here has centered around the development of a world energy model⁽³⁾ built in two parts and called ENDEM and FUELCOM, respectively.

ENDEM (Energy Demand Model) is a representation of our analysis of energy demand development on a regional basis for 15 different end-use categories (steelmaking, chemicals, residential/commercial space heat, transportation, etc.) as a function of assumptions about macroeconomic variables such as population, GNP per capita, and trade balances. FUELCOM (Interfuel Competition Model) represents our analysis of the competition among different fuels (oil, coal, gas, nuclear, hydro, and others) for each of the end-use markets in each region. FUELCOM calculates market clearing prices for each fuel in each region based upon obtaining supply/demand balances at each point in the energy network from resource production, through conversion and transportation links, to end-use consumption in each of the demand markets used by ENDEM.

The approach used in this study to integrate the demand and supply work is an iterative process. At first a tentative economic projection (GNP growth rates, trade flows, industrial production, consumption) is used to calculate tentative energy demand projections by end-use category for each region (at the highest level of regional aggregation) in ENDEM. These projections are used in FUELCOM to obtain an overall energy demand/supply balance at a market clearing price for each fuel in each region over the entire time horizon. This tentative energy balance is compared by the analyst with the assumptions on energy prices and trade flows implicit in ENDEM. If they are consistent and reasonable in the judgment of the analyst, a converged solution is assumed. If they are not consistent, a somewhat revised economic outlook is made to take into account the new information on energy prices and trade flows, and the process is repeated until a converged solution is obtained. When this process is completed at the first level of regional disaggregation and a satisfactory convergence obtained, a further regional disaggregation is begun using the larger region results as constraints on the more detailed analysis.

The principal outputs of the energy model are projections of the regional market clearing prices for fuels over time, associated production quantities, flows through transmission links, capacities of conversion processes, and demands for distributed fuels. Clearly, the projections can be sensitive to the inputs to the model. By varying the key model inputs and assumptions over reasonable ranges of uncertainty, the sensitivity of the projections to these inputs are determined.

Results--Demand

Long-range projections of world energy demand have been changing substantially in recent years. Today's estimate for total primary energy demand for the year 2000 is more than 20 percent lower than earlier estimates.⁽⁴⁾ For example, Exxon's recent estimate of world energy demand for the non-Communist world in 1985 of 125 million barrels of oil equivalent per day is down 24 percent from estimates of 165 million barrels of oil equivalent per day made in 1973 for the same region. These differences are related to changing views of the future growth of regional macroeconomic indicators such as GDP and population, as well as to changes in the relationship of energy consumption to these variables and to price. The quadrupling of world oil prices since 1973 (shown in Figure 1) has had an important impact on all of these estimates. Even if demand often appears to be somewhat inelastic to price changes in the short term, long-term effects of the increases shown in Figure 1 are making big changes in year 2000 projections.

The regional variation in anticipated primary energy consumption obtained in this analysis is shown in Table 1. Although OECD nations still account for nearly half of world energy consumption in year 2000, in general, developing nations will show higher growth rates of energy consumption than developed nations because they are starting from much lower absolute values, have higher population growth rates, less room for improvements in the efficiency of consumption, and are expected to make considerable effort to "narrow the gap" in GDP per capita.

The changing relationship anticipated between energy and GDP is most dramatic in the United States. In 1970, a barrel of oil equivalent energy was used to generate about \$140 in gross domestic product (in constant 1978 dollars). By the year 2000, it is expected that the same amount of energy will generate about \$191 in GDP or a 37 percent increase in economic efficiency in energy use. These efficiency improvements are achieved despite the fact that electricity consumption is expected to grow faster than total energy, and average electric power efficiencies are lower than for the direct consumption of fuels. Such changes are occurring worldwide, although not so dramatically in nations that have historically not had access to the same abundance of relatively low-cost energy as the United States.

Table 1

PRIMARY ENERGY CONSUMPTION
(Millions of Barrels of Oil Equivalent per Day)*

	<u>1960</u>	<u>1970</u>	<u>1980</u>	<u>2000</u>
United States	20.7	31.7	38.9	58.6
Canada	1.8	3.0	4.5	7.3
Western Europe	12.5	22.0	27.3	46.3
Japan	1.8	5.6	8.8	17.9
Mexico/South America	2.2	4.2	7.5	20.9
Africa	1.0	1.8	3.4	7.6
Middle East	0.7	1.4	3.3	10.5
Centrally Planned Economies	18.2	27.1	42.9	87.5
Remainder	<u>2.2</u>	<u>4.6</u>	<u>7.6</u>	<u>19.1</u>
Total	61.1	101.4	144.2	275.7

* For most of this paper, the units of energy demand will be expressed in oil equivalent barrels to evaluate how changes in forecasts or assumptions can affect world oil trade--oil being the "swing fuel" in international energy forecasting.

The results of the FUELCOM interfuel competition analysis corresponding to the ENDEM regional energy demand of Table 1 is shown in the highly aggregated curves of Figure 2. There are no dramatic surprises shown in this figure. World demand for all forms of primary energy is expected to continue to grow to the end of the century but at considerably lower rates than for the most recent 25-year historical period. The average historical growth for 1950 to 1975 was about 5 percent, whereas for the forecast period the analysis indicates world average demand growth of about 3.4 percent.

Oil, coal, natural gas, and nuclear energy are all expected to play major roles in supplying the increased energy consumption, while hydroelectric energy supplies will become increasingly important in some of the less developed areas.

Worldwide, nuclear power generation growth rates, although still considerable, will be substantially lower than most projections of the recent past because of previously unanticipated political, social, and economic problems. Gas consumption, on the other hand, will probably grow more rapidly than expected.

Primary Resource Economics

One of the most difficult and important considerations in analyzing energy supply and demand balances is to quantify the long-term economics of primary resource

production. In the classical economic sense, a long-term dynamic supply curve that specifies a price-volume relationship across a 50-year time horizon or longer is required for each resource. The key issues that must be considered with regard to primary resources are: depletion, reserves, lease cost, production, development, exploration, technological change such as enhanced oil recovery or advanced mining techniques, and wellhead or mine-mouth price.

The main shortcoming of most published resource estimates is that price is not explicitly included; only quantity is considered. Differences among estimates can thus be due to differences among assumptions and definitions as well as to differences of opinion or uncertainty about the resource base itself. To analyze strategic energy decisions and to estimate resource availability, considering resource volume estimates alone is not sufficient; joint price-volume relationships for each resource must be estimated and made explicit.

Resource supplies represented in FUELCOM on a regional basis are crude oil, natural gas, coal, nuclear fuel, hydroelectricity, oil shale, and tar sands in specific regions. Each of these is described in each resource basin by a different supply curve giving the marginal cost of incremental production of that resource as a function of total cumulative production in that basin. Probable in-place resources, past discovery and development histories, and expected future finds are defined in the analysis. In estimating the costs of reserves, price-dependent costs such as lease bonus payments, royalties, and production taxes are distinguished from ordinary exploration, development, and production costs.

Specifically excluded from the marginal cost is economic rent (lease bonus payment and additional profits above the 15 percent return on investment). The marginal cost of a resource is the minimum acceptable price at which the supplier would be willing to develop and sell that resource. Economic rent, reflected in a price higher than the minimum acceptable price, is computed by FUELCOM as a function of the prices of other energy sources and the dynamic characteristics of the market. For OPEC producers, a specific cartel pricing algorithm is used.⁽³⁾

FUELCOM uses regional marginal cost estimates including 26 oil resource curves, 26 gas resource curves, 22 coal curves, and 13 miscellaneous resource curves, including estimates of the costs of hydropower, nuclear fuel, shale oil, and tar sands in different regions. As an example of this type of curve, Figure 3 illustrates the marginal cost curves for world cumulative supplies of crude oil, natural gas, and coal. These world total curves are much too aggregated for use in FUELCOM, but are valuable to illustrate several important points. As shown, coal is available in vast quantities at low recovery cost. Recently,⁽⁵⁾ the estimated in-place coal resource base of the world was increased over 18 percent above the 1974 estimates at the 1978 World Energy Conference. Similar modifications in estimates of traditional supplies of oil and gas are being made showing increases in production potential from old and new areas, e.g., Mexico, China, Canada, the North Sea, etc.

From the results shown in the curves of Figure 2, the cumulative world consumption of oil anticipated from 1975 to 2000 is 700 billion barrels. For natural gas and coal, the cumulative consumption is 340 and 460 billion barrels of oil equivalent, respectively. Although there is not sufficient information in the curves of Figure 3 to calculate a year 2000 market clearing price for each resource, it is apparent that world supplies of these resources are by no means exhausted at the end of the century. In fact, there is considerable uncertainty as to whether the market prices of conventional supplies will even reach the levels required to make sources of synthetic hydrocarbons commercially competitive by that time. Superimposed on the marginal cost resource curves of Figure 3 are the minimum cost estimates found in the literature⁽⁶⁾ for synthetic crudes from coal, synthetic natural gas (SNG), and oil from shale. The early 1978 posted price of OPEC marker crude oil is

also shown for comparison. In this economic environment, because of price competition from conventional supplies, it is not likely that any unconventional supplies of energy will become commercially available on a global scale before the end of the century. However, in specific locations, shale oil, heavy oils, and synthetic fuels from coal may contribute a measurable fraction of regional energy supplies.

As an example of evolving trade patterns, Figure 4 shows how petroleum production patterns have changed since 1950 and are expected to change in the future. In 1950 there were four significant production areas in the world--North America, Central and South America, the Middle East, and the Soviet Union. By the end of the century, according to this analysis, there will be several more. The Middle East, of course, remains a major supplier of oil to the world, although its share of world markets will be smaller in the future. An important result of this analysis is the growing role of producers that are not presently in OPEC--Mexico, the United Kingdom, Norway, China, and several nations in Africa and Asia. Each is faced with the need to develop supplies and to market them to provide capital for economic development. In addition, considerable development of coal and nuclear resources displaces oil and gas from utility and industrial markets. Since OPEC must continue to function as the marginal supplier of petroleum to maintain control over international oil prices, all of these development impact strongly upon cartel production growth rates and together suggest that--for a time--the organization will find itself in the passive position of attempting to preserve its gains. Future growth in world demand for oil will very likely be significantly slower than the pace that was seen in the years prior to 1974. Non-OPEC oil production will continue to grow, probably at a rate higher than many observers expect. If the organization is to continue to set and maintain the world price of oil, it must also support the price for all producers of oil moving in international trade. Many of the newer oil exporters such as Norway, the United Kingdom, and China are not likely to become part of OPEC because of their history, politics, or because--for one reason or another--they do not view membership in the cartel as in their best interests. A special problem for the cartel is that non-OPEC producers can take advantage of the cartel price without assuming any of the burdens associated with withholding production to support prevailing price levels. As mentioned previously, it is expected that those who do join OPEC will increase the diversity of cartel membership and the complexity of production allocation and pricing decisions to be settled. The combination of these factors is likely to place pressure on OPEC's market share and--at least over the near term--continue to reduce the ability and willingness of cartel members to make higher real prices stick.

* The author is now at the Electric Power Research Institute.

REFERENCES

1. Energy Supply-Demand Integrations to the Year 2000, Workshop on Alternative Energy Strategies, The MIT Press, Cambridge, Mass. and London, England (1977).
2. The International Energy Situation: Outlook to 1985, CIA, No. ER 77-10240 U (April 1977).
3. A more complete discussion of the SRI World Energy Model as well as references to other documentation may be found in the following paper: J. B. Kopelman and N. L. Weaver, "Energy Modeling as a Tool for Planning," Long Range Planning, II (February 1978).
4. World Energy Conference, Executive Summary, "World Energy Demand to 2020" (August 15, 1977).
5. World Energy Resources, published for the World Energy Conference by IPC Science and Technology Press, p. 209 (1977).
6. Fuel and Energy Price Forecasts, Volume 2, Electric Power Research Institute (EPRI) Report EA-433 (February 1977).

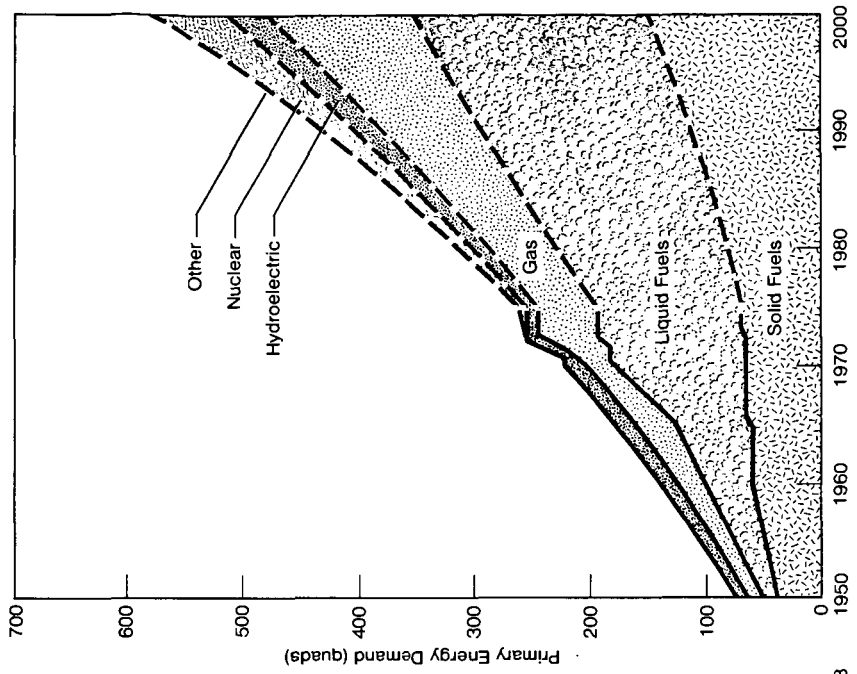


Figure 2. World Energy Consumption

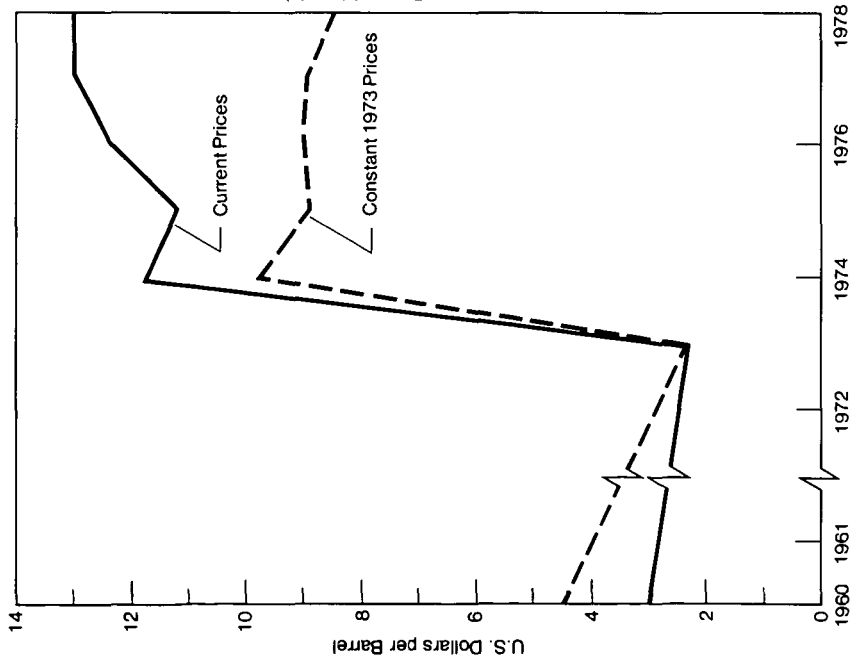


Figure 1. OPEC Prices of Oil

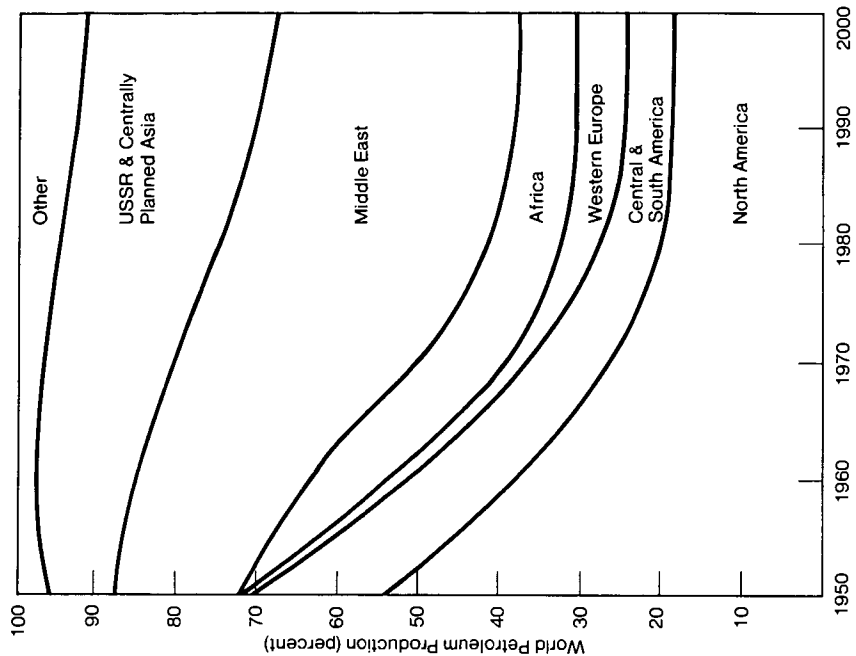


Figure 4. World Petroleum Production

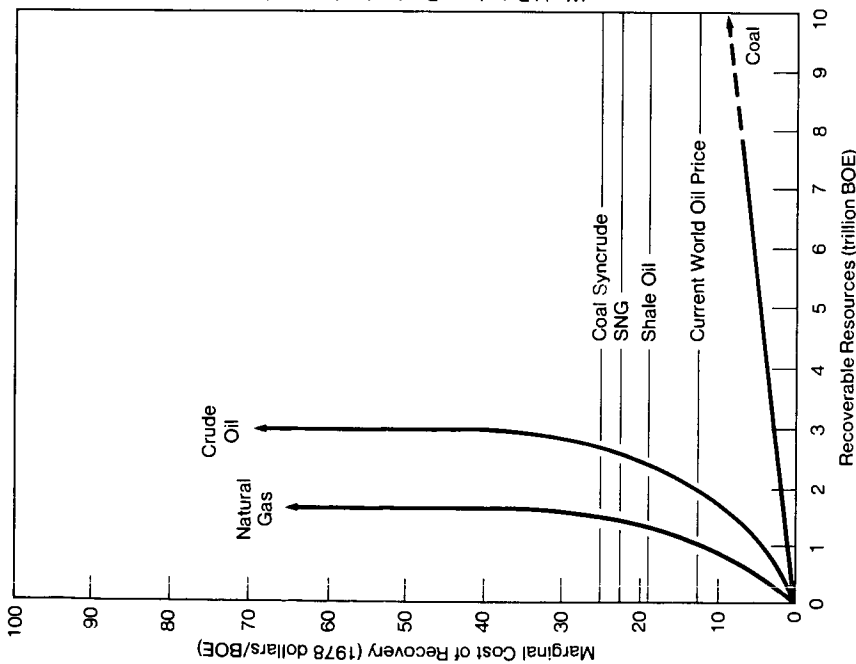


Figure 3. World Hydrocarbon Resources in 1975

FORETELLING THE ENERGY FUTURE

H. DuMoulin and E. V. Newland

Shell International Petroleum Company Limited,
Shell Centre,
London SE1 7NA.

Introduction

Half a decade has passed since the world economic system suffered the shock of a massive increase in oil prices. In the intervening years there have been many conflicting forecasts of future energy developments, ranging from "no problem" to alarmist warnings of another, even greater, shock to come - a second energy crunch. The latter variety have tended to predominate. The multiplicity of forecasts would be confusing enough and undoubtedly contribute to indecision and lack of action by the policy makers, but the picture is still further obscured by the current situation. At the time of writing (November 1978), oil consumption is only just back where it was five years ago, energy supply is in potential surplus and the sense of urgency seems to be gone. What is the truth? Is the second energy crunch, so widely predicted, real or not? If it is, how can the confusing messages be rationalized so that the actions necessary to ameliorate it can be set in motion?

A Methodology for Coping with Uncertainty

"Those who foretell the future lie, even if they tell the truth" Arab Proverb

This quote is appropriate at the beginning of a discussion on the future of world energy supply and demand in view of the important role which the Middle East has had, and will continue to have, in shaping the future world energy scene. This particular proverb also makes another very important point - the future cannot be predicted. In fact there are many possible futures dependent on how events and decisions yet to be taken are linked and interact. Assertions about the future in general and about energy developments in particular may or, more likely, may not, turn out to be accurate but if we are to avoid confusion, indecision and too many mistakes, we need a methodology to cope with the uncertainties.

A scenario is logically coherent, future state of the world. It is not what will happen but what can happen - a subtle but important distinction. We can distinguish, and will be referring to, three distinct types of scenario - the archetype, the phantom and the exploratory scenario (see Box 1). Archetype scenarios form a starting point; they provide alternative views of the world or of specific issues in rather stark terms, i.e. the future economic framework, oil price developments etc. Phantom scenarios are similar, but they consider issues which have a low probability of occurring but a major impact on the future if they do occur. Exploratory scenarios are rather different; they combine the variables that emerge as important from the essential analyses of the archetype and phantom scenarios to develop routes or pathways into the future. This involves making assumptions about how the world will react to a given set of conditions, so exploratory scenarios tend to evolve into second generation response scenarios.

The scenarios have several functions. Their construction is a learning process which helps us to understand the past and the present and to structure in a rational way the uncertainties of the future. As a possible instrument of change, they have an important role in strategic planning. By identifying the features common to all scenarios - the pre-determined elements - we provide a hardcore of information, some solid facts on which we can base our plans.

The scenarios also provide a rational framework for discussion with outside organisations such as governments, academic institutions etc. We can thus share our view of the world in an unemotional and professional way. This is particularly important in the international energy sphere, where as we have mentioned, the dialogue has become confused because of the concentration on conflicting single-line forecasts.

<u>A WORLD OF INTERNAL CONTRADICTIONS</u>	<u>BUSINESS EXPANDS</u>	<u>BOX 2</u>
- A world which fails to liberate the forces making for growth	- Barriers to growth removed	
- Systems proliferate and decay, alienation is widespread	- Systems performance improved, alienation mitigated	
- Greater government intervention in the market economy	- Reached by reaction against low growth	
- Diversion of resources to non-marketed sectors. Low commitment of risk capital	The Condition	
- Low growth of international trade (protectionism)	- Effective political leadership	
- Strong move towards further egalitarianism	- Governments understand and foster the process of wealth creation	
- GDP growth 2.6 - 3.0%	- Strong links into the international trade system	
	- GDP growth 4 - 4.5%	

We can get some idea of how demand for energy might develop by quantifying the archetype scenarios. One way of doing this would be simply to look how demand has increased with economic growth in the past and to project this, or a subjectively modified relationship, into the future. Such type of analyses quickly indicates that demand for energy, and for oil in particular, will grow to exceed available supply - to result in a gap or the next crunch - any time from the early 80's onwards, depending on the economic growth rates chosen. But such an analysis is far too simplistic. The historic relationship between energy and economic growth was established over a long period of abundant, low-priced oil. The oil price hike in 1973/74 was enough to begin to change our way of using energy, our attitudes towards conservation, self-sufficiency etc. and changes in oil price in the future remain a key element in influencing future demand. Hence it became clear that the price-dimension had to be introduced in the energy quantification work as a critical separate variable.

The price of a commodity is normally determined by the supply/demand interplay, i.e. provided supply is free to increase in pace with demand. If there is interference with the free supply/demand play, as there has been in the case of oil, then the price could be driven up to the eventual cost of alternative fuels. In theory, this upper level should provide a new norm for oil prices, but, in practice, because of the long lead times necessary to change the pattern of energy supply, the point at which some consumers, or more particularly consuming countries, will find it difficult to pay may well be reached earlier. Considering the economic disruption that has already been caused by the price rises of 1973/74, it would seem that we are already close to some consumers' ability to pay at current prices. At this stage, economics have been completely overtaken by political forces and there is no economic theory that will tell you what the oil price is going to be. It is a question of "realpolitik".

There are forces pushing the price in both directions and, as a lever to extract insight, we can develop these into two oil price scenarios. Upward pressure leading to Escalating Prices in real terms stems, inter alia, from the influences of those producing countries which have, or face, balance of payments difficulties. Particularly those with limited oil reserve to production ratios will argue most strongly that the price should escalate in real terms to reach the cost of alternative means of obtaining oil or gas (e.g. derived by synthesizing coal) at a not too distant point in the future, say 1990. Higher oil, and hence energy, prices will also render the exploitation of the gas reserves, which most of these producers possess, much more attractive - such projects almost invariably

require expensive liquefaction, conversion or pipeline projects to deliver the gas to distant consumers. Then there is the perception that most OECD countries are in a better position to pay for oil; there is a general belief that U.S. imports will continue to increase and of course there can always be further accidents in the Middle Eastern political situation. These and other factors would tend to push the oil price up in real terms, i.e. by considerably more than the rate of global inflation.

The major forces pushing in the direction of Price Moderation include the concern, particularly expressed by the key producing country, Saudi Arabia, with the economic stability of the West. Other factors such as major new oil discoveries or a belated success for President Carter's energy policy in the USA may also have a part to play. There has been considerable restraint on the part of the producers since 1974 so that it would appear that, at present, we are in a "symbiosis" scenario which could keep prices roughly at today's level - although inflation corrections could either over or under compensate from time to time. Whether this price moderation scenario will prevail is far from certain and depends inter alia on future geopolitical developments. Our purpose for developing these contrasting, essentially politically based, archetype price scenarios was as a tool to increase the understanding of the interaction with the other scenario parameters (described above) in the energy supply and demand field.

Exploratory Scenarios for Energy - combining the important variables from the archetype scenarios.

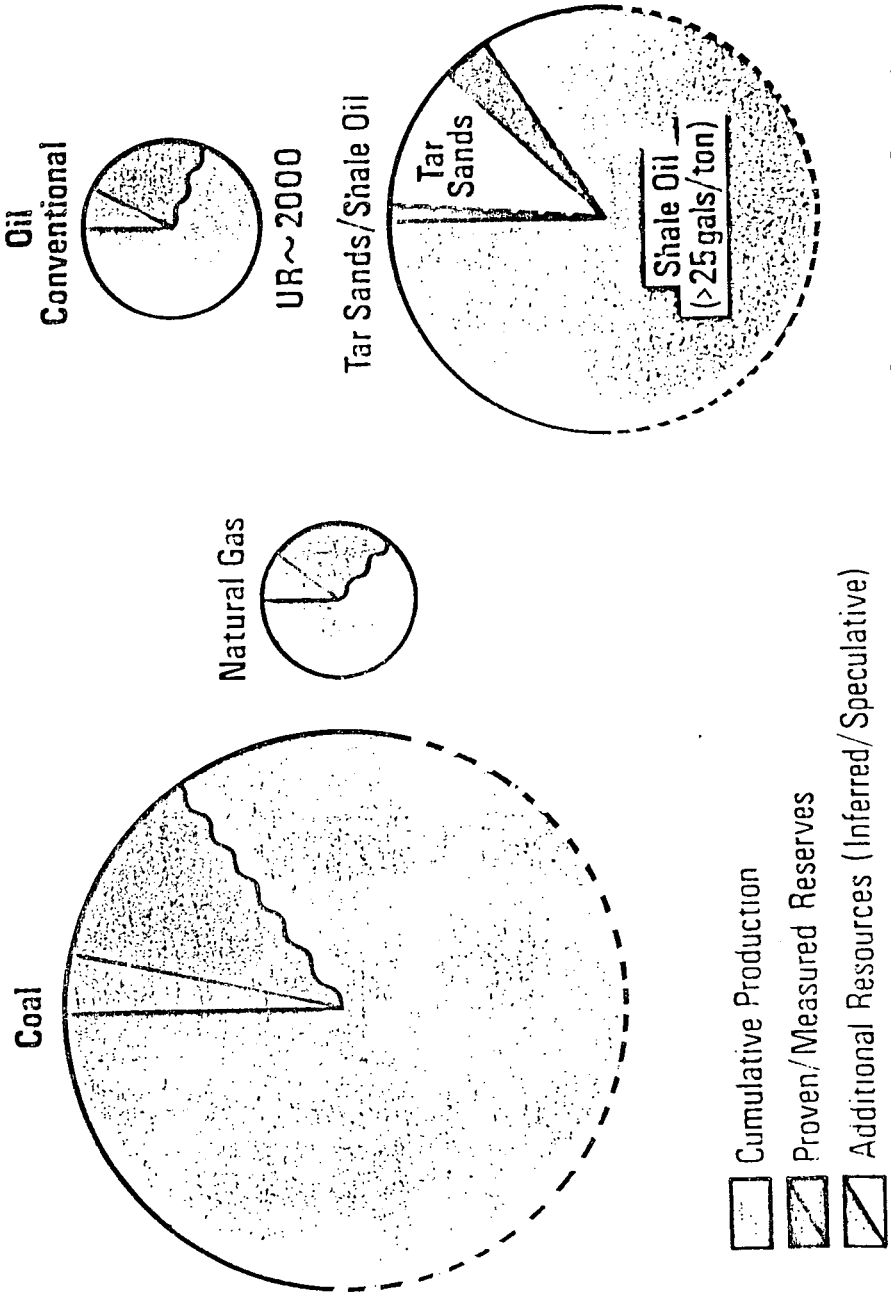
It is clear that the relationship between economic growth and the amount of energy needed to fuel that growth can change in the future, but to get an idea of by how much and in what ways it may change we need to take a detailed look at the markets - the end uses for energy. Similarly, one can use the price scenarios to test for the price sensitivity of demand, but price elasticity is an unreliable concept and we have not found any really worthwhile study that we could use with confidence. No short cut, using for example ex-ante assumptions about changing income and price elasticity of demand for energy, appeared satisfactory. Thus we were driven to the conclusion that a detailed market breakdown coupled with subjective judgement on how each will be affected by higher prices was needed. We had to assess how consumers will react to prices under the different economic scenarios and, more importantly, how governments will react. This is because the private consumer (micro) reaction is often insufficient in view of the national (macro) problem created in balance of payments terms as a result of an oil price increase. For example, an increase of one dollar in the price of a barrel of crude oil can be very serious in balance of payments terms, yet the price of gasoline at the pump, if the crude price increase were spread evenly over the products, would not go up by more than about two cents a gallon.

One way in which governments have already reacted to the earlier price hikes is in the encouragement of energy conservation. Again, the individual consumer is unlikely to use the same criteria for deciding whether or not to implement energy-saving methods. A detailed market breakdown approach turned out to be the only way to manage the assessment of just how much conservation and substitution may be achieved.

Fossil fuel resources, as shown in Figure 1 which looks a bit like planets in the solar system, appear more than adequate but, to come down to earth again, there are economic, societal and geopolitical problems to be overcome if shortages are to be avoided. The warnings of a world rapidly running out of oil are well known and we shall return to these below, but each of the "big three" fossil fuel alternatives also has its problems. There is a great deal of gas around, but most of it is in the wrong place - a long way from the market. Similarly, there is plenty of coal but general aversion to dig it out and reluctance to burn it. The importance of the potential role of tar sand and more particularly, shale oil, in the international energy context has been exaggerated.

World Fossil Fuel Resources

(Estimated Ultimate Recoverable Resources)



UR = Ultimate Economic Recovery in 10⁹ Barrels of Oil Equivalent

n.b. The size of the circles should be taken as indicative only of the order of magnitude of hydrocarbon resources. With the exception of conventional oil, insufficient exploration has been carried out to define the size of the resources base accurately and the technologies for exploiting the reserves are not yet fully developed.

If one looks outside the carbon-based, fossil fuels spectrum nuclear energy is, of course, very important, but generally most unpopular. This is an area where a phantom scenario can be useful. We developed a scenario called Nuclear Disappointment in 1975 to analyse the effects of a major slowdown of such magnitude that at the time it was considered highly unlikely, but would, of course, have a major impact on the world energy situation. Such slowdown in the rate of introduction of nuclear power would have resulted from the lack of consensus over the complex set of technical, economic and socio/political issues surrounding it.

Solar energy and its derivatives, wind, waves, biomass, etc. are superficially attractive because of their abundance, renewable nature and familiarity. The problems arise from their intermittent, diffuse and sometimes unpredictable characteristics. It is too early to say which of the many alternatives will ultimately prove successful and become significant but all are likely to make some contribution depending on local conditions.

At the 1977 World Energy Conference, a Delphi exercise put the ultimately recoverable world crude oil resource base at about 2×10^{12} barrels. About three-quarters of this total is thought to be outside Communist areas (WOCA) and if this was developed at the fastest technically feasible rate, production would peak in the 90's and then start to decline (Figure 2). We also know that the oil-producing countries have many other considerations and they will undoubtedly choose to develop their resources at a slower rate. Analysis of the production profiles for individual countries suggests that the maximum acceptable level of production will be considerably lower than the technical ceiling resulting in a flatter profile of what we call "The Oil Mountain". nevertheless, there is still significant growth ahead, so that liquid fuels, even from conventional sources, will be with us for many decades to come. The real point, and the reason for the debate about the next energy crunch, is that the demand for oil is likely to be constrained by available supply within the next 20 years, as we shall discuss below.

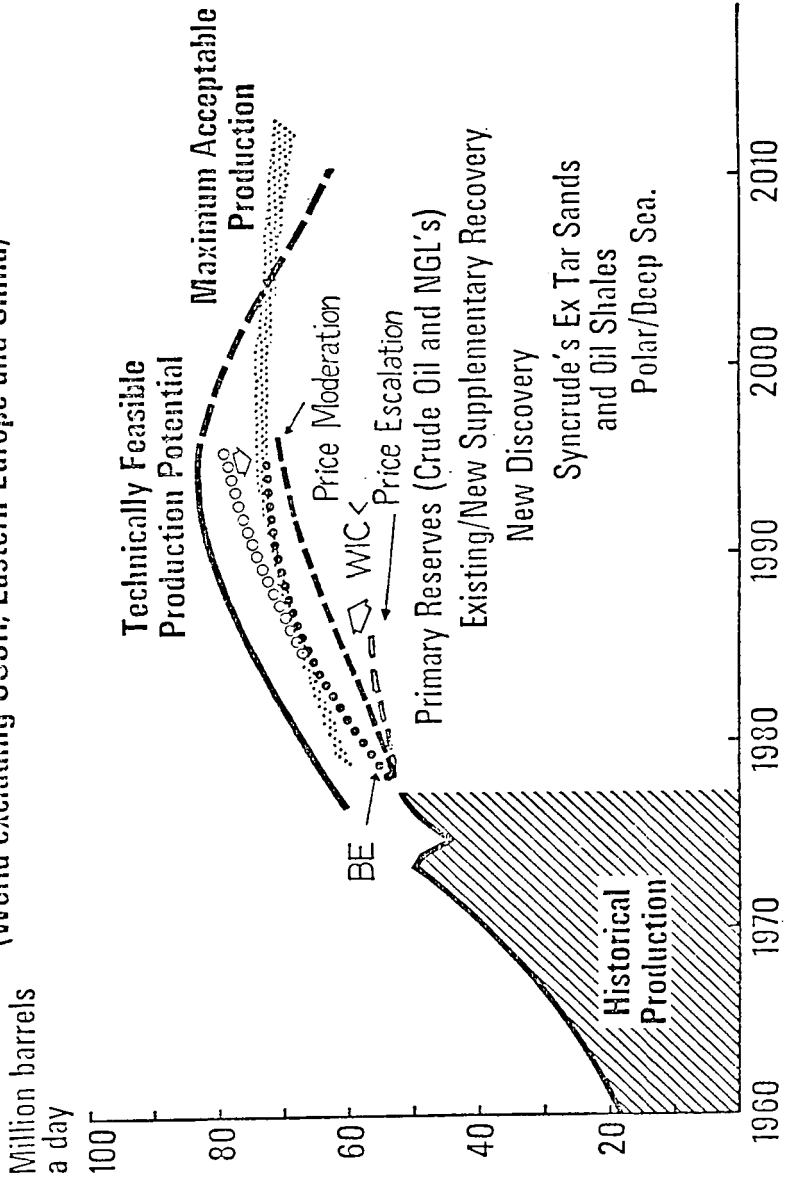
There are critics of the oil industry who think this picture is overly pessimistic and that there may be far more oil to be found than has been assumed. It is certainly true that there are vast reserves of low-grade oil in the form of tar-sands, oil shale etc. (Figure 1) which are only now beginning to be developed and there will undoubtedly be further discoveries of conventional oil as well as improvements in recovery techniques from known reserves. The profile in Figure 2 requires approximately half the oil produced in the year 2000 to come from such "new" sources. This assumes that the huge capital needed can be made available and that the associated technical and environmental problems can be solved. However, the north Sea oil fields have taken over 10 years to bring to present levels and the next oil province might be in even more hostile territories requiring longer to develop. So even if there is a lot more oil, it is not going to change the early part of the production profile very much, but could extend the plateau in Figure 2. The resource base (including unconventional oil) may be adequate but money, technical skills and time may not be.

The Next Oil Crisis - A Mirage?

When we compare the oil demand figures obtained by quantifying the exploratory scenarios with the resource base (Figure 2) some interesting response situations are revealed. For example, we can put a low probability on rapidly escalating oil prices in a low growth world (WIC) because we found that the resulting reduction in oil offtake was such that it would not seem to be in OPEC's interest to follow this route. On the other hand, a low growth world coupled with prices which are approximately constant or rising only slowly in real terms - price moderation - appears at first sight to be a perfectly tenable one. Oil constraints could, in theory, be avoided for the rest of this century, even though the threat of impending crisis might stay with us. This mirage effect, i.e. a crisis which stays on the horizon but recedes as it is approached, could result if low economic growth allows time for some efficiency improvements to be made and for alternatives and new oil to be brought on stream. As an illustration of the physical

The Oil Era - A Perspective

(World excluding USSR, Eastern Europe and China)



effort required by the year 2000, even in this low growth scenario, it is interesting to note that one is talking about some additional:

- 700 Nuclear Power Stations
- 650 Coal Mines
- 60 Liquefied Natural Gas Projects or similar developments
- 7 Oil fields of Nigeria's size plus a roughly equivalent amount of new supplementary recovery from existing reserves.
- 17% Energy conservation relative to 1973 consumption per unit of economic activity

Naturally the above is of an illustrative nature only but it is important to realise that lead times are long (ranging from say 5 to 12 years) and that a considerable effort in related infrastructure will also be required (coal terminals, unit trains, coal burning equipment in power stations, to mention but a few). Figure 3 illustrates what would happen if no action were taken in the field of non-oil energy and the savings assumed in the WIC scenario. Whilst it is physically possible to develop new energy supplies and to achieve the efficiency improvements a prolonged period of low growth would not be the best environment from which the necessary investment decisions could be taken and might give us other, perhaps more serious, difficulties to cope with.

The Energy Outlook - Some Conclusions.

The quantification of the exploratory scenarios was carried out by a detailed end-use analysis of the various energy-using sectors. The analysis has shown that, under all scenarios, future demand for energy is likely to grow more slowly than in the past. A retrospective breakdown of the results shows that there are three major reasons for this: lower economic growth, structural changes and saturation effects in the developed countries and improvements in end-use efficiency. The relative importance of these factors is illustrated with the total energy projections in Figure 4.

Whilst the energy intensive primary and secondary sectors of the industrialised countries move towards saturation, relatively faster growth in demand can be expected from the developing countries. Since these countries are not yet so tightly locked into an oil-consuming demand pattern, greater opportunities might exist here for exploiting alternative energy sources, particularly biomass, although it is unreasonable to suggest that they will not require large volumes of liquid fuels, particularly for transport and other preferred uses for energy liquids.

In summary, to return to the question posed in the introduction, as we see it the next energy crunch is either going to be a mirage or it might show itself as a series of mini crises. The future remains uncertain, the outcome remains scenario dependent, but then, as we said, scenarios carry the seeds of their own discontinuity and are therefore likely to pull towards each other. It is a near certainty that a rapid take-off in demand is likely to be followed by a rapid increase in the price of oil which in turn would slow down the world economy and means that the world is in an economic trap - it could be called the "new economic reality".

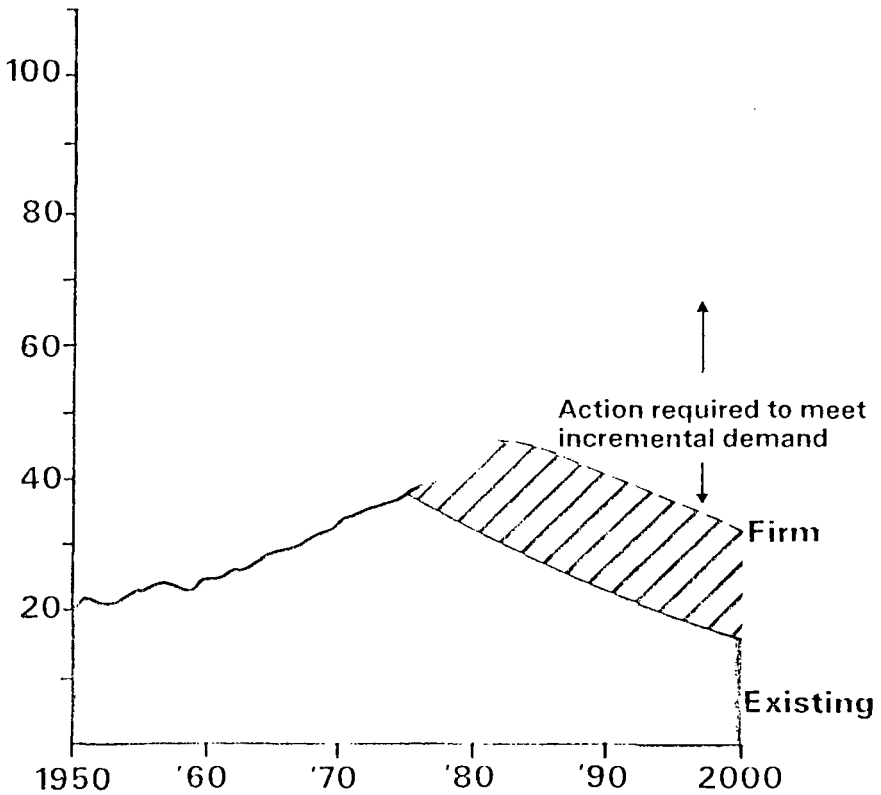
Thus the mirage represents a relatively smooth energy flight under a rather dull and gloomy (economic) sky. The mini crises seem like more of a bumpy ride, i.e. periods of sunshine (economic growth) followed by thunderstorms (oil price increases in real terms). Naturally, a political upset in the Middle East could disturb the delicately balanced oil supply and demand equation at any time. A sudden drop in the supply ceiling as a result of such a geopolitical scenario is hard to plan for but the emergency sharing scheme of the International Energy Agency has been designed to cope with such a contingency. Figure 5 is an attempt to illustrate these scenario conclusions.

To end with Aristotle again, which seems apposite, "knowledge springs from amazement, and amazement comes from an appreciation of contradictions".

FIGURE 3

**NON-OIL ENERGY PRODUCTION
REQUIRED IN WOCA
UNDER WIC CONDITIONS
(Under BE approximately 66% higher)**

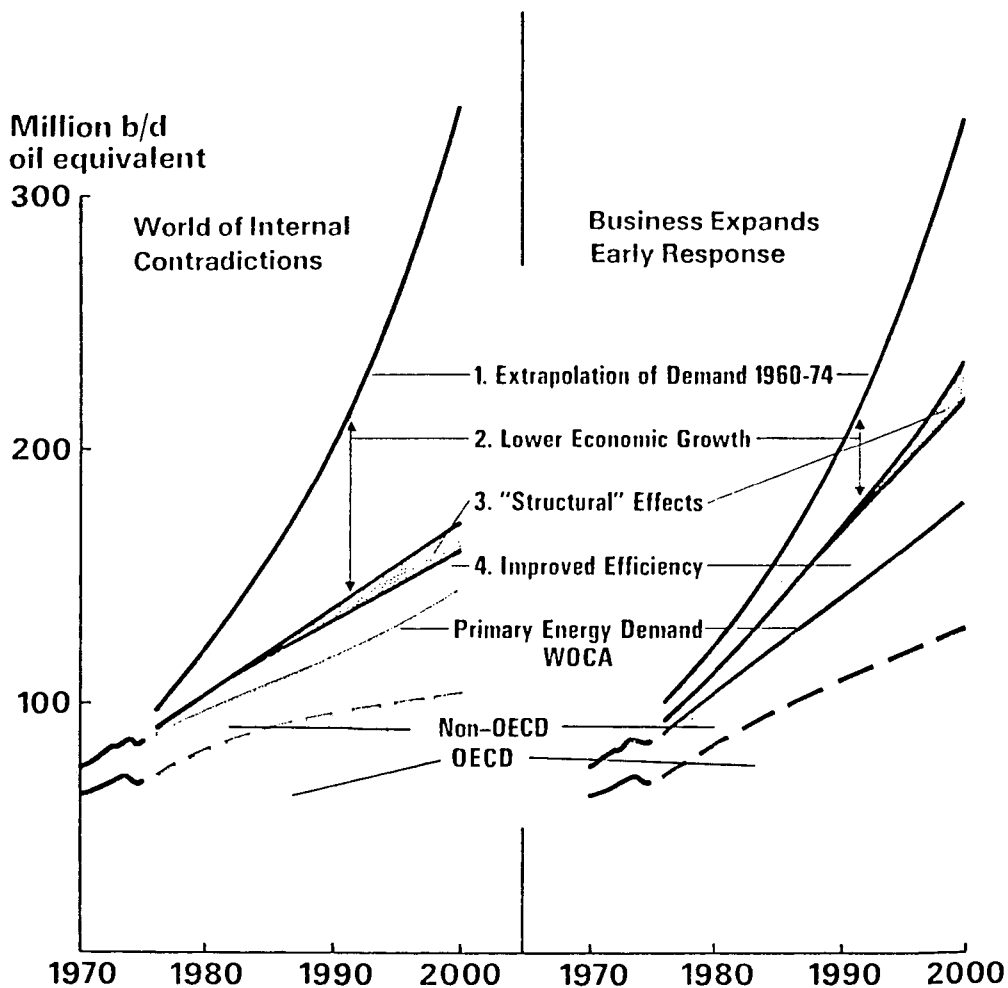
Million b d o.e.



n.b. The rate of decline of existing and new firm productive capacity has been calculated on the basis of historic depletion rates of coal and gas resources

FIGURE 4

WOCA PRIMARY ENERGY DEMAND



THE NEXT OIL CRISIS

OIL SUPPLY
OIL DEMAND



MIRAGE

As a result of low economic growth, reaction and pre-emptive action to avoid impending crises, oil supply ceiling remains above demand.



MINI CRISES

Demand hits the oil supply ceiling accompanied by price rise, fall in demand and subsequent repeat of cycle. Crisis made more critical by miscalculation of height of ceiling.

There is also the possibility that the supply ceiling may fall most likely as a result of a political accident.



FIGURE 5

FUTURE WORLD OIL PRICES

Kenneth L. Kince1

U.S. Department of Energy
12th & Pennsylvania St., N.W.
Washington, D.C. 20461

Introduction

This paper summarizes the major findings of an analysis prepared for the Office of Policy and Evaluation, U.S. Department of Energy. The purpose of the study was to delimit a range of world crude oil prices that might occur between now and 1990.¹

Unlike analyses of most physical systems, analyses of the international energy system are dominated by uncertainty. Two major sources of uncertainty dealt with in this analysis are the future level of OPEC production capacity and future rates of economic growth. Both of these factors affect the balance between supply and demand, hence the price, in the world oil market. In recognition of such uncertainties, the approach taken posits a range of assumptions for each of these factors.

Methodology

The world oil price projections, presented below, were derived from simulations involving four major analysis systems (see Figure 1):

- 1) The Oil Market Simulation model, which projects world crude oil supply, demand, and prices on a regional basis;
- 2) The Mid-Term Energy Market model (formerly the Project Independence Evaluation System, or PIES), which simulates domestic energy supply and demand and equilibrium prices for the various types of energy;
- 3) The International Energy Evaluation System, which is an international counterpart of the Mid-Term Energy Market model; and,
- 4) The Data Resources (DRI) model of the U.S. economy.

The analysis was initiated by making preliminary estimates of future world oil prices with the Oil Market Simulation (OMS) model. OMS is a reduced form, parametric representation of the world oil market. The model calculates a price of oil that will balance total world supplies with total world demands. These preliminary estimates indicated that even with moderate rates of economic growth, world oil prices might double, or even triple, by 1990.

The initial estimates were preliminary in the sense that they were derived using a calibration of the OMS model which was consistent with world oil price levels of around \$15 per barrel. In order to recalibrate elasticities in the OMS model to be consistent with much higher world oil prices, it was necessary to use the other three models to analyze the adjustments of energy supply and demand and economic activity to high oil price levels.

¹ The views and interpretations expressed in this paper are those of the author and do not necessarily reflect a position of the Department of Energy. For a more complete presentation of this analysis, see (1).

To gain further insight into this problem, it may be useful to follow the adjustments which occur in the OMS model if world oil supply and demand are not in equilibrium. When demand exceeds supply, consumers bid up the price of oil. As a result, the following three adjustments are set in motion:

- o An increase in the price of oil encourages an increase in the production of additional oil supplies;
- o An increase in the price of oil causes the quantity of oil demanded to decline and the demand for alternative energy forms to increase; and,
- o Increases in the price of oil adversely affect the rate of inflation and trade balance in countries dependent on oil imports which reduce their rate of economic growth. This decline in economic activity reduces both their total demand for energy and their demand for oil.

The magnitude and net effect of these adjustments vary not only from one region to another, but according to the magnitude and timing of the price increase. Thus, the Mid-Term Energy Market model and the DRI macroeconomic model were used to analyze the adjustments within the domestic energy system and the domestic economy to alternative world oil price trajectories. The International Energy Evaluation System was employed in a similar fashion to analyze the adjustment of foreign energy systems. These results provided the information necessary to recalibrate the OMS model.

Results

Two ranges of future world oil prices were projected with the OMS model based on two economic growth scenarios. Table 1 shows the range of economic growth rates used to define the optimistic and pessimistic growth scenarios. The optimistic growth rates are consistent with those reported in the Energy Information Administration's (EIA's) Annual Report to Congress (see 2, page 67). The pessimistic growth rates were arbitrarily assumed to be one percentage point lower.

For each economic growth scenario, ranges of world oil prices were determined by constraining the level of OPEC production capacity according to the optimistic and pessimistic estimates shown in Table 2. These estimates are also consistent with data reported in EIA's Annual Report, see (2, page 81), and suggest that development of Saudi Arabia's production potential presents the major uncertainty in this area.

Figure 2 illustrates the range of world oil prices projected for each economic growth scenario. In this figure and throughout this discussion, oil prices are expressed in 1978 dollars per barrel delivered to the East Coast of the United States. The upper end of each price range corresponds to the pessimistic estimate of OPEC capacity, 36.5 million barrels per day in 1990, whereas the lower end corresponds to the more optimistic estimate of 43.5 million barrels per day.

As shown in Table 3, the real price of oil could begin to rise as early as 1982 and reach the \$26-37 per barrel by 1990, if the optimistic growth scenario becomes a reality. Realization of the lower economic growth estimates could delay any real price increases until the 1985-1988 period with prices reaching \$16-21 per barrel range by 1990.

Conclusion

Based on the findings of this analysis, it is not unlikely the recent leveling off of real oil prices will come to an end in the next decade. Exactly when oil prices could

begin to rise in real terms and to what levels is highly uncertain. It must also be noted that although such increases are likely, they are not inevitable. A number of events, such as extensive energy conservation, accelerated development of new energy sources, or the adoption of aggressive energy policies in the United States and elsewhere could significantly delay another round of escalation in world oil prices. The potential effects of these and other factors are the subject of an ongoing analysis within the Energy Information Administration.

References

- (1) Energy Information Administration, An Evaluation of Future World Oil Prices, Analysis Memorandum AM/IA-78-05, June 1978.
- (2) Energy Information Administration, Annual Report to Congress, Volume II, DOE/EIA-003612, Washington, D.C., April 1978.

Table 1

Economic Growth Assumptions
(Average Annual Rates)

<u>Country or Region</u>	<u>1975-1985</u>		<u>1985-1990</u>	
	<u>Optimistic</u>	<u>Pessimistic</u>	<u>Optimistic</u>	<u>Pessimistic</u>
United States	4.2	3.2	3.1	2.1
Canada	4.2	3.2	3.1	2.1
Japan	5.6	4.6	5.6	4.6
OECD Europe	3.6	2.6	3.8	2.8
Australia/New Zealand	4.1	3.1	4.5	3.5
Developing Countries	6.6	5.6	6.2	5.2
OPEC	5.5	4.5	4.4	3.4

Table 2

Range of OPEC Production Capacities
(Millions of barrels per day)

<u>Country</u>	<u>1985</u>		<u>1990</u>	
	<u>Optimistic</u>	<u>Pessimistic</u>	<u>Optimistic</u>	<u>Pessimistic</u>
Saudi Arabia	12.0	10.0	17.0	12.0
Kuwait	3.0	3.0	4.3	3.0
United Arab Emirates	3.0	3.0	3.2	2.5
Other Arab OPEC	8.0	8.0	8.3	8.3
Other OPEC	<u>12.8</u>	<u>12.8</u>	<u>10.7</u>	<u>10.7</u>
Total OPEC	38.8	36.8	43.5	36.5

Table 3
Summary of World Oil Price Analysis

	<u>Year of Initial Price Increase</u>	<u>World Oil Price</u> ¹	
		<u>1985</u>	<u>1990</u>
<u>Optimistic Growth</u>			
Optimistic Capacity	1982	19.00	26.00
Pessimistic Capacity	1982	21.00	37.00
<u>Pessimistic Growth</u>			
Optimistic Capacity	1988	14.50	16.00
Pessimistic Capacity	1985	15.00	21.00

¹ Prices are stated in 1978 dollars per barrel, C.I.F. East Coast of the United States.

Figure 1
 Overview of Analysis Methodology

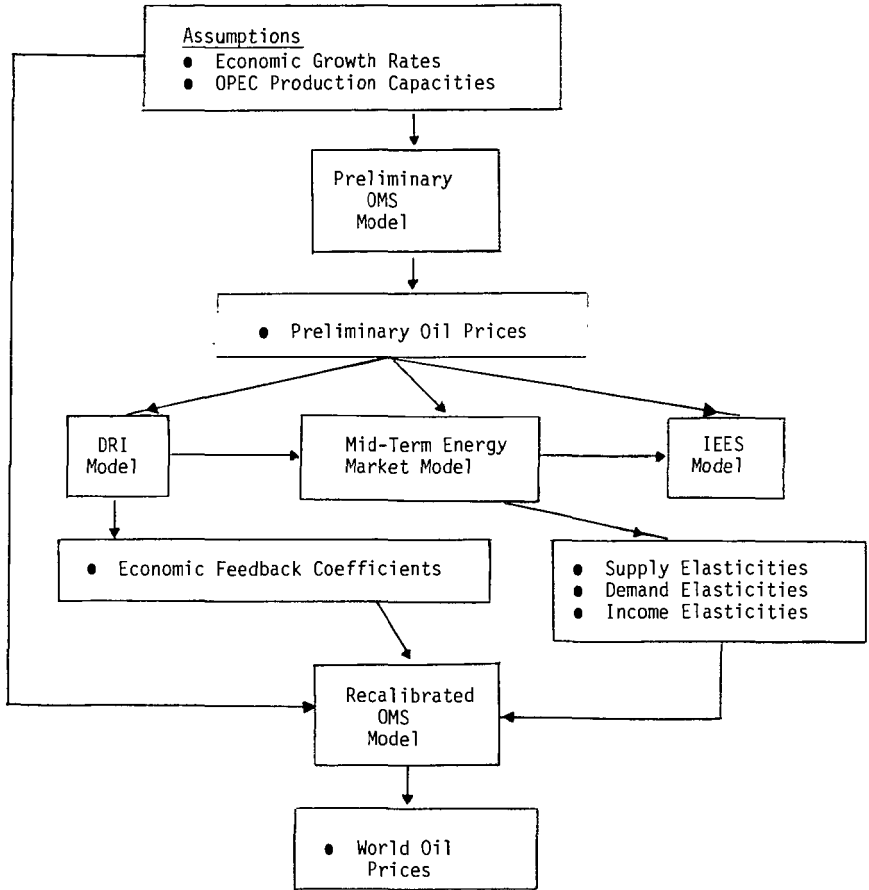
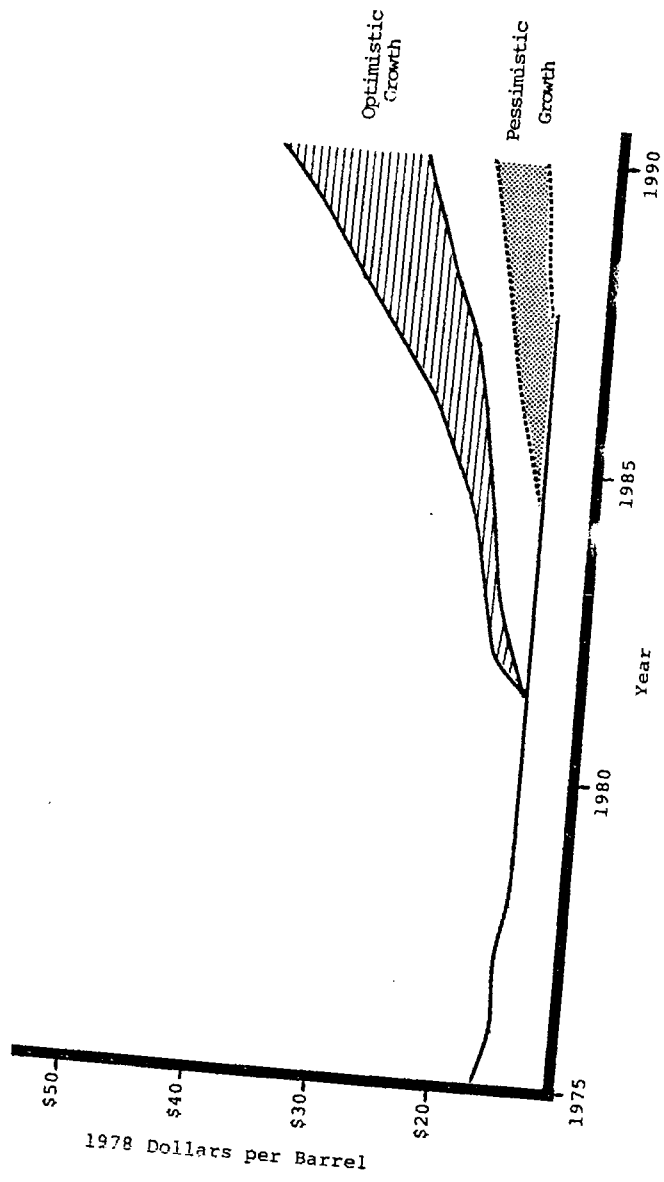


Figure 2
WORLD OIL PRICE PROJECTIONS



ABSTRACT - FUTURE OF NATURAL GAS, G. J. MacDonald. The MITRE Corporation, 1820 Dolley Madison Boulevard, McLean, Virginia 22102.

Some fraction of natural gas found in deposits not associated with petroleum may have an abiogenic origin with the gas produced by igneous activity or as a result of the outgassing of primeval hydrocarbons accumulated during the formation of the earth. Evidence for an abiogenic origin include the ratios of the stable isotopes of carbon and hydrogen in methane, temperatures deduced from isotopic ratios of coexisting methane and carbon dioxide and methane and water, the bulk chemical composition of the gas deposits, the age and geologic setting of the deposits, the presence of methane in volcanic emissions and hydrothermal gases and the accumulation of large quantities of methane in the cold waters of recent lakes in the volcanic regions of the East African Rift Zone. The possible existence of abiogenic methane could greatly alter estimates of the remaining economically recoverable natural gas. In the United States, major structural features that could trap gas of whatever origin have probably been discovered. However, difficult to discover, stratigraphic traps are known to exist and exploration for these would be aided by knowledge of the source of the methane. Abiogenic methane could be expected to accumulate, for example, in the vicinity of regions of igneous activity or near deep faults that penetrate basement rocks but that do not reach the surface. Such regions have not been favored in conventional exploration of hydrocarbons.

THE POTENTIAL CONTRIBUTION OF COAL TO WORLD ENERGY FUTURES

MR. LESLIE GRAINGER

NCB (IEA SERVICES) LTD., 14/15 LOWER GROSVENOR PLACE, LONDON SW1.

Introduction - IEA Coal Research

Since IEA Coal Research exists precisely to examine and develop the subject given in the title, this paper will mainly be devoted to describing the activities of that body.

The International Energy Agency was formed in 1974 by O.E.C.D. countries, in response to problems arising from discontinuities in the supply and price of oil at that time. One objective of the IEA was to encourage alternative to oil, especially through Research and Development programmes of a collaborative nature. The potential energy alternatives were divided into discrete technical fields; the U.K. was nominated the lead country for coal. Certain projects were initially proposed in 1975 and were each accepted by a sufficient number of countries to make a viable set of programmes. The principles behind these initial proposals have proved durable. The early progress of the work has already provided substantial new information, both technical and also about the methods by which countries can work together. This experience, assisted by the fact that IEA Coal Research is detached from immediate responsibilities within the coal industry and therefore in a more objective position, is allowing a clearer picture of the future world potential for coal to be developed progressively.

The IEA provide no central funds for the R & D groups and there were initially no administrative procedures of financial conventions. The only asset at the beginning was that most of the countries who had joined IEA through their mutual interest in the problems of oil dependence also perceived that coal provided a means of alleviating those problems and were willing to send representatives, generally without mandates however, to the early meetings of a Coal Working Group.

From the outset it seemed essential that the Working Group should sponsor one major "hardware" project. However, it also seemed that several questions needed to be answered if the IEA countries were to be influenced further in the direction of coal, both for long-term resource planning and for short and medium term R & D programming. It was proposed that this should be done by the establishment of "Service Projects" or office studies. The service projects and the questions they were designed to answer are:

- (a) Resources and Reserves. Is the coal really there? In circumstances making economic recovery plausible? Can output be greatly increased and the product made more widely available?
- (b) Mining Technology Clearing House. Is the technology for recovering coal adequate? Is the technology capable of developing in ways which will meet increasing stringencies in human and environmental
- (c) Technical Information Service. Is the coal industry fragmented and disunited or is it capable of co-operation in order to maximize the impact of developing technology on an international scale?
- (d) Economic Assessment Service. Will coal be economically competitive? How, when and where.

The hardware project chosen was Pressurised Fluidised Bed Combustion (PFB) at a total programme cost now expected to be in excess of \$40m. The annual cost of the Service projects described above is of the order of \$2m. An organisation, referred to here as IEA Coal Research, has been set up to carry out this work, to make further proposals and to exploit the achievements for policy guidance.

Resources and Reserves of Coal

The World Energy Conference (WEC) is the best current source of information on energy resources, since the different sources are discussed both separately in relation to each other and because such a wide spectrum of countries participate in a constructive manner. Thus, whatever uncertainties there may be in the data, the results and conclusions have a very important political validity.

The WEC Coal Resources Study was carried out by Peters and Schilling of Bergbau-Forschung, Germany; their results, which were not in any way challenged, are summarized in Table 1; Fig. 1 shows the planned coal production. "Technically and Economically Recoverable Reserves" are those which could be produced using current technology at a cost which would be economic at current prices. These reserves, defined on this stringent basis, represent only 6% of the total resource base but would nonetheless last for 250 years at current outputs. Only a small shift in prices, technology or in accuracy of exploration would be needed to transform a substantially further proportion of resources into the economic reserves category. Furthermore, the resource base itself is still expanding, as a result of increasing interest. Fig. 1 is based on output figures assessed mainly from plans stated by various countries. Line 1, which shows the annual output rising from 2.6b. tones to about 7.0 in 2020, could be achieved even if output were restricted to an operationally conservative level based only on present reserves. If the reserves were doubled, say by a small change in the economic base, line 3 reaching nearly 9.0b. could be achieved and sustained for a very long time. Thus, there can be little real doubt about the feasibility of a very large increase in coal production, so far as technical reserves are concerned. It should be noted that the increase, about 3% per year, follows the trend established over many decades. Producing countries expect to have about 10% of their output available for export. At some time, therefore, perhaps within two or three decades, coal will probably re-assume from oil its former leadership, both as a source of energy and as a form of traded energy.

IEA Coal Research, while welcoming these figures and not doubting their implications, felt that more information would be needed in support of this "second coming" of coal, especially in view of the very important decisions on which would be necessary for exploitation. It is noteworthy that the World Energy Conference is itself becoming more interested in improving coal assessment methods and that the United Nations is arranging a meeting early in 1979 to produce a common classification system as a prerequisite to a world assessment.

IEA Coal Research is linked to the data bank of the U.S. Geological Survey. Its immediate objectives are, first to compare different assessment systems and nomenclatures used in various countries, leading to a common synthesis, and, second to provide a preliminary catalogue of all known World coalfields. The first of these tasks is virtually complete and the second, covering more than 3000 deposits, should be completed early in 1979. It is already clear that there is no reason to believe that the WEC estimates are over-stated in total.

Aggregations compiled from disparate components do not form a suitable basis for national and international policy decisions, whether these are for investments in mining and utilisation within a single country or for multi-national planning which depends on trading, implying harmonious developments in the exporting and importing countries. The assessment of deposits requires study of the following factors, some of which are interlinked of course:

- (i) Existence: how much coal in total exists in the ground;
- (ii) Coal type; what sort of coal exists and what are its potential uses,
- (iii) Extractability: what proportion of the coal in the ground could be brought to the surface;
- (iv) Usefulness: what proportion of coal brought to the surface could be used;
- (v) Potential Cost: of bringing the coal to the ground;
- (vi) Potential Proceeds: of the coal so recovered;
- (vii) Accessibility: whether the coal is immediately accessible or whether some obstacle has to be removed first;

A proposed classification form based on these factors is given in Appendix 1. The definitions of accessibility are:

- (i) accessed by current working, or those for whose development capital expenditure has been committed;
- (ii) a) accessible to current technology within existing legal and environmental restraints and with existing infrastructure;
- and,
- b) coal which remains accessible in previously worked but abandoned areas;
- (iii) dependant for their exploitation on the provision of infrastructure (transport, housing, etc.);
- (iv) accessible only after some defined change in circumstances such as
 - a) removal of environmental prohibitions;
 - b) removal of other legal restraints (e.g.licenses);
 - c) the development of a new technology (e.g. underground gasification);

In the diagram the ratio of costs to proceeds, C/P, is used to provide a measure of economic viability and certain boundaries, at ratios of 1, 2, and 4, are suggested. The setting of these boundaries and the rules for the calculating C and P are difficult matters, which affect the categorisation of "reserves". These reserves may be thought of as being column A of the diagram, at accessibilities 1 down to 3 (including costs of infrastructure). It will be apparent that less knowledge is needed for the lower parts of the diagram.

Some conclusions which may be derived from these early attempts to develop assessment and classification system are:

1. In assessing potential coal recovery it is essential to consider the deposit as a whole and to understand the effect of progressive removal of seams.
2. There is little point in attempting to assess total coal in country or

in a particular deposit beyond the point of ensuring adequate supplies for the next 50 years.

3. It is desirable to establish the physical parameters of deposits to enable potentially recoverable coal to be related to current technology; it is also necessary to ensure that technical research and development is appropriate to its future context.
4. Any new modified system has to be based on the fact that, for the most part, operators generate the information they need and are only interested in wider assessments which benefit their activity. These wider assessments should help to steer the operator as well as national and international policy.
5. Coal is a wasting asset and continuation of the policy of taking first the best of what is left is only valid if the second best can or is likely to be recovered later, and if coal to be abandoned is adequately identified.

Mining Technology

This is not the place to explain detailed mining developments but it is important to emphasize the urgency now attached to this subject throughout the world. Substantial success has in fact already been achieved in practice but this is often over-looked, possibly due to adverse publicity over industrial relations. Coal mining technology is likely to be largely transformed over the next couple of decades, probably not through any revolutionary discovery but through an evolutionary procedure using information now available or well advanced in development and, most important, through investment. All this should make coal a more reliable energy source with more predictable costs.

This confidence has been enhanced by the studies so far carried out by the IEA Mining Technology Clearing House (MTCH). Mining research and development has expanded very rapidly recently - there are several times as many scientists and engineers engaged now compared with ten years ago. MTCH has catalogued over 2000 R & D projects in the eight co-operating countries alone and from this has developed critiques and overviews which should help in rationalisation and collaboration as well as suggesting lines for future emphasis. MTCH has boundaries with other IEA Coal Research work, for obvious being with Resources and Reserves. An example is that, since coal is a wasting asset, percentage recovery is becoming an increasingly important measure of efficiency. Monitoring recovery performance is a key function especially in relating recovery to the needs of economy and conservation now under the impact of changing extraction technology.

Mining technology is closely linked to transport and utilisation. In this connection, particular interest has been focussed on hydraulic mining and transport. This subject, and several others identified through the surveys are currently under consideration as possible co-operative "hardware" projects in mining technology.

Technical Information

A key function of the Technical Information Service (TIS) is the production of Coal Abstracts, a service which was previously greatly missed. A perusal of this journal, incidentally, quickly gives a clear impression of the tremendous current interest and activity in coal. All information is of course computerized, with international links. Besides the standard information service, including the preparation of a Coal Thesaurus, TIS provides, for organisations in member countries, an Enquiry Service and a Selective Dissemination of Information Service. In addition, a series of Special

Technical Reviews of key topics is being prepared; these will review all the available literature on the topic and provide constructive summaries and appraisals, suitable for non-experts but useful also to experts because of the comprehensiveness of the sources used. Reviews already issued include:

- a) Underground Transport in Coal Mines.
- b) Carbon Dioxide and the "Greenhouse Effect".
- c) Combustion of Low Grade Coal.

Topics under preparation or consideration include:

- a) Surface Transport of Coal.
- b) Loading and off-loading of Coal to/from Ships/Rail.
- c) Hot Gas Cleanup.
- d) Combustion of coal with control of Particulates and NOx.
- e) Methane Prediction in Coal Mines.
- f) Monitoring of Coal Quality.
- g) Conversion of Oil-fired Plants to Coal firing.
- H) Materials Problems During High Temperature Coal Conversion.
- i) High Temperature Gas Turbine.

The Review on Carbon Dioxide has been received with particular interest and this applies in general to other matters relating to environmental impact. It is believed that these questions are now of sufficient importance to merit more direct and original investigation than appropriate for TIS and proposals are being made for a separate Service to be established; this might benefit from association with other organisations.

Economic Assessment

This must be the central feature of any organisation studying the future contribution of coal. Even environmental factors have economic impact. The Economic Assessment Service (EAS) considers the cost and availability of coal, its transport and its utilisation, in relation of course to alternatives and different timescales, under the following main headings:

- a) Economic and Technical Criteria for Coal Utilisation Plant.
- b) Technical and Economic Factors Associated with Effluent Disposal.
- c) Cost and Availability of Coal.
- d) Transport of Coal.
- e) Coal Conversion Economics.
- f) Costs of Coal Conversion Plant.
- g) Fuel Costs and Demand for Coal.

h) Relative Costs of Coal Based Energy.

Although the conversion of coal into gases and liquids, including feedstocks, is of great importance, combustion is likely to remain the most important outlet for sometime. Accordingly, under (h) above, attention has so far been focussed on:

- (i) The competitive position of coal in electricity generation .
- (ii) The competitive position of coal in direct heating for industry.
- (iii) The competitive merits of gas vs. electricity vs. direct coal heating in industry.

Item (i) is particular importance, especially in view of discussion surrounding the future of nuclear power. In economic comparisons between coal and nuclear power, there remain substantial uncertainties and areas reflecting judgement or policies. In the case of nuclear power, reports of capital cost vary considerably and fuel costs are also uncertain partly due to uranium resources but also because the fuel cycle has not been closed. In the case of coal, flue-gas desulphurisation (FGD), if needed, may amount to 20% of total plant costs. Finally, interest rates and projections of future real costs are dominant but subjective items and results also depend crucially on load factor. The resulting comparisons are therefore quite complicated and the various nuclear and coal cases overlap substantially. In the U.K., however, at present it is considered that if a "medium cost" nuclear case is compared with coal based generation without FGD (not required at present or projected) the breakeven price of coal would be £1.2/GJ. If 100% FGD were required, the breakeven price would be £0.81/GJ (current British price £0.95). Another comparison, on British data, makes the assumption that nuclear capital costs will stabilise either at present levels ("medium") or at 25% higher ("high") and calculates the maximum real annual coal cost inflation which could be suffered for coal to remain competitive. The results are:

100%FGD/medium nuclear	Not competitive
100%FGD/high nuclear	2.2%
No FGD/medium nuclear	2.5%
No FGD/high nuclear	5.3%

In the U.K. such annual rates of coal costs increase do not seem credible, in the light of current investment, nor can 100% FGD be regarded as at all likely. Each country will have its own attitude to FGD but the effect that this has had on the breakeven coal cost - a reduction by one-third, say - should be borne in mind when assessing any benefits from sulphur suppression especially to very low levels.

These studies have now also considered the economic impact of the introduction of Fast Breeder Reactors. At this stage it is very difficult to see how the FBR can be justified even in comparison with thermal reactors without making assumptions which are either incredible with regard to the growth of nuclear electricity or which make thermal reactors themselves much less attractive.

Perhaps more directly relevant, at least to IEA Coal Research, a preliminary assessment has been made of the comparison between conventional coal generating costs (with FGD) and fluidised combustors both atmospheric (AFB) and pressurized (PFB). The first results, expected as percentage savings in electricity cost are:

PERCENTAGE SAVINGS IN ELECTRICITY COSTS

Coal Price	High Sulphur		Low Sulphur	
	AFB	PFB	AFB	PFB
£1/GJ	13-15%	7-8%	4-3%	3-4%
£2/GJ	12-14%	9%	4-3%	4-5%
£3/GJ	11-13%	10%	4-3%	4-6%
OVERALL	11-15%	7-10%	4-3%	3-6%

The main "hardware" project of IEA Coal Research is an experimental unit based on PFB. This project has been described elsewhere. It is expected to be commissioned in the early Spring of 1979 and has initially a two year programme of work mainly on combustion factors, with particular attention to the quality of off-gases for direct use in turbines. Proposals for adding a gas turbine, which would effectively convert the test equipment into a pilot plant, are being considered. The earliest that this could be completed is about the end of 1981 which probably corresponds to the need to complete the basic combustion programme first.

The preliminary economic assessment quoted above, whilst showing reasonable potential for fluidised combustion power generation where FGD must be practiced on high sulphur coals do not show much saving with low sulphur or any advantage for PFB over AFB. This obviously calls for collaboration between the technical and economic studies. Apart from better engineering to reduce capital costs, from which the more complex system should benefit most, consideration will have to be given to other ways in which the competitiveness of PFB can be increased initially as a guide to further experimentation. In the calculations above, PFB, is taken as having only 3 percentage points advantage in thermal efficiency over AFB. Clearly if this can be increased, so will the economic benefit and this would be compounded by fuel price increase. Thus, great emphasis must be put on thermal efficiency, which is most likely to be increased by higher temperatures. In addition, the system itself will need further examination, including continuous reconsideration of the duty of PFB, in conjunction with other processes and within the broader study of energy flows.

Similar studies to those described above on combustion will be required on other coal conversion processes and these are in hand by EAS, as are combinations of processes (Coalplexes). Coalplexes, intermediates may be transferred and more than one product is available. It is likely that hydrogen costs will be a key factor in economic studies in the future, not only for coal but for the whole family of fossil fuels. This has led to suggestions of a sequential use of hydrocarbons and this may result in separation procedures as an initial step in coal processing, in order to recover fractions having a higher hydrogen content or small molecular size; the residues could be gasified and/or combusted. Obviously, the development of more elegant utilisation systems for coal will require re-optimisation of quality requirement for mining and preparation of transport methods.

Conclusions and Predictions

The resources of coal are very large indeed, so large that the rate at which the world decides to exploit them is a matter of choice based on economics and investment policies, rather than resource constraints. It seems highly probable that output will be increased several-fold over the next few decades, without the danger of a sharp peak followed by a rapid decline which may occur in the case of oil and gas. Coal is fairly well distributed and is readily transportable and storable, so that trading should become much more important in the wake of oil. Practically all countries should therefore seriously consider their policies for coal and most would benefit by doing so through international collaboration. Countries possessing ample coal may need capital to make large investments in developing these resources; potential importers need to invest in handling and utilisation equipment. Coal may be transported as such or converted into coal products in the producing countries and the merits the alternatives need careful consideration on a case-by-case basis. Partnerships between producers and users should therefore be formed at an early stage and a wide range of options involving current and future processes considered.

The understanding of how to get and how to use coal is developing progressively. Within individual countries a new approach to mining and distribution is necessary. Hydraulic mining and transport, for example could help to separate mining from its traditional environmental impact and might also provide flexibility in the location of energy conversion and consumption centres. Utilisation patterns will certainly change sequentially, in timescales which may be consistent both with the peaking and run-down of other hydrocarbons and also sequence from low to high value uses will be based on adding more hydrogen which will increasingly be derived from coal.

The development and economic progress of new coal conversion processes will call for re-optimisation of all the stages in getting, preparing and using coal including schemes where the more valuable portions are removed before the residue is used for the crude outlets. Envisaging the complex nature of the coal industry in the next century is perhaps more difficult than trying to see the modern petroleum industry from its origins at Titusville might have been. Still, it should be attempted now and progressively updated.

For the present however the most important outlet for coal is combustion. For electricity generation coal is likely to continue to compete successfully and will become very important for direct heating. Fluidised Combustion, in various forms, will be the main contributing technological factor.

All countries will be affected by the optimal use of coal will all benefit from the extension of collaborative arrangements. IEA Coal Research has demonstrated some ways in which this collaboration might progress.

Hard Coal (bituminous coal and anthracite)

Continent	Geological resources		Technically and economically recoverable reserves	
	in 10 ⁶ t. c. e.	percentage	in 10 ⁶ t. c. e.	percentage
Africa	172 714	2	34 033	7
America	1 308 541	17	126 839	26
Asia	5 494 025	71	219 226	44
Australia	213 890	3	18 164	4
Europe	535 664	7	94 210	19
Total	7 724 834	100	492 472	100

Brown Coal (subbituminous coal and lignite)

Continent	Geological resources		Technically and economically recoverable reserves	
	in 10 ⁶ t. c. e.	percentage	in 10 ⁶ t. c. e.	percentage
Africa	190	--	90	--
America	1 408 838	59	71 081	49
Asia	887 127	37	29 626	21
Australia	49 034	2	9 333	7
Europe	55 241	2	33 762	23
Total	2 400 430	100	143 992	100

Total

Hard Coal	7 724 834	76	492 472	77
Brown Coal	2 400 430	24	143 992	23
Gesamt	10 125 264	100	636 364	100

Table 1: The Distribution of World Coal Resources, grouped by Continents

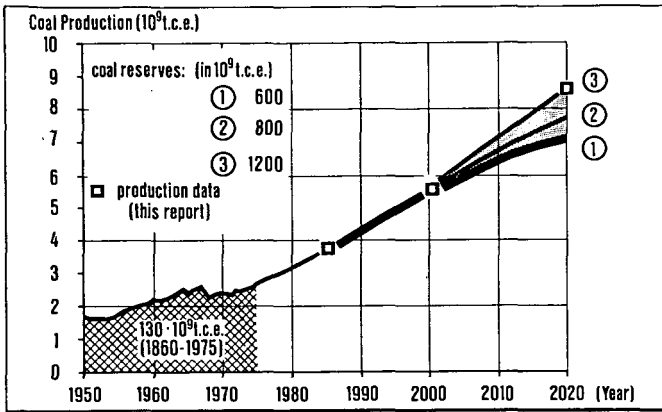


Fig. 1: Future Trend in World Coal Production, based on Different Amounts of Coal Reserves

MAIN CLASSIFICATION

Date of assessment.....

Coal type.....

Location.....

Decreasing
accessibility

Decreasing
economic viability



tonnes x 10⁹



Access Category		Assurance Bracket	Economic Category			
			Coal recoverable at:-			D Coal in place
			A C/P ≤ 1	B C/P ≤ 2	C C/P ≤ 4	
1	1. Accessed	most likely maximum minimum				
2	2. Accessible	most likely maximum minimum				
(a)	Total of 1 & 2	most likely maximum minimum				
3	Accessible after provision of infrastructure	most likely maximum minimum				
(b)	Total of 1, 2 and 3	most likely maximum minimum				
4	Accessible subject to other conditions	most likely maximum minimum	X			
(c)	Total of 1-4	most likely maximum minimum				
5	Inaccessible	most likely maximum minimum				
(d)	Total 1-5	most likely maximum minimum				

- Notes:
1. Economic category A is included within B, B within C and so on.
 2. Access categories 1 to 5 are separate from one another and do not include one another.
 3. The most usual view of 'reserves' - currently economic accessible coal - is represented in Column A, line (a).
 4. Coal in place (Column D) may be limited by excluding coal below a given thickness or depth, varying from country to country. Such limits will be recorded.

JAPANESE ENERGY OUTLOOK AND INTERNATIONAL COOPERATION

Masao Sakisaka
President
National Institute for Research Advancement

1. Formation of a High-Energy-Consumption Type Economy

It was after the 1960s that the Japanese economy has become that of high-energy-consumption type. The volume of energy consumed during fifteen years up to 1975 far exceeded the volume consumed ever since the beginning of Meiji Era up to 1960. Average annual per capita energy consumption during the recent five years was about 4.5 times that in the period prior to World War II. The transition of the economy to that of high-energy-consumption type coincided with the shift of energy from hydraulic power and coal to petroleum.

Energy consumption grew during the 1960s by an average annual rate of 13%. In Japan technological innovation bloomed in the 1960s. Materials industry such as metals, chemicals, and synthetic textile developed modern mass production systems. And mass assembling industry such as automobiles and home use electric appliances developed based on the supply of such materials of a good quality for a low price. Consumers durables rapidly saturated homes, and "throwaway" became a common place. Equipment investments increased in industries, and public investments such as roads and highways and ports and harbors also increased. Heavy and chemical industries was much developed, and the economy grew rapidly. An "affluent society of mass production and mass consumption" was formed.

2. Fragility of Energy Supply Base

This "affluent society" is a grand house built on petroleum. Demand for primary energy expanded from the 95 million tons of 1960 to 284 million tons in 1970, and 87% of this increase was supplied by petroleum--almost all imported.

When rapid economy growth began in Japan under technological innovation, rapid increase in petroleum production began in Middle East and Africa. International oil companies raced to increase their market shares and reduce the price of petroleum. OECD could not stop it. The world entered into an oil age. The Japanese economy took full advantage of low-priced petroleum

supply. But since the beginning of 1970, the international petroleum situation largely changed. Due to worldwide expansion in petroleum consumption, the demand and supply of petroleum became tight. The position of OPEC was strengthened, and nationalism rose in oil producing countries where the government intensified controls over their petroleum resources. The era of abundant supply of low-priced oil ended, and the world entered the era of high-priced oil.

3. Change in Growth Pattern and The Decline of Energy Elasticity

At the time the world's oil situation changed, the pattern of Japanese economic growth also changed. Since the beginning of the 1970s increase in private equipment investments slowed down because new technology had been introduced into all sectors, environmental destruction had advanced, and the spread of consumers durables slowed down. Metals, chemicals, and other materials production increase slowed down. Such growth pattern change and industrial structure change naturally affected energy consumption. And this tendency was accelerated by the energy price hike and economic stagnation since the oil crisis of the fall of 1973.

A review of energy consumption in relation to GNP indicates that consumption in the industrial purposes had been on the decline while that for household purposes had consistently increased. Energy consumption for transportation purposes remained little changed since the 1960s. The ratio of household consumption of energy to total consumption was still too small to cover in full the decline in industrial consumption, and energy elasticity to GNP had declined.

4. Future Economic Growth and Energy Consumption

Japanese economy will need to grow by about 6% annually in order to sustain full employment, to accomplish fuller social security, and to develop public facilities. And it is believed that the economy would have that much of potentiality provided that there would be no limit on energy supply. It will be 0.9 in consideration of the elasticity during the period from 1970 through 1976, future recovery of equipment investment rate, and the estimate (0.91) under the New Energy Plan of the Government of West Germany, energy demand under economic growth of about 6% will be 660 million KL in 1985. Conservation of energy can depress the demand to less than the indicated. If 5.5% saving is achieved, demand will be 625 million KL in 1985.

5. Continuously High Future Reliance on Petroleum

Policy for stable energy supply is conceived of in the direction as indicated below.

- (1) Domestic resources will be exploited as much as possible.
- (2) Development of nuclear power generation will be propelled at social consensus, while making efforts to increase its safety and reliability.
- (3) Of imported energy, the utilization of natural gas and coal will be expanded.
- (4) While reducing reliance on imported petroleum through the above listed measures, petroleum supply source will be diversified.

The possibility of Japan's domestic resources exploitation is low. Also, the development of nuclear power generation will proceed only slowly due to citizens' movement against nuclear power generation. The government inevitably will lower the previous development target of 49,000 MWe by 1985 to 26,000 MWe. Even if smooth operation of these nuclear power plants is assumed, the total volume of energy supplied from domestic sources, including such plants, will be only about 84 million KL (in terms of petroleum).

Therefore, an overwhelming portion of energy demand will have to depend on imports. In order to diversify imported energy, the potential was estimated under the policy that the importation of natural gas (liquidified) and coal will be increased as much as possible.

The total potential supply volume of energies other than petroleum, as discussed in the above, is only 195 million KL (in terms of petroleum), and the balance must depend on imported petroleum. Assuming that 5.5% conservation will be accomplished by 1985, said energy demand will be 625 million KL, which means that 430 million KL (or from 7.4 million barrels per day) of petroleum will have to be imported.

If economic growth of about 6% is to be sustained, continuously greater amounts of petroleum will have to be imported. Even if the source is diversified to China and Indonesia, and overwhelmingly large portion of import will have to come from Middle East. In view of the political instability in Middle East, the energy base of the Japanese economy is extremely fragile.

6. World Limit to Oil Production

Petroleum experts believe that the petroleum production of the world (excluding communist countries) will reach its peak in the first half of the 1990s and will subsequently continue to decline. Main reasons for this are deterioration of discovery rate (new Petroleum fields) and the preservation policy of oil producing country governments.

Discover rate will drop due to the worsening of natural conditions, rise in development costs, decline in investment potentials of international oil companies and national companies. Gap between increasing production volume and discovery rate will open in the shape of scissors,

Long Term Projection of Energy Demand and Supply Balance

Fiscal Year	(Unit)	F.Y. 1975		F.Y. 1985	
		Actual		Projection	
Demand of Energy before Conservation	M.KL			660	
% of Reduction of Energy Demand by Conservation	%			5.5	
Energy Demand after Conservation	M.KL	390		625	
Type of Primary Energy	M.KW	Actual	%	Estimate	%
Hydro General	M.KW	17.80	5.7	19.50	3.7
Electric Pumped storage	M.KW	7.10		19.50	
Geothermal	M.KW	0.05	0.0	0.50	0.1
Domestic Oil Natural Gas	M.KL	3.50	0.9	8.00	1.3
Domestic Coal	M.TON	18.60	3.4	20.00	2.2
Nuclear	M.KW	6.62	1.7	26.00	6.1
Imported LNG	M.TON	5.06	1.8	24.00	5.5
Imported Coal (steam coal)	M.TON	62.34 (0.50)	13.1	93.00 (6.00)	12.0
Sub Total	M.KL	104.00	26.7	195.00	31.2
Imported Oil	M.KL	286.00	73.3	430.00	68.8
Grand Total	M.KL	390	100	625	100

causing reductions in the volume of proven deposits. When production reserve ratio (R/P) declines to a certain level (10-15), production increase reaches its limit. This is the physical limit of petroleum production increase.

On the other hand, it is doubtful if all oil countries will continue to produce petroleum at the maximum production rate. While countries whose economic developmental potentials are high (Iran, Iraq, Algeria, etc.) will need to increase their revenue by increasing oil production, oil countries of Arabian Peninsula will adopt policy to restrict the volume of oil production due to their excessive revenue from oil, as has already been done by Kuwait and the United Arab Emirates and will eventually be done by Saudi Arabia, the country of world's greatest petroleum resource. When Saudi Arabia curbs the production, oil production of the world will begin to shrink. It is highly possible that the transition from production increase to production decline will take place often the latter half of the 1980s.

If OECD countries fail to conserve on energy and to develop and to expand the utilization of a substitute energy by the time of this transition, but increase demand for OPEC oil, the world will suffer from an oil shortage. Industrial nations will fight each other for securing oil (in which USSR will join), and the price of oil will surely rise and the world politics and economy will be hurt substantially.

The lead time for energy conservation and the successful development of a substitute energy is from ten to fifteen years. Unless OECD countries establish a goal for reduced petroleum consumption in the future and immediately intensify their policy efforts for the energy conservation and substitution of petroleum chronic shortage of petroleum will be inevitable. And if this situation is not avoided, non-oil producing developing nations will be hurt seriously.

OUTLOOK ON COAL RESOURCES AND COAL MINING TECHNOLOGY. R. Yamamura.
Coal Mining Research Centre, Kanda Jinbocho 2-10, Chiyoda-ku, Tokyo, Japan

Since the end of the nineteenth century Japan has spent a great effort to the development of industries and made a splendid achievement in it. During this period, the coal mining industry had exploited coal mines in all parts of the country, and produced about 2.5 billion tons of coal for the use as the foundation of the development.

Japanese coal is geologically of Paleogene period of Cenozoic era. Being located at the edge of the Continent of Asia, it was subject to the influence of the orogenic movements which resulted in that, a wide range of coal varying from lignite to anthracite is available in Japan owing to the accelerated coalification, while the state of mines is worse than many other countries due to the geological deformation.

However, the difficulties in coal mining have been overcome to a considerable extent through the accomplishment of the advanced systems of the technologies for all mechanized long-wall mining, hydraulic mining, under-sea mining and centered control of mine safety, etc.

In order to meet the future global energy demand, the exploitation of the huge amount of coal resources in the countries around the Pacific is becoming important. Japan, as a member country with its energy being largely dependent on importation, is eager to cooperate with them by offering its mining technologies as well as its mine management knowledges.

GEOPOLITICAL ASPECTS OF NEW OIL:
THE SEARCH FOR ADEQUATE AND CONTINUOUS SUPPLY

Melvin A. Conant

CONANT AND ASSOCIATES, INC.
9901 Phoenix Lane
Great Falls, Virginia 22066

However much energy forecasts vary, depending upon a large number of economical, geological, technical, and political assumptions, there is widespread agreement on certain trends. These are 1) if the industrial world experiences, over the next decade, a better-than-recent average economic growth rate of 4-4.5% and 2) if the energy consumption growth rate is nearly comparable, then the world community of nations will almost assuredly be competing intensely for oil in world trade. And if, as we have been warned will occur, the U.S.S.R. is included among these nations, there will then be an even greater increase in oil prices as a result of a chronic shortage of oil. For many importing states, the general condition will be one of an inability to compete with a few large energy consumers while coping with major social, economical, and political issues, and a lack of available alternative energy sources. Finally, underlying all these concerns will be the importance of Middle East supply as the major source of oil in world trade.

Dependence upon Middle East sources for a very high proportion of oil in world trade appears to be one of the "constants" in energy equations. Possessing today some 60% of proven and probable reserves, the Middle East may well remain the most prolific source of international oil through our lifetime. The Middle East today supplies the U.S. with nearly 50% of its oil imports (crude and products), approximately 80% of West Europe's import requirements, and 77% of Japan's. From nowhere else comes such a profusion of oil; there are no other truly giant conventional petroleum deposits (it is possible that Mexico's deposits could rival those of the Mid-East but the information is presently too incomplete).

Obviously, Middle East supply brings with it serious and mounting concerns. As long as it remains such an important source of world oil, we will have to accept that it is a commodity which is plagued by risks of continuing political instability whose origins are very deep in history; it is by no means summed up only in the Arab-Israeli dispute. We must understand that we are dealing with ancient rivalries derived from cultural, religious, and economic differences between the peoples of the Nile and the Fertile Crescent of the Tigris and Euphrates and between the Muslim peoples of the Arab world and those of Persia.

The contemporary usage of "Lebanon," "Syria," "Iraq," "Jordan," the "United Arab Republic" (Egypt), "Iran" (Persia), "Saudi Arabia," and "Israel," which implies nation-states of a form familiar to the Western world, misleads us again and again. Regardless of the modern names, we are still witnessing the break-up of one of the great imperial systems -- the Ottoman Empire. This fragmenting process is made infinitely more complex by the strategic importance of oil to the industrial world, and by the intervention of western powers into the affairs of the region.

The point should be clear that access to Middle East oil will always be inextricably bound to the prevailing political trends; it will not be expressed in relatively simple, commercial terms. The combination of these factors lends great urgency to the task of reducing dependence upon the region, by diversifying our sources of oil and encouraging the rapid development of non-conventional petroleum deposits (shale, tar sands, and the so-called "heavy" oils) and of alternatives to oil itself. Of all these courses of action, the search and exploitation of new deposits of crude are tasks which can be undertaken with minimum delay as the technology of exploration exists: we can lay the pipe, we have the tankers and the refineries already.

In order to minimize the "geopolitics" of oil, by decreasing one's dependence upon a single, politically sensitive area, one must take into consideration the number of factors which would contribute to easy access to oil. These would be seeking out regions for exploration which are 1) controlled by non-Communist countries; 2) distant from the Middle East; 3) dependent upon earnings from oil; 4) within a comparatively short distance from the commercial markets; 5) areas whose political objectives are such as to find them not part of any cohesive bloc; and finally, 6) regions whose reserves are of such magnitude that they would be useful alternatives to a reasonable proportion of Middle East supply.

In the case of Japan, for example, the most obvious "zones" of interest would center upon the prospective regions of offshore South East Asia, Indonesia, and the South China Sea. Others would be China (a future possibility), the Soviet East Siberian and Sakhalin fields (also a future possibility), Alaska, the Canadian Arctic, and Alberta (the last named Canadian sources being of considerable interest at the present time). Another Japanese security zone for alternatives to Middle East oil would also, surely, include some exports from Mexico and, eventually, from the Venezuelan Orinoco region.

By how much would Japan have to reduce its Middle East dependence to gain added security? Today, Japan imports a total of about 5 MMB/D; of that, 3.5 MMB/D come from the Gulf proper. The volumetric flow will increase, assuredly, with time. But if Japan had in existence a substantial strategic petroleum reserve (perhaps in the order of four months total imports, or 600 MM barrels) over and above an increased commercial inventory and were also fortunate enough to obtain perhaps 1.5-2 MMB/D from other zones, the problem of oil supply security for Japan might be manageable.

The United States is in a different situation. Faced with the prospect of declining onshore reserves and an uncertain amount of additional offshore oil, its present 50% dependence upon oil imports -- approximately 8 MMB/D (3 MMB/D than Japan's total imports) -- compels it to examine oil supply zones less vulnerable to disruption than the Middle East. An inner and primary zone would include Venezuela, Mexico, and Canada. Others, more greatly dispersed, would be Nigeria, the polar latitudes, and the Falkland-Argentine shelf.

The Orinoco Valley belt in Venezuela is still thought to contain one of the most extensive sources of oil with some 700 billion barrels of oil (perhaps 70 billion barrels recoverable by the application of known techniques). A conservative billion barrel estimate of Mexico's oil is 12 billion barrels "proven," 30 billion barrels "proven and probable," and 60 billion barrels "in place." The Canadian "heavy" oil and tar sands are, potentially, of comparable significance: possibly 954 billion barrels of oil, from which some 27 billion barrels could be put in the market using present day techniques.

The overlap of Japanese and U.S. oil security zones need be of no concern; the successful development of the great unexploited regions of Alberta, the Canadian Arctic, Mexico, and Venezuela would make available to the industrial world an additional volume of substantial size which would, in time, diminish the strategic significance of Middle East Oil.

These reserves are known to exist. We may not, at present, be fully cognizant of the necessary technology to exploit these diverse reserves, nor have the required funds, nor be sure of whether the various interested governments will use every incentive to encourage their exploitation. But the oil is there -- it does not have to be discovered.

Perhaps the greatest unknown is the political aspect, the extent to which government policy may encourage or inhibit exploitation. For example, current Canadian estimates warn, despite the enormous amounts of oil in the tar sands, and the existing heavy oil, that Canadian production is to decline (1978: 565 MMB/D; 1985: 282 MMB/D; and 1990: 221 MMB/D) while demand increases (1978: 687 MMB/D to 1990: 836 MMB/D). Is this to be the case?

Although none of these zones, from the Japanese, U.S., or the rest of the industrial world's perspective, is going to be developed soon, the launching of a major effort to exploit these resources would be an important signal to OPEC generally -- and to OAPEC in particular.

Thinking in these terms, one is reminded that the U.S. possesses a truly extraordinary oil resource whose extraction may prove to be not much more difficult than that of the deposits of Venezuela's Orinoco. The total oil in place in the U.S. oil shale deposits is

estimated at 2 trillion barrels, of which 80 billion may be recoverable with current techniques. (Estimated production for 1980: 100 MB/D; for 1985: 400 MB/D, all based on present levels of commitment.) Apart from capital and technical problems, however, the successful exploitation of these shale deposits is made more difficult through other conflicting interests, such as environmental impacts on the surrounding regions, the diversion of scarce water supply, conflicts of jurisdiction and purpose between the Federal government and state governments and also between various agencies within the Federal government itself.

With all these complications, the present judgment is that, as vast as the shale deposits are, we are less likely to develop them as assiduously as we would the resources of other countries -- barring a shock similar to the 1973-74 Arab embargo. Yet it is this vast domestic resource (plus, of course enormous coal deposits) which makes the crucial difference between the U.S. and Japan.

Another factor which one must take into account in attempting to reduce dependence upon Middle East oil is the still largely unknown effects of enhanced recovery techniques -- prolonging the life of oil fields, thus permitting a greater volume of oil to be produced. It is the unique contribution of chemists, chemical and petroleum engineers, and geologists which has accomplished some of the task. There is hope that they may be able to make even greater strides in the area of enhanced recovery techniques. For example, the usual estimate for the extraction of oil without the employment of such recovery techniques is about 25%. As a general rule, the employment of secondary techniques (injection of water, gas) and the wider use of tertiary techniques (injection of heat and/or chemicals) may increase the amount of recoverable to 32%. It is possible that these techniques could increase the volume of oil from known reserves world-wide by as much as 250,000 MMB, thereby significantly prolonging their useful life.¹ There is every reason to believe that such techniques, applied under similar conditions, would also increase the overall yield of new oil reserves.

Confounding many of our hopes for limiting reliance upon the Middle East and increasing oil in world trade from other sources is the too-infrequently discussed subject of the "finding rate" for new oil. The brutal fact is that for the last thirty years -- outside the Middle East and the Soviet Union -- we do not believe there has been discovered a single proven or probable reserve of more than 25 billion barrels. Neither Libya, Nigeria, Alaska, the North Sea, nor Mexico qualify as exceeding that level. Yet, if we are to preserve a reserve-production ratio of 10:1 (and some now advocate a more conservative ratio of 15:1) a discovery of such magnitude will be required annually -- the discovery of two North Slopes, if you prefer.

¹See Andrew R. Flower, "World Oil Production, Scientific American, March 1978, pp. 42 and 44.

Other views which divert us from a prudent thinking-through of oil supply problems are the classical economists' theory of supply always meeting demand, or that OPEC states will always be willing to produce enough oil for their "customers," or simply that oil has always been found when needed and will still continue to do so. The naivete of these views has yet to be appreciated.

The assumption that supply will meet demand for economic reasons ignores some of the realities of our crucial dependence on oil. It does not consider that in time of chronic shortage, a number of nations may both be unable to pay escalating costs for oil and, for reasons of their oil-dependent economies, be unable to go below a certain level of supply without risking an economic disaster, with severest social and political consequences. Wars have been fought over scarce resources. The "law" of the market place is not always one, when applied, that is accepted peacefully by all involved.

The argument found in so many forecasts of "OPEC Supply Required to Balance" should be banished from our midst unless qualified by the word "desired" for "required." We believe we have in Saudi Arabia an interesting and instructive example of why an oil exporter may find it to be in its own long term interest not to produce at levels desired or even required by oil consumers: it is wasting an irreplaceable asset; oil left in the ground is virtually certain to increase in value over time. If exported, the revenues from today's sales cannot be fully employed, so the surplus is invested in overseas markets whose ups and downs, combined with the erosion worked by inflation, warn of further losses.

There is a pernicious belief that the producing states are economic animals certain to pursue rational, economic goals (as defined by western, industrial states). Hence security and maximum supply can be taken for granted; if, in the passion of a moment, states should act irrationally, they soon come to their senses. It is a line of reasoning which should be re-examined.

Most curious of all is the near-religious conviction that undiscovered reserves of oil are vast and will be discovered in time to ease any future energy crunch. What is an "undiscovered" reserve? It is merely speculation based upon a mix of some geological evidence and surmise, for the most part, which may "prove" to be accurate. However, there is little scientific evidence to support these speculations and scarcely more practical application of drilling to further investigate such predictions.

The prudent man must inquire more into the likelihood that enough oil will be found to give us more time to accomplish a safe passage through what may someday be described as transition from our present dependence upon oil to the use of alternative energy sources.

The search for more adequate and continuous supply may well be unsuccessful; geology, economics, and politics may be against us. Time is not necessarily on our side and we cannot assume ultimate victory in terms of oil. Nor, however, can we just accept this pessimistic scenario; comprehending the scope of our problems may lead to a clearer concept of our opportunities. This is a point which does not appear to have been fully realized in the capital of the world's energy colossus -- the United States whose domestic energy options are so varied as to set it apart from most other industrial nations for whom foreign exploration may be the only alternative to continuing, large dependence upon imported oil.

AUSTRALIA'S ENERGY POLICY: A GAS UTILITY VIEW

R.D. PALMER

GAS & FUEL CORPORATION OF VICTORIA, 171 FLINDERS ST., MELBOURNE. AUSTRALIA. 3000.

Australia has been called the world's largest island but it is really the world's smallest continent. Dry and sparsely inhabited, with only two cities of world renown and more sheep than people, the "Great South Land" (as early European explorers called it) is nevertheless a highly urbanised industrial country. Some 25% of civilian employment is in manufacturing, compared with 26% for Japan and 23% for the United States. Our gross domestic product in 1975 was 5,700 US dollars per head, compared with 7,120 for the United States and 4,450 for Japan. However, the Japanese economy was clocking up an average 7.8% real G.D.P. growth rate from 1960 to 1975, while Australia only managed 3.1% and the United States 2.5%.

Three million of Australia's 14 million population live in Sydney, the largest city. By contrast, about 9 million of Japan's more than 100 million people live in Tokyo and New York is home to about 8 million of the over 200 million United States citizens. The land areas of these three nations range from 377,000 square kilometres for Japan to 9,363,000 for the United States. Australia is a little smaller than the United States with 7,682,000 square kilometres. Her population, if evenly spread over the land mass, would live and work with a mere two persons per square kilometre. The comparable figure for the United States is 23 while Japan has 300 persons per square kilometre.

Only about 3% of Japan receives under 800 millimetres of rainfall annually, yet fully 88% of Australia is as dry as this. The United States figure is about 55%. Yet from Australia's dry northern and western regions comes exportable mineral wealth which now eclipses in value the agricultural staples on which the country has historically depended for external solvency.

A glance at the atlas will convey a better impression of Australia's economic assets and liabilities. First, as they say, the bad news. The continent is isolated from her four major trading partners, namely Japan (32% of exports/19% of imports), the United States (11% of exports/21% of imports), and the Association of South East Asian Nations (7% of exports/5% of imports). The distances in kilometres (by air) start at 3,347 (Darwin to Singapore), then climb through 7,817 (Sydney to Tokyo) and 11,242 (Melbourne to San Francisco), before reaching 14,500 (Perth to London).

Australia has not yet reached industrial maturity and is still a net importer of capital. The economic composition of imports reflects this fact, being heavily weighted in favour of plant and machinery, transport equipment, industrial inputs and fuels and lubricants. Finished consumer goods typically represent less than a fifth of total imports. The commodity composition of imports shows that mechanical machinery predominates with almost 17% of the total, followed by miscellaneous manufactures (13%), petroleum (10%), motor vehicles (10%), chemicals (9%) and electrical machinery (almost 9%).

The importance of transport equipment and fuels and lubricants in overcoming what one Australian historian has termed "the tyranny of distance" was foreshadowed in my remarks about isolation. The east-west distance from Sydney to Perth is 3,400 kilometres, with the Adelaide to Darwin journey from south to north almost as lengthy. To make matters worse, the bulk of Australia's secondary industry is situated within a narrow crescent connecting Sydney to Melbourne. The products issuing forth from Australia's south-eastern factories and workshops must be transported vast distances to reach consumers in the other capital cities and the country towns which serve the agricultural districts and mining projects to which I now turn.

Now for the good news. Australia's extreme geological age and size means that it encompasses most of the world's geological and climatic zones. Every mineral of commercial significance (except graphite and sulphur) is in production, along with such a quantity and variety of agricultural produce that food, beverages and tobacco represent less than 5% of imports. Australia's export income is principally generated by coal (12%); wheat, wool and iron ore (8% each); meat and alumina (6% each); and sugar (4%).

Australia's primary industries are much less geographically concentrated than its secondary ones. Coal from the productive seams around Blackwater fuels Queensland power stations and is exported through Gladstone. Wheat from the Wimmera-Mallee district around Horsham in Victoria is railed to flour mills in Melbourne and exported through Geelong. Wool from Goulburn in the Southern Tablelands of New South Wales is sold at auction in Sydney and exported. Iron ore from Mt. Tom Price in the Pilbara region of Western Australia is pelletized at Dampier and exported or shipped to the Kwinana steelworks. Bauxite is mined at Weipa in Queensland and treated to produce alumina, which is shipped to Bell Bay in Tasmania for smelting. Sugarcane is grown along the Queensland central coast and crushed in mills, with the product being exported through Mackay and other bulk handling ports. Uranium reserves are located in the Northern Territory in the far north, whilst oil and gas are produced in Bass Strait in the far south.

Within what kind of legislative restraints do Australian export industries operate? Politically, Australia is a federation of six States and two Territories. There is a bicameral Parliament in Canberra, the National Capital, consisting of a House of Representatives and a Senate on the United States model. However, the United Kingdom's Westminster system of government is followed, with an elected Prime Minister who appoints a Cabinet of elected politicians rather than calling on outside talent, as the American President does. The Senate is only nominally a House representing States' interests, as it almost always divides along party lines. Party discipline is strong within the current Government (Liberal Party/National Country Party) and Opposition (Australian Labor Party), so lobbying by interest groups is in general only successful if directed at the top men. Permanent heads of Government departments are also influential, as Acts of Parliament typically leave room for a lot of "administrative discretion", giving quasi-legislative power to the top bureaucrats. In addition, there are the Courts, who often place fresh interpretations on the Constitution, the Statutes and the Regulations made thereunder by the administrative wing of Government. The various State Parliaments operate in similar fashion, although of course confined to matters within their boundaries.

The Australian federation is more centralist than, say, the Canadian one, due to Canberra's control over the most lucrative tax bases, particularly personal incomes, sales turnover and imports. Power over the mining industry though, is much more under the control of the States. Each Government includes a Minister of Minerals and Energy (or equivalent), who approves applications for exploration leases. All minerals discovered become Crown property, but promising leases are almost invariably converted into mining tenements for exploitation by the successful prospecting company, which pays royalties to the Crown and may have to abide by other negotiated terms and conditions. The Australian Government receives a 40% share of offshore petroleum royalties and levies an excise tax on crude oil, although control of other seabed resources remains firmly in State hands,

Through its Bureau of Mineral Resources, the Australian Government supplies geological and economic information to the mining industry. It can control the export of certain metals, petroleum and petroleum products and all raw and semi-processed minerals. Government assistance is given in the form of income tax concessions on capital subscribed to mining ventures and direct subsidies to the industry. Commonwealth and State Ministers meet regularly to co-ordinate policies through the Australian Minerals and Energy Council.

Australia's Fossil Fuel Resources:

The problem of estimating Australia's energy resources is very difficult. An attempt has been made by the Federal Government's National Energy Advisory Committee (1) and most of the information in this note comes from this source. The term resources usually refers to that quantity of material that can be economically extracted. New technical developments and/or increases in prices can make previously identified sub-economic resources, economic. As well as identified resources there are usually considerable quantities of undiscovered resources (i.e. hypothetical and speculative). The National Energy Advisory Committee has used the McKelvey classification, Figure 1. On this basis, Australia's fossil fuel resources are shown in Table 1.

Table 1

Proven Economically Recoverable Australian Fossil Fuel Reserves - At December 1977.

(million terajoules)

<u>State</u>	<u>Crude</u> <u>Oil</u>	<u>Natural</u> <u>Gas</u>	<u>Gas</u> <u>Liquids</u>	<u>Black</u> <u>Coal</u>	<u>Brown</u> <u>Coal</u>	<u>Total</u>
Victoria	8.0	7.8	2.3	-	377*	395
New South Wales	-	-	-	252	-	252
Queensland	-	0.1	-	256	-	256
South Australia/ Northern Territory	0.3	3.5	0.9	9	4	18
Western Australia	0.8	18.8	3.4	8	-	31
Tasmania	-	-	-	2	-	2
Australia (approx.)	9.2	30.2	6.6	527**	381	954

* Based on 38 580 megatonnes of economically recoverable resources.

** Based on 20 260 megatonnes of economically recoverable resources.

Sources:

Crude Oil, Natural Gas and Gas Liquids - The Petroleum Newsletter No. 72 - Department of National Development.

Black Coal and Brown Coal - Australia's Energy Resources - an assessment. National Energy Advisory Committee No. 2.

Note 1 : Total figures are rounded out to the nearest whole numbers.

Note 2 : Resources which are relatively very small have been omitted.

Note 3 : Gas liquids are shown separately from crude oil and natural gas.

Commonly, they occur together in the ground, but are separated in the treatment plant immediately after extraction, and are therefore quoted separately.

Note 4 : Western Australian Petroleum reserves includes those at Carnarvon and Bonaparte Gulf.

Note 5 : Conversion factors - terajoules x 10⁶ = 237 million barrels of gas liquids.
 (average) = 166.3 million barrels of crude oil
 = 0.92 tcf. of natural gas
 = 38.4 million tonnes of black coal
 = 102.5 million tonnes of brown coal

Although the above Table 1 follows the McKelvey classification, the figures for crude oil, natural gas and gas liquids include the reserves of the North West Shelf. The North West Shelf fields although not currently being produced have been included as they are presently being assessed for future development. Table 1 lists only conventional fossil fuels and ignores shale oil, uranium and thorium.

The following comments expand the information shown in Table 1 for the various fuels.

Petroleum Fuels:

(a) Crude Oil:

At December, 1977 some 9.2 million terajoules (TJ) of crude oil was estimated to be economically recoverable. This is a known and demonstrated quantity. Potential still exists for more discoveries (1). It is estimated that a 90% probability exists for finding an additional 9.3 million TJ ($1,550 \times 10^6$ barrels). To find an additional 39.1 million TJ ($6,500 \times 10^6$ barrels) the probability is believed to be around 10%.

(b) Natural Gas:

The economically recoverable quantity of sales gas is put at 30.2 million TJ (28 tcf.). As with crude oil, potential still exists for future discoveries. The probability of finding an additional 32.9 million TJ (30 tcf.) is estimated at 80%. This probability declines to only 20% for an additional 65.8 million TJ (60 tcf.).

(c) Gas Liquids:

This includes condensate and L.P. gas. In terms of size they are an important resource and total 6.6 million TJ ($1,560 \times 10^6$ barrels). This is not much smaller than crude oil at 9.2 million TJ. It is considered (1) that an 80% probability exists for finding an additional 5.2 million TJ ($1,240 \times 10^6$ barrels). To find 16.8 million TJ ($3,980 \times 10^6$ barrels) the probability is only 20%.

Black Coal:

The economically recoverable quantity of black coal shown is 527×10^6 TJ (20,260 million tonnes). However, there are at least 4.4 times this quantity in the identified inferred category as shown on Figure 2.

Identified sub-economic resources of coal are very large. For example, the Cooper and Pedirka Basins in South Australia contain 3 trillion tonnes of coal ($78,000 \times 10^6$ TJ) at a depth between 1,400 and 4,000 metres. In addition, considerable scope exists for future discoveries. Figure 2 summarizes the position for black coal. It is important to note that as the price of black coal increases or as new technologies develop the quantity of coal classified as an economic resource can be increased considerably.

Brown Coal:

Economically recoverable brown coal is situated primarily in Victoria and totals 381×10^6 TJ (39,000 million tonnes). Identified and demonstrated sub-economic resources total an additional 265×10^6 TJ (27,128 million tonnes). Identified and inferred sub-economic quantities are very large with at least 54,000 million tonnes in Victoria. Undiscovered categories are also likely to be large. Figure 3 summarizes the position for brown coal.

Australia's Fossil Fuel Demand:

A demand forecast for internal consumption to the year 2000 has been prepared using the Federal Government's Department of National Development latest projections (2) to 1986/87 and then extending those to the year 2000. Average growth rates, annual use and cumulative demand to the year 2000 are shown in Table 2.

Table 2

Fuel	1976/ 2000	Annual Use		Cumulative Demand
	Growth	TJ x 10 ³		TJ x 10 ³
	P.a.	1976	2000	1976/2000
Black Coal	4.8	749.9	2 289.7	35 315.5
Brown Coal	4.0	289.9	753.4	11 980.9
Oil	2.6	1 255.3	2 331.6	44 250.5
Natural Gas	5.7	212.8	800.9	14 152.8
Total	3.8	2 507.9	6 175.6	105 699.7

Table 3 shows the relationship between the cumulative use of fuels from 1976 to the year 2000 and total economic resources of fuels.

Table 3

Fuel	Cumulative Demand	Economically Recoverable Resource	% Depleted
	TJ x 10 ³	TJ x 10 ³	
Black Coal	35 315.5	527 000	6.7
Brown Coal	11 980.9	381 000	3.1
Oil	44 250.5	9 200	- 381.0
Natural Gas	14 152.8	30 200	46.9

The position for oil and natural gas is not good. The cumulative requirement for natural gas will result in the consumption of almost half the economic resource by the year 2000. This however, understates the position as 18 x 10⁶ TJ of natural gas are located at the North West Shelf and will be used primarily for export. For oil the situation is even worse as known reserves are completely inadequate representing only 21% of the cumulative demand to the year 2000.

Australia is well endowed with black and brown coal. Cumulative consumption of black coal to the year 2000 of 35 million TJ will only consume 6.7% of current economic resources. With 60 x 10⁶ tonnes of black coal exported per annum for 24 years at an average heating value of 26 gigajoules (GJ) per tonne an additional 37 million TJ would be consumed. With exports and domestic consumption 13.8% of the black coal resources would be utilized. However, as noted in the previous section it is estimated that there is at least 4.4 times the quantity of black coal stated in Table 3 that is suitable for mining. With these resources the percentage used by the year 2000 would be close to 3%.

The position for brown coal is good with only 3% of economically recoverable resources being used by the year 2000. Considerable potential exists for enlargement of these resources.

Natural Gas for the Future:

As explained earlier, the population of Australia and the major concentration of its industry is in the south-eastern corner of the continent. The resources of natural gas not yet committed to customers and the most prospective areas for further gas discovery are in the north-western corner. The distance between these two is 4,000 kilometres and the cost of a pipeline system to bring this gas to Eastern States was estimated (3) in 1976 to be \$1,600 million. The alternative of liquefaction in the north-west and transport by ship to the Eastern States, evaluated over a 20 year period, was less attractive than a pipeline.

Such a pipeline must cross four State boundaries, and its cost would be such that the gas utilities could find difficulty in financing such a project. It would therefore seem appropriate for it to be a Commonwealth Government project but so far the Government has not made any commitment.

Against the background of resource availability described earlier all gas utilities are confronted with planning problems. The following description of those confronting the Gas and Fuel Corporation of Victoria is given as a typical example.

The Gas and Fuel Corporation supplies 700,000 residential consumers and in addition, supplies industry in the reticulated area with 81% of its secondary energy needs (excluding electricity). It has maintained a strong campaign to convert all stationary uses of liquid fuels to natural gas both in its own interest and in its perception of the interest of the Government to minimize dependence on oil. The natural gas distributed in Victoria is obtained from the Bass Strait gas and oil fields under long term contracts which also provide options over any future discoveries. It is assumed in forecasts of the future that the price of gas from these sources will allow natural gas in the market place to maintain its competitiveness with oil and electricity. Competition does exist from solid fuels but is limited to very large users away from urban areas where clean air requirements make solid fuel uncompetitive. Market growth for natural gas will therefore be dependent on such fundamentals as population growth, industrial development and changes in living habits. On the other hand, growth may be neutralized by community adoption of energy conservation objectives, such as insulation of homes, re-cycling of materials, efficient designs of homes and efficient designs of industrial equipment. There are great unknowns in this area but the best estimates to date indicate that known reserves of natural gas in Bass Strait are equal to the cumulative demand up to 2005 at least, and success in conservation education could extend this period.

This does not however take account of the deliverability of gas from the reserves. When a comparison is made of the best estimate of maximum deliverability from the Bass Strait fields with the maximum daily demand of the market, it is found that a shortfall could exist from 1990 onwards. There are many solutions to this problem, partly from the demand and partly from the supply side. From the demand side conservation should be looked at seriously.

The Corporation is engaged in a major programme of community education. It is actively engaged in the promotion of insulation, it runs energy management courses for industry and provides technical consultancy services to industry. It has sponsored and built demonstration low energy homes. It operates a central energy information centre to provide information to the public. It is developing and demonstrating gas/solar installations for domestic and commercial use. This programme is aimed at reducing the use of gas by wise use, not by conversion to some other form of energy which could be against the national interest. Success in the programme could postpone the deliverability shortfall into the late 1990's.

From the supply side we can consider a number of solutions:

Storage:

The prospects of increased peak deliverability through the use of storage in geological structures are doubtful. At present an L.N.G. peak shaving plant is being built and expansion of this concept is a likely means of postponing peak deliverability problems. In addition, of course, such storage gives security against plant and platform breakdowns and thus serves a double purpose. The present plant is being built in conjunction with an air separation plant producing oxygen and nitrogen and it is hoped that the combined plant will give significant energy savings as well as capital cost savings.

Discovery of Additional Reserves in Victoria:

Exploration in Victoria to date has been concentrated in the Gippsland Basin offshore. What exploration has been carried out onshore and in the offshore Otway Basin has had no success, and active exploration in these areas has ceased. Even in offshore Gippsland there have been no additions to gas reserves by new discoveries for many years. Nonetheless, it is believed that diligent exploration could yield new gas discoveries sufficient to provide the required deliverability through the 1990's. To this end, the Corporation has set up an exploration subsidiary which in conjunction with a joint venturer has commenced exploration over 2,500 sq. kilometres offshore Gippsland.

New Long Term Supply Sources:

Chief amongst these lie the prospective resources of the North West Shelf. However, the problem of transport across the 4,000 kilometres to a market which will be small at the start and grow as a result of market growth and reduced deliverability from existing sources, is difficult to solve without some form of Government involvement in the financing of the lines and explicit Government policy on availability of reserves of gas.

Another alternative long term supply source is S.N.G. from brown coal of which there are tremendous reserves in Victoria. Since it does appear that S.N.G. from brown coal can be delivered to the market at a price competitive with oil from brown coal or electricity from brown coal, this should be a viable alternative by the late 1990's and may well be, in the long term, the main source of gaseous fuel to the State.

As can be seen, the solution to the supply problem in Victoria does not present any technical difficulty. All the above alternatives are possible with today's technology. The difficulty lies in the choice of the most effective method or combination of methods. For example, the lead time for an S.N.G. from a coal plant might be ten years and for a trans-continental pipeline 7 years. A lot could change during this time so that a decision to take one route as against another could be found to be incorrect with disastrous financial consequences.

The first priority therefore must be to remove the risk of such error being caused. The major change that can take place during a 6-10 year gestation period to secure long term supply is new discoveries of gas close to Victoria. For this reason exploration throughout Victoria and adjacent areas must be carried out as soon as possible. This does not necessarily suit the private enterprise explorer looking for immediate inland sales.—Consequently some Government or utility intervention either to carry out exploration or to compensate the explorer for his holding costs seems to be necessary. Assuming that this exploration work has still shown a demand for North West Shelf gas in the Eastern States, a prior requirement for construction of a pipeline is the dedication of reserves to it to ensure its economic viability. At present the Commonwealth attitude to export of L.N.G. is uncertain. Permission has been given to export 52% of the present known commercial reserves which after allowance for plant fuel and losses is equivalent to almost 65%. For such a project as this pipeline at least 20 year's requirements would seem the minimum dedication. This quantity does not seem available at present.

Taking our risk minimizing exercise a step further, even with North West Shelf gas, a case can be made for the installation of a coal conversion plant in 1990's. However, the capital cost of these plants and the risks inherent in such a large project makes it unlikely that any utility could afford a plant of the required size without Government involvement in the financing and risk sharing.

All in all this points towards an inevitable Government involvement in ensuring the continued smooth supplies to customers in Eastern Australia.

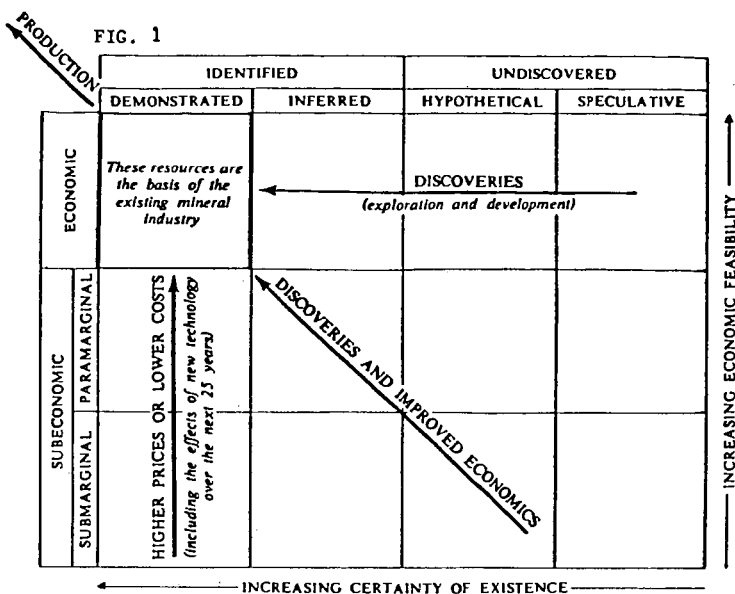
Summary:

From this description of the particular problems of one gas utility, general conclusions with regard to a national energy policy can be drawn. If it is desirable to minimize Australia's dependence on oil, then widespread replacement of oil in stationary applications by gas should be encouraged. To achieve this, confidence in long term availability and stability of price must be encouraged by:-

- (a) Government action to ensure a proper level of exploration by all possible means.
- (b) Explicit Government policy on natural gas export so as to maintain sufficient resources dedicated to inland use to justify investment in distribution and utilization facilities.
- (c) Government commitment either to construct or to guarantee the viability for private investors of large energy projects such as a trans-continental pipeline and coal conversion plants.

References:

1. Australia's Energy Resources, an assessment. National Energy Advisory Committee Report No. 2.
2. Demand for Primary Fuels Australia 1976/77 to 1986/87. Report by Department of National Development - April 1978.
3. Australian Natural Gas Utilization and Transportation Study. Prepared for The Pipeline Authority - October 1976.



Resource classification diagram showing the general progression of non-renewable resources as a result of exploration, research, development and production.

FIG. 2 AUSTRALIA'S RESOURCES OF BLACK COAL (10⁴ tonnes)

		IDENTIFIED		UNDISCOVERED	
		DEMONSTRATED	INFERRED	HYPOTHETICAL	SPECULATIVE
ECONOMIC	PARAMARGINAL	In situ 36 300 (a) Recoverable Coking 11 880 (a, c) Non-coking 8380 (a, c)	In situ At least 160 000 Recoverable At least 89 000 (b)		
	SUBMARGINAL				
SUBECONOMIC	PARAMARGINAL	Very large (d) +		Very large (d)	Relatively small (d)
	SUBMARGINAL				

← INCREASING CERTAINTY OF EXISTENCE →

↑ INCREASING ECONOMIC FEASIBILITY ↓

(a) Results of drilling since 1973 will increase this figure. (b) A mining recovery rate of 55.8 per cent is assumed (see text). (c) For reasons given in the text, distinctions between coking and non-coking coals are becoming increasingly less meaningful. (d) No quantitative assessment available.

FIG. 3 AUSTRALIA'S RESOURCES OF BROWN COAL (10⁶ tonnes)

		IDENTIFIED		UNDISCOVERED	
		DEMONSTRATED	INFERRED	HYPOTHETICAL	SPECULATIVE
ECONOMIC	PARAMARGINAL	In situ 40 930 (a) Recoverable 39 000	Small (b)		
		In situ 27 128	Very large (c) (Only partly assessed)	Very large (b)	Small (b)

← INCREASING CERTAINTY OF EXISTENCE →

↑ INCREASING ECONOMIC FEASIBILITY ↓

- (a) Total includes 5000 million tonnes in Victoria located beneath township planning scheme areas.
 (c) Includes at least 54 500 million tonnes in Victoria. (b) No quantitative assessment available.

COAL STRUCTURE AND COAL SCIENCE: OVERVIEW AND RECOMMENDATIONS

Richard C. Neavel

Exxon Research and Engineering Co., P.O. Box 4255, Baytown, Texas 77520

Coal is a sedimentary rock accumulated as peat and composed principally of macerals, subordinately of minerals, and containing water and gases in submicroscopic pores. Macerals (mas' er - als) are organic substances derived from plant tissues and exudates that have been variably subjected to decay, incorporated into sedimentary strata, and then compacted, hardened, and chemically altered by natural (geological) processes.

Coal is not a uniform mixture of carbon, hydrogen, oxygen, sulfur, and minor proportions of other elements; nor is it, as is often implied, simply a uniform, polyaromatic, "polymeric" substance. Rather, it is an aggregate of microscopically distinguishable, physically distinctive, and chemically different macerals and minerals.

Coal is analogous to a fruitcake, formed initially as a mixture of diverse ingredients, then "baked" to a product that is visibly heterogeneous. The heterogeneous nature of coal is evident in Figure 1, a photomicrograph of a polished surface of a piece of typical coal. The different macerals reflect different proportions of incident light and are therefore distinguished as discrete areas exhibiting different shades of gray. It should be evident that any attempt to characterize the chemical structure of this coal without recognizing the organization of the elements and molecules into discrete substances would be like trying to describe the essence of a fruitcake by grinding it up and analyzing its elemental composition.

The heterogeneity of coal, exemplified by Figure 1, is inherited from the diversity of source materials which accumulated in a peat swamp. Coals may be compared, contrasted and classified on the basis of variations in the proportions of these microscopically identifiable components. Such a classification is referred to as a classification according to type. Coals may also be classified according to how severely geological alteration processes, referred to collectively as metamorphism, have affected their properties. This is classification according to rank. These two classification methods are independent and orthogonal; therefore, within certain limits, any type of coal can be found at any rank.

Classification according to type involves the relative proportions of both the inorganic substances and the different organic substances. Because only the organic material is altered by metamorphic processes, rank classification is independent of inorganic content. Inorganic material is significant in commercial uses of coal, and its presence must be accounted for in scientific studies. The present discussion, however, concentrates on the properties of the organic substances, because only the organic macerals make coal the valuable material that it is.

In Figure 1, selected areas are identified as vitrinite, liptinite, and inertinite. These terms refer to the three major classes of macerals recognizable in all ranks of coal except those of the highest ranks. A few of the more significant features of these major classes of macerals and of their more important subclasses are summarized in Figure 2. It can be seen from Figure 2 that the differentiation of coals according to type, viz. according to the content of materials assignable to each of the maceral classes, is really a differentiation according to the ingredients which initially accumulated as peat to form that coal. Although the rank scale according to ASTM has been arbitrarily divided, and

specific segments have been identified by an epithet (i.e., lignitic, bituminous, anthracitic coals), there are no such well-recognized classes of coal types.

In this sense, there is essentially a continuous series of coals of different types, defined by microscopic quantification of their maceral (and mineral) contents. Particles of crushed coal, when cemented together as a solid block with a catalytically solidified resin or plastic, can be polished and examined microscopically. Individual particles derived from different layers of a coal seam, may differ significantly in maceral and mineral contents. Recognition of this feature has led to the concept of the microlithotype, wherein each particle can be classified according to its maceral content. In this procedure, arbitrary classes of particles are recognized according to specific maceral proportions as shown in Table 1. It is important that the scientist or technologist recognize that particles of the different microlithotypes are likely to perform quite dissimilarly when analyzed or processed; therefore, coals must be sampled carefully to prevent the selection of non-representative particles.

Each of the materials recognized as belonging to a specific maceral class (according to the criteria shown in Figure 2) has physical and chemical properties that depend upon its composition in the peat-swamp and the effects of subsequent metamorphic alteration. Thus, for instance, in all coals there is material derived from the structural tissues ("wood") of plants. These "woody" substances (lignin, cellulose) are the dominant components of plants, and hence their derivatives dominate in typical coals. In the peat swamp, some of the woody tissues may have been pyrolyzed by fire, forming a carbon rich char recognized as fusinite in the coal. In some coal layers, this may be the dominant maceral, and such layers would be referred to as fusinite-rich types of coal.

Much more commonly, though, the woody tissues accumulated below a water covering where imperfectly understood, largely microbiological processes converted them to humic substances of somewhat variable composition. These humic substances were subsequently altered by metamorphic processes (heat, pressure) into substances classifiable as one of the vitrinite macerals. Therefore, the physical and chemical properties of the vitrinitic materials in a specific coal were largely conditioned by the magnitude of temperature and pressure to which they were subjected after burial. Thus, one could say that the properties of the macerals in a given coal reflect the rank of the coal; or more correctly, one should say that the rank of the coal reflects the properties of macerals as conditioned by the severity of the metamorphic processes to which the coal was subjected.

One of the properties of macerals that changes progressively with metamorphic severity is the microscopically measurable reflectance of polished surfaces. Using a sensitive photomultiplier cell mounted on a microscope, it is possible to measure objectively the absolute percentage of incident light reflected from very small areas (5 μ m diameter) of polished coal surfaces. In Figure 3 is shown a series of reflectance distributions, each representing a sampling of the material in a coal of the rank indicated. These distributions are arbitrarily constructed to show what would happen to a given peat if it were to be subjected to increasingly more severe metamorphism. Recognize, of course, that these are "slices" through a continuum, and that no jump from rank to rank is implied. Properties such as carbon content, oxygen content, degree of aromaticity, and many others, could be substituted for the reflectance scale and a similar sort of picture would emerge. In Table 2, some typical values are shown for selected properties of vitrinite macerals in different rank coals. In Table 3, a number of the properties of non-vitrinite macerals are compared to those of vitrinite from coal of the same rank.

Typical U.S. coals are relatively vitrinite-rich, therefore analyses of whole coals, when appropriately corrected for inorganic content, reflect, to a first approximation, the composition and properties of the included vitrinite. For this reason, the parameters employed to classify coals according to rank, reflect the

rank (stage of metamorphic development) of the vitrinite. Calorific values or fixed carbon yields are calculated to a so-called mineral-matter-free basis for use in the ASTM classification of coals according to rank (1). It is essentially impossible to obtain inorganic-free samples; therefore, to represent organic matter accurately in comparative studies of any of the organic properties of coal, analytical data must be converted to an inorganic-free basis. Commonly, a dry, ash-free (DAF*) basis is employed. It is preferable, however, to convert to a dry, mineral-matter-free (DMMF) basis, as discussed by Given and Yarzab (2). In fact, the most meaningful assessment of coal rank or of the properties of coals of different ranks should be done with samples of concentrated vitrinite or on samples where the vitrinite comprises more than about 80% of the organic fraction. Because reflectance is closely correlative with many rank-sensitive properties and its determination can be made on vitrinite alone, it has become a widely accepted parameter to designate the rank of a coal (see Figure 4). Unfortunately, even when a reflectance value is available, it may not be reported in scientific publications. I strongly recommend that petrographic analyses and vitrinite reflectance be reported for samples on which structural studies are conducted.

Although many properties of vitrinites appear to change in a more or less parallel fashion as a result of metamorphism, there is considerable scatter in their correlation. Figure 5 is offered as evidence of this contention. The data plotted in Figure 5 are from coals containing more than 80% vitrinite on a DMMF basis (3). It is obvious that the progression from high to low H/C and O/C values reflects the influence of more severe metamorphic alteration; in other words coals toward the lower H/C and O/C end of the band are higher rank. However, the fact that the data do form a band, rather than a linear progression, implies that there is not a simple scale which defines the rank progression. As Given and his co-workers have so eloquently shown, the geological/geographical disposition of U.S. coals appears to exert some, as yet undefined, influence on the intercorrelations of coal properties (4).

Clearly, neither geology nor geography are coal properties and hence cannot be "measured". Different source materials, depositional conditions (including especially sulfur availability), and time/temperature/pressure conditions during metamorphism, interacted so as to provide a multitude of potential paths which different coals (or even vitrinites in different coals) followed to their present condition. In other words, the concept of a single rank progression is more fallacy than fact.

As unifying, underlying concepts, type and rank certainly can be validly employed to envision why coals have the properties that they do. However, it is time for a re-evaluation of coal classification concepts. How can we measure rank when we analyze coals of different types and when there is no simple rank progression even when vitrinite or vitrinite-rich coals are compared? And how can we assess type when maceral identification criteria are highly subjective, except for reflectance measurements that routinely are not even applied to the liptinite and highly variable inertinite macerals? And, finally, how can coals be classified scientifically when empirical and derived properties like calorific value and fixed carbon yield are employed as classifying parameters?

A scientific classification should be based first on the fundamental properties of the vitrinite in coals. This means, at the very least that element concentrations and molecular structure configurations must be assessed. The structural properties of most importance to classification and process responses

*Not 'MAF', which is often unfortunately used as an abbreviation for moisture-and-ash-free.

appear to be: (1) the nature of hydrogen bonding and physical entanglement that cohere molecular moieties, (2) the nature of cyclical structures (e.g., ring condensation index, aromaticity, heteroatoms), (3) amount and distribution of hydroaromatic hydrogen, (4) scissle bridging structure (e.g., ether, sulfides, polymethylenes), (5) functional group characteristics (esp. oxygen- and sulfur-containing), and (6) organic/inorganic interactions. To develop the basis of a scientific classification, these determinations need to be made on a large number of vitrinite-rich coal samples spanning a wide range of rank. Because coals are sensitive to oxidation and moisture changes during handling, these samples must be carefully collected, prepared and preserved.

It is fairly evident that because of the complex interactions of depositionally-influenced and metamorphically-influenced properties, the fundamental chemical/structural properties will need to be related to each other in a complex statistical fashion. A multivariate correlation matrix such as that pioneered by Waddell (5) appears to be an absolute requirement. However, characterization parameters far more sophisticated than those employed by Waddell are required. One can hope that, as correlations between parameters become evident, certain key properties will be discovered which will allow coal scientists and technologists to identify and to classify vitrinites uniquely. Certain optical properties might prove valuable in this respect. It would then not be necessary for every laboratory to have super-sophisticated analytical equipment at its disposal in order to classify a coal properly. By properly identifying/classifying the vitrinite in a coal, one could then estimate accurately the many other vitrinite properties available in the multivariate correlation matrix.

Of course, elucidation of vitrinite properties and establishment of unique vitrinite class identifiers would not solve all of the problems of coal classification. Further work needs to be done to characterize the inorganic materials in coals, especially developing simple tests for quantification of inorganic species.

Once vitrinites could be properly identified and classified, then it would be necessary to characterize and to identify uniquely the members of the other maceral classes. It is probable that liptinite properties change in some fashion correlative with the changes wrought by metamorphism on vitrinite. Therefore, classification of vitrinite would automatically classify liptinite. Whether inertinite changes with rank is uncertain; but it is certain that far better differentiation of fusinites needs to be employed for it is evident that fusinite reflectance values span wide ranges in a given coal.

A multivariate vitrinite classification, supplemented by information about the inorganic matter and the proportions and properties of associated macerals, would be of little value if it could not be used to predict the response of a given coal in a processing system and thereby provide an estimate of the value of that coal. Consequently, it will be necessary to relate the scientific classification to the responses of coals in such processes as pyrolysis, liquefaction, gasification, combustion, and coke-making. This can only be done by relating the fundamental, classifying properties to empirically determined processing responses on a substantial number of samples. Again, they should be vitrinite-rich and cover a broad range of ranks.

Only through the conduct of an integrated program more or less along the lines that I have outlined is Coal Science ever going to move out of the era of the 1950's where it is now mired. The scattered probes of coal structural properties on a bewildering range of poorly selected, poorly collected, poorly prepared, poorly preserved and poorly characterized coal samples will lead us only into further confusion. Progress in Coal Science can only be made when scientific and technological investigations on coal result in a comprehensive integration and synthesis of data and information. The essence of science is

"the reduction of the bewildering diversity of unique events to manageable uniformity within one of a number of symbol systems" (6). Present investigations of coal structure hardly conform to that definition today, and therefore hardly deserve the epithet of Coal Science.

References

1. Annual Book of ASTM Standards, Designation D388, standard specification for the classification of coals by rank.
2. Given, P. H., R. F. Yarzab, Problems and solutions in the use of coal analyses, Coal Res. Sect., Penn. State Univ., Tech. Rpt. No. FE 0390-1, 1975.

Given, P. H., The use of daf and dmmf ultimate analyses of coals, Fuel, 55, 256, 1976.

Given, P. H., W. Spackman, Reporting of analyses of low-rank coals on the dry, mineral-matter-free basis, Fuel, 57, 219, 1978.
3. Spackman, W., and others, Evaluation and development of special purpose coals; final report, Coal Res. Sect., Penn. State Univ., Tech. Rpt. No. FE 0390-2, 1976.
4. Abdel-Baset, M. B., R. F. Yarzab, P. H. Given, Dependence of coal liquefaction behavior on coal characteristics. 3. statistical correlations of conversion in coal-tetralin interactions, Fuel, 57, 89-94, Feb. 1978.
5. Waddel, C., A. Davis, W. Spackman, J. C. Griffiths, study of the inter-relationships among chemical and petrographic variables of United States coals, Coal Research Section, Penn. State Univ., Tech. Rpt. FE-2030-9, 1978.
6. Huxley, Aldous, Education at the non-verbal level, Daedalus, spring 1962.

TABLE 1. CLASSIFICATION OF MICROLITHOTYPES

	<u>Micro lithotype</u>	<u>Maceral</u>	<u>Volume Percent</u>
Monomaceralic	Vitrite	Vitrinite (V)	> 95%
	Liptite	Liptinite (L)	> 95%
	Inertite	Inertinite (I)	> 95%
Bimaceralic	Clarite	V + L	> 95%
	Vitrinerite	V + I	> 95%
	Durite	I + L	> 95%
Trimaceralic	Duroclarite	V + I + L	V > (I + L)
	Clarodurite	V + I + L	I > (L + V)
	Vitrinertoliptite	V + I + L	L > (I + V)
	Carbominerite	V, L, I and Mineral Matter (MM)	MM > 20%, < 60%

TABLE 2. SELECTED PROPERTIES OF VITRINITES IN
COALS OF DIFFERENT RANKS

	<u>Liq.</u>	<u>Sub-Bit.</u>	<u>Bit.</u>	<u>Anth.</u>
Moisture Capacity, Wt.%	40	25	10	< 5
Carbon, Wt.% DMMF	69	74.6	83	94
Hydrogen, Wt.% DMMF	5.0	5.1	5.5	3.0
Oxygen, Wt.% DMMF	24	18.5	10	2.5
Vol. Mat., Wt.% DMMF	53	48	38	6
Aromatic C/Total C	0.7	0.78	0.84	1.0
Density (He, g/cc)	1.43	1.39	1.30	1.5
Grindability (Hardgrove)	48	51	61	40
Btu/lb, DMMF	11,600	12,700	14,700	15,200

DMMF = Dry, Mineral-matter-free basis. These are typical values for rank classification. Sulfur and nitrogen are rank-independent and not shown.

TABLE 3. PROPERTIES OF MACERALS COMPARED TO VITRINITE IN SAME COAL
 (Subbituminous and High-Volatile Bituminous Only)
 Magnitude of property greater than (>), less than (<), or
 equal to (=) that of associated vitrinite.

<u>Optical Properties</u>	<u>Inertinite</u>			
	<u>Semi-Fusinite</u>	<u>Fusinite</u>	<u>Micrinite</u>	<u>Exinite</u>
Reflectance	>	> >	>	<
Fluorescence				>
<u>Chemical Structure</u>				
Basic carbon structure				=
Molecular weight				>
H/C ratio	<	< <	=	>
H aliphatic/H total; -CH ₂ ; hydroaromaticity				>
Fraction aromatic C; rings/unit		>	>	<
Oxygen _{OH} /Oxygen _{Total}		<		<
Unpaired spins by ESR		>		<
Unpaired spins of fusinite with same carbon as vitrinite		>		
<u>Reactivity</u>				
Methane sorption		>		
Decomposition temperature				<
Oxidizability				<
Reduction with Li in EtDA		<	=	<

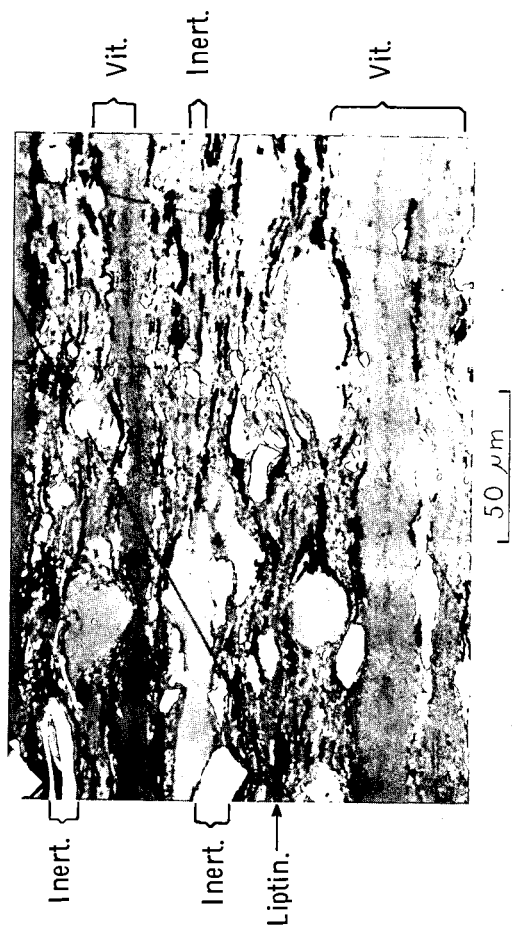
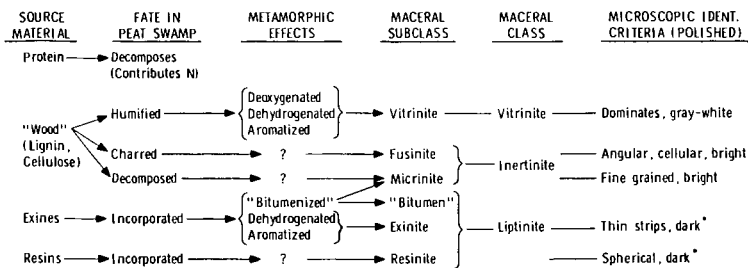


Figure 1. Photomicrograph of polished surface of a high-volatile bituminous coal.
Vit. = Vitrinite; Inert. = Inertinite; Liptin. = Liptinite

FIGURE 2. PRINCIPAL MACERAL CLASSES



* In Low-Vol Bituminous and Anthracites, Liptinite Indistinguishable from Vitrinite

FIGURE 3. REFLECTANCE DISTRIBUTION OF MACERALS IN TYPICAL COALS

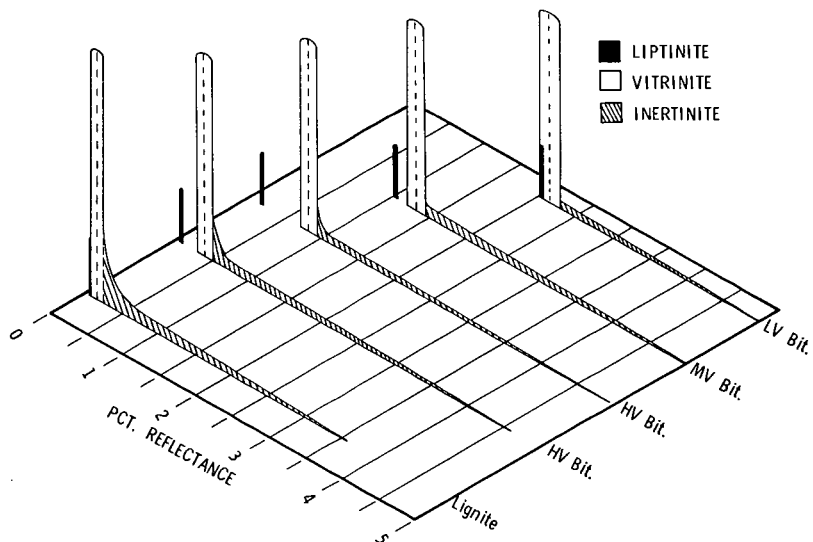


FIGURE 4. CORRELATION OF REFLECTANCE OF VITRINITE AND CARBON CONTENT OF COALS. DATA FROM REF. 3

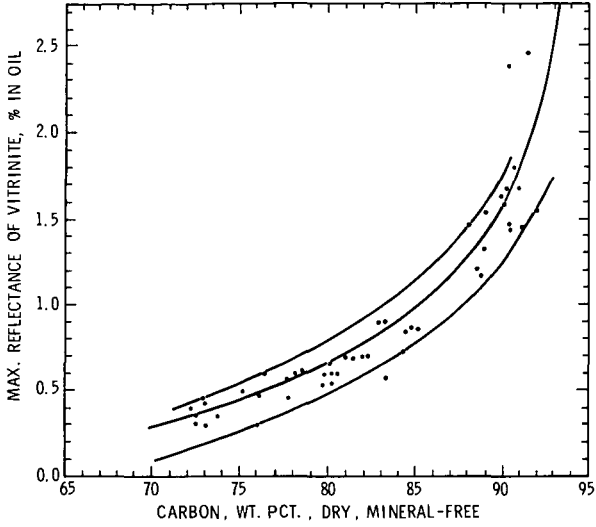
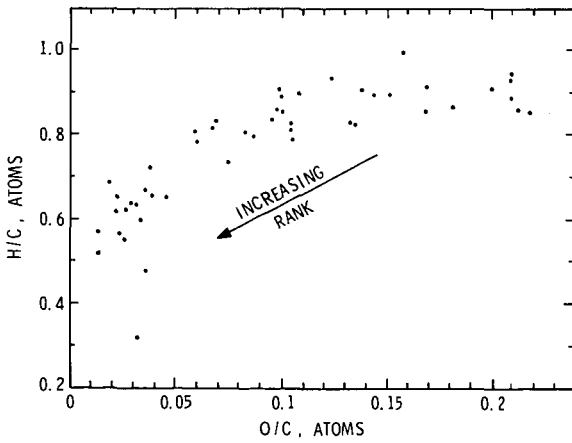


FIGURE 5. CORRELATION OF ATOMIC H/C AND O/C FOR COALS OF DIFFERENT RANKS. DATA FROM REF. 3



NATURE OF THE FREE RADICALS IN COALS, PYROLYZED COALS,
AND LIQUEFACTION PRODUCTS

H. L. Retcofsky, M. R. Hough

Pittsburgh Energy Technology Center, U. S. Department of Energy
4800 Forbes Avenue, Pittsburgh, PA 15213

R. B. Clarkson

Varian Associates, Instrument Division
611 Hansen Way, Palo Alto, CA 94303

Electron spin resonance (ESR) spectrometry has been the favored instrumental tool to probe the nature of the free radicals in coals and materials derived from coal (1). Recently, it was shown that these free radicals are also amenable to study by electron nuclear double resonance (ENDOR) spectrometry (2,3). The ENDOR technique is becoming increasingly popular in free radical studies because frequently the resulting spectra are much more highly resolved than corresponding ESR spectra of the same materials (4).

As a first step toward elucidating the role of free radicals in the liquefaction of coal, the stable radicals present in coals, pyrolyzed coals, and liquefaction products require characterization. In the present characterization study we have applied both the ESR and ENDOR techniques. For many of the samples examined, it was found that great care must be taken during sample preparation to ensure reliability of the spectral data.

Coals. ESR measurements on non-anthracitic and young anthracitic coals can be made with little difficulty. It is best to evacuate the samples since it has been shown that the ESR spectra of fusains, petrographic constituents found in nearly all coals, are quite sensitive to the presence or absence of air (oxygen) in the sample (5). Contrary to other evidence in this report (5), high rank anthracites and meta-anthracites do require dilution of the samples with a non-conducting medium to prevent errors in ESR measurements due to microwave skin effects. For example, the ESR intensity of a meta-anthracite from Iron County, Michigan increased significantly rather than decreased after the sample was diluted with KBr.

For non-anthracitic coals, the observed variation of the ESR g value with coal rank suggested that the naturally occurring radicals in coals become more "hydrocarbon-like" as coalification progresses (6). Evidence supporting this hypothesis is depicted in Figure 1. The plot of ESR g values vs oxygen contents of the coals suggests that the unpaired electrons in low rank coals interact with oxygen atoms in the sample. Statistical treatment of the data revealed that the g values of only two of the coals fall outside the area bounded by the dashed lines drawn \pm twice the standard error of estimate from the linear regression line. These two coals are somewhat unique in that they contain an usually high content of organic sulfur (7). In the second plot of Figure 1, the abscissa has been changed to reflect the sum of the oxygen and sulfur contents of the coals, (each element being weighted according to its spin-orbit coupling constant). This latter plot exhibits much better statistics, suggesting that the unpaired electrons interact with sulfur as well as with oxygen. Attempts to extend the statistical treatment to nitrogen in the samples were inconclusive.

Pyrolyzed Coals. A number of investigators have applied ESR techniques to pyrolyzed coals (1). At least two groups of investigators (8,9) have reported g values less than that of the free electron for certain coals heated to commonly used liquefaction temperatures. One group (9) attributed these low g values to the

presence of sigma radicals. During the present investigation, we observed a similar g value dependence with heat-treatment temperature for hvAb coal from the Ireland Mine (Pittsburgh bed) in West Virginia.

It had been shown previously (10) that incorrect ESR g values were obtained for heat-treated sucrose if proper dispersal techniques were not used. With this in mind, we measured the effect of sample dilution on the apparent g value of Ireland Mine coal heat-treated to 450°C. The results, shown in Figure 2, show that the true g value of the sample in question is actually higher than that of the free electron. This suggests that great care must be exercised when applying ESR techniques to heat-treated coals. This problem will undoubtedly present some obstacles to the in situ ESR studies of coal pyrolysis and coal liquefaction planned by many laboratories.

Liquefaction Products. A few ESR studies of liquefaction products from coal have been reported (6,11,12). One group of investigators (6) concluded from ESR studies of coal-derived asphaltenes that charge-transfer interactions are relatively unimportant binding forces between the acid/neutral and base components.

ESR results from our on-going efforts to elucidate the changes in chemical structure that occur during coal liquefaction are given in Table 1. The samples examined were obtained from a liquefaction run in the Pittsburgh Energy Technology Center's 10 lb coal/hr process development unit (13). The run was made without added catalyst. The samples included the process coal and its pyridine extract, and the preasphaltenes, asphaltenes, and oils separated from the centrifuged liquid product. It can be seen that the free radical contents change in the order: process coal < preasphaltenes >> asphaltenes > oils. The g values suggest the presence of "hydrocarbon-like" radicals with perhaps some interaction between the unpaired electrons and heteroatoms in the asphaltene and oil fractions. The line widths appear to increase (at least crudely) with increasing hydrogen contents of the samples.

ENDOR Studies. In contrast to the ESR spectra of coals, which generally consist of a single line devoid of any resolvable fine structure due to hyperfine interactions, the ENDOR spectra (at least in the present study) are rich in detail (Figure 3). These results are quite surprising in light of spectra published several months ago which showed only a single band at the so-called free proton frequency (2). In an attempt to experimentally deduce the reasons for this apparent discrepancy of results, we found a reversible effect of air (oxygen) on the ENDOR spectrum, i.e., the hyperfine lines were observed for evacuated samples, but disappeared upon admission of air to the samples.

The fact that an ENDOR spectrum is observed under the experimental conditions employed is unambiguous proof that the unpaired electrons in the coal couple with nuclear spins, undoubtedly protons, in the sample. This provides additional support for the free radical interpretation of the ESR spectrum. The magnitude of the hyperfine interactions, i.e., none greater than 10 gauss, indicates that none of the radicals has a high unpaired electron spin density at a particular carbon atom.

Table 1. MAF analyses, carbon aromaticities, and electron spin resonance data for materials produced from the liquefaction of West Virginia (Ireland Mine) hvAb coal in the Pittsburgh Energy Technology Center's 10 lb coal/hr process development unit.

	COAL		PREASPHALTENES	ASPHALTENES	OILS
	Solid Coal	Pyridine Extract			
<u>MAF Analysis, %</u>					
C	78.5	81.7	86.9	87.3	86.6
H	5.6	5.9	5.1	6.3	8.2
O	9.7	8.0	4.8	3.6	3.3
N	1.2	1.9	2.2	2.0	1.2
S	4.9 ₁	2.6	0.9	0.9	0.7
f_a	$0.76^{\underline{1}/}$	$0.73^{\underline{1}/}$	$0.84^{\underline{1}/}$	$0.77^{\underline{2}/}$	$0.63^{\underline{2}/}$
<u>ESR Data</u>					
Free Spins/Gram	1.4×10^{19}	9.0×10^{18}	2.0×10^{19}	2.4×10^{18}	9.4×10^{17}
g value	2.0027 ₇	2.0031 ₂	2.0027 ₉	2.0032 ₉	2.0030 ₇
Linewidth, gauss	5.9	5.7	6.6	7.3	8.7

$\underline{1}/f_a$ determined by cross-polarization ^{13}C NMR.

$\underline{2}/f_a$ determined by high-resolution ^{13}C FT NMR.

REFERENCES

1. For reviews of the early literature see (a) H. Tschamler and E. De Ruitter, "Chemistry of Coal Utilization", Suppl. Vol. H. H. Lowry, Ed., Wiley, New York, 1963, p. 78; (b) W. R. Ladner and R. Wheatley, Brit. Coal Util. Res. Assoc. Monthly Bull., 29, 202 (1965); and (c) D. W. Van Krevelen, "Coal", Elsevier, Amsterdam, 1961, p. 393.
2. S. Schlick, P. A. Narayana, and L. Kevan, J. Am. Chem. Soc., 100, 3322 (1978).
3. H. L. Retcofsky and M. R. Hough, "Electron Spin Resonance Studies of Coals and Coal Liquefaction", Paper presented at the 29th Pittsburgh Conference on Analytical Chemistry and Applied Spectroscopy, Cleveland, Ohio, February 27-March 3, 1978.
4. L. Kevan and L. D. Kispert, "Electron Spin Double Resonance Spectroscopy", Wiley, 1976, p. 2.
5. H. L. Retcofsky, J. M. Stark, and R. A. Friedel, Anal. Chem., 40, 1699 (1968).
6. H. L. Retcofsky, G. P. Thompson, M. Hough, and R. A. Friedel, Chapter 10 in "Organic Chemistry of Coal", John W. Larsen, Ed., ACS Symposium Series, No. 71, 1978, p. 142.
7. R. M. Eloffson and K. F. Schulz, Preprints, Am. Chem. Soc. Div. Fuel Chem., 11, 513 (1967).
8. S. Toyoda and H. Honda, Carbon, 3, 527 (1966).
9. L. Petrakis and D. W. Grandy, Anal. Chem., 50, 303 (1978).
10. L. S. Singer, Proc. Fifth Carbon Conf., 2, Pergamon Press, 1963, p. 37.
11. D. L. Wooten, H. C. Dorn, L. T. Taylor, and W. M. Coleman, Fuel, 55, 224 (1976).
12. T. F. Yen, Private Communications.
13. P. M. Yavorsky, S. Akhtar, J. J. Lacey, M. Weintraub, and A. A. Reznik, Chem. Eng. Prog., 71, 79 (1975).

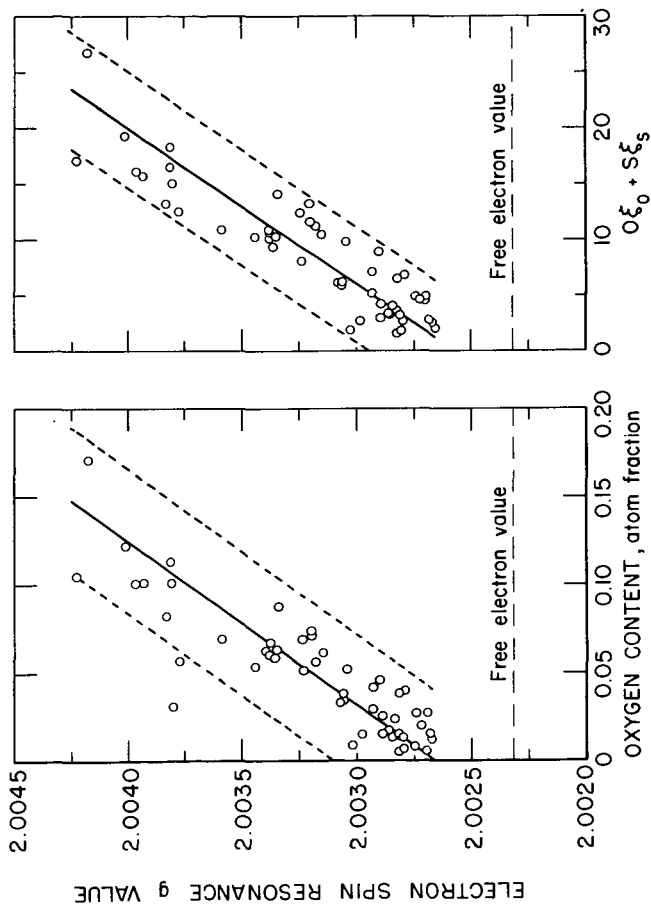


Figure 1. Functional dependences of the electron spin resonance g values of vitrains from selected coals.

11-4-77 L-15681

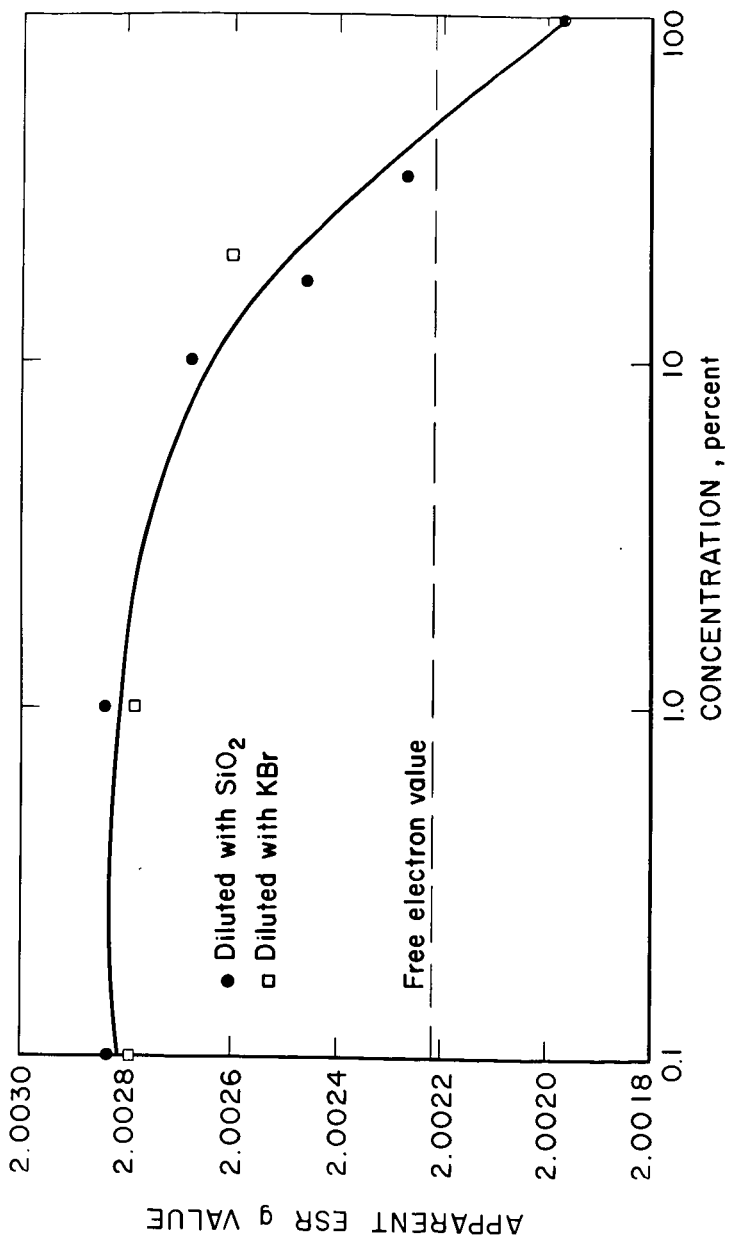


Figure 2. The effect of sample dilution on the apparent electron spin resonance g value of Ireland Mine hvAb coal heat-treated to 450°C.

11-29-78 L-16340

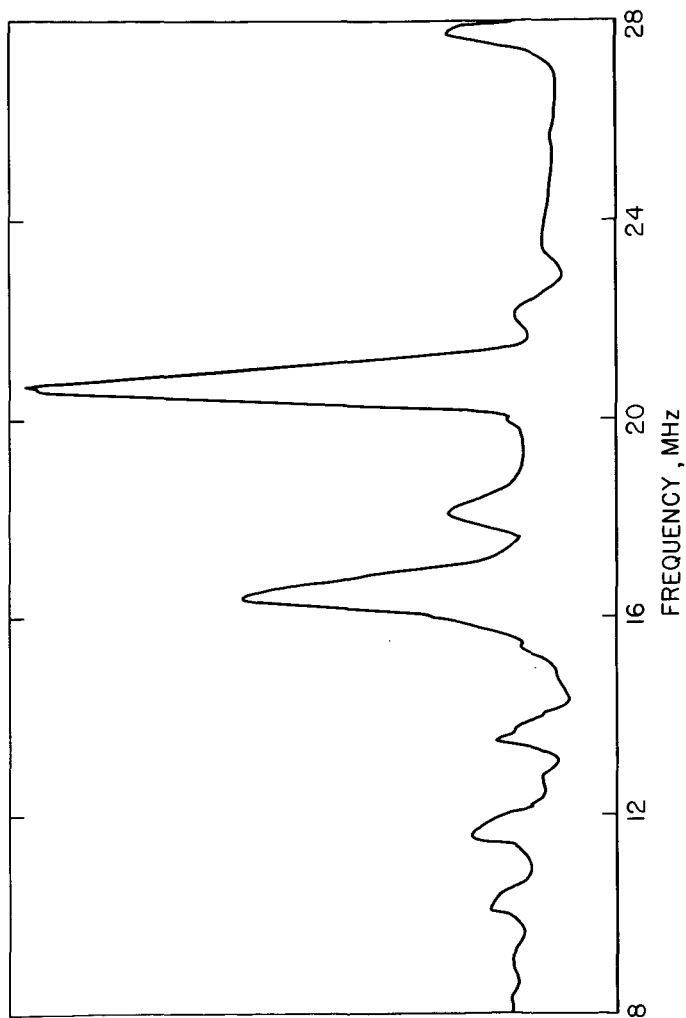


Figure 3. Electron nuclear double resonance (ENDOR) spectrum of vitrain - rich Pittsburgh coal.

2-7-78 L-15839

A Tentative Identification of Average Aromatic Ring Size in an Iowa Vitrain and a Virginia Vitrain

B. C. Gerstein, L. M. Ryan, and P. Dubois Murphy

Ames Laboratory, U. S. Department of Energy, and
Department of Chemistry, Iowa State University
Ames, Iowa 50011

Introduction

A knowledge of the average aromatic ring size in coals is useful not only in indicating the appropriate chemistry one might use for conversion to fuel oil, but also as an indicator of possible physiological effects of contact with coals and coal products. In principle, NMR offers the capability of a direct determination of average ring size via an identification of the fractions of ^{13}C and ^1H in coals. Three factors prevent use of conventional NMR for this purpose in solid coals. The first is the effect of homonuclear and heteronuclear dipolar interactions which lead to linewidths of hundreds of ppm for both ^1H and ^{13}C in solid coals^(1a,b). The second is the fact that even in the absence of dipolar broadening, chemical shift anisotropies of ^1H can be as large as 34 ppm⁽²⁾ for, e.g. the single species ^1H in $\text{H}_2\text{O}(s)$, such that a randomly oriented solid sample containing many protons in different chemical environments would exhibit an NMR spectrum in which individual protons could not be easily identified. A similar statement applies to NMR spectra of ^{13}C in solids. A third factor peculiar to coals is the possibility of an enormous number of chemically shifted species of a given nucleus, leading to NMR spectra which are still severely overlapping in the absence of broadening due to dipolar and chemical shift interactions.

In the present work, cross polarization to enhance sensitivity⁽³⁾ combined with strong heteronuclear decoupling⁽⁴⁾ and magic angle spinning⁽⁵⁾ to remove heteronuclear dipolar broadening and chemical shift anisotropy broadening are used to distinguish aliphatic from aromatic ^{13}C in Pocahontas #4 vitrain, and Star vitrain. Combined rotation and multiple pulse (NMR) spectroscopy (CRAMPS)⁽⁶⁾ are similarly used to narrow NMR spectra of ^1H in these coals. The ratios of aliphatic to aromatic ^1H and ^{13}C thus inferred are used to estimate an average aromatic ring size in the samples investigated.

Experimental

The NMR spectrometer used for determinations of spectra of both ^1H and ^{13}C has previously been described, (1a) as have the probes used for magic angle spinning^(7, 8). The Virginia coal "Pocahontas #4" was supplied by H. L. Retcofsky of the Pittsburgh Energy Research center of the U. S. Department of Energy. A vitrain portion of the Iowa coal "Star" was supplied by Dr. D. L. Biggs of the Iowa State University Department of Earth Sciences and the Ames Laboratory of the U. S. Department of Energy. The coals were analyzed for major constituents and free radical content as previously reported. (1) Results of these analyses are given in Table I.

Results

The high resolution solid state spectra of ^{13}C in both coals are shown in Figure 1. The high resolution solid state spectrum of ^1H in 2,6 dimethylbenzoic acid is shown in Figure 2, as an indication of the resolution available with equipment used in the present experiments. The high resolution solid state spectra of ^1H in both coals are

shown in Figures 3 and 4. Also indicated in Figures 2 - 4 are the Lorentzian lines used to approximate the total experimental spectra, indicated by crosses (+), and the sum of these lines indicated by the smooth curve through the experimental points.

The mole ratios of aromatic hydrogen to aromatic carbon implied by the elemental analyses given in Table I, and the fractions of aromatic to total hydrogen and carbon calculated from the results of estimating the integrated areas associated with these species as shown in Figures 2 - 4 yield the following values for (H_{Ar}/C_{Ar}): Pocahontas #4, 0.53; Star, 0.40. At first thought, these numbers seem a bit surprising, because Pocahontas, having the higher carbon content, is an older coal, and one would expect a larger ring size to correspond to the more "graphitized" material. A bit of reflection, as illustrated by the entries in Table II, might help to remove the ambiguity.

TABLE I

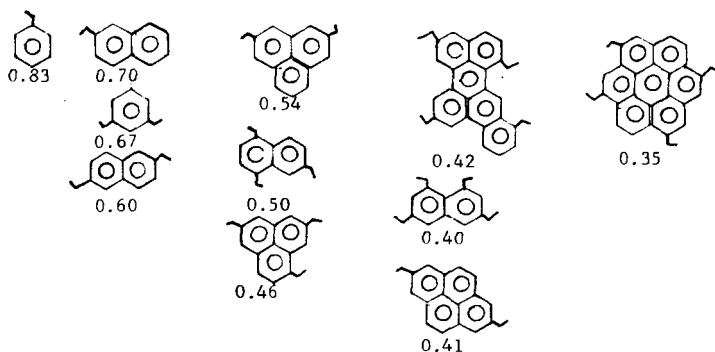
Elemental analyses, Wt% (maf), free radical concentration, and fractions of aromatic hydrogen and carbon.

SAMPLE	% C	%H	%N	%S	$[e^-]$, spins $g^{-1} \times 10^{-19}$ a	$\frac{Ar}{f_C}$	$\frac{Ar}{f_H}$
Pocahontas #4 Vitrain	90.3(2)	4.43(4)	1.28	0.85	4	0.86	0.77
Star Vitrain	77.0(1)	6.04(4)	1.17(14)	5.02	1.6	0.71	0.31

^a Determination made on unheated sample

Table II

Average aromatic ring size as a function of H_{Ar}/C_{Ar} and connectivity



The point to be made from Table II is that the average aromatic ring size inferred from the aromatic hydrogen to carbon ratios depends a good deal upon the number of side chains, or functional groups, indicated by the symbol \wedge in Table II, connected to the ring in question. We see that a value of 0.53 for this ratio is not inconsistent with an average ring size of three, with two connections per polyaromatic ring. On the other hand, a value of 0.40 is not inconsistent with an average ring size of two, with four connections per polyaromatic ring. (but is also not in disagreement with an average ring size of four to six, as indicated in the fourth column of Table II). Our present prejudice is that the average polyaromatic hydrocarbon ring size in the older coal should be greater than that in the younger. With what we feel are reasonable values for connectivities, we thus infer that the average polyaromatic hydrocarbon ring size in Pocahontas #4 is no greater than three, and that in Star no greater than two, the values thus inferred being dependent upon the assumption that on the average, the younger coal has more aliphatic chains attached to the rings. Inference from ^{13}C spectra alone yield similar values⁽⁹⁾.

One source of error in the above inferences is the fraction aromatic carbon, since it is known that not all carbon are polarized in cross polarization experiments⁽¹⁰⁾. A second most obvious source of error is the accuracy of resolving the high resolution solid state spectra of protons in these coals. The former error would tend to increase the ring size on the average, since it is quite probable that the carbons not seen in cross polarization experiments are in the neighborhood of stable free radicals, characterized by relatively large polyaromatic hydrocarbon rings. Relaxation times of protons under the spin locking conditions of the cross polarization experiments⁽¹¹⁾ may be sufficiently short to obviate effective cross polarization. Spin counting of protons with, and without strong homonuclear decoupling indicates that at least 95% of the protons in the present samples are being detected under the high resolution solid state techniques used in the present work.

ACKNOWLEDGEMENT

This work was supported by the Office of Chemical Sciences of the Division of Basic Energy Sciences of the U.S. Department of Energy.

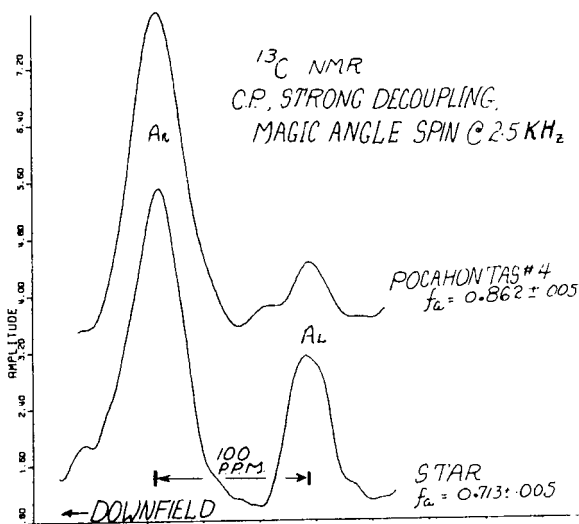


Figure 1.

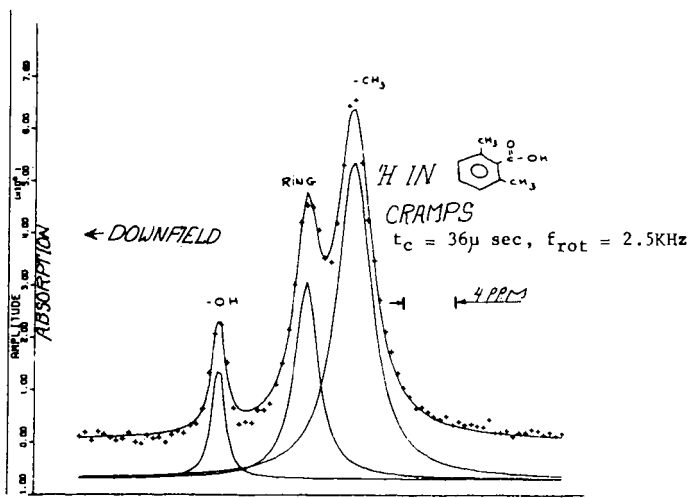


Figure 2.

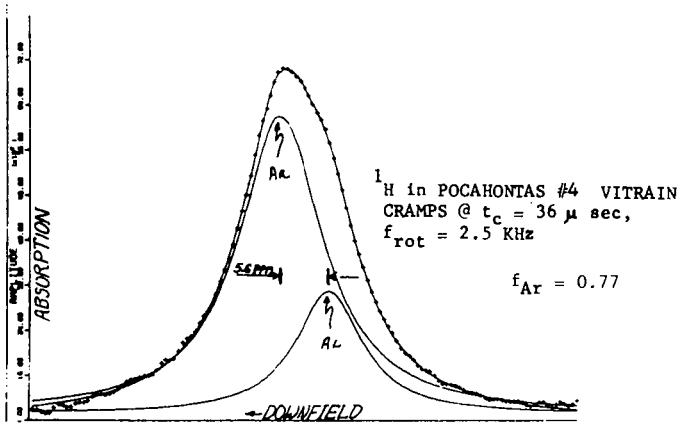


Figure 3.

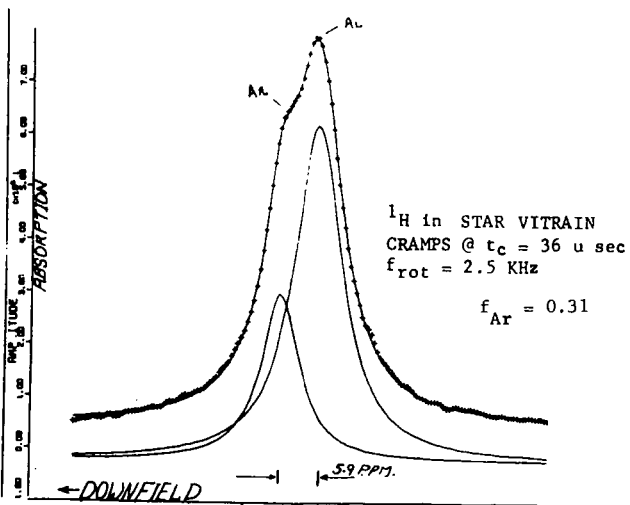


Figure 4.

References

1. a) B. C. Gerstein, C. Chow, R. G. Pembleton, and R. C. Wilson, J. Phys. Chem. 81, 565-70 (1977).
- b) H. L. Retcofsky and R. A. Friedel, J. Phys. Chem. 77, 68-71 (1973)
2. L. M. Ryan, R. C. Wilson, and B. C. Gerstein, Chem. Phys. Lett. 52, 341-4 (1977).
3. S. R. Hartman and E. L. Hahn, Phys. Rev. 128, 2042-53 (1962).
4. A. Pines, M. G. Gibby, and J. S. Waugh, J. Chem. Phys. 59, 569-95 (1973)
5. E. R. Andrew, in "Progress in Nuclear Magnetic Resonance Spectroscopy" Vol. 8, Part 1, Ed. J. W. Emsley, J. Feeney, and L. H. Sutcliffe, Pergamon Press (1971).
6. B. C. Gerstein, R. G. Pembleton, R. L. Wilson, and L. M. Ryan, J. Chem. Phys. 66, 361-2 (1977).
7. R. G. Pembleton, L. M. Ryan, and B. C. Gerstein, Rev. Sci. Instr. 48, 1286-9 (1977).
8. P. D. Murphy and B. C. Gerstein, Report #IS-4388, Iowa State University, (1978).
9. H.L. Retcofsky and D.L. VanderHart, Fuel 57, 421 (1978).
10. D.L. VanderHart and H.L. Retcofsky, Fuel 55, 202 (1976).
11. B.C. Gerstein "Fingerprinting Solid Coals Using Pulse and Multiple Pulse Nuclear Magnetic Resonance", Chapter 52, in Vol 3, Analytical Methods for Coal and Coal Products, Ed. Clarence Karr, Jr., Academic Press (circa 1979).

Temperature Dependence of ^1H NMR Absorption in Coal and Pitch

Kunio Miyazawa, Tetsuro Yokono, Yuzo Sanada

Coal Research Institute, Faculty of Engineering,
Hokkaido University, Sapporo, 060, Japan

Introduction

Many kinds of reactions such as pyrolysis, depolymerization, condensation occur simultaneously in complicated way when coal and tar pitch are heated over temperature range from 350°C to 500°C. In order to understand the processes of coal liquefaction and coal carbonization, it is important to clarify the characteristics of reaction behaviors for coal and tar pitch over the temperature range.

It is well known that pitch, solvent refined coal (SRC) and coking coal produce various kinds of mesophase at the early stages of carbonization [1-3]. The mechanisms of many chemical reactions and physical transformations relating to mesophase formation are studied by quenching techniques. Such research techniques as polarized light-microscopy and so on can be extremely fruitful. On the other hand, direct observation of phenomena at reaction temperatures may yield more easily interpretable or more relevant results. Line shape of NMR corresponding to mobility of molecule and/or segment in coal and tar pitch have been measured at the temperature range of mesophase formation.

No report has been appeared on direct measurement of change of hydrogen aromaticity (f_{Ha}) at higher temperature occurring pyrolysis and carbonization. This paper deals with observation of resolved NMR spectra corresponding to aromatic and aliphatic protons at high temperatures in a tar pitch. High resolution NMR spectra for thermally decomposed polyvinyl chloride were observed by S. Shimokawa et al. [4] over the temperature range from 350°C to 450°C using the same apparatus at Hokkaido University.

Experimental

The experiments were done by using a Bruker Sxp 4-100 pulsed Fourier transform (FT) spectrometer with a high temperature probe and an improved JEOL 3H electromagnet (0.88T) with a 60 mm gap operating at 36.4 MHz for the ^1H NMR. In order to improve the resolution of a spectrum at high temperatures, a home-built shim system was used [4]. Outlines of the high temperature probe and flowing gas system are illustrated in Fig. 1. The samples as received were heated in the high temperature probe and NMR spectra were obtained simultaneously. No heat-treatment was done before measurements. Kureha pitch was heated at 10°C min⁻¹ and the others were heated at 5°C min⁻¹ to various given temperatures under nitrogen gas flushing. In the case of the resolved NMR spectra for ethylene tar pitch, the heating rate employed was 2°C min⁻¹. Characteristics of all samples so far studied are shown in Table 1.

Results and discussion

Temperature dependence of molecular and/or segmental motion

Representative proton NMR spectra for coals and solvent extracts from coal are shown in Fig. 2. Apparently, there is no structure in the lines. Increasing temperature produces changes in the spectra. In order to discuss the broadening behavior quantitatively, the values of the line widths at half-height ($\Delta H_{1/2}$) were utilized. Temperature dependence of $\Delta H_{1/2}$ is shown in Fig. 3. It is obvious that there are three different groups with respect to temperature dependence of $\Delta H_{1/2}$. The value of $\Delta H_{1/2}$ of the first group to which Taiheiyō coal belongs decreases and then increases rapidly with increasing temperature. The behavior of $\Delta H_{1/2}$ of the second group, Yubarishinko coal and β -component (pyridine soluble, chloroform insoluble fraction of a coal [5]) of Yubarishinko coal, resembles that of the first group, but the curve of $\Delta H_{1/2}$ is shifted to higher temperatures. The third group, which includes γ -component (pyridine soluble, chloroform soluble fraction of a coal [5]) of Yubarishinko coal, coal tar pitch and ethylene tar pitch, indicates that the values of $\Delta H_{1/2}$ remain small over

a wide temperature range. This suggests that the molecules and/or segments in them are mobile throughout the temperature range.

The carbonization process at low temperatures has been studied by the method of polarized-light microscopy. The formation of low temperature carbons by solidification from a liquid phase proceeds through the separation of an optically anisotropic mesophase.

Optically anisotropic textures of mesophase from the samples heat-treated at the early stages of carbonization are classified into five types corresponding to isotropic, fine mosaic, coarse mosaic, fibrous and domain. It has been found that there is a close relation between the spin-lattice relaxation time, T_1 , observed with pulsed FT NMR at room temperature and microstructure of mesophase, transformed from the parent matrix of coal. That is, the longer the relaxation time is, the more sufficient the growth of mesophase from the matrix occurs as shown in Table 1. The parent materials, which give the fibrous/domain texture at the early stages of carbonization, have the longest relaxation time so far as being described in the table. There is also an excellent relation between the microstructure of mesophase and the temperature dependence of $\Delta H_{1/2}$. The minimum value of the line width at half-height with respect to the temperature dependence of $\Delta H_{1/2}$ is expressed as $\Delta H_{1/2, \min}$ and used for characterization of mesophase texture. $\Delta H_{1/2, \min}$ of isotropic mesophase is larger than that of coarse or fibrous/domain mesophase and the temperature of isotropic mesophase corresponding to $\Delta H_{1/2, \min}$ is lower than that of fine mosaic mesophase. The values of $\Delta H_{1/2}$ in coarse mosaic or fibrous mesophase keep small over a wide temperature range (see Fig. 3). But no distinction was observed between coarse mosaic and fibrous textures concerning the broadening behavior of NMR.

Regarding the concentration of free radicals and the line width, these values remain almost constant up to about 400°C for coals of different rank [6]. Therefore, it seems that the contribution of free radicals on the NMR line width is not so important as that of the proton dipole-dipole interaction.

At higher temperatures we estimate the value of T_1 following equation,

$$t = T_1 \ln 2$$

where t is the time at the amplitude of the Free Induction Decay (FID) following the 90° pulse being equal to zero. Pulse sequence used was 180°- τ -90° in this experiment.

Fig. 4 shows the relation between the T_1 of ethylene tar pitch and the inverse of temperature. T_1 of ethylene tar pitch has the value of 400 ms at room temperature. It decreases with the increase of temperature, and reaches a minimum value at about 150°C. As is shown in the figure, T_1 has a maximum value of 190 ms at 340°C, and decreases rapidly with the increase of temperature.

It is clearly marked that the aromaticity of ethylene tar pitch increases with increase of temperature at 340°C and the formation of mesophase for the sample heat-treated becomes observable by an optical microscope. Rotational correlation time for aromatic lamellae, which are stacking parallel each other in the mesophase, is long due to being in rigid state. Accordingly T_1 becomes short. However, more detailed discussion will be made with further experiments.

NMR line simulation by means of computer

A proton NMR spectrum from Kureha pitch at 450°C (15 min) (a) and a comparison of the experimentally observed spectrum with a computer simulated spectrum (b) are illustrated in Fig. 5. The spectrum (a) contains considerable intensity in the wings of the line, and the ratio of the width at one-eighth height to that at one-half height, indicated by the symbol $R(8/2)$, is 6.4. The ratio for a pure Lorentzian line is 2.64 and for a pure Gaussian line is 1.73 [7]. By means of computer simulation the NMR line for the mesophase in Kureha pitch is composed of at least three different components, i.e. one Gaussian component with value of proton spin-spin relaxation time $T_2=7$ microseconds and two Lorentzian components with those of $T_2=210$ and 636 microseconds at 36.4 MHz, respectively. The fractions are also estimated as 0.85, 0.05 and 0.10, respectively. Kureha pitch at the early stages of carbonization contains 85 percent rigid structures from the view point of general NMR behavior [8].

In some liquid crystal systems broad partially resolved spectra with little structure attributed to proton dipole-dipole interaction have been observed [9-11]. On the other hand, such spectra were not observed in this study, so that the

ordering parameters of the samples employed would be expected to be very small. This result is compatible with that of ESR study reported by Yamada et al. [12].

Resolved NMR spectra at thermal decomposition temperature

In order to improve the resolution at higher temperature, a home-built shim system was attached with the magnet of NMR spectrometer. Typical ^1H NMR spectra for ethylene tar pitch are shown in Fig. 6. On heating at about 84°C , a broad resonance with no resolved structure becomes observable. And then at about 123°C , the NMR spectrum shows two discrete lines apparently, 200 Hz apart. That is, the lines correspond to the resonance due to aromatic and aliphatic protons. Assignment of the two peaks was done by comparing with the ones of a pure compound, acenaphthylene, which has the value of 0.75 hydrogen aromaticity (f_{Ha}). At about 208°C , the NMR spectrum becomes narrow and separately due to the rapid tumbling of molecule in ethylene tar pitch. This suggests that the molecules exhibit the random motion similar to that in isotropic solution and the value of the dipolar tensor over all orientation in them is almost zero in the vicinity of this temperature. However, fine structures due to the protons attached to α , β and γ carbons refer to aromatic rings were not able to observe at the higher temperatures, because of superposition of protons having various chemical shifts.

The intensity of aliphatic protons is higher than that of aromatic ones up to 208°C , at which the intensity change is observable. The values of f_{Ha} are able to elucidated from the intensity of the splitted spectra. However, two lines merge and broaden raising at about 430°C . Heating of the specimen at higher temperatures accelerates the degree of broadening of the spectrum. Therefore, it is difficult to observe the spectrum in the range of a usual high resolution NMR sweep width.

The spectrum obtained with a wider sweep width (25kHz) are shown in Fig.

7. For the spectrum in the figure, the ratio of the width at one-eight height to that at one-half height, indicated by the symbol $R(8/2)$, is 7.0. This line shape is designated as "Super Lorentzian" [13] which contains considerable intensity in the wings of the line. After the measurement of the NMR spectra at 470°C , the sample was immediately quenched to room temperature and observed by polarized light-microscopy. And it was confirmed that the bulk mesophase was produced at 470°C .

When a magnetic field is applied, it is known that the direction of alignment of c-axes of mesophase spherules is aligned perpendicular to that of the magnetic field by interacting magnetic anisotropy of polycondensed aromatic molecules with the magnetic field applied [14]. On heating of ethylene tar pitch beyond 430°C in a magnetic field, a dipolar tensor is only partially averaged due to less chaotic molecular motion in a magnetic field. Resulting line becomes broad but is not as broad as solid. The structure of the mesophase produced in an NMR magnetic field is more rigid than that of isotropic liquid.

Table 2 summarizes range of sweep width for various NMR type at 36.4 MHz of resonance frequency. Generally, the sweep width of broad line NMR is the order of $10^5 \sim 10^6$ Hz, while that of high resolution NMR is about 10^3 Hz at 36.4 MHz for a proton. But the NMR spectrum of the mesophase obtained from ethylene tar pitch shown in Fig. 7 was swept over 2.5×10^4 Hz. Thus, the sweep width of the NMR spectrum for the carbonaceous mesophase is intermediate between those of broad line NMR and high resolution NMR. It seems that the result is supported by that obtained by J. J. Fink et al. [15]. They have measured the line width of 2.3×10^{-4} to 3.1×10^{-4} T for conventional nematic and smectic liquid crystals.

Conclusion

It could be concluded from the above results that the materials which give spherical mesophase on heating show a narrowing of the NMR with increasing temperature which corresponds to so-called softening and plastic stages. Moreover, the degree of motional narrowing of the proton NMR spectra reflects the degree of fluidity at the plastic stage. The temperature dependence of hydrogen aromaticity would be monitored directly by using the NMR high temperature technique.

Chemical reactions such as pyrolysis, depolymerization, condensation could be clarified. Moreover, application of the technique seems to be promising in the mechanism of coal liquefaction as well as that of mesophase formation.

Acknowledgement

The authors express their sincere thanks to Messrs. S. Shimokawa and E. Yamada for the experimental assistance and helpful discussion.

References

- [1] J. D. Brooks and G. H. Taylor, *Carbon*, 3, 185 (1965)
- [2] H. Honda, H. Kimura, Y. Sanada, S. Sugawara and T. Furuta, *Carbon*, 8, 181 (1970)
- [3] J. Dubois, C. Agache and J. L. White, *Metallography*, 3, 337 (1970)
- [4] S. Shimokawa and E. Yamada, *J. Phys. Chem.*, submitted
- [5] R. V. Wheeler and M. J. Burgess, *J. Chem. Soc.*, 649 (1911)
- [6] J. Smidt and D. W. van Krevelen, *Fuel*, 38, 355 (1959)
- [7] C. P. Poole, Jr. and H. Farach, *The Theory of Magnetic Resonance*. John Wiley & Sons, Inc. (1972)
- [8] A. Abragam, *The Principles of Nuclear Magnetism*, Clarendon Press, Oxford (1961)
- [9] A. Saupe and G. Englert, *Phys. Rev. Letters*, 11, 462 (1963)
- [10] K. R. K. Easwaran, *J. Mag. Res.* 9, 190 (1973)
- [11] J. C. Rowell, W. D. Phillips, L. R. Melby and M. Panar, *J. Chem. Phys.*, 43, 3442 (1965)
- [12] Y. Yamada, K. Ouchi, Y. Sanada and J. Sohma, *Fuel*, 57, 79 (1978)
- [13] K. D. Lawson and T. J. Flautt, *J. Phys. Chem.*, 72, 2066 (1968)
- [14] L. S. Singer and R. T. Lewis, 11th Biennial Conference on Carbon, Gatlinburg, Tennessee, Prepring, CG-27 (1973)
- [15] J. J. Fink, H. A. Moses and P. S. Cohen, *J. Chem. Phys.*, 56, 6198, 1972
- [16] T. Yokono, K. Miyazawa and Y. Sanada, *Fuel*, 57, 555 (1978)
- [17] T. Yokono and Y. Sanada, *Fuel*, 57, 334 (1978)

Table 1
Characteristics of samples used

Sample	weight % (d.a.f.)					f_a 1)	T_1 (ms) 2)	Optical texture in carbonized coal
	C	H	N	S	O			
Taiheiyō coal	77.0	6.0	1.4	0.1	15.5	0.70	18	isotropic
Hongei coal	93.1	3.2	1.0	2.7	-	0.70	58	isotropic
Miike coal	83.5	6.2	1.2	1.8	7.3	-	421	fine mosaic
Yubarishinko coal	86.6	5.9	2.0	0.3	5.2	0.80	438	fine mosaic
β-component of Yubarishinko coal	82.2	5.7	2.2	-	-	0.78	531	fine mosaic
γ-component of Yubarishinko coal	87.8	7.0	1.5	-	-	0.80	719	coarse mosaic
Kureha pitch	95.2	4.2	0.1	0.2	0.3	0.86	952	fibrous/domain
Ethylene tar	94.3	5.5	0	0.1	0.1	0.78	1103	fibrous/domain
Coal tar pitch	92.1	4.8	1.3	0.3	1.5	0.83	1560	fibrous/domain

1) values obtained from proton spin-spin relaxation time at -100°C [16]

2) proton spin-lattice relaxation time [17]

Table 2
 Range of sweep width for various NMR at 36.4 MHz of
 resonance frequency [$H_0=0.88T$]

NMR	Range of sweep width (Hz)
High resolution	10^3
Intermediate	10^4
Broad line	$10^5 \sim 10^6$

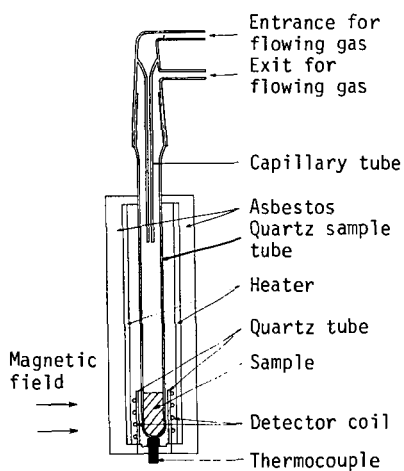


Fig. 1 Outlines of the high temperature probe and flowing gas system.

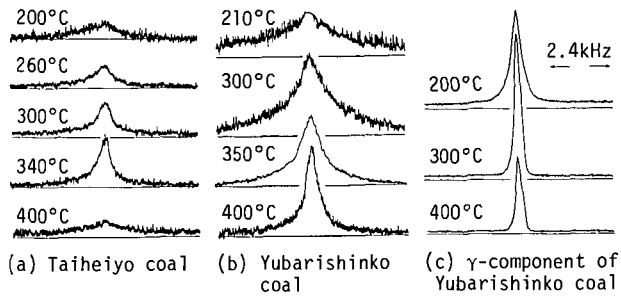


Fig. 2 Proton NMR spectra of Taiheiyo coal (a), Yubarishinko coal (b) and γ -component of Yubarishinko coal (c) at high temperatures.

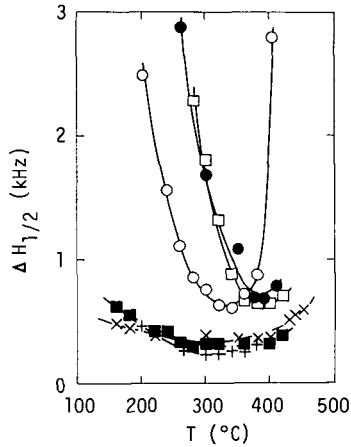


Fig. 3 Temperature dependence of the line width at half-height ($\Delta H_{1/2}$):
 ○ Taiheiyo coal, ● Yubarishinko coal,
 □ β -component of Yubarishinko coal,
 ■ γ -component of Yubarishinko coal,
 + Coal tar pitch and × Ethylene tar pitch.

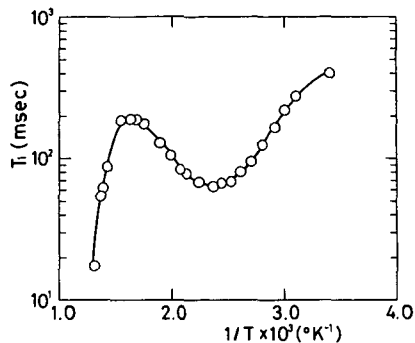


Fig. 4 Temperature dependence of spin-lattice relaxation time (T_1) of ethylene tar pitch.

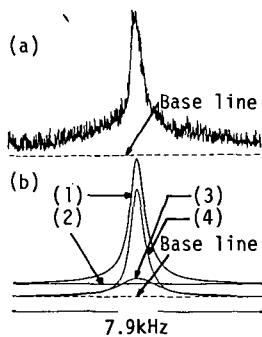


Fig. 5 A proton NMR spectrum of Kureha pitch at 450°C (for 15 min) (a) and a comparison of the experimentally observed spectrum with a computer simulated spectrum (b): (1) Total simulated curve, (2) Gaussian component with $T_2=7 \mu\text{s}$, (3) Lorentzian component with $T_2=210 \mu\text{s}$ and (4) Lorentzian component with $T_2=636 \mu\text{s}$.

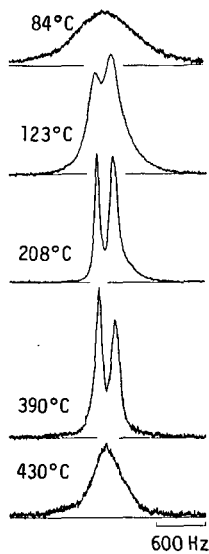


Fig. 6 Proton NMR spectra of ethylene tar pitch at high temperatures.

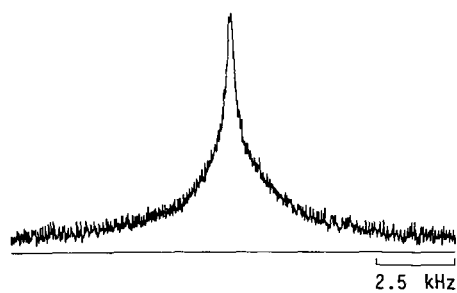


Fig. 7 A proton NMR spectrum of ethylene tar pitch at 470°C.

MAGNETIC RESONANCE STUDIES OF LABELED GUEST MOLECULES IN COAL

L. B. Ebert, R. B. Long, R. H. Schlosberg, and B. G. Silbernagel

Corporate Research Laboratories, Exxon Research and Engineering Co.
P.O. Box 45, Linden, NJ 07036

We have used magnetic resonance techniques to probe the time scales of motion for a series of labeled guest molecules imbibed in subbituminous Wyodak and bituminous Illinois #6 coals. Nuclear magnetic resonance (NMR) was used to study a suite of such guests which were either deuterated or fluorinated, while electron spin resonance (ESR) was used to examine paramagnetic TEMPOL spin labels. These labeled guest molecules can be observed directly with a minimum amount of interference from the nuclei and paramagnetic species naturally occurring in the coal. By choosing a variety of differently labeled species, a broad range of time scales for molecular motion can be examined. The rate and nature of the motion provides information about the environment of the guests in the coal structure.

Dry coal samples (10-20 mesh) were exposed to various solvent vapors while contained in closed jars. The solvent uptake was monitored by periodic weighing of the sample during the exposure period. As shown for C_6H_6 and C_5H_5N in Illinois #6 coal (Figure 1), the uptake pattern depends upon the choice of solvents: benzene uptake approaches an asymptotic value in roughly one week while pyridine continues to be included over a much longer time period. The amounts of imbibed labeled molecules in the coals used for the present study, shown in Table 1, range from ~ 0.1 - ~ 10 m mole of solvent/gm of coal.

In most liquids, rapid molecular motion causes averaging of the interactions between nuclear and electronic spins and their environment. If the rate of motion becomes sufficiently slow, these interactions are no longer averaged and a change in the magnetic resonance signal, typically a broadening, is observed. This averaging process has been studied in many liquids and solids and relatively simple theories have been developed which predict the characteristic times for motion required for the onset of averaging for different electronic and nuclear spins (1). For example, in 2-fluoropyridine the ^{19}F NMR is broadened by dipolar interactions, principally with protons on the same molecule, and motion on a time scale shorter than 250μ sec is needed to average the interaction. For the $-CF_3$ components of hexafluoropropanediamine, this characteristic time is $\sim 100 \mu$ sec. The 2H nuclei in deuterated labels are broadened by the stronger nuclear electric quadrupolar interaction and more rapid motion ($\sim 5 \mu$ sec) is required for averaging. Interactions of the much larger electronic moments in the paramagnetic TEMPOL spin labels require times on the order of 10^{-8} sec to be averaged. A combination of these labels allows us to survey rates of motion which vary by over a factor of one million.

The derivative of the ^{19}F NMR absorption of 2-fluoropyridine in Illinois #6 coal is shown in Figure 2. A narrow NMR line is seen at 300K, with no evidence for the broad component which would indicate molecules moving more slowly than 250μ sec. No broad 2H NMR line is seen in coal samples containing D_2O . However both broad and narrow components are seen in coals with C_6D_6 and C_5D_5N guests. The derivative of the 2H NMR for C_6D_6 in Illinois #6 is shown in Figure 3. The same data is displayed at two levels of gain to show the two satellites which occur on either side of the intense central component. Very roughly, comparable numbers of nuclei contribute to the narrow and broad components. The C_6D_6 molecules contributing to the central absorption are moving on time scales shorter than 5μ sec and the 2H quadrupole interaction is completely narrowed. The satellite splitting for the broad C_5D_5N component is twice as large as in the C_6D_6 case. From the

magnitudes of these broad spectra (2) we infer that the C_6D_6 molecules are still spinning about their C_6 symmetry axis at times shorter than 5μ sec, while the C_5D_5N molecules are not. The restricted motion of this class of C_6D_6 molecules suggests that they may be sterically confined by the nearby coal matrix. The absence of rapid motion for this class of C_5D_5N molecules may reflect a chemical interaction between the molecules and the coal matrix.

ESR studies of the TEMPOL spin label also show this slowing down process in the coal. Immediately after adding a TEMPOL solution to a coal sample, a narrow triplet ESR signal from the TEMPOL in the liquid is super-imposed on the carbon radical signal in the coal (Figure 4A). The narrow TEMPOL lines broaden as time passes while the total EPR signal does not change, again implying the loss of averaging due to slower motion of the molecules (Figure 4B). The characteristic time of motion is therefore longer than 2×10^{-8} sec. The reduction of the narrow triplet signal intensity (Figure 4C) is proportional to $\exp(-\alpha t^{1/2})$ suggesting that this slowing of the motion reflects diffusion of the TEMPOL labels into the coal.

Pulsed NMR studies of the narrow component of the resonance line also show the change in motion of a molecule when introduced into the coal solid. The energy exchange between ^{19}F nuclei in 2-fluorophenol and their environment was determined in the free liquid and for molecules included in coal by using spin lattice relaxation (T_1) measurements. T_1 is frequency independent for both systems, but the relaxation time is much shorter for the guest molecules in coal: $T_1 = 13 \pm 3$ m sec, in comparison with $T_1 = 1.5 \pm 0.3$ sec for the free liquid at the same temperature (300K). These data imply characteristic times of motion for the guest species. A factor of 100 slower than for the free species.

In summary, a combination of labeled molecular probes and different observation techniques provides information on the environment and motion of molecular species in coal. The range of characteristic times of motion is indicated schematically in Figure 5. As illustrated in the case of the spinning C_6D_6 molecules, the type of the motion may also be deduced in some cases.

REFERENCES

1. This averaging phenomenon is discussed by A. Abragam, "Principles of Nuclear Magnetism" (Oxford, 1961), Chapter X.
2. See R. G. Barnes in "Advances in Nuclear Quadrupole Resonance", J. A. S. Smith, Ed. (Heyden and Sons, London, 1974), v. 1, p. 235 ff.

TABLE 1: MOLECULAR UPTAKE DURING THE SWELLING PROCESS

Coal Type	Imbibing Molecule	Millimoles Imbided/Gram of Coal
Wyodak:	D_2O	8.49
	C_5D_5N	8.93
	C_6D_6	1.26
Illinois #6:	D_2O	5.79
	C_5D_5N	6.21
	C_6D_6	2.08
	2-Fluorophenol	4.83
	4-Fluorophenol	1.88
	2-Fluoropyridine	6.09
	C_2F_6	0.47
	Hexafluoro Propane Diamine	0.29

Figure 1:
Examples
of the
Swelling
Process:

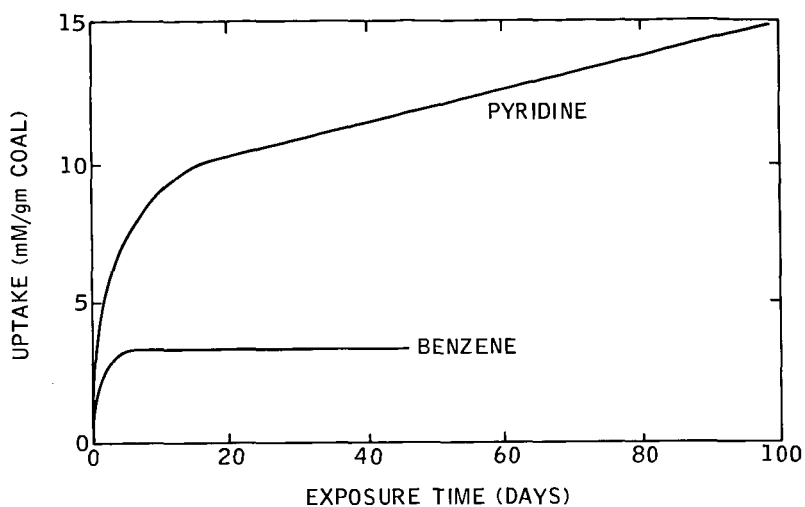


Figure 2: The ^{19}F
NMR of Illinois #6
Coal swelled with
2-fluoropyridine
shows only a narrow
component.

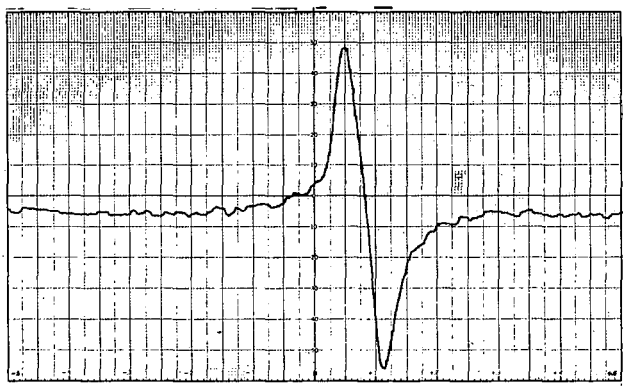


Figure 3: Both narrow
and broad ^{2}D NMR
signals are observed in
Illinois #6 coal
swelled with C_6D_6 .

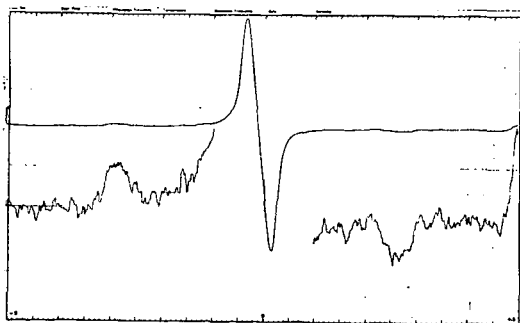
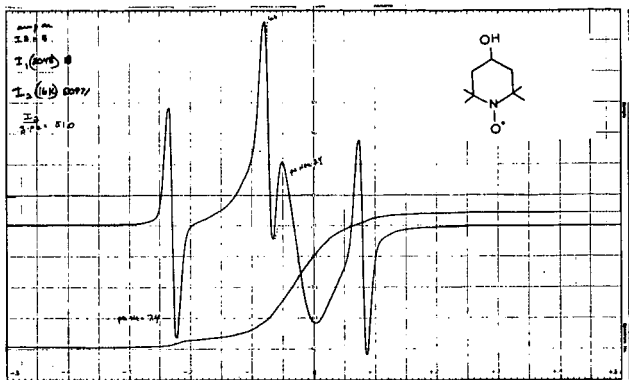
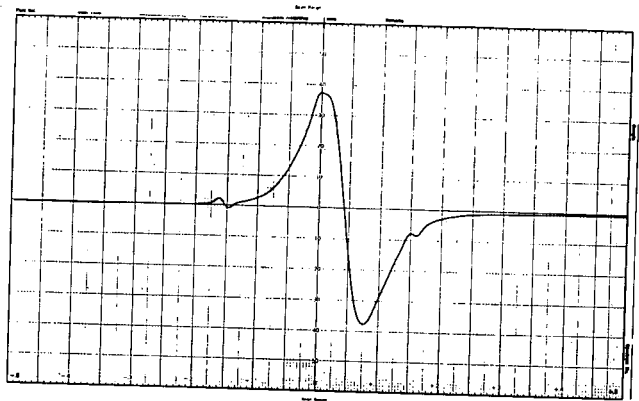


Figure 4: Coal Swelling with a paramagnetic spin label (TEMPOL)

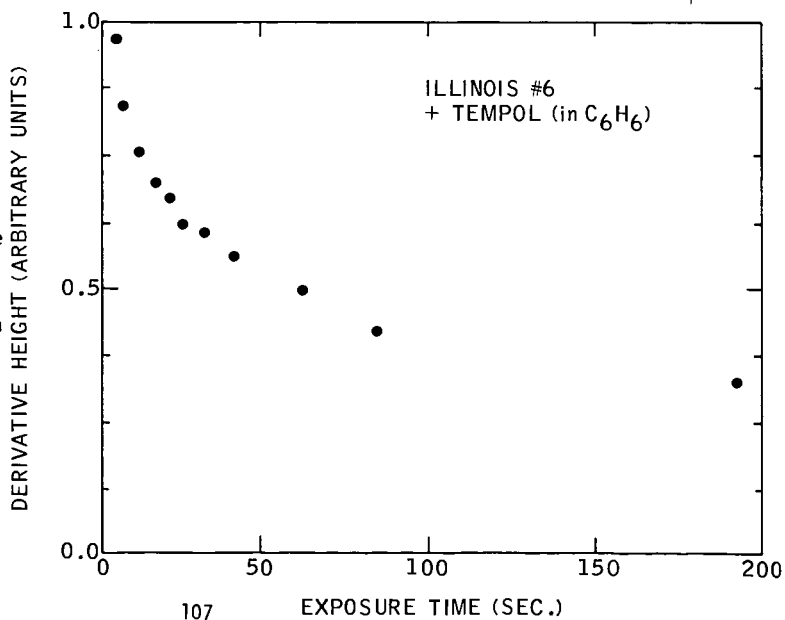
A. Upon initial exposure of TEMPOL to coal, the narrow spin label triplet signal is superimposed upon the carbon radical signal from the coal.



B. At long times, only a trace of the triplet TEMPOL signal remains.



C. An example of the loss of TEMPOL signal intensity with time for Illinois #6 coal exposed to a solution of TEMPOL in benzene.



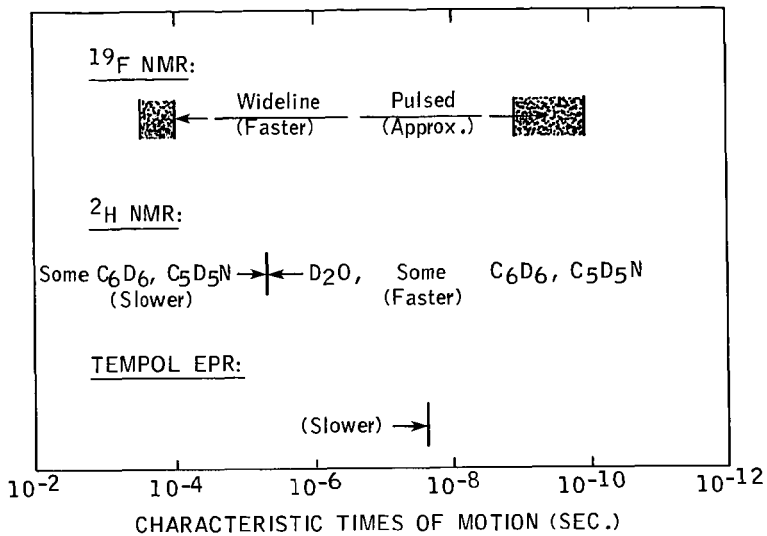


Figure 5: A survey of characteristic times of motion probed by the current labeled molecules.

CARBOXYLIC ACIDS AND COAL STRUCTURE. A. L. Chaffee, G. L. Perry and R. B. Johns.
School of Chemistry, University of Melbourne, Parkville, Victoria 3052, Australia.

The emphasis will be on fatty acids, particularly monocarboxylic and dicarboxylic acids as environmental indicators. Fatty acid data will be presented for a number of Lithotypes of Brown Coal from the LaTrobe Valley, Victoria, and a series of Australian Black Coals of varying rank. For the Brown Coal the relationship between fatty acids and Lithotype (which is believed to reflect the environment by deposition) will be discussed. The diagenetic changes which fatty acids in the coal structure undergo with depth of burial will also be discussed in relation to Lithotypes.

Structural Characterization of Coal: Lignin-Like Polymers in Coals

Ryoichi Hayatsu, Randall E. Winans, Robert L. McBeth,
Robert G. Scott, Leon P. Moore, and Martin H. Studier

Chemistry Division
Argonne National Laboratory, Argonne, Illinois 60439

INTRODUCTION

Although lignins are major constituents of vascular plants from which coals are derived, their roles in the coalification process and resulting coal structures have not been defined. On the basis of chemical and biological degradations, lignins are considered to be polymers of propylphenyl compounds, coniferyl alcohol and related alcohols (1-3). Because of their great abundance, high resistance to biological degradation and characteristic occurrence in land plants, isolation of coal degradation products related to these lignin compounds should shed some light on the roles, if any, played by lignins during coalification and in the final structure of coals. To date such studies have had only limited success.

Although fulvic and humic acids have been degraded successfully with alkaline solutions to produce lignin-related phenols (4-6), this method has not proved to be useful for coals. Reductive degradations of soil and coal-derived humic acids with sodium amalgam have been reported to produce a variety of phenolic compounds (9-10); however, several investigators have found that this procedure gives only a few phenols in very small amounts, because of the degradation of phenolic rings (11-12).

Many oxidative degradations have also been carried out to break coal down into simpler species; however, isolation and identification of phenols such as p-hydroxybenzene derivatives, vanillic and syringic groups, which are characteristic lignin oxidation products, have not been definitely confirmed yet. In general, commonly used oxidants destroy phenolic rings or give complex products (13-15). Some of the oxidants such as nitrobenzene produce reaction by-products that may interfere with the analysis of the oxidation products (16-18). To obtain lignin oxidation products from coals, we resorted to the alkaline cupric oxide oxidation method which has been successfully applied to analysis of lignins in plants (16), fulvic and humic acids (18-19), and land-derived marine sediments (16).

EXPERIMENTAL

Seven coals were used in this study (Table 1). To remove trapped organic materials (20-21), four coals (samples 1-4) were extracted with benzene-methanol (3:1, refluxing for 48 hours) and 2.5% aq.-NaOH (20-35°C for 16 hours) before oxidation. Since the alkaline extractable material was found to be negligible for samples 5-7 these coals were only extracted with benzene-methanol.

Each coal sample (5g) was oxidized with alkaline cupric oxide (51.9 g of $\text{CuSO}_4 \cdot 5\text{H}_2\text{O}$, 37.3 g of NaOH and 185 ml of H_2O) at 200°C for 8-10 hours* by the method of Greene et al. (22). After the reaction mixture had cooled, it was centrifuged. The alkaline supernatant was acidified with HCl to pH 2. After concentration of the acidic solution, the slushy residue was repeatedly extracted with benzene-ether (1:3). The residue was further extracted with methanol. Materials soluble in alkali only were also isolated from all samples. To recover non-oxidized coal, the alkaline insoluble residue was treated several times with concentrated HCl, and finally washed with water. A summary of the oxidation products is shown in Table 2.

Solid probe mass spectrometric analysis (20) showed that the benzene-ether extracts consist mainly of organic acids. Therefore, these extracts were derivatized with d₆-dimethylsulfate to yield d₃-methyl labelled derivatives. The derivatives were analyzed by GC-TOFMS and high resolution MS using techniques which have been previously described (20). Authentic samples of phenolic acids derivatized with d₆-dimethylsulfate or diazomethane were also analyzed by GCMS for reference.

Gas chromatograms of the derivatives obtained from samples 1 and 2 are shown in Fig. 1a and in Fig. 1b with numbered peaks identified in Table 3. The methanol extracts and fractions soluble in alkali only were found to consist essentially of humic acid-like materials by solid probe MS.

To obtain detailed information of the CuO-NaOH oxidation, control experiments with 15 model compounds and a polymer were carried out using the procedure employed for the coals. The results are shown in Table 4.

RESULTS AND DISCUSSION

As shown in Table 2 and in Table 3, most informative is the identification of large amounts of p-hydroxy and 3,4-dihydroxybenzoic acids in the oxidation products of samples 1 and 2. These are regarded as lignin oxidation products. It is interesting to note that, while no o- and m-hydroxybenzoic acids were found in the oxidation products of samples 1 and 2, all three isomers were identified in small amounts in other rank bituminous coals (samples 3, 5, 6). From sample 3, 3,4-dihydroxybenzoic acid was also isolated in small amount, however this compound was not detected in the oxidation products of other bituminous coals (samples 4-6).

It is interesting that bituminous (sample 4) gave organic acids qualitatively similar to those of lignite coal (see Table 2).

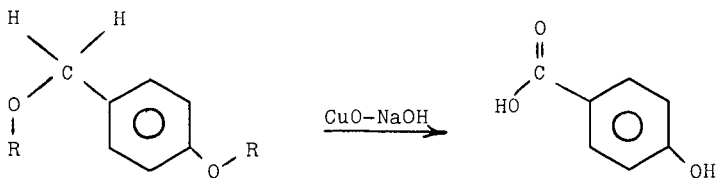
* In general, lignin, plant materials, fulvic and humic acids and marine sediments are oxidized at 170°C for 3-4 hours, however this condition has been found to be not strong enough to oxidize coals.

identified compounds were p-hydroxybenzoic acid, 4-hydroxy-1,3-benzenedicarboxylic acid, benzene di and tricarboxylic acids. No o- or m- isomer of hydroxybenzoic acid was detected. We have found that solvent extractable hydrocarbons obtained from this coal consist mainly of n-alkane (C₁₁ to C₃₁). This is quite different from other results which showed that aromatic hydrocarbons were the major solvent extractable material of several bituminous and anthracite coals (20,23). Indeed, petrographic analysis shows that this coal has a high content of sporinite (14.3 wt %) and low content of vitrinite (30.2 wt %) (24). Anthracite coal (sample 7) did not yield any organic solvent extractable oxidation products.

Some acids not found in oxidation products of lignins, land plants and marine sediments were found in the oxidation products of coals. Among these were phenolic di and tricarboxylic acids and hydroxynaphthalenecarboxylic acids. From some soil fulvic and humic acids, phenolic polycarboxylic acids have been found in the oxidation products together with considerable amounts of fatty acids. Therefore, phenolic esters of fatty acids are considered to be present in these soil acids (5,18). However, little or no fatty acids were observed in the coal oxidation products.

Trihydroxybenzoic acid or its methoxy derivatives (syringic group) which are obtained from the oxidation of lignins, fulvic and humic acids and marine sediments were not found in any of our oxidation products. We have found that the authentic syringaldehyde and 2,6-dimethoxyphenol were largely degraded by the oxidation (Table 4). This may account for the fact that we did not observe them, however the syringic groups may have been degraded during coalification.

All phenolic acids identified were found as OCD₃-derivatives. The mass spectra showed the complete absence of OCH₃-group. It is confirmed that no isotope exchange of the H in OCH₃ with D occurred under our procedures. Although partial demethylation reaction during the oxidation cannot be excluded from the control experiment (see Table 4), it is probable that the phenolic acids found were derived mainly from the fission of ether linked aromatic systems as shown in the example below rather than from aryl methoxy units.



R = alkyl (C \geq 2), aryl

Indeed, it is known that very little or no methoxy groups are present in bituminous coals (25-26). In the lignite coal (sample 1) aryl methoxy groups are not present in significant amounts (26).

Nonhydroxy benzene, naphthalene, pyridine and thiophene carboxylic acids and humic acid-like materials found in the oxidation products might be derived from non-lignin or extensively transformed lignin polymers.

The oxidation of methyl groups of aromatic compounds has been found to be ineffective. Therefore, relatively large amounts of methyl-substituted phenolic and benzene carboxylic acids were isolated from the coal oxidation. Our control experiments also indicated that, while the CuO-NaOH oxidation of alcohol, aldehyde, ketone, quinone and ether is effective, methyl groups and methylene bridges are not oxidized significantly.

CONCLUSIONS

1. Although one cannot rule out the possibility that plant polyphenols (27) could be one of the important precursors for coal formation, the present work shows that lignin-like polymers have been incorporated into the macromolecules of coals, and are still identifiable in lower rank coals. Evidence for this is the identification of p-hydroxy- and 3,4-dihydroxy-benzoic acids which are known lignin oxidation products.

2. The lignin-like polymers contain more highly cross-linked structures increased in aromaticity compared with the original lignins. Phenolic polycarboxylic acids and hydroxynaphthalene-carboxylic acids which were identified are not found in the CuO-NaOH oxidation products of lignins and plant materials.

3. It is obvious that extensive transformation of lignin-like polymers occurred perhaps through reactions (28-29) such as demethylation, demethoxylation, dehydrogenation, oxidation, cleavage of ring structures, re-condensation, etc. during coalification from lignite to bituminous and anthracite coals. This is shown by the fact that (a) lower rank coals gave higher yields of the CuO-NaOH oxidation products; (b) higher phenolic acid/benzenecarboxylic acid ratio is shown for the lower rank of coals; (c) very little or no dihydroxy-benzoic acid was identified in the oxidation products of higher rank coals (samples 3-6); (d) more naphthalene- and heterocarboxylic acids are found in the oxidation products of higher rank coals. Finally, major parts of lignin-like polymers are transformed into non-lignin type polymers at later stage of coalification. Indeed, the later coalification product, anthracite coal (sample 7) did not yield any phenolic acid by the oxidation.

4. In a previous paper (21) we characterized aromatic acids trapped in lignite coal, and have found that these acids are qualitatively quite similar to those obtained from the present oxidation of the same pretreated coal. This indicates that the trapped acids were derived mainly from the oxidative degradation of lignin-like polymers during the coalification. We have also observed that no trapped organic acid is isolated from the anthracite coal which no longer contains lignin-like polymers.

ACKNOWLEDGEMENT

This work was supported by the Division of Basic Energy Sciences of the Department of Energy.

REFERENCES

1. Freudenberg, K. and Neish, A. C., *Constitution and Biosynthesis of Lignin* (Springer Verlag, New York), 1968.
2. Bolker, H. I. and Brenner, H. S., *Science* 170, 173 (1970).
3. Grimshaw, J., *Rodd's Chemistry of Carbon Compounds*, S. Coffey, Ed., Vol. 3, Part D, Chapter 16, Elsevier Scientific Publ. Co., New York (1976).
4. Dubach, P., Mehta, N. C., Jakab, T., Martin, F., and Roulet, N., *Geochim. Cosmochim. Acta* 28, 1567 (1964).
5. Neyroud, J. A., and Schnitzer, M., *Canad. J. Chem.* 52, 4123 (1974).
6. Schnitzer, M., and Neyroud, J. A., *Fuel* 54, 17 (1975).
7. Pew, J. C., and Withrow, J. R., *Fuel* 10, 44 (1931).
8. Sharma, J. N., and Wilson, M. J. G., *Fuel* 40, 331 (1961).
9. Burges, N. A., Hurst, M. H., and Walkden, G., *Geochim. Cosmochim. Acta* 28, 1547 (1964).
10. Bimer, J., Given, P. H., and Raj, S., *ACS Symp. Series No. 71*, 86 (1978).
11. Stevenson, F. J., and Mendez, J., *Soil Sci.* 103, 383 (1967).
12. Schnitzer, M., DeSerra, M. I. O., and Ivarson, K., *Soil Sci. Soc. Am. Proc.* 37, 229 (1973).
13. Forrester, A. R., and Wardell, J. L., *Rodd's Chemistry of Carbon Compounds*, S. Coffey, Ed., Vol. 3, Part A, Chapter 4, Elsevier Scientific Publ. Co., New York (1971).
14. Musgrave, O. C., *Chem. Rev.* 69, 499 (1969).
15. Bearse, A. E., Cox, J. L., and Hillman, M., *Production of Chemicals by Oxidation of Coal*, Battelle Energy Program Report, Columbus, Ohio (1975).
16. Hedges, J. I., and Parker, P. L., *Geochim. Cosmochim. Acta* 40, 1019 (1976).
17. Bugur, K., Gaines, A. F., Guleg, A., Guger, S., Yurum, Y., and Olcay, Y., *Fuel* 52, 115 (1973).
18. Neyroud, J. A., and Schnitzer, M., *Soil Sci. Soc. Am. Proc.* 38, 907 (1974).
19. Griffith, S. M., and Schnitzer, M., *Soil Sci.* 76, 191 (1976).
20. Hayatsu, R., Winans, R. E., Scott, R. G., Moore, L. P., and Studier, M. H., *Fuel* 57, 541 (1978).
21. Hayatsu, R., Winans, R. E., Scott, R. G., Moore, L. P., and Studier, M. H., *Nature* 275, 116 (1978).
22. Green, G., and Steelink, C., *J. Org. Chem.* 27, 170 (1962).
23. Unpublished results.
24. Spackman, W., Davis, A., Walker, P. L., Lovell, H. L., Stefanko, R., Essenhigh, R. H., Vastola, F. J., and Given, P. H., *Evaluation of Development of Special Purpose Coals*, Final Report FE-0390-2, September 1976, ERDA.
25. Dryden, I. G. C., *Chemistry and Utilization of Coal*, Suppl. Vol., H. H. Lowry, Ed., Chapter 6, John Wiley, New York (1963).
26. Unpublished results from selective aq.-Na₂Cr₂O₇ oxidation of coals derivatized with d₆-dimethylsulfate.
27. Timell, T. E., Ed., *Proceeding of the 8th Cellulose Conference I. Wood Chemicals - A Future Challenge*, John Wiley & Sons, New York, 1975; see also Reference no. 3.
28. Flaig, W., *Coal and Coal-Bearing Strata*, D. Murchison and T. S. Westoll, Eds., Chapter 10, Oliver and Boyd, London 1968.
29. Swain, F. M., *Non-Marine Organic Chemistry*, The University Press, Cambridge (1970).

Table 1
 Elemental Analysis of Samples* (maf %)

No.	Sample	C	H	N	S	O (by diff)	H/C
1	Lignite (Sheridan Wyoming)	66.4	4.8	1.5	1.1	26.2	0.87
2	Bituminous (IL. #2)	73.9	5.2	1.4	3.4	16.1	0.84
3	Bituminous (IL #6)	77.7	5.4	1.4	4.1	11.4	0.83
4	Bituminous (Ohio PSOC#297)	80.5	5.6	1.6	2.9	9.4	0.83
5	Bituminous (Pitt. #8)	82.0	5.5	1.4	3.7	7.4	0.70
6	Bituminous (Penn. PSOC#258)	86.5	4.8	1.3	2.6	4.8	0.67
7	Anthracite (Penn. PSOC#85)	91.0	3.8	0.7	1.2	3.3	0.50

* All samples were pretreated to remove solvent extractable trapped organic materials and were dried at 110-120°C for 16-18 hours under vacuum before oxidation.

Table 2
Summary of CuO-NaOH Oxidation Products

Wt % of fraction ^b	Sample No. ^a						
	1	2	3	4	5	6	7
Organic acid (Benzene-ether extract)	35.3	19.6	17.1	7.0	14.7	1.3	-
Humic acid A (Methanol extract)	54.3	61.0	46.2	9.3	39.5	69.5	-
Humic acid B (only aq. alkali soluble)	≤ 1.0	≤ 1.5	16.1	51.0	20.2	2.0	7.5
Non-oxidized coal ^c	11.0	21.0	22.2	30.4	26.5	32.0	95.0
Wt % of identified acids ^d							
Phenolic	66.6	54.1	14.6	41.0	8.3	5.8	-
Benzene carboxylic	26.0	36.2	69.4	50.2	62.7	76.7	-
Naphthalene carboxylic	2.0	3.3	6.2	5.5	22.9	10.6	-
Heterocyclic ^e	-	1.6	3.5	2.0	2.0	3.2	-
Aliphatic dibasic	2.6	1.0	1.4	-	≤ 1.0	≤ 1.0	-
Others	2.8	3.8	4.9	1.3	3.5	3.0	-
Ratio of Phenol/Benzene Acid	2.56	1.49	0.21	0.82	0.13	0.07	-

^aSee Table 1 for information.

^bWt % was obtained from coal sample on a dry, ash free basis.

^cSmall amount of insoluble Cu-salts are present.

^dWt % was obtained from each benzene-ether extract. Determination was made from the gas chromatograms of their methyl esters.

^eThiophene- and pyridine carboxylic acids for samples 2-6, and pyridine tricarboxylic acids for sample 1.

- Not found.

Table 3

Organic Acids Identified as Their d_3 -methyl Esters by GC-MS and
High Resolution MS

Peak No.	Compound
1	Succinic acid
2	C ₃ -dibasic acid
3	Benzoic acid
4	Methylbenzoic acid
5	p-Hydroxybenzoic acid
6	Hydroxytoluic acid
7	1,2-Benzenedicarboxylic acid
8	1,4-Benzenedicarboxylic acid
9	1,3-Benzenedicarboxylic acid
10	Methylbenzenedicarboxylic acid
11	Dihydroxybenzoic acid
12	Pyridinedicarboxylic acid
13	3,4-Dihydroxybenzoic acid
14	Dimethylbenzenedicarboxylic acid (naphthoic acid, minor)
15	Hydroxybenzenedicarboxylic acid (4-hydroxy-1,3-benzenedicarboxylic acid, largest peak)
16	Methylhydroxybenzenedicarboxylic acid
17	1,2,4-Benzenetricarboxylic acid
18	1,2,3-Benzenetricarboxylic acid
19	1,3,5-Benzenetricarboxylic acid
20	Methylbenzenetricarboxylic acid
21	Pyridinetricarboxylic acid
22	Naphthalenedicarboxylic acid
23	Hydroxybenzenetricarboxylic acid
24	1,2,4,5-Benzenetetracarboxylic acid
25	1,2,3,4-Benzenetetracarboxylic acid
26	1,2,3,5-Benzenetetracarboxylic acid
27	Methylbenzenetetracarboxylic acid
28	Dihydroxy-diphenyldicarboxylic acid (T)
29	Hydroxynaphthalenedicarboxylic acid
30	Benzenepentacarboxylic acid

T indicates that identification is tentative.

Table 4

CuO-NaOH Oxidation of Model Compound at 200°C for 8-10 Hours

Compound	Type of Reaction	Major Product ^a	Yield mol %
4-Methylbenzyl alcohol	-CH ₂ OH → -COOH	4-Methylbenzoic acid	93
β-Naphthyl methylcarbinol	-CH ₂ OH → -COOH	β-Naphthoic acid	77
Benzaldehyde	-CHO → -COOH	Benzoic acid	95
4-Methoxybenzaldehyde	-CHO → -COOH	4-Hydroxybenzoic acid	89(45)
2,6-Dimethoxyphenol	-OCH ₃ → -OH	b	-
Syringaldehyde	-CHO → -COOH	3,4,5-Trihydroxybenzoic acid	4.5 ^c
Dibenzoylmethane	-CO-CH ₂ - → -COOH	Benzoic acid	76
1,4-Naphthoquinone	-CO-C → -COOH	Phthalic acid	91
Phenylacetic acid	-CH ₂ -CO- → -COOH	Benzoic acid	68
Diphenyl ether	-O- → -OH	Phenol	67
Dibenzyl ether	-H ₂ C-O-CH ₂ - → -COOH	Benzoic acid	81
Diphenyl methane	-C-C- → -COOH	Benzoic acid	11
Poly-(4-methoxystyrene)	-C-C → -COOH	4-Hydroxybenzoic acid	6 ^d
1-Methylnaphthalene	-C-C → -COOH	1-Naphthoic acid	3
2,4-Dimethoxytoluene	-C-C → -COOH	2,4-Dihydroxybenzoic acid	5(58)
3,4-Dimethoxytoluene	-C-C → -COOH	3,4-Dihydroxybenzoic acid	7(52)

^aAll products were derivatized with d₆-dimethylsulfate or diazomethane, and analyzed by GCMS.

^bAbout 16.9 wt % of the oxidation product was obtained under the same conditions (170°C for 4 hours) employed for plant materials, humic acids and marine sediments. The product consisted mainly of polymerized material. Very small amount of trihydroxy compounds (2-3%) was detected by GCMS.

^cMost of syringaldehyde was degraded.

^dShown as wt %.

^eNumber in parenthesis shows % of demethylation from -OCH₃ group.

FIGURE CAPTION

Fig. 1a. Gas chromatogram of methyl esters of the organic acid fraction from lignite; Fig. 1b, from bituminous coal. The analysis was carried out on a Perkin-Elmer 3920B gas chromatograph interfaced to a modified Bendix model 12 time-of-flight mass spectrometer with a variable split between a flame ionization detector and the source of the mass spectrometer. The separation was made on a 15.2 m x 0.51 mm SCOT column coated with OV 17 and temperature programmed from 100-250°C at 4°C min⁻¹.

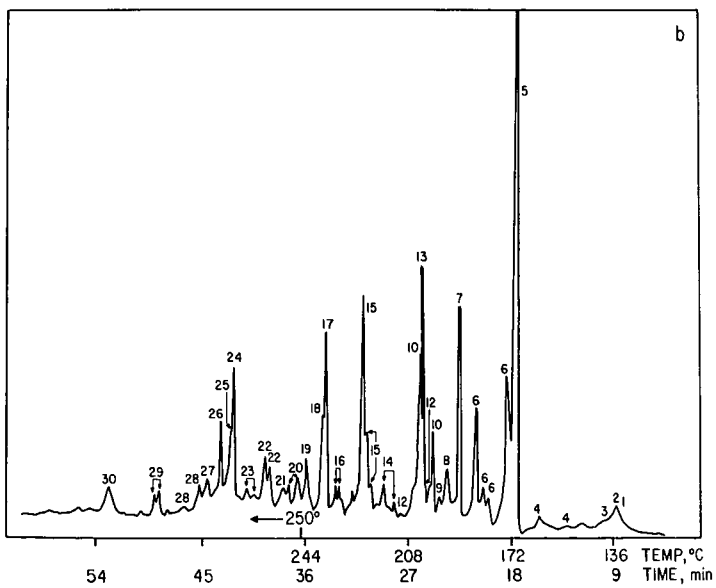
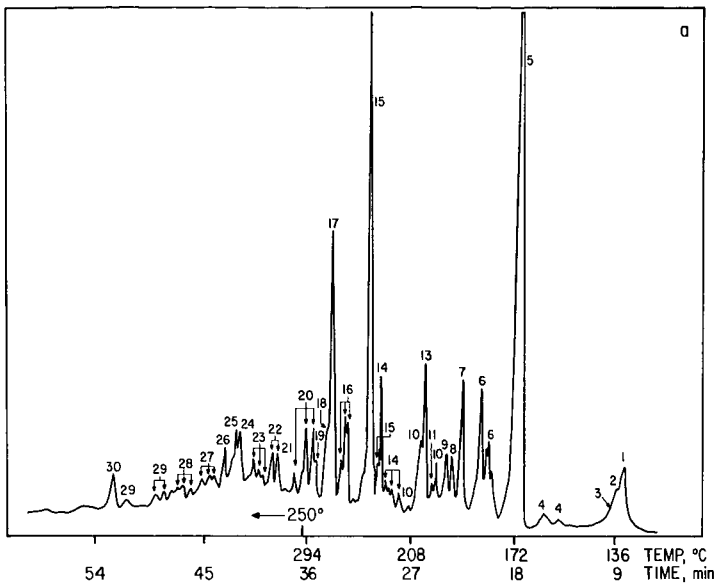


Figure 1

SHORT TIME REACTION PRODUCTS OF COAL LIQUEFACTION
AND THEIR RELEVANCE TO THE STRUCTURE OF COAL

Malvina Farcasiu

Mobil Research and Development Corporation
Central Research Division
P. O. Box 1025
Princeton, New Jersey 08540

INTRODUCTION

The subject of the chemical structure of coal is almost as controversial as it is complex. The complexity of this problem is partially due to the lack of homogeneity and solubility of coals, as well as to the large variety of organic rocks labeled as coals.

A fundamental question is whether we can even consider a chemical structure for a specific coal. Experimental data indicates that there are similarities in the physical properties of some groups of coal and in their behavior toward different chemical reactions; this at least allows us to speak of elements of structure in coal.

Traditionally, both physical and chemical data have been used to study coals. Both kinds of methods require a large amount of experimental work and highly specialized competence in the understanding and application of the method itself. This makes it quite difficult for any individual to master all the aspects of this kind of research. Fully aware of this reality, I will try to present some of our present concepts on coal structure. These concepts are based on data available in the literature as well as from our own experiments. The main idea is to use as much information as possible, which has been obtained by methods as different as possible, and to question all the data, especially those which can be proven by a single method only. One should mention that previous work by Given [1] and Wiser [2] was based on a similar approach. In this paper we will discuss some new data, which was not available to them when they proposed several representative coal average structures.

RESULTS AND DISCUSSION

The first step in the chemical analysis of a coal is the determination of its moisture-ash-free elemental composition. For example, for two coals which have been extensively studied for liquefaction behavior the elemental composition, calculated for 100 atoms is:

<u>Coal</u>	<u>Elemental Composition</u>
Illinois #6 (Monterey)	$C_{50.8}H_{43}O_{4.8}S_{0.8}N_{0.6}$
Wyodak	$C_{48.4}H_{42.4}O_{8.6}S_{0.07}N_{0.5}$

A look at the above data gives several hints about coal structure:

1. For each 100 atoms in coal over 90 are atoms of carbon and hydrogen. Stoichiometry dictates that the majority of the chemical bonds in coal will be carbon-carbon and carbon-hydrogen.
2. Oxygen is the main heteroatom and understanding its chemistry during any coal transformation is essential. For each reaction performed for the usual purpose of removing sulfur and nitrogen, understanding what happens to oxygen is very important, as well as how its reactivity affects those of N and S functions.

Looking at possible coal structures, two aspects are relevant:

- a) the chemical functions in which the heteroatoms appear,
- b) the carbon skeleton of the rest.

The most important chemical functionalities in coal are [3]: for oxygen: phenols, ethers, carboxylic acids, quinones; for nitrogen: pyrrole and pyridine derivatives.

These functionalities can be present in larger or smaller relative amounts in a given coal, but, qualitatively, all the coals contain the same kind of chemical functions.

The carbon skeleton of coal is perhaps the most controversial aspect of the research on coal structure. Three major questions are of interest in this field:

1. What is the percentage of aromatic carbons?
2. How condensed are the aromatic ring structures?
3. What is the carbon skeleton of the aliphatic portion of the coal?

The percentage of aromatic carbon can now be determined by solid-state ^{13}C -NMR. Alex Pines from the University of California at Berkeley made the quantitative measurements for the coals discussed in this paper.

To answer the other two questions related to the carbon skeleton, several approaches can be taken.

One of them is a careful structure determination of the short time reaction products of the thermal liquefaction of coal [4]. During the last four years we worked on a research project supported in part by the Electric Power Research Institute. One of the purposes of this project was to establish the chemical composition of short contact time thermal liquefaction products (including structure). We will now discuss how this data can be used to obtain information about coal structure.

In the short time of 2-5 minutes, coal dissolves in the presence of an H-donor; in the absence of an added catalyst only a few bonds are actually broken. Work at Mobil [4], Exxon [5] and Oakridge National Laboratory [6] indicates that none of the following reactions take place:

- Hydrogenation of aromatic polycyclic hydrocarbons,
- Destruction or formation of polycyclic saturated structures.

A corollary of this is: if these polyaromatic or polycyclic saturated structures are present in coal, they should be identified in the thermal liquefaction products.

Many of the chemical functionalities are also stable in these conditions, especially the O,S,N heterocyclic structures. Water formation by phenol dehydrogenation is also minimal. We found that in coal conversions even at long reaction times (up to 90 minutes) in the absence of an added catalyst, the -OH bonded to a monoaromatic ring is stable. In the same conditions, dehydroxylation of naphthenic phenols does occur [7].

The degree of ring condensation of the aromatic part can be semi-quantitatively determined in coal liquids [4]. It has been found that in the short time liquefaction products, the majority of the aromatic rings are as in benzene and naphthalene. These data are consistent with the data obtained by Hayatsu, Scott, Moore and Studier [9], using an oxidative method and with the uv-visible spectroscopy data reported by Friedel and Queiser [10]. I conclude then that in the subbituminous and bituminous coals studied by us and others, the aromatic carbons are not present in significant amounts as highly condensed rings.

Concerning the carbon skeleton of the aliphatic portion, there are no methods for direct identification. However, for a given formula if the total number of C and H is known, as well as the percentages of aromatic and aliphatic carbon and hydrogen a possible structure for the aliphatic part may be inferred.

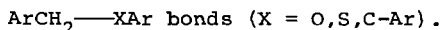
Possible average chemical structures present in short time reaction products have been determined by a methodology we have already reported [4,8]. Fractions with average molecular structures as in Figures 1-4 are consistent with the experimental data.

As shown in Figure 1 for a given molecular formula, there is a relationship between the degree of aromatic ring condensation and the degree of aliphatic ring condensation.

The relative number of aliphatic hydrogens and carbons is consistent with the presence of some polycondensed aliphatic structures. The number of the polycondensed aliphatic rings seems quite high in certain Wyodak coal liquids obtained in a thermal process at short reaction time (Figure 4). It is likely that such structures are also present in Wyodak coal. Other experimental data are also in favor of this explanation. For example, the oxidative method used by Deno et al. [11], gives selective oxidation of aromatic structures only if polycondensed aliphatic rings are not present. The results obtained by this method for Wyodak coal are nonreproducible and the oxidation products are difficult to analyze.

Another approach is a direct calculation of the possible number of the aliphatic rings. The calculation is based on the elemental analysis of the coal and the percent of aromatic carbon obtained by ^{13}C -NMR in solid state [4]. Based on this method, the Wyodak coal used in the liquefaction study to obtain data as in Figure 2 contained 44-50% aromatic carbon. This would be consistent with 2 to 8 aliphatic rings for 100 atoms of carbon. We should note that some other samples of Wyodak coal for which we measured the aromatic content were somewhat more aromatic (50-70% aromatic carbon).

The data we presented are based on the similarity of the elements of structure in coal and in the short contact time, noncatalytic liquefaction products. These elements of structure could be bound together with low energy thermally labile bonds. As described in the literature [4,6], these weak bonds could be:



An important practical consequence of knowing the coal structure and the structure of its short time liquefaction products is the understanding of the possible limits of reduction of H-consumption for the liquefaction of a particular coal. In Figure 5 we make such correlations. This aspect will be discussed more fully in the future.

ACKNOWLEDGMENTS

The work presented here was conducted under a program jointly sponsored by EPRI and Mobil Research and Development Corporation. Co-workers in this project are J. J. Dickert, T. O. Mitchell and D. D. Whitehurst. Technical assistance was provided by B. O. Heady and G. Odoerfer

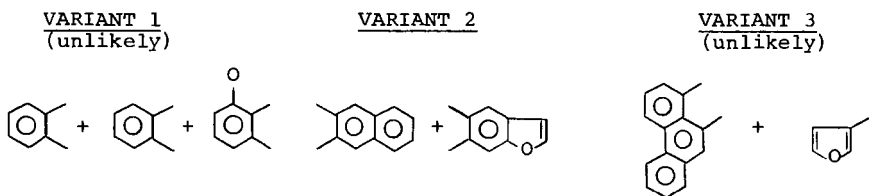
REFERENCES

1. P. H. Given, *FUEL*, **39**, 147 (1960).
2. W. Wiser, Storch Award Address, ACS Meeting, Miami, 1978.
3. W. Francis, "Coal", Edward Arnold Publishers, Ltd., London, 1961.

- 4a. D. D. Whitehurst, M. Farcasiu and T. O. Mitchell, "The Nature and Origin of Asphaltenes in Processed Coals," EPRI Report AF-252, First Annual Report Under Project RP-410, February 1976.
- 4b. D. D. Whitehurst, M. Farcasiu, T. O. Mitchell and J. J. Dickert, Jr., ibid, Second Annual Report, July 1977.
- 5a. T. Aczel, M. L. Gorbaty, P. S. Moa, R. H. Schlosberg, FUEL, 54, 295 (1975).
- 5b. T. Aczel, M. L. Gorbaty, P. S. Moa, R. H. Schlosberg, Preprints of the 1976 Coal Chemistry Workshop organized by EPRI, ERDA, NSF and SRI, Menlo Park, Calif., p. 165 (1976).
6. B. M. Benjamin, V. F. Raaen, P. H. Maupin, L. L. Brown and C. J. Collins, FUEL, 57, 269 (1978).
7. D. D. Whitehurst, M. Farcasiu, T. O. Mitchell, J. J. Dickert, Jr., "The Nature and Origin of Asphaltenes in Processed Coals," EPRI Project RP-410, Third Annual Report, to be published.
8. M. Farcasiu, FUEL, 56, 9 (1977).
- 9a. R. Hayatsu, R. G. Scott, L. P. Moore, M. H. Studier, Nature, 257, 378 (1975).
- 9b. R. Hayatsu, R. E. Winans, R. G. Scott, L. P. Moore and M. H. Studier, Preprints ACS-Division of Fuel Chemistry, Vol. 22, No. 5, p. 156 (Chicago 1977).
10. R. A. Friedel, J. A. Queiser, FUEL, 38, 369 (1959).
11. N. C. Deno, B. A. Greigger, S. G. Stroud, FUEL, 57, 455 (1978).

General Formula $C_{31}H_{27}O_2$
 Aromatic Moiety $C_{18}H_{10-11}$ (1H -NMR, ^{13}C -NMR)

Aromatic Structures Considered



Possible Average Structures

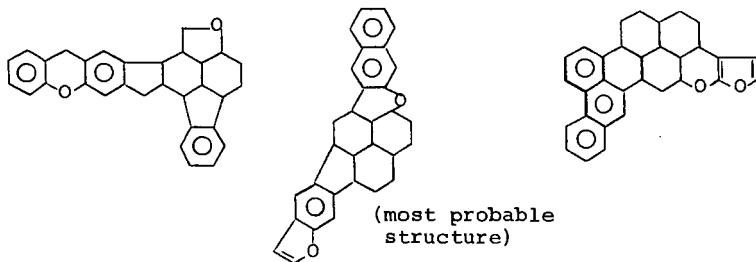
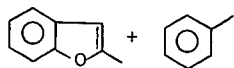


Figure 1: Possible Average Structure for a Short Contact Time Fraction SESC-3 of Monterey Coal.

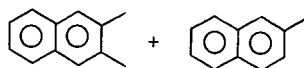
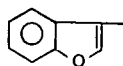
General Formula $C_{43}H_{38}O_2$
 Aromatic Moiety $C_{26}H_{18}$ (1H -NMR, ^{13}C -NMR)

Aromatic Structures Considered:

VARIANT 1



VARIANT 2



Possible Average Structures:

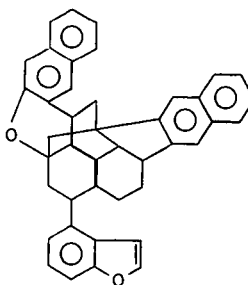
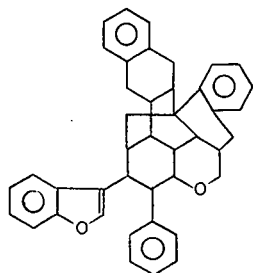
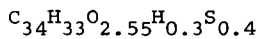


Figure 2: Possible Average Structures for Wyodak SESC-3 Short Contact Time SRC

Figure 3: Fraction SESC-4 Monterey Coal Short Contact Time SRC



% Aromatic C = 59

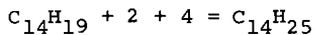
% Aromatic H = 43

Aromatic Part $C_{20}H_{14}$

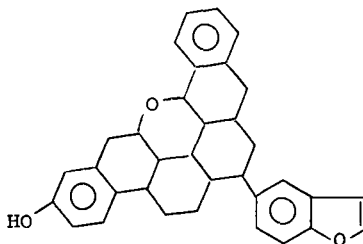


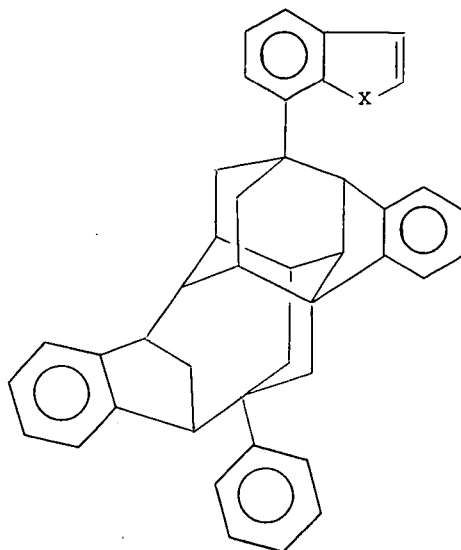
Aliphatic Part $C_{14}H_{19}$

1 Aliphatic Ether + 4 Substitutents



$C_{14}H_{26}$ -- 3 Condensed Aliphatic Rings





Calculated Based on Experimental Data:

$C_{43}H_{36}NO_2$

Av. MW = 600

Aromatic $C_{27}H_{18-19}$ (1H -NMR, ^{13}C -NMR)

In formula:

(62% Aromatic C, 52% Aromatic H)

$C_{26}H_{18}$

Benzylic (2-3 ppm)

H_{10}

H_3

Aliphatic

C_{16}

H_7

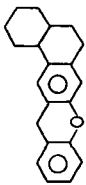
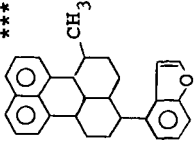
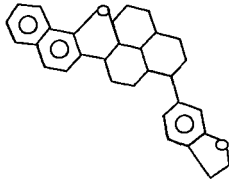
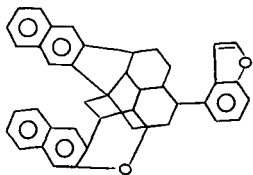
C_{16}

$H?$

H_{18}

Figure 4: Average Carbon Skeleton Formula for Wyodak SRC

Figure 5: Comparison of Structures and Hydrogen Consumption for Four Coals

Coal	Kentucky	Hiawatha	Monterey	Wyodak
Composition	$C_{100}H_{82}N_1O_9.4$	$C_{100}H_{84}N_2O_9.5$	$C_{100}H_{88}N_1.6O_{13.2}S_1.74$	$C_{100}H_{86}NO_{18}$
No. polycondensed saturated rings/100C	Coal: 4 SESC-3: 2 SCT*: 2	6 4	6 4	10 5
Structure				
g H consumed/100g coal during liquefaction (Normalized to 100% conversion)	SCT: 0.43 LCT**: 0.96	0.63 2.03	0.89 2.80	

*SCT = Short Contact Time <2 min.

**LCT = Long Contact Time >30 min.

***Ca. 30 min. contact time.

DEDUCTION OF THE STRUCTURE OF BROWN COAL
BY REACTION WITH PHENOL

R.J. Hooper* and D.G. Evans[†]

* D.S.I.R. Industrial Processing Division, Private Bag, Petone, New Zealand

† Centre for Environmental Studies, University of Melbourne, Parkville, Victoria
3052, Australia.

INTRODUCTION

To make any real progress in the ability to predict and control the liquifaction of coal by hydrogenation it is necessary to know what chemical reactions are occurring. Modern preparative and analytical techniques such as elution chromatography, mass spectroscopy and proton nmr have made the task of characterizing the products of liquefaction reactions much easier than hitherto, but the task of characterizing the coal before reaction remains almost as intractible as ever, because these new methods depend on the analysis samples being in the liquid form (or in the case of mass spectroscopy, able to be completely vaporized).

This is not a new problem, of course. Over the years many solubilization techniques have been suggested as tools for deducing coal structure, e.g. oxidation, hydrogenation, alkaline hydrolysis, pyrolysis and extraction with powerful solvents (either alone or in conjunction with other methods such as thermal pre-treatment, use of ultrasonics, etc.). These suffer from one of two disadvantages: with the relatively mild physical methods insufficient coal is got into solution to be useful (less than 20% is typical); but with chemical methods, including pyrolysis, the treatment is so harsh that interpretation of the structure of the original coal in terms of that of the products is of dubious validity. In particular, use of elevated temperatures, as in pyrolysis or other thermal treatments, is to be avoided, as free radicals formed by cleaving fragments off the main body of the coal molecule may polymerize to form structures which were not present in the original coal.

If it is accepted that coal cannot be got into solution without altering its structure to some extent, we should look for methods in which these changes are not large enough to prohibit the drawing of adequate deductions about the structure of the original coal, while at the same time presenting the reacted coal in a form suitable for structural examination. This would require at least 80% of the coal to be solubilized, with the soluble material low enough in molecular weight to ensure that it in turn is soluble in mild organic solvents, as required for preparative techniques such as solvent fractionation or chromatography.

The methods we considered were Friedel-Crafts reactions of various kinds (alkylation and acylation) and depolymerization of the coal by using it to alkylate phenol, as first proposed by Heredy and co-workers (1), and extensively investigated by them (1-5) and by Ouchi and co-workers (6-11). From the recent review of these methods by Larsen and Kuemerrle (12) it appears that molecular weights of the coal fragments produced are higher for alkylation and acylation methods (typically several thousand, even after allowing for the added acyl or alkyl groups) than for the material depolymerized in phenol (less than a thousand). The only disadvantage of phenol depolymerization, compared with the other methods, was its relatively weak action on very high rank coals (< 90%C, daf). This did not concern us, as we were interested in examining brown coals from the Latrobe Valley, Victoria, Australia, with very low rank (65-70%C, daf). We therefore chose this method, which had already been shown by Ouchi and Brooks (9) to be very effective for this type of coal. We perhaps underestimated the difficulties that chemically combined phenol would cause us, as will be discussed later.

In our plan of attack we first depolymerized the coal using conditions suggested by Imuta and Ouchi (11), then divided it into five fractions of progressively increasing polarity, using solvent fractionation, then analysed these fractions separately by elemental and functional group analysis, and further characterized the fractions by running infrared and proton nmr spectra on them. After allowing for the effects of combined phenol these data were put together to build up a composite picture of the structure of the original coal. Heredy et al. (5) have carried out a similar investigation on a series of coals of different ranks. The present work differs from theirs in that it used a more powerful catalyst for the phenolation, a more decisive solvent fractionation scheme, and infrared as well as nmr analysis for characterizing the fractions. Also our coal was lower in rank than any of those they tested.

EXPERIMENTAL

Coal used

The coal tested was Morwell brown coal from Victoria, Australia. Its composition on a dry basis is shown in Table 1. This coal contains over 60% moisture as mined. It was ground wet to 80% < 25 mesh, and used in the wet state (60% moisture).

Phenolation reaction

179 g of wet ground coal, 75 g of p-toluenesulfonic acid catalyst and 1300 g of laboratory grade phenol were heated under nitrogen, and the water was removed from the coal by boiling at 183°C (the boiling point of phenol is 181.8°C). The remaining mixture was refluxed at 183°C for 4h, after which the phenol was removed by steam distillation, leaving a solid, black, tarry material of low melting point, which was separated by decantation, and extracted by refluxing for 2h with 1200 ml of ethanol/benzene azeotrope (65% benzene, 35% ethanol). The insoluble material was filtered off and dried in a vacuum oven for 12h at 50°C and 16kPa pressure (these conditions were later used to remove excess solvent from all the fractions - see Figure 1 below).

Solvent fractionation

To facilitate later structural analysis the coal was separated into structural types using the solvent fractionation scheme shown in Figure 1.

Analysis

The original coal and the various fractions were analysed for carbon, hydrogen and oxygen by the C.S.I.R.O. Microanalytical service. Ash contents were determined in a standard ashing furnace (13). Phenolic, carboxylic and carbonyl oxygen contents were determined by the State Electricity Commission of Victoria, using methods developed by them for brown coals (14).

Infrared spectra of the original coal and the fractions were measured on a Perkin Elmer 457 Grating Infrared Spectrophotometer. Liquid samples (fractions A and B) were analysed as a thin film or smear. Solid samples (C, D and original coal) were analysed in KBr discs containing 0.3% by mass of sample. These were prepared by grinding the KBr mixture for 2 minutes in a tungsten carbide TEMA grinding barrel, drying for 24h in a vacuum desiccator over phosphorus pentoxide, then pressing into discs at 10 tons force, at room temperature but under vacuum. Because fraction A was dominated by phenol a sample of it was further separated by elution chromatography in an attempt to separate from it material less dominated by phenol. Elution was carried out in a silica column, using elutants in the following order:

hexane, chloroform, methanol.

Proton nmr spectra were recorded on a Varian HA 100 nmr spectrometer at room temperature, with tetramethylsilane (TMS) as internal standard, with a sweep width of 0 to 1000 Hz from TMS. For fraction A a solution of deuterated chloroform was used; fractions B and C were not soluble in CDCl_3 and pyridene $-d_5$ had to be used; fractions D and the whole coal were barely soluble even in pyridene $-d_5$, but enough dissolved to get spectra. These will not, of course, be representative of the whole material.

RESULTS

Yields and compositions

Table 1 shows the yields of the five fractions per 100 g of original dry coal and their compositions, including a breakdown of the oxygen into carboxylic, phenolic and other oxygen. Note that part of the ash-forming material has been removed by the solubilizing process (much of the non-organic material in Morwell coal is ion-exchangeable, and would have been replaced by hydrogen ions from the p-toluene-sulfonic acid; this was confirmed by ash analysis: e.g. ash from the original coal contained 50% SiO_2 and 10% MgO , whereas fraction D ash contained 80% SiO_2 and only 1% MgO). As the total yield of fractions was 202 g/100 g of original coal 102 g must have been added. This consists of combined phenol and unseparated solvents, as will be discussed later. This dilution results in the fractions having higher carbon contents and lower oxygen contents than the original coal. The hydrogen content decreases from A to D as the fractions become less aliphatic and more aromatic and polar.

Infrared spectra

The infrared spectra of the fractions and the original coal are shown in Figure 2. The spectra of the eluted sub-fractions of fraction A are not given here.

As already mentioned fraction A is dominated by phenol; nevertheless strong aliphatic absorptions can be seen at 2920, 2850, 1460 and 1380 cm^{-1} . The spectra of subfractions A1 (eluted by hexane, a very small part of A) and A2 (eluted by chloroform, about a quarter of A) showed these aliphatic absorptions very strongly. The spectrum for A1 showed little else, and this sub-fraction is probably virtually pure paraffins. The spectrum for A2 resembled the spectra for phenol ether and phenetole ($\text{C}_6\text{H}_5\text{OC}_2\text{H}_5$). Absorption due to hydrogen-bonded hydrogen is negligible, showing that all the phenol in this sub-fraction has been converted to ethers. The spectrum for subfraction A3 (which constitutes about three quarters of A) was dominated by phenol, but some aliphatic absorptions still showed, and this sub-fraction may well consist of phenol bonded to small coal fragments by methylene bridges. The absorptions for A, A2 and A3 at 1250 cm^{-1} are probably due to ether oxygen.

Fraction B is in many ways similar to fraction A, but with much weaker aliphatic absorption. It has a strong absorption due to hydrogen-bonded hydrogen at 3400 cm^{-1} , a weak aromatic absorption at 3030 cm^{-1} and many other absorptions characteristic of phenol. It also shows weak aliphatic absorptions at 2920, 1460 and 1380 cm^{-1} , and ether oxygen absorption at 1250 cm^{-1} .

Fractions C, D and E have spectra similar to those of the original coal. Phenol no longer dominates, although the hydrogen bonded -OH absorption at 3400 cm^{-1} is still strong. Aliphatic absorption is weak in C and E and negligible in D. The shoulder at 1700 cm^{-1} due to carboxylic oxygen, which was quite strong for the whole coal, is also quite pronounced for fractions C and D. (It was absent from fractions A and

B). This checks well with the data in Table 1 obtained by chemical analysis. The broad absorption from $1200-1000\text{ cm}^{-1}$ present in the whole coal is also present in fractions C and D although absent from A, B and E. Doubtless oxygen groups contribute to this, but we believe it is mainly due to silica, which is a major constituent of the ash. It could be virtually removed by deashing the coal with strong acids or by float/sink separations.

Nmr spectra

Figure 3 shows nmr spectra for fractions A, B, C and E.

Table 2 shows the forms the protons are present in, as determined from these spectra. The data for fraction D and the whole coal are shown in brackets, as these samples were virtually insoluble in pyridine, and the spectra represent only the small soluble portions. This table demonstrates the difficulties the coal chemist faces in trying to use proton nmr on physical solutions of coal: e.g. the soluble part of the whole coal shows no hydrogen-bonded protons despite the evidence of table 1; it shows no triaromatic or methylene bridge protons, despite the presence of appreciable amounts of these in the fractions; on the other hand it shows far more methylene α and methylene β than do the fractions.

The nmr data confirm and amplify the infrared data: hydrogen bonded protons are present from phenolic and carboxylic groups in the coal and phenol groups added into the chemically combined phenol. The monoaromatic content (of fractions A and B especially) is high, also because of added phenol, but di-ring aromatic material is also present in all fractions (even triaromatic in C), which must have come from the original coal. The aliphatic material observed in the infrared spectra of A, B and C is now seen to consist principally of methylene bridges and short, branched aliphatic chains (α and β - methyl predominate).

DISCUSSION

Combined phenol

The total combined phenol was estimated as follows:

Using the yield and composition data of Table 1 elemental balances were drawn up, as in Table 3. The third last line gives the masses of the various constituents of the added material. The second last line gives the amount of phenol this would account for, assuming all the added oxygen was from phenol (none from ethanol or methanol). The last line gives the remainder, which is close in composition to benzene (which could be present as a contaminant in fractions B and C). In the fractionation scheme shown in Figure 1 ethanol contamination of any fraction is unlikely, but pentane contamination of fraction A and methanol contamination of D and E are possible. We rejected these because pentane was not picked up from fraction A by hexane elutriation while preparing subfraction A1 (this was negligible in mass), and D was too deficient in hydrogen and oxygen to contain any appreciable amount of methanol. Methanol could have been present in E, but the mass of this fraction was so small that any such effect would be negligible.

Distribution of hydrogen on a phenol - and solvent-free basis

We can now determine the distribution of hydrogen in the original coal, but first we have to estimate the hydrogen distribution in fraction D, which could not be determined by nmr analysis. In another paper presented to this Congress (15) we reported results of the hydrogenation of fractions A to D in tetralin. Fraction D yielded a low-hydrogen residue, which still could not be analysed by nmr, and a high-hydrogen

liquid product separated by boiling off excess tetralin. From its nmr analysis and the known amount of functional group hydrogen in the original fraction (0.05 g/100 g original coal) we concluded that the aliphatic hydrogen in the original fraction was about 0.3 g/100 g, and the remaining 0.8 g of hydrogen/100 g was aromatic hydrogen of various kinds.

In Table 4 the results of the nmr analyses (Table 2), the estimates of combined phenol and contaminant benzene (Table 3), and the above estimates of the distribution of hydrogen in fraction D are manipulated to give a composite estimate of hydrogen in various forms in the original coal (the aromatic hydrogen in fraction D is assumed to follow the same pattern as in A, B and C, and the aliphatic hydrogen is also assumed to be distributed as in A, B and C). From this we can calculate by difference the hydrogen present in various forms in the original coal (second last line of Table 4).

Distribution of structural types

The distribution of hydrogen calculated above, together with the distribution of functional group oxygen (Table 1), between them define a statistically probable structure for Morwell brown coal. Rather than attempt to draw a structure we give in Table 5 estimates of the numbers of carbon atoms associated with each type of hydrogen atom that not only predict approximately the correct mass of carbon per 100 g of coal but also allow for approximately the required number of substituents in the aromatic groups, and for the bridges connecting the groups. There may, of course, also be some carbon not associated with hydrogen, such as acyl bridges and tertiary carbons in side chains (see later). We note in passing that the greatest difficulty in meeting the above requirements is in accommodating the oxygen not accounted for in functional groups.

We will conclude with a brief discussion of the forms taken by the three main structural groups: oxygen groups, aromatic groups and aliphatic groups.

Oxygen groups: As seen from Table 1, 25% of the dry coal was oxygen, 5% in the form of phenolic groups, 5% carboxylic, and 3% carbonyl. The present work throws little light on the remaining 12%. Some ethers are thought to be present, but we cannot confirm this: ethers noted in fractions A and B could have come from the phenolation reaction. There was some indication of the presence of benzofuran groups from the infrared spectra of residues left after the reaction of fractions C and D with tetralin (15). No doubt other heterocyclic oxygen is present also.

Aromatics: The presence of relatively large proportions of higher aromatic structures (diphenyl, naphthalene and polynuclear) is noteworthy, and unexpected from previous studies on brown coal (16, 17). The total aromatic content may have been overestimated slightly by the procedure used to estimate the hydrogen distribution of fraction D, but this would make little difference to the contents of the higher aromatics.

Aliphatics: The most surprising result of this work is the high methylene bridge content (more than 25% of all hydrogen), which again was not expected from earlier models (16). However it should be noted that in the study by Heredy et al. (5) similar to the present one 12% of the hydrogen in a lignite was found to be in the form of methylene bridges. It seems unlikely that these bridges were formed by the phenolation reaction (indeed Heredy's favored mechanism requires the prior presence of such bridges, and the large content found in this work appears to confirm his mechanism as being the most important one in the phenolation reaction). If the quantities in Table 5 are calculated out in terms of the numbers of structures rather than their masses, we get 0.45 mole of aromatic groups per 100 g of coal and 0.65 mole of methylene bridges per 100 g. This means that there is more than one bridge per aromatic group, i.e. a high degree of crosslinking must be present, probably in

a three-dimensional network. Possibly dihydroanthracene structures may also be present.

Another surprising result is the high number of β -methyl and β -methylene groups (0.23 mole/100 g coal) without corresponding α -methylenes (only 0.02 mole/100 g). This could be explained only by the presence of tertiary butyl groups (note that Swann et al. (18) recovered 2,6-di-*t*-butyl-4-methylphenol from a similar brown coal by evacuation at 35°C). The material reported here as β -methyl occurred at $\delta = 1.2$ (Figure 3), which Heredy et al. (5) interpret as β -methylene groups in naphthenic rings. If they are right this would put quite a different complexion on this finding; however their interpretation differs from those of other authorities (e.g. Ref. (19)), and would require a simultaneous occurrence of α -methylene groups, which is not borne out by our Figure 3.

REFERENCES

- (1) Heredy, L.A. and Neuworth, M.B. Fuel 1962, 41, 221.
- (2) Heredy, L.A., Kostyo, A.E. and Neuworth, M.B. Fuel 1963, 42, 182.
- (3) Heredy, L.A., Kostyo, A.E. and Neuworth, M.B. Fuel 1964, 43, 414.
- (4) Heredy, L.A., Kostyo, A.E. and Neuworth, M.B. Fuel 1965, 44, 125.
- (5) Heredy, L.A., Kostyo, A.E. and Neuworth, M.B. Adv. Chem. 1966, 55, 493.
- (6) Ouchi, K., Imuta, K. and Yamashita, Y. Fuel 1965, 44, 29.
- (7) Ouchi, K., Imuta, K. and Yamashita, Y. Fuel 1965, 44, 205.
- (8) Ouchi, K. Fuel 1967, 46, 319.
- (9) Ouchi, K., and Brooks, J.D. Fuel 1967, 46, 367.
- (10) Ouchi, K., Imuta, K. and Yamashita, Y. Fuel 1973, 52, 156.
- (11) Imuta, K. and Ouchi, K. Fuel 1973, 52, 174.
- (12) Larsen, J.W. and Kuemerrle, E.W. Fuel 1976, 55, 162.
- (13) BS1076 Part 3 1973.
- (14) McPhail, I. and Murray, J.B. Victorian State Electricity Commission, Sci. Div. Rep. MR-155, 1969.
- (15) Hooper, R.J. and Evans, D.G. Paper to Coal Liquifaction Fundamentals Symposium, ACS/CSJ Congress, Honolulu, 1979.
- (16) Anon. Coal Research in C.S.I.R.O. No. 6, March 1959, p12.
- (17) van Krevelen, D.W. "Coal", Elsevier, Amsterdam, 1961.
- (18) Swann, P.D., Harris, J.A., Siemon, S.R. and Evans, D.G. Fuel 1973, 52, 154.
- (19) Bartle, K.D. and Smith, J.A.S. Fuel 1965, 44, 109.

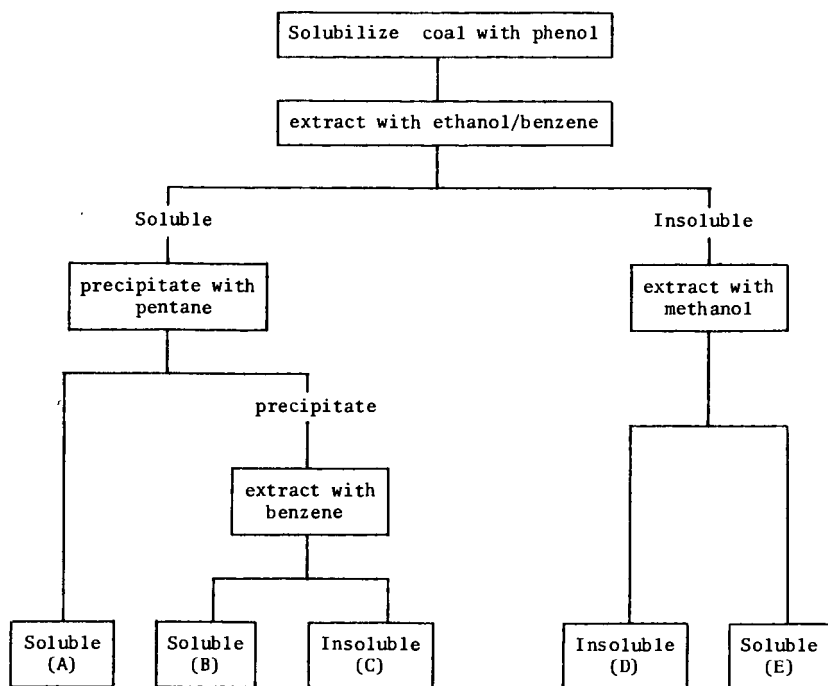


Figure 1: The fractionation scheme used to separate coal into four soluble fractions and an insoluble residue.

	fraction						Whole Coal
	A	B	C	D	E	Composite	
yield, g/100g original coal	28	66	78	28	2	202	100
composition, mass %							
C	76	74	69	71	56	72	63
H	7	6	5	4	6	5	5
O phenolic	4	4	3	6	ND	(4)	5
O carboxylic	0	1	3	2	ND	(2)	5
O carbonyl	ND	ND	ND	ND	ND	ND	3
O total	17	16	21	18	24	18	25
ash	ND	ND	2	3	ND	(1)	4
unaccounted	1	4	3	4	14	4	3

Table 1: Yields and compositions of the fractions. ND means not determined. Ash contents were not determined on fractions A, B and E, which were liquids. Functional group oxygen was not determined on fraction E because insufficient of it was available. The figures in brackets for the composition of the composite should be little affected.

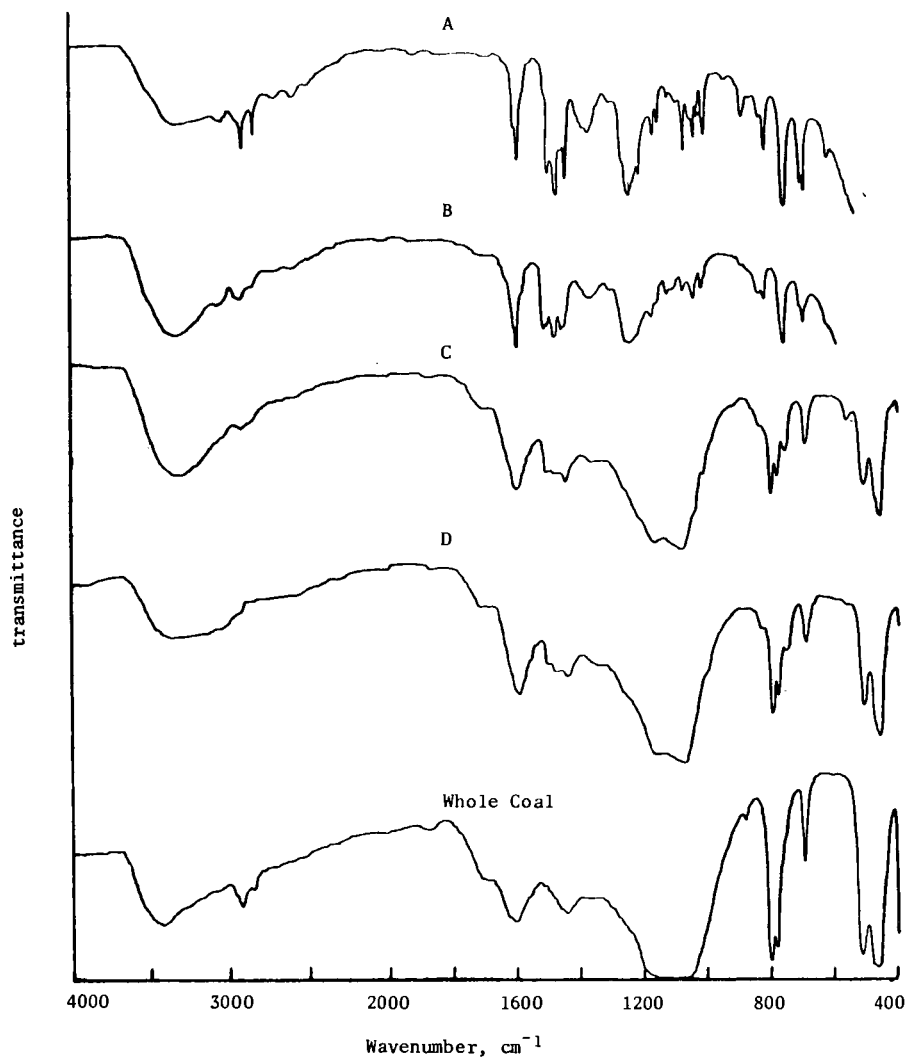


Figure 2: Infrared spectra for the original coal and the fractions A to D separated by the fractionation scheme shown in Figure 1. Fractions A and B, thin film; C, D and whole coal, KBr disc.

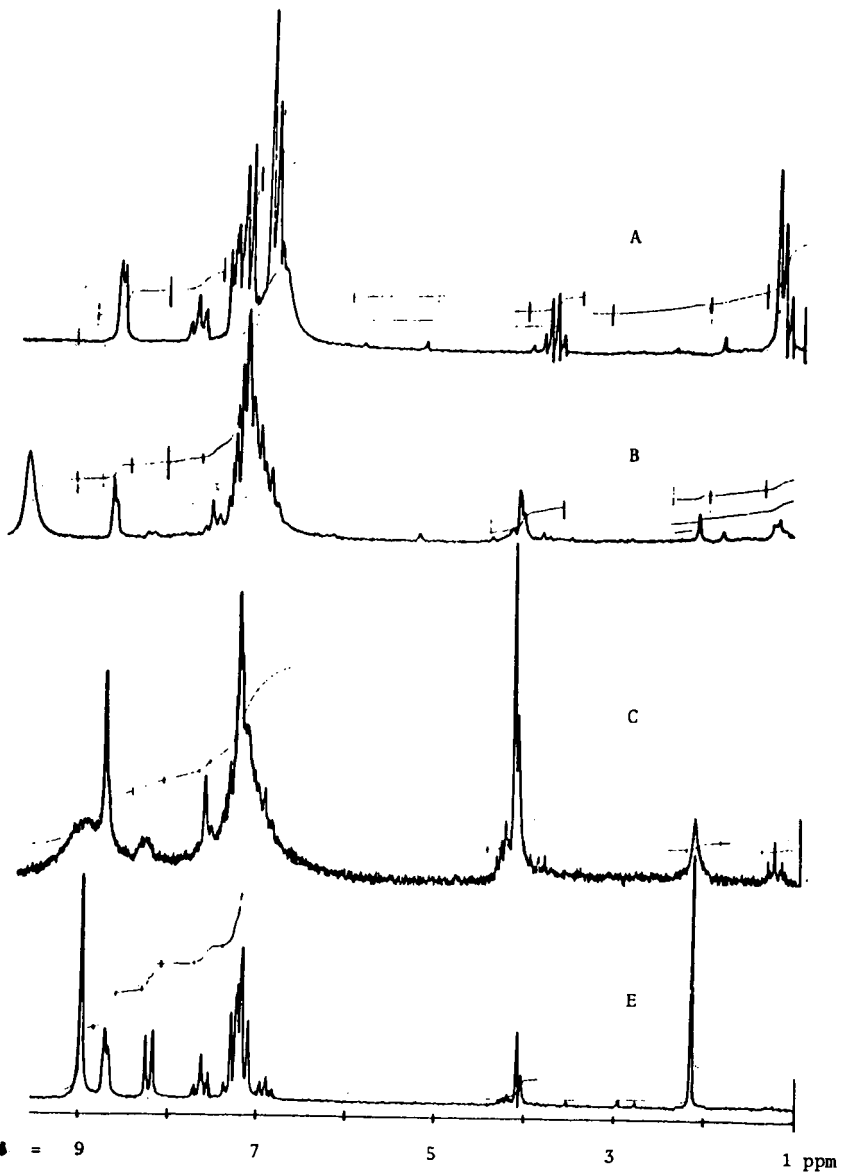


Figure 3: Nmr spectra for fractions A, B, C and E. A is dissolved in CDCl_3 ; B, C and E in pyridene $-d_5$.

δ ppm	proton type	fraction					Composite	Whole Coal
		A	B	C	D	E		
> 8.0	hydrogen bonded	7	17	19	(0)	27	(15)	(0)
8.7-8.0	triaromatic (5)	0	0	6	(10)	0	(3)	(0)
8.0-7.2	two-ring aromatic (5)	6	10	8	(48)	13	(63)	(46)
7.2-6.2	monoaromatic	63	58	44	(35)	37		
5.8-4.3	olefinic	1	0	0	(0)	0	(0)	(0)
4.3-3.4	methylene bridge	4	9	17	(trace)	9	(10)	(0)
3.4-3.2	acetylinic	0	0	0	(0)	trace	(0)	(0)
3.2-2.4	methin, methylene α	3	0	0	(0)	0	(3)	(11)
2.4-2.0	methyl α		1	4	(4)	15		
2.0-1.4	methylene β	3	1	0	(0)	0	(1)	(4)
1.4-1.0	methyl β	13	4	1	(4)	0	(5)	(39)
1.0-0.6	aliphatic γ	0	0	0	(0)	0	(0)	(3)

Table 2: Distribution of protons by type in the various fractions as measured from nmr spectra. Figures are % of the total protons in the particular fraction. Allowance has been made for residual protons in the deuterated solvents (CDCl_3 for A, pyridene- d_5 for others). The figures for fraction D and the whole coal are put in brackets to indicate that these samples were barely soluble and the spectra do not represent the whole material, only the small soluble part. α , β , γ refer to the positions of these protons with respect to aromatic rings.

fraction	C	H	O	ash	un- accounted	total
A	21	2	5	0	0	28
B	49	4	11	0	2	66
C	54	4	16	1	3	78
D	20	1	5	1	1	28
E	1	0	0	0	1	2
total original coal	145	11	37	2	7	202
added material	63	5	25	4	3	100
added phenol	82	6	12	-2	4	102
remainder	54	4	12	0	0	70
	28	2	0	-2	4	32

Table 3: Materials balances on material added to the coal by phenolation and fractionation. All figures are g/100 g of original dry coal.

	hydrogen bonded	aromatic			meth. bridge	aliphatic				total
		tri	di	mono		α CH ₂	α CH ₃	β CH ₂	β CH ₃	
A	0.14	0.00	0.12	1.23	0.08	(0.02	0.04)	0.06	0.25	1.94
B	0.67	0.00	0.40	2.30	0.36	0.00	0.04	0.04	0.16	3.97
C	0.74	0.23	0.31	1.72	0.66	0.00	0.16	0.00	0.04	3.86
D	(0.05)	(0.03	0.10	0.65)	(0.16	0.00	0.04	0.02	0.07)	1.12
E	0.03	0.00	0.02	0.04	0.01	0.00	0.02	0.00	0.00	0.12
total	1.63	0.26	0.95	5.94	1.27	0.02	0.30	0.12	0.52	11.01
phenol	0.74	-	-	3.01	-	-	-	-	-	3.75
benzene	-	-	-	2.46	-	-	-	-	-	2.46
coal	0.89	0.26	0.95	0.47	1.27	0.02	0.30	0.12	0.52	4.80
total	1.63	0.26	0.95	5.94	1.27	0.02	0.30	0.12	0.52	11.01

Table 4: Hydrogen present in various forms in fractions, original coal, combined phenol and benzene contaminant, g/100 g original dry coal (figures in brackets have involved making some assumptions about the distribution).

hydrogen type	atomic C/H	mass C/H	H (Table 4) g/100 g coal	C g/100 g coal
monoaromatic	6/2	36	0.47	17
two ring aromatic	10/4	30	0.95	28
triaromatic	14/4	39	0.26	10
α methylene	1/2	6	0.02	0
β methylene	1/2	6	0.12	1
methylene bridge	1/2	6	1.27	8
α methyl	1/3	4	0.30	1
β methyl	1/3	4	0.52	2
carboxyl	1/1	12		2
total				69

Table 5: Calculation of carbon in various structural forms, g/100 g dry coal.

THE CHEMISTRY OF ACID-CATALYZED COAL DEPOLYMERIZATION

Laszlo A. Heredy
Rockwell International, Energy Systems Group
8900 De Soto Avenue, Canoga Park, California 91304

Since its introduction in the early 1960's, acid-catalyzed depolymerization has become a widely used method to convert coal into soluble products for structural investigations. It was first shown by Heredy and Neuworth⁽¹⁾ that coal could be depolymerized by reacting it with phenol-BF₃ at temperatures as low as 100°C. The method was based on the assumption that coal contains aromatic structures linked by aliphatic bridges, such as methylene bridges, which are sufficiently reactive to participate in an acid-catalyzed transarylation reaction. This general type of structure was proposed by Neuworth, et al.,⁽²⁾ to explain the chemistry of low-temperature pyrolysis of coal. The overall reaction of this proposed structure with phenol-BF₃ is illustrated in Figure 1. One of the final products of the depolymerization is dihydroxy-diphenylmethane.

The depolymerization reaction was modified by Ouchi, Imuta, and Yamashita⁽³⁾ who substituted p-toluenesulfonic acid (PTSA) for BF₃ as the catalyst and increased the reaction temperature to 180-185°C. A very high degree of depolymerization, with pyridine soluble product yields over 90%, was achieved under these conditions. Darlage and Bailey⁽⁴⁾ investigated the effects of reaction temperature, various solvents and coal preoxidation on depolymerization product yields using a number of acid catalysts. They found that meta-substituted phenols were more effective aromatic substrates for the depolymerization reaction than phenol. The preoxidation of coal, particularly of some sulfur-rich bituminous coals, with dilute aqueous nitric acid considerably increased the yield of depolymerization products.⁽⁵⁾

A general review of the acid-catalyzed coal depolymerization method has been published recently by Larsen and Kuemmerle.⁽⁶⁾ The objective of this paper is to discuss some specific aspects of the chemistry of coal depolymerization.

I. THE RELATIVE REACTIVITIES OF VARIOUS BRIDGE STRUCTURES TOWARD PHENOL-BF₃

Although no systematic studies have yet been reported regarding the relative reactivities of aliphatic bridge structures, or more generally, aliphatic-aromatic carbon-carbon bonds, which may be present in various coals, toward phenol-BF₃, some important trends have been established in model compound experiments.^(1,7) The results of these experiments are summarized in Tables 1 and 2 and in Figure 2.

The data on isopropyl group transfer in Table 1 show that the secondary aliphatic-aromatic carbon-carbon bond is much more reactive when it is located on either a phenolic ring or on a phenanthrene ring than on a nonactivated benzene ring. The relative reactivities of the secondary carbon bond in the first two structures could not be evaluated because the isopropyl group transfer went to completion both in the case of ortho-isopropylphenol and of retene. The data on n-propyl group transfer in Table 2 show, as expected, that a bond between a primary aliphatic carbon and an aromatic carbon is less reactive than a secondary carbon-aromatic carbon bond under otherwise similar conditions.

Figure 2 shows the comparison of the relative reactivities of four aromatic-aliphatic carbon-carbon linkages. A comparison of the reactivities of the two linkages a' and b', which involve primary aliphatic carbon atoms, clearly show enhanced reactivity at bond a' due to the activating effect of the phenolic hydroxyl group. A comparison of the reactivity of linkage a' with that of the corresponding bond in para-n-propylphenol (Table 2) indicates that the reactivities of (-CH₂-CH₂-) substituted aromatics are similar whether the substitution is in a bridge or in a chain structure. The relative reactivities found with model

compound B indicate that -CH₂- bridges can play a special role in coal depolymerization because in this case bonds on both sides of the bridge structure are activated (compare the reactivities of bonds b and b', respectively).

It is probable that cleavage of aliphatic ether bonds contributes to coal depolymerization, particularly in the case of lignites and subbituminous coals. Although the reactivity of various ethers with phenol-BF₃ has not been investigated, several studies on the BF₃-catalyzed cleavage of various aliphatic ether linkages have been reported.^(8,9) It was shown that the reaction of ethers with benzene gives alkylbenzenes. The relative ease of reaction varied considerably with different ethers. Diisopropyl ether and dibenzyl ether reacted vigorously with benzene upon saturation with BF₃. Isopropyl, phenyl, and benzyl ethyl ethers reacted violently. On the other hand, ethyl, isoamyl, and n-amyl ethers reacted only at higher temperatures and elevated pressures (150°C and 10-20 atm).

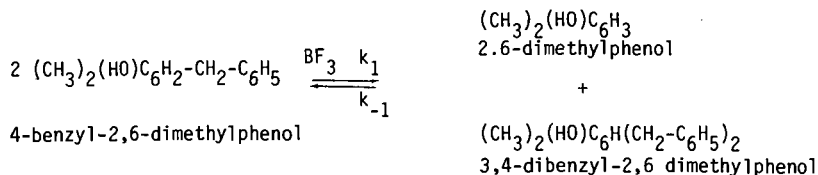
II. INVESTIGATION OF THE KINETICS OF BF₃-CATALYZED BENZYL GROUP TRANSFER

Kinetic investigations of BF₃-catalyzed benzyl group transfer in benzylphenol systems were reported by Heredy.⁽¹⁰⁾ These systems were chosen for investigation because of the particular interest in the role that -CH₂- bridges may play in coal depolymerization.

One of the investigations was made with para-benzylphenol. Experiments were made first with the para-benzylphenol/phenol (1-¹⁴C)/BF₃ system to study the rate of benzyl group transfer from benzylphenol to phenol (1-¹⁴C). It was found, however, that the rate of benzyl group transfer to para-benzylphenol was much faster than to phenol (1-¹⁴C), and therefore, no meaningful kinetic measurements could be made on the latter system. In another experiment, the kinetics of benzyl group transfer was studied in the para-benzylphenol-BF₃ system. The kinetic measurements were made in sealed glass tubes at 100°C using a para-benzylphenol to BF₃ mole ratio of 6.25/1.0. The two principal reactions which take place in this system are shown in Figure 3. In agreement with the reaction scheme shown in Figure 3, the rate of disappearance of the sum of para- and ortho-cresols followed a second order rate equation. The ratio of the initial reaction rates of reaction 1a to 1b was found to be approximately 4.0. In addition to phenol and benzene, significant amounts of diphenylmethane and some para-cresol were formed during the latter part of the reaction. Also, isomerization to ortho-benzylphenol took place as a result of the reverse reactions of 1a and 1b.

A more detailed kinetic study of benzyl group transfer was made using the 4-benzyl-2,6-dimethylphenol/BF₃ system. This system was selected for investigation for the following reasons: (a) In the benzylphenol/BF₃ system two parallel major reactions have taken place giving dibenzylphenol and phenol in one reaction, and hydroxybenzylphenols and benzene in the other. It was expected that the additional activating effect of the two methyl groups on the phenolic ring will sufficiently enhance the reactivity of the methylene-aromatic carbon-carbon bond on the side of the phenolic ring to make the cleavage of that bond the predominant reaction; (b) The chemical shifts of the benzyl protons and of the 2-methyl protons of the starting material and of the main products were sufficiently different to permit the quantitative analysis of the reaction mixture by proton NMR spectrometry. The chemical shifts of the benzyl -CH₂- groups and of the methyl groups in the starting material and in the products are shown in Table 3.

The reaction which was studied is shown in the following equation:



The kinetic measurements were made in CS₂ solution at 70°C using sealed NMR sample tubes as the reactors. After the completion of the prescribed reaction period each sample tube was quickly cooled to room temperature and transferred to the NMR spectrometer for recording the spectra. When a solution of 4-benzyl-2,6-dimethylphenol and BF₃ (mole ratio 4.5 to 1.0) was used, the absorption under the methylene peak (3) and the methyl peak (2) increased from an initial value of zero as the reaction advanced, showing the formation of 3,4-dibenzyl-2,6-dimethylphenol. Independent gas chromatographic analysis showed the formation of an equivalent amount of 2,6-dimethylphenol. Reaction rate constants were determined for both the forward (k₁) and the reverse (k₋₁) reactions for three different BF₃ concentrations. The following correlations were determined:

$$\text{Rate (forward reaction)} = k_1 [\text{BF}_3] [(\text{CH}_3)_2(\text{HO})\text{C}_6\text{H}_2\text{-CH}_2\text{-C}_6\text{H}_5]^2$$

$$\text{Rate (reverse reaction)} = k_{-1} [\text{BF}_3] [(\text{CH}_3)_2(\text{HO})\text{C}_6\text{H}(\text{CH}_2\text{-C}_6\text{H}_5)_2] [(\text{CH}_3)_2(\text{HO})\text{C}_6\text{H}_3]$$

At 70°C and at a concentration of BF₃ = 1.0 moles per litre, k₁ = 2.6 ± 0.3 × 10⁻⁴ min⁻¹ lit. moles⁻¹ and k₋₁ = 16.0 ± 1.8 × 10⁻⁴ min⁻¹ lit. moles⁻¹. The benzyl group transfer in this system is clearly a bimolecular substitution reaction where the rate determining step involves a reaction between a protonated benzyl compound (benzenium ion) and a phenolic compound or its BF₃- complex. There is no indication of the formation of the benzyl cation in this particular system. It should be noted here that the data obtained on the transfer of n-propyl groups (Table 2) indicate that, similarly, the main reaction in that transfer does not involve the formation of the 1-propenium cation. If that were the case, isomerization to the 2-propenium cation would take place with the predominant formation of iso-propylphenols. On the other hand, the formation of diaryl-methenium cations was indicated in model compound studies reported by Franz et al.,⁽¹¹⁾ who studied the behavior of triaryl-methanes under depolymerization conditions using both PTSA and phenol-BF₃ as the catalyst.

III. COMMENTS ON THE CHEMISTRY OF COAL DEPOLYMERIZATION

After reviewing the information on the reactivities of various bridge structures which may be present in coal, it will be instructive to summarize available data on coal depolymerization yields as a function of coal rank. One can attempt then to correlate the product yields obtained by depolymerization with various structural features of coals over the coalification range which has been investigated.

Depolymerization yields determined with phenol-BF₃ at 100°C are summarized in Table 4,⁽¹²⁾ and the yields obtained with phenol-PTSA depolymerization at 185°C are shown in Figure 4.⁽³⁾ In the case of the phenol-BF₃ catalyst, the phenol-soluble product yield was the highest (75%) for the lignite. It gradually decreased to about 10% for the low-volatile bituminous coal, although the low product yield obtained with subbituminous coal does not fit this correlation. In the case of depolymerization with phenol-PTSA, the pyridine-soluble product yield was over 90% for coals of 70-84% C content; for coals with higher C content, the yield dropped sharply and it reached about 10% for a coal with 93% C. Benzene-ethanol was a more selective solvent than pyridine for fractionating the depolymerization products obtained with PTSA catalyst: a linear relationship between the yield of the soluble extract and the carbon content of the starting coal was observed.

The following comments can be made with regard to a correlation of the coal depolymerization product yields with the relative reactivities of aliphatic carbon and oxygen bridge structures in coal:

- (1) In low-rank coals, particularly in lignites, the cleavage of aliphatic ether and benzyl ether oxygen bonds may contribute significantly to depolymerization. Many of the aliphatic bridges, which participate in depolymerization, may be linked to single phenolic rings. The reactivity of an aliphatic structure linked to a

phenolic ring is sufficient to permit its participation in the depolymerization reaction. On the other hand, spectrometric studies indicate⁽¹³⁾ that these coals do not contain significant amounts of sufficiently reactive condensed aromatic structures which could participate in depolymerization.

- (2) In high-volatile bituminous coals (C = 80-84%), the breaking of aliphatic bridges is seen as the major means of depolymerization. Many of these bridges may be linked to phenolic rings, others to condensed aromatic rings such as phenanthrene. Ether oxygen bonds play a less important role because most of these bonds are in aromatic ethers which do not react with BF₃.
- (3) In higher rank bituminous coals (C > 84%), the depolymerization product yield decreases sharply with increasing rank. It is probable that this decrease is related to the nature of the aliphatic bridge structures. It is postulated that in lower rank coals a sufficient number of the bridge structures are short aliphatic chains (N_C = 1 to 4). On the other hand, in higher rank coals, nearly all of the bridge structures are condensed hydroaromatic rings; with structures of this type, several bonds must be broken between two aromatic groups to effect depolymerization.
- (4) Among the aliphatic bridge structures, -CH₂- bridges may play a particularly important role in coal depolymerization. Even if the number of such bridges is relatively small, the probability of their cleavage is high because, in general, both carbon-carbon bonds of the bridge are activated under the reaction conditions used in coal depolymerization. This view is supported by experimental data obtained in depolymerization studies made with phenol-BF₃ where the yield of soluble depolymerized products was proportional to the amount of -CH₂- bridge structures found in the soluble products.⁽¹²⁾

REFERENCES

1. L. A. Heredy and M. B. Neuworth, *Fuel*, **41**, 221 (1962)
2. E. A. Depp, C. M. Stevens, and M. B. Neuworth, *Fuel*, **35**, 437 (1956)
3. K. Ouchi, K. Imuta, and Y. Yamashita, *Fuel*, **44**, 29 (1965)
4. L. J. Darlage and M. E. Bailey, *Fuel*, **55**, 205 (1976)
5. L. J. Darlage, J. P. Weidner, and S. S. Block, *Fuel*, **53**, 54 (1974)
6. J. W. Larsen and E. W. Kuemmerle, *Fuel*, **55**, 162 (1976)
7. L. A. Heredy, A. E. Kostyo, and M. B. Neuworth, *Fuel*, **42**, 182 (1963)
8. J. J. O'Connor and F. J. Sowa, *JACS*, **60**, 175 (1935)
9. W. J. Monacelli and G. F. Hennion, *JACS*, **63**, 1722 (1941)
10. L. A. Heredy, *Studies on the Chemistry and Mechanism of Transbenzylation*, Doctoral Dissertation, Carnegie Institute of Technology, Pittsburgh (1962)
11. J. A. Franz, J. P. Morrey, G. L. Tingey, W. E. Skiens, R. J. Pugmire, and D. M. Grant, *Fuel*, **56**, 366 (1977)
12. L. A. Heredy, A. E. Kostyo and M. B. Neuworth, *Fuel* **44**, 125 (1965); *Coal Science, Advances in Chemistry Series*, **55**, 493 (1966)
13. H. L. Retcofsky, *Applied Spectroscopy*, **31**, 116 (1977)

TABLE 1
 BF₃-CATALYZED ISO-PROPYL GROUP TRANSFER TO PHENOL (1-¹⁴C)

Starting Compound*	Conversion (%)	Product Distribution (wt %)		
		para-isopropyl-phenol (1- ¹⁴ C)	ortho-isopropyl-phenol (1- ¹⁴ C)	Residue
Cumene	8.0 ⁺	3.5	0.8	3.7
ortho-isopropylphenol	100.0	74.5	14.5	11.0
Retene (1-methyl-7-isopropylphenanthrene)	100.0 ⁺⁺	61.5	10.2	28.3

*Starting compound to labelled phenol molar ratio: 1 to 20. Reactions performed at 100°C for four hours. Mixture saturated with BF₃

+Benzene, in an amount equivalent to the isopropylphenols, was also recovered

++A methylphenanthrene fraction, in an amount equivalent to isopropylphenols, was also recovered

TABLE 2
 BF₃-CATALYZED REACTION OF PARA-N-PROPYLPHENOL WITH PHENOL (1-¹⁴C)

Reaction Conditions:
 Ratio of para-n-propylphenol to phenol (1-¹⁴C): 1 to 20
 Mixture saturated with BF₃ at reaction temperature
 Temperature: 100°C
 Reaction Period: 4 hours

<u>Product Distribution (wt %):</u>	
para-n-Propylphenol (unreacted)	: 18.0
para-n-Propylphenol (1- ¹⁴ C)	: 43.0
ortho-n-Propylphenol (1- ¹⁴ C)	: 14.5
para-iso-Propylphenol (1- ¹⁴ C)	: 5.3
ortho-iso-Propylphenol (1- ¹⁴ C)	: 1.2
Residue	: 18.0
Total	: 100.0

TABLE 3
CHEMICAL SHIFT VALUES OF METHYLENE AND METHYL
 PROTONS OF BENZYL DERIVATIVES OF 2,6-DIMETHYLPHENOL

COMPOUND	CHEMICAL SHIFT (ppm)*			
	METHYLENE		METHYL	
	(3)	(4)	(2)	(6)
2,6-DIMETHYLPHENOL	---	---	2.08	2.08
4-BENZYL- 2,6-DIMETHYLPHENOL	---	3.70	2.03	2.03
3,4-DIBENZYL- 2,6-DIMETHYLPHENOL	3.80	3.70	1.95	2.10

*TETRAMETHYLSILANE = 0.00 ppm

TABLE 4
 DEPOLYMERIZATION OF COALS OF DIFFERENT RANKS WITH PHENOL-BF₃ AT 100°C

Coal Type	C, % dmmf	Total Soluble ^(a) Yield, %	Combined Phenol Content of Soluble Fraction, %
Lignite	70.6	75.2	41.2
SubB	76.7	23.4	32.8
hvab	82.4	47.4	16.3
hvab	85.1	28.8	12.4
hvab	85.8	25.0	13.0
lvb	90.7	9.8	15.5

^(a) Coal-derived part of phenol soluble material

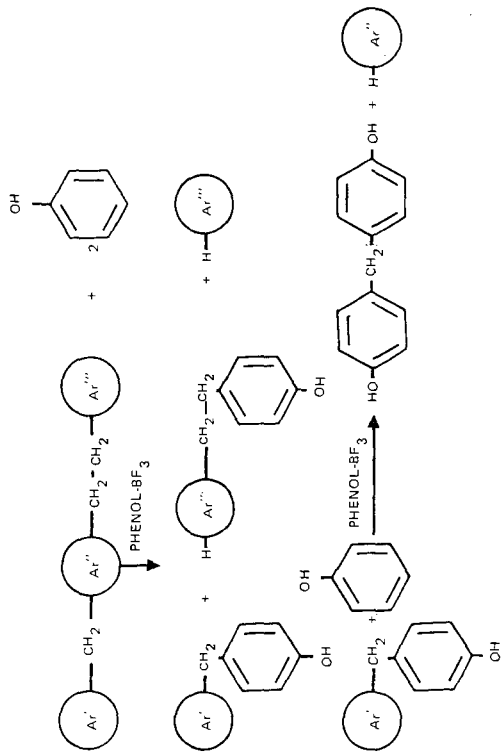
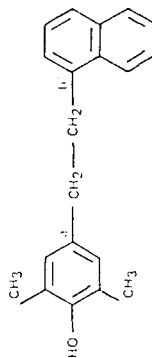


Figure 1. Copolymerization via Transalkylation with Phenol-BF₃

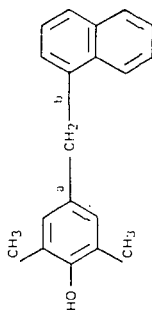
FIGURE 2
 RELATIVE REACTIVITIES OF MODEL COMPOUNDS WITH PHENOL-BF₃

<u>Model Compound</u>	<u>Reacting Bond</u>	<u>Relative Reactivity</u>
A	a'	77
A	b'	2
B	a	70
B	b	41

Model Compound A:



Model Compound B:

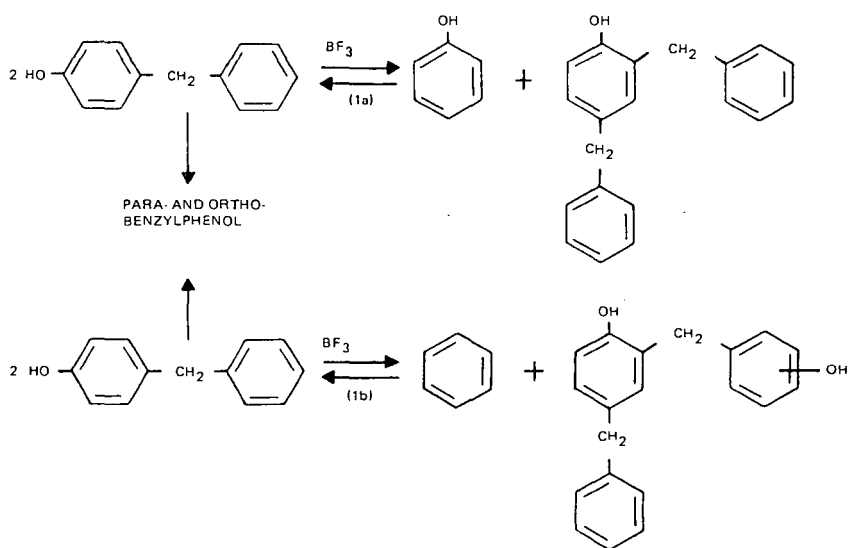


Reaction Conditions:

Ratio of Model Compounds to Phenol: 1 to 10
 Mixture Saturated with BF₃ at Reaction Temperature
 Temperature: 100°C
 Reaction Period: 4 hours

FIGURE 3.

BF₃-CATALYZED BENZYL GROUP TRANSFER IN BENZYLPHENOLS



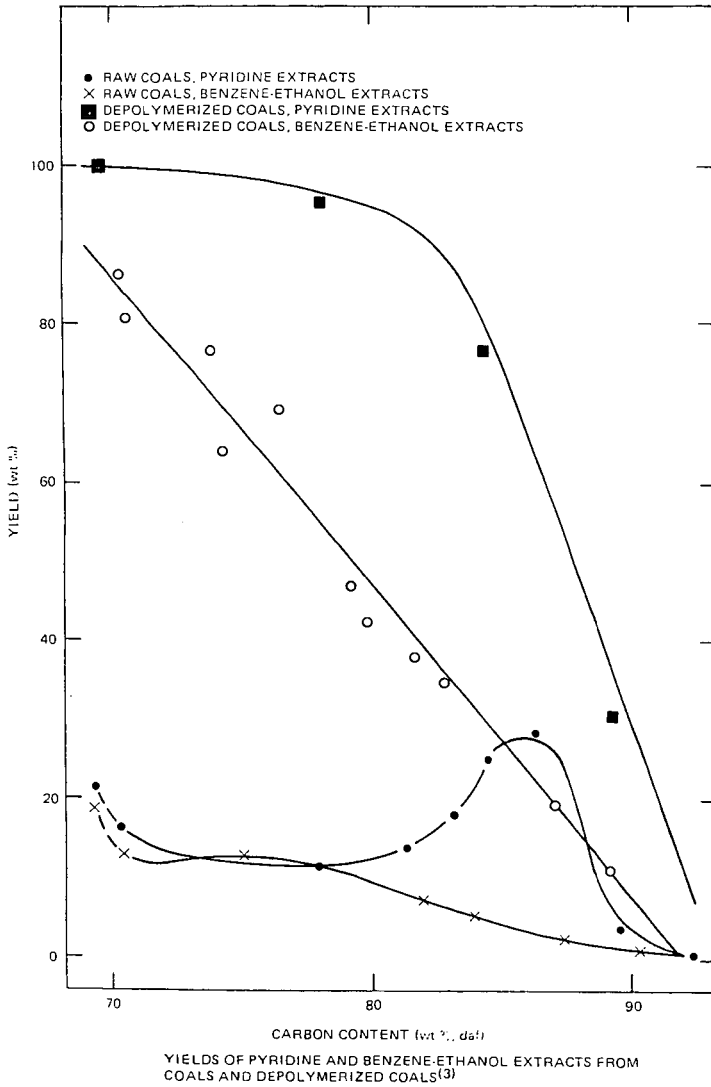


FIGURE 4. -

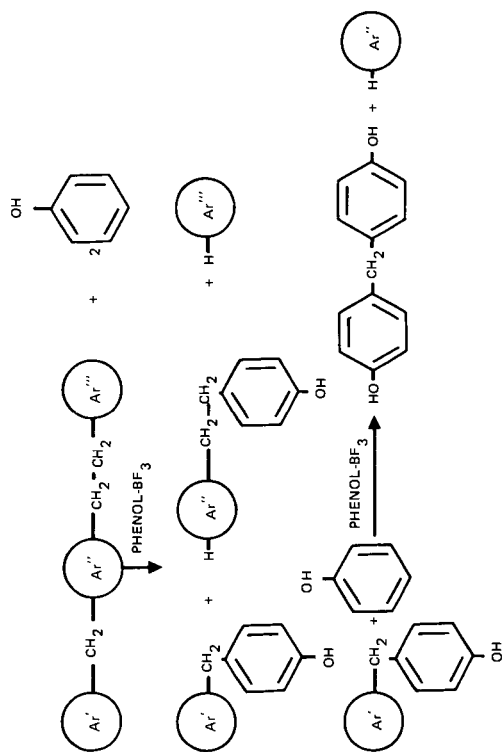
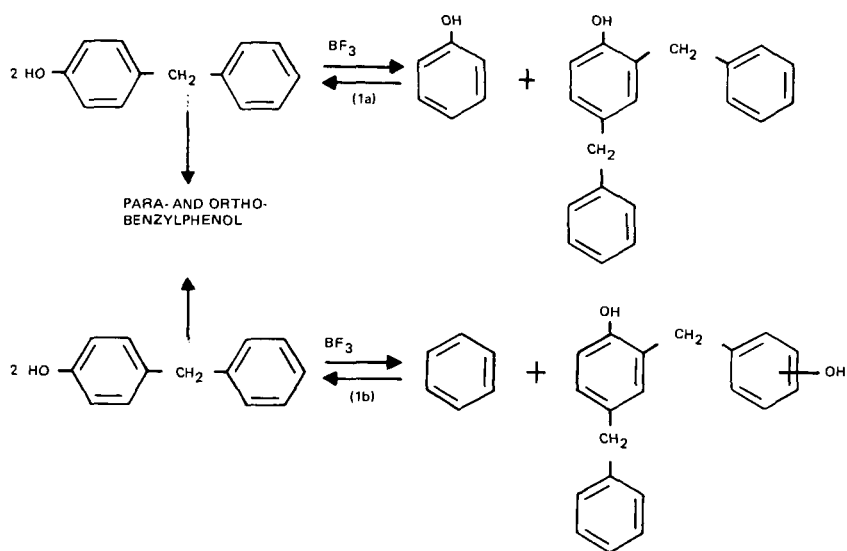
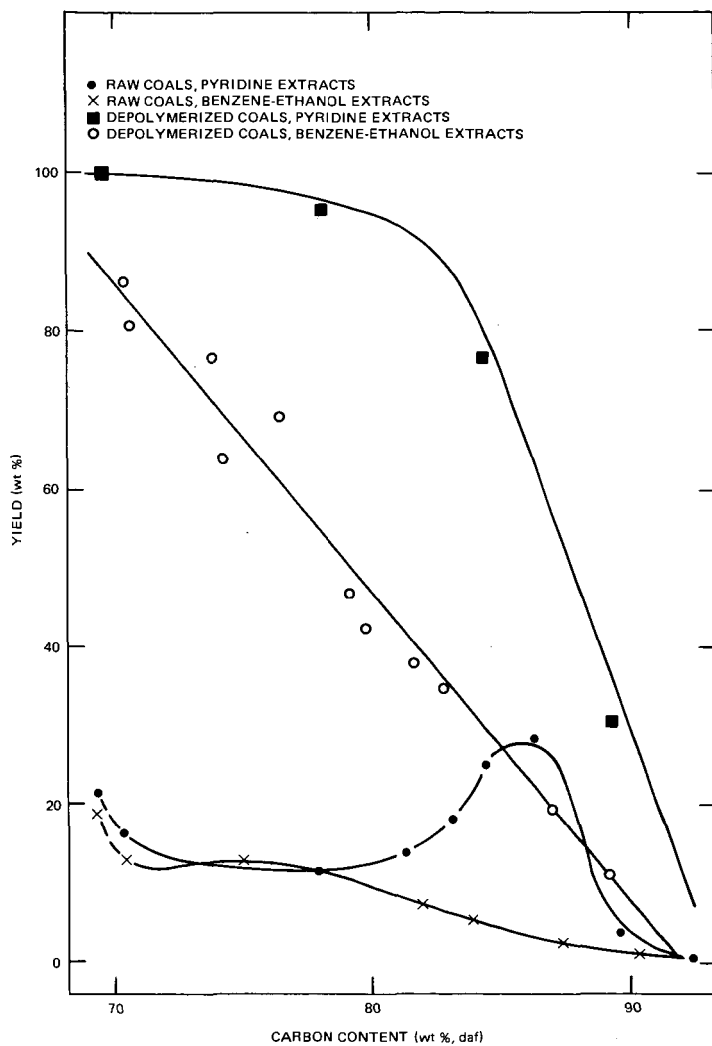


Figure 1. Coal Depolymerization via Transalkylation with Phenol-BF₃

FIGURE 3.

BF₃-CATALYZED BENZYL GROUP TRANSFER IN BENZYLPHENOLS





YIELDS OF PYRIDINE AND BENZENE-ETHANOL EXTRACTS FROM
 COALS AND DEPOLYMERIZED COALS⁽³⁾

FIGURE 4.

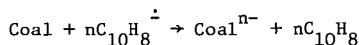
COAL ALKYLATION REACTION. THE CHARACTERISTICS
OF THE ALKYLATION REACTIONS AND PRODUCTS

Lawrence B. Alemany, C. Indhira Handy and
Leon M. Stock

Department of Chemistry
The University of Chicago
Chicago, Illinois 60637

INTRODUCTION

Sternberg and his associates found that the treatment of many coals with alkali metals in the presence of electron transfer agents formed polyanions which could be alkylated to form compounds which were soluble in common organic solvents including heptane and benzene (1). More recently, we discussed the proton and carbon nmr spectra of typical gpc fractions of polybutylated Illinois No. 6 coal (2). This work revealed that there were significant differences in these fractions with variations in the degree of aromaticity, the ratio of C-butylation to O-butylation, the extent of butylation on aliphatic and aromatic carbon atoms, and the amount of carbonyl and vinyl derivatives. In addition, the low molecular weight fractions contained paraffinic hydrocarbons which presumably were liberated as the coal matrix collapsed. The results obtained in this work are compatible with the essential features of the reaction process proposed by Sternberg and his associates (1,2). He suggested that the electron transfer agent, naphthalene, transfers electrons from the metal to molecular fragments in the coal. Under these conditions,



the aromatic molecules of the coal are reduced, and the basic anions produced under the experimental conditions react with acidic hydrogen atoms to yield aryloxides and stable carbanions. Ether cleavage and elimination reactions also occur under these experimental conditions. In addition, carbon-carbon bond cleavage reactions take place. Also, carbonyl compounds are reduced to semiquinones or ketyls. In the presence of sufficient concentrations of soluble electron transfer reagents, an equilibrium mixture of soluble and insoluble polyanions containing carbanions, aryloxides, mercaptides, ketyls, nitrogenous bases and so forth is generated. Because few rearrangement reactions occur under basic conditions the structures of the anionic products are quite closely related to the structures of the molecular fragments in coal. These anionic compounds are readily alkylated by primary iodides. However, the alkylation reaction is complicated by competitive electron transfer reactions which yield butyl radicals. Thus, the coal alkylation reactions occur by the reactions of the nucleophilic anionic compounds with the alkyl iodide and by the reactions of the aromatic hydrocarbon compounds with the butyl radical.

The rich chemistry of the coal polyanion and the presumably close relationship between the structures of the coal polyanion and the initial coal molecules prompted us to study the reaction conditions and the reaction products carefully and then to examine the reaction of the coal polyanion with 90%-enriched butyl iodide-1-C-13.

EXPERIMENTAL PART

Materials.--Successful alkylations require the use of thoroughly purified reagents in an air and moisture-free environment. The reagents used in this work were all carefully purified by distillation or recrystallization shortly before use. The Illinois No. 6 coal samples (Anal.: C, 70.19; H, 5.18; N, 0.62; Cl, 0.14; S(pyritic), 0.82; S(sulfate), 0; S(organic), 2.71; O(by diff.) 11.43; Ash, 8.19) were dried at 100° in vacuo for 16 hrs. Tetrahydrofuran was refluxed in a nitrogen atmosphere over lithium aluminum hydride for 4 hrs prior to distillation from the hydride. The distillate was stored under argon. Tetrahydrofuran could not be purified as readily by distillation from potassium. We found that the resonances of vinyl, carboxyl and other unidentified groups were present in the nmr spectra of concentrated samples of the distillate when potassium was used as the purification reagent.

Preliminary Experiments.--Initial work centered on the study of the reaction of potassium with tetrahydrofuran and with naphthalene in tetrahydrofuran.

Potassium (20 mmol) was added to tetrahydrofuran (50 ml) under argon. Aliquots free of potassium were withdrawn periodically. These aliquots were hydrolyzed and titrated to determine the extent of the reduction of the solvent. This reaction was negligible even after 5 days, Figure 1A.

In the next experiment, potassium (20.1 mmol) was added to a stirred solution of naphthalene (3.10 mmol) in tetrahydrofuran (50 ml) under argon. The characteristic dark green solution of naphthalene radical anion and dianion formed within 4 min. Aliquots free of potassium were withdrawn from the reaction mixture. These aliquots were hydrolyzed and titrated to determine the extent of conversion of naphthalene to the radical anion and dianion. After about 4.5 hrs, the titrimetric procedure revealed that the naphthalene was converted to a mixture equal in reducing power to 80% dianions. The reaction was followed for 5 days. The results are shown in Figure 1B.

In the third experiment of this series, potassium (20.1 mmol) and naphthalene (3.10 mmol) in tetrahydrofuran (50 ml) were allowed to react for 4.5 hrs. Coal (0.860g) was then added. The reaction mixture immediately became brown. During the next several days the reaction mixture changed color as the reactions proceeded. Aliquots free of potassium but containing solid coal particles were withdrawn from this mixture and titrated to determine the extent of conversion of the coal to the coal polyanion. In certain instances, aliquots free of potassium and solid coal particles were withdrawn from the reaction mixture and titrated to determine the extent of conversion of the solid coal to soluble anionic substances. The reaction was allowed to proceed for 5 days at ambient temperature under argon. An aliquot of the mixture was then withdrawn to establish the extent of the reaction. The results are shown in Figure 1C.

The results obtained in several experiments revealed that 21 ± 1 negative charges per 100 carbon atoms were introduced into the coal.

Coal Alkylation with Butyl Iodide-1-C-13.--Potassium (26.1 mmol) was added to a stirred solution of naphthalene (3.14 mmole) in tetrahydrofuran (45 ml) under argon. After 45 min, -325 mesh coal (1.00g) and an additional wash quantity of tetrahydrofuran (10 ml) were added. The mixture was stirred for 5 days. The excess potassium (2.98 mmol) was removed. A small quantity of insoluble coal (0.041g) was unavoidably lost in the removal of the metal. A solution of 90%-enriched butyl iodide-1-C-13 (6.88g) in tetrahydrofuran (10 ml) was added to the stirred solution in 15 min. This quantity corresponds to a 2-fold excess of the amount of reagent needed for the alkylation of a coal polyanion with 21 negative charges per 100 carbon atoms and naphthalene dianion. Potassium iodide began to precipitate from the reaction mixture almost immediately. The alkylation reaction was allowed to proceed for 2 days. Potassium iodide rapidly settled from the reaction mixture when stirring was interrupted.

The reaction mixture was then exposed to the atmosphere and the coal product was isolated. The mixture was centrifuged and the very dark brown, tetrahydrofuran-soluble material was removed by pipet. Fresh solvent was added to the residue and the mixture was stirred. The mixture was then centrifuged and the soluble material was removed by pipet. This procedure was repeated several times. The final extracts were clear, pale yellow solutions. The combined extracts were filtered through a 1.4μ frit. The filtrate was concentrated in vacuo at 50°C to yield a freely flowing, dark brown material (2.252g). Residual volatile materials were removed in several stages in vacuo. The amounts of material present after 2 hrs were 1.956g; after 16 hrs, 1.678g; after 41 hrs, 1.581g; and after 68 hrs, 1.521g. This product is dark brown and does not flow.

Water was added to dissolve the potassium iodide present in the tetrahydrofuran-insoluble material. The mixture was then stirred and subsequently centrifuged to yield a clear, yellow supernatant solution and a small residue. This residue was treated in the same way several times to extract all the water soluble materials. The final extracts were colorless and did not yield a precipitate when treated with sodium tetrphenylborate. The residue obtained in this way was dried in a stream of dry nitrogen to constant weight (0.686g).

The water-soluble material was filtered through a 1.4μ frit. An aliquot of the solution was treated with excess sodium tetrphenylborate. The potassium tetrphenylborate which precipitated was collected and dried. This analysis indicates that 18.1 meq of potassium ion were formed in the reaction.

The tetrahydrofuran-soluble portion of the butylated, carbon-13 labelled Illinois No. 6 coal (1.5208g) was chromatographed on silica gel (Baker, 60-200 mesh, 24g) to remove materials such as the electron transfer agent and the related reduction and alkylation products. These materials were eluted with pure hexane (about 250 ml) and 5:95 tetrahydrofuran: hexane (about 250 ml). The dried eluent weighed 0.9967g. The coal products were then eluted with pure tetrahydrofuran (about 250 ml) followed by 50:50 tetrahydrofuran: methanol (about 250 ml) and pure methanol (about 250 ml). The dried eluent weighed 0.5350g. The recovery was virtually quantitative.

A portion of the coal product (168.1 mg) was dissolved in pure tetrahydrofuran (2 ml) and chromatographed on Styragel(R) gpc columns (Waters Associates). Columns with a molecular weight exclusion limit of 10,000 (2 x 61 cm.) and 2,000

(2 x 61 cm.) were connected in series. Tetrahydrofuran was used as the mobile phase ($0.36 + 0.01 \text{ ml min}^{-1}$). About 30 fractions (3.7 to 3.8 ml) were collected in each experiment. The tetrahydrofuran was removed in vacuo and a stream of filtered, dry nitrogen was used to remove the final traces of the solvent. The coal product obtained with C-13 labelled butyl iodide was partitioned into 17 fractions (total weight 178.4 mg). Samples to be used for nmr spectroscopy were dried thoroughly at 25° at about 5 torr for 40-45 hrs to remove the remaining traces of tetrahydrofuran.

The spectroscopic methods used in this study have been described previously (2).

Other Alkylation Experiments.--In other experiments, lithium and sodium were used in place of potassium. 1,2-Dimethoxyethane was used in place of tetrahydrofuran. Butyl chloride, butyl bromide, butyl mesylate, butyl triflate, and methyl iodide were used in place of butyl iodide. The conditions used in these experiments were very similar to the conditions used in the procedures described in the previous paragraphs. The isolation procedure was modified in those cases where the ionic salt, e.g. sodium iodide, was soluble in tetrahydrofuran. In these instances, the tetrahydrofuran-soluble product was washed with water to remove the salt prior to further study.

Repetitive Alkylation Reaction.--The tetrahydrofuran-insoluble materials were, in certain instances, subjected to a second alkylation reaction. In these cases, there were three notable differences in the experimental results. First, the green color of the naphthalene dianion persisted for a significantly longer time following the addition of the coal residue. Second, gas evolution, presumably butene-1, was detectable during the addition of butyl iodide or butyl mesylate but, significantly, not during the addition of methyl iodide. Third, the rate of formation of potassium iodide was much more rapid such that the rate difference between butyl iodide and methyl iodide was not evident.

The reaction products were separated into tetrahydrofuran-soluble and tetrahydrofuran-insoluble fractions as already described. The chromatographic separations and spectroscopic investigations were also performed as described.

RESULTS AND DISCUSSION

The rates of reduction of tetrahydrofuran (A), naphthalene (B), and Illinois No. 6 coal (C) are shown in Figure 1. These preliminary experiments established that potassium reacted only very slowly with tetrahydrofuran under the experimental conditions used for the formation of the coal polyanion. Naphthalene was rapidly converted to a mixture of anion radicals and dianions under the same conditions. The initial reaction between the electron transfer reagent and the Illinois No. 6 coal was quite rapid. However, the reaction slowed to nearly constant rate after about 12 hours. During the last four days of reaction the coal molecules acquired about 0.1 negative charges per 100 carbon atoms per hour.

The titrimetric data indicated that the coal polyanions derived from this coal quite reproducibly had 21 ± 1 negative charges per 100 carbon atoms when potassium was used as the reducing agent. The evidence obtained in the magnetic resonance work on the reaction products suggests that these negative charges reside largely on the oxygen atoms of the phenoxide and alkoxide residues and on the carbon skeletons of the aromatic fragments of the coal structure.

Potassium is a much more effective reducing agent than either sodium or lithium. This feature of the reaction is illustrated by the extent of reduction (measured by the number of negative charges per 100 carbon atoms) and the extent of alkylation (measured by the number of alkyl groups introduced and the weight of the reaction products). The results are summarized in Table I.

TABLE I
THE REDUCTION AND ALKYLATION OF ILLINOIS NO. 6 COAL WITH
LITHIUM, SODIUM, AND POTASSIUM

Reagent Pair	Reduction ^a	Alkylation ^b
Lithium, Butyl iodide	12.0	12.2 (0.78g)
Sodium, Butyl iodide	12.9	13.2 (1.17g)
Potassium, Butyl iodide	19.3	20.1 (1.52g)

^aNegative charges acquired per 100 carbon atoms.

^bButyl groups introduced per 100 carbon atoms. The weight of tetrahydrofuran-soluble product obtained from 1.00g of coal.

The reactions of the coal polyanion with methyl iodide and butyl iodide were compared in tetrahydrofuran. The reaction could be monitored quite readily by the rate at which potassium iodide precipitated from solution. We estimate that methyl iodide is about 10-fold more reactive than butyl iodide under these conditions. This result, of course, suggests that the SN2 reactions of the coal polyanion are more significant than the electron transfer reactions. Although there is a clear distinction in the reaction rate, the extent of the alkylation reaction is the same for methylation and butylation with about 21 alkyl groups introduced per 100 carbon atoms. The amount of tetrahydrofuran-soluble alkylation product is also similar for methylation and butylation under comparable conditions.

The observations concerning the butyl halides and sulfonates are summarized in Table II.

TABLE II
ALKYLATION REACTIONS WITH BUTYL DERIVATIVES

Reagent, equivalents ^a	First Reaction		Second Reaction		Total %
	Solubility, ^b %	Residue, ^c g	Solubility, ^b %	Residue, ^c g	
BuCl, 2.0	23	1.00	--	--	--
BuBr, 2.0	51	0.64	--	--	--
BuI, 2.0	62	0.49	74	0.18	79
BuOSO ₂ CH ₃ , 2.0	64	0.51	polymer	--	--
BuOSO ₂ CF ₃ , 2.0	polymer	--	--	--	--

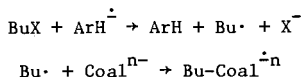
^aBased on the number of negative charges acquired by the coal.

^bThe percentage of the original coal which has been converted to soluble product. The values reported here have been corrected for the extent of the alkylation reaction.

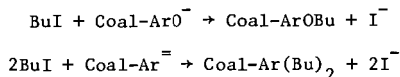
^cThe weight of the tetrahydrofuran-insoluble residue. No correction has been applied for either alkylation or mineral matter.

The reactions of the potassium coal polyanion with the butylation reagents differed markedly. Both the percentage of soluble product and the weight of residue indicate that the reactions of the chloride and the bromide are distinctly less effective than the reactions of the iodide. The butyl sulfonate esters were much more reactive. In one case, the mere addition of freshly distilled butyl triflate to tetrahydrofuran at room temperature caused the polymerization of the solvent. In the other case, the addition of butyl mesylate to the reaction mixture was effective for the production of soluble products in 64% conversion. However, when the reaction was repeated with the residue, a polymerization reaction ensued and a gas, 1-butene, was evolved from the reaction mixture.

These observations indicate that butyl iodide is adequately reactive for the alkylation of the polyanion. This reagent effectively converts more than 90% of the original carbonaceous matter in the coal to soluble alkylation products. The fact that the reactions of butyl chloride and butyl bromide do not give similar results suggests very strongly that SN2 reactions rather than electron transfer reactions are primarily responsible for the production of soluble materials. This interpretation is based on the fact that the reactivities of nucleophiles with butyl iodide, bromide, and chloride are in the approximate order 100:60:1 and that these substitution reactions are all slow relative to the electron transfer reactions of the butyl halides with anion radicals. To illustrate, the rate constants for the reactions of primary alkyl iodides with anion radicals of the kind formed under the conditions of these experiments are about 10^7 l/mole sec (3). The rate constants for the reactions of primary alkyl iodides with nucleophiles are much smaller, only about 10 l/mole sec in the fastest processes (4). Thus, we infer that the butyl halides all undergo rapid electron transfer reactions to produce butyl radicals during the initial stages of the alkylation process. We also infer that this process is less important



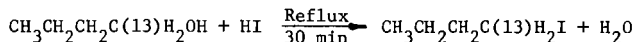
for the formation of soluble products than the alkylation reactions



which proceed much more slowly. Indeed, we observed that the precipitation of potassium iodide from the reaction of butyl iodide with the coal polyanion appeared to be complete only after about 24 hrs. Thus, the much slower reactions of the polyanion with the other halides would not be complete in 48 hrs.

In another experiment, we tested the utility of 1,2-dimethoxyethane as a solvent for the reaction. The results obtained in this experiment revealed that the coal polyanion was formed to the same extent as in tetrahydrofuran. In addition, the alkylation of the polyanion with butyl mesylate proceeded to give 65% soluble product. This datum is comparable with the result for butylation in tetrahydrofuran, 64%. Hence both solvents are equally useful for the alkylation reaction.

When we were satisfied that the alkylation reaction could be accomplished both effectively and reproducibly, we undertook the synthesis of C-13-enriched butyl iodide. Conventional procedures were used to produce the desired compound in 90% isolated yield using concentrated hydroiodic acid.



The coal alkylation reaction was carried out using the enriched compound and the products were separated using the procedures described in the Experimental Part. The proton and carbon nmr spectra of one fraction (comparable to fraction 9 in the previous report (2)) are presented in Figures 2 and 3.

The proton nmr spectra of the coal products obtained in this work are quite similar to the spectra of the products obtained by Sun and Burk and discussed previously (2). No additional comments on this aspect of the work are necessary.

The carbon nmr spectra, on the other hand, provide much new information concerning the alkylation reaction. To illustrate, the resonances at $\delta 67.7$, 72.9 , and 64.2 indicate that O-butylation has occurred dominantly on aryloxides with concomitant butylation on alkoxide and possibly carboxylate fragments. The broad band of resonances at $\delta 35$ indicate that C-butylation is also important and that butyl groups are bonded to quaternary and tertiary sp^3 carbon atoms and possibly to aromatic carbon atoms. These results and the other spectroscopic data for other fractions enriched in carbon-13 will be discussed.

ACKNOWLEDGEMENT

This research was supported by the Department of Energy under contract EF-77-S-02-4227.

REFERENCES AND NOTES

1. (a) H.W. Sternberg, C.L. DelleDonne, P. Pantages, E.C. Moroni, and R.E. Markby, Fuel, **50**, 432 (1971). (b) H.W. Sternberg and C.L. DelleDonne, ibid., **53**, 172 (1974).
2. L.B. Alemany, S.R. King, and L.M. Stock, ibid., **57**, 000 (1978).
3. B. Bockrath and L.M. Dorfman, J. Phys. Chem., **77**, 2618 (1973).
4. S. Bank and D.A. Juckett, J. Amer. Chem. Soc., **97**, 567 (1975).

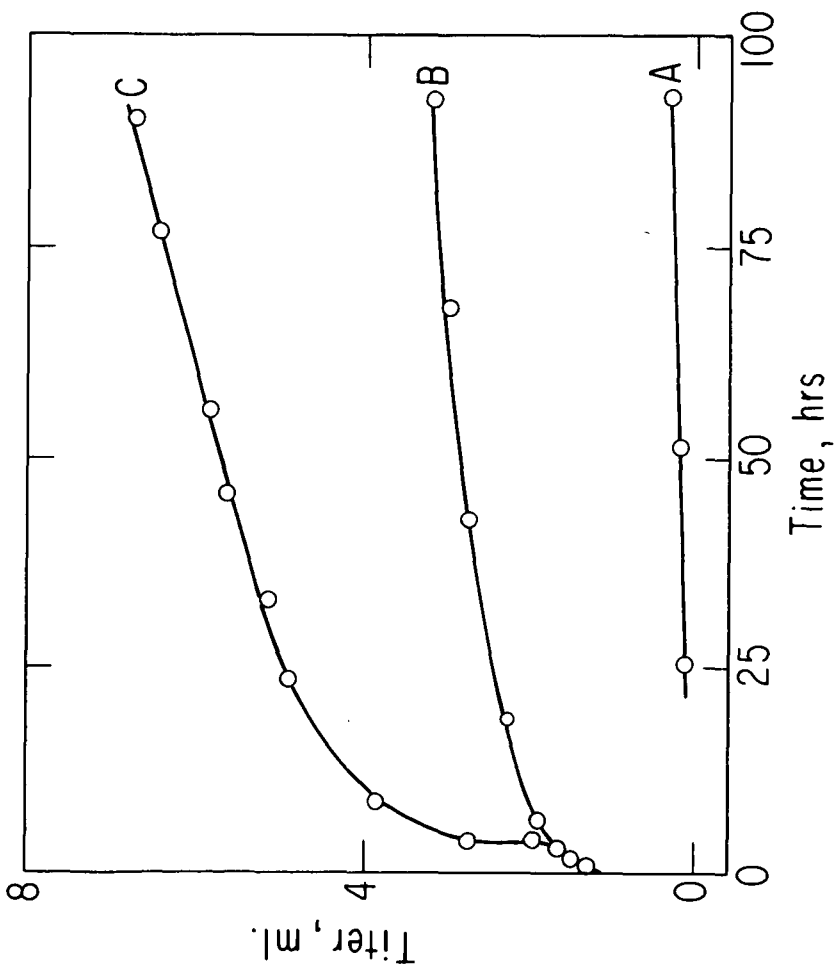


Figure 1.—The rates of reduction of tetrahydrofuran (A), naphthalene (B), and Illinois No. 6 coal (C) are presented by a comparison of the titer required for aliquots of separate reaction mixtures over 100 hrs.

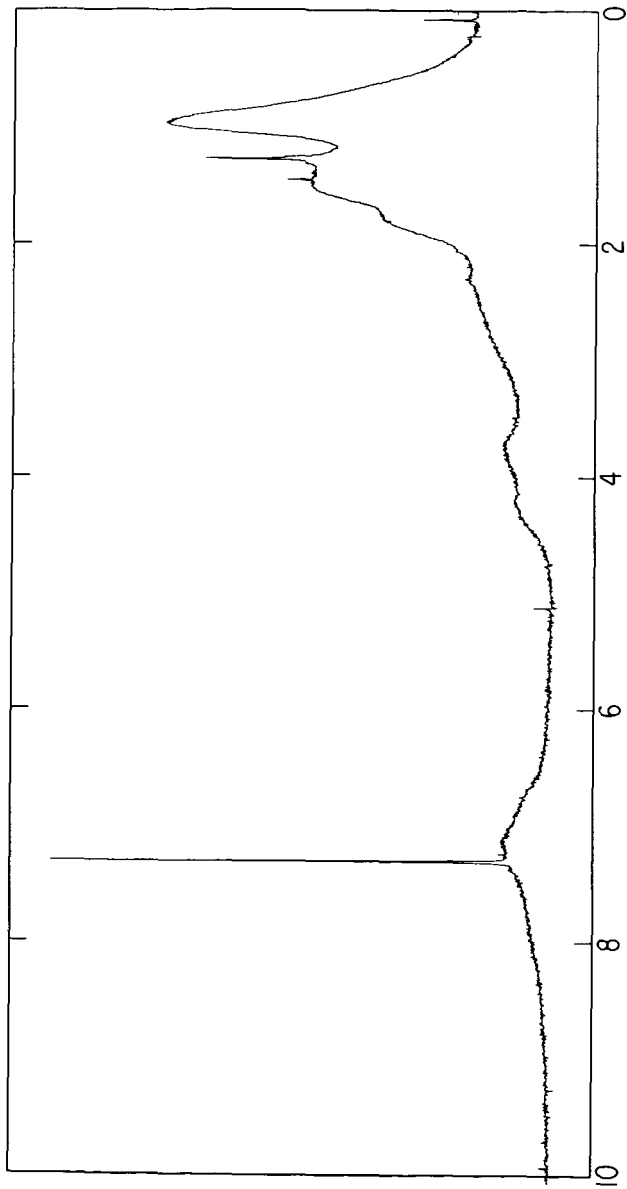


Figure 2.--The proton nmr spectrum of a representative fraction of coal butylated with the C-13 enriched reagent. The intense signal at $\delta 7.3$ results from residual chloroform.

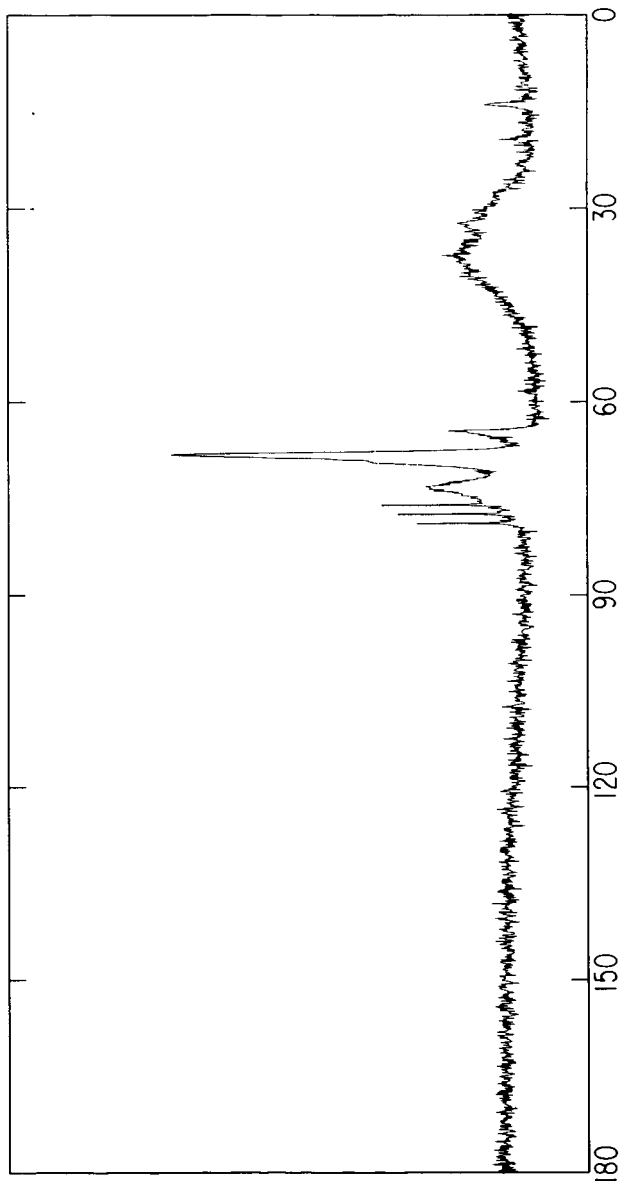


Figure 3.--The carbon nmr spectrum of a representative fraction of coal butylated with the C-13 enriched reagent. The three sharp signals at about $\delta 77$ result from chloroform.

DATA ON THE DISTRIBUTION OF ORGANIC SULFUR FUNCTIONAL GROUPS IN COAL

By: Amir Attar and Francois Dupuis

Department of Chemical Engineering, University of Houston, Houston, Texas 77004

1.0 Introduction

Coals contain inorganic sulfur compounds, like iron pyrite and gypsum and organic sulfur, which is bound to the organic matrix. Detailed reviews of sulfur functional groups in coal were recently published by Attar (1977)(1) and Attar and Corcoran (1977)(2). The chemistry, the kinetics and the thermodynamics of reactions of the sulfur were described by Attar (1978) and therefore will not be reviewed here in detail.

This work had two objectives:

1. to identify and quantify the organic sulfur group functionalities in different coals, and
2. to examine the implications of these functionalities on potential desulfurization processes.

The main results are:

1. The majority of the organic sulfur in high ranked coals, i.e., LVB is thiophenic while in low ranked coals, i.e. lignites, most of the organic sulfur is thiolic or sulfidic.
2. 18-25% of the organic sulfur is in the form of aliphatic sulfides in all coals.
3. Part of the organic thiols are present in the form of ionic thiolates, presumably of calcium.
4. Coals containing mainly thiolic groups can be easily desulfurized.

2.0 Principle of the Method of Analysis

Detailed description of the principle of the method of analysis was published by Attar and Dupuis (1978)(4). Therefore only the main points will be described here.

1. All the organic sulfur functional groups can be reduced to H_2S if a sufficiently strong reducing agent is used.
2. Each sulfur group is reduced at a rate which can be characterized by a unique activation energy and a frequency constant.
3. If a sample which contains many sulfur groups is reduced and the temperature is gradually increased, each sulfur group will release H_2S at a different temperature given by:

$$\frac{A_i RT_{mi}^2}{\alpha E_i} = c \frac{E_i}{RT_{mi}} \quad (1)$$

where T_{mi} is the temperature of the maximum E_i and A_i are the activation energy and the frequency factor, and α is the linear rate of temperature increase. The rate of evolution of H_2S from the reduction of the i -th group can be described by:

$$\frac{d[H_2S]_i}{dt} = \frac{A_i}{\alpha} [H_2S]_{i0} \exp\left[-\frac{E_i}{RT} - \frac{A_i RT}{E_i} - c \frac{E_i}{RT}\right] \quad (2)$$

where $[H_2S]_{i0}$ is the total amount of H_2S that reduction of the i -th group would release. The detailed derivation of the previous equations was done by Jüntgen (1964)(5), and Jüntgen and Van Heek (1968)(6).

4. The value of T_{mi} is a characteristic unique to the sulfur functionality reduced and the area of each peak is proportional to the quantity of sulfur present in the form of the group reduced.

The implication of these discussions is that the area of the peak whose maximum is at T_{mi} is proportional to the concentration of sulfur present in the sample in the form of the i -th group. Therefore, quantitative determinations of the i -th sulfur group can be accomplished by determining the area of each peak.

3.0 Experimental

The experimental system consists of six parts:

1. a reduction cell,
2. a gas feed and monitoring system,
3. a hydrogen sulfide detector,
4. a recorder,
5. an integrator, and
6. a temperature programmer.

Figure 1 is a schematic diagram of the experimental system. The coal sample is placed in the reduction cell with a mixture of solvents catalyst and a reducing agent. The gas flow rate is then adjusted and the temperature is programmed up. The rate of evolution of H_2S is recorded vs. the cell temperature and the signal of each peak is integrated using the integrator. A more detailed description of this system was recently published by Attar and Dupuis (1978)(4).

The data described in this paper were derived using an improved version of the same experimental system. The following modifications were made:

1. stronger reducing conditions were used in order to obtain more complete reductions of the organic sulfur,
2. the sensitivity of the detector was improved, and
3. the cell design was changed and now it is possible to obtain detailed analysis on a routine basis.

Figure 2 shows a typical kinetogram.

4.0 Results and Discussion

The distributions of sulfur functional groups (USFG) in four types of solids are described:

1. sulfur containing polymers with well characterized sulfur functional groups,
2. raw coals,
3. treated coals, and
4. iron pyrite.

The analysis of the DSFG consists of two parts:

1. the qualitative assignment of a peak of a kinetogram to a given chemical structure, and
2. the determination of the quantity of each sulfur group in the (coal) sample.

4.1 Qualitative Identification of the Sulfur Groups

Tests of polymers with a known structure were used to identify the temperature at which each sulfur group releases its sulfur. Four polymers were tested:

1. polyphenylene sulfide (7) as a representative of aromatic sulfides,
2. polythiophene as a representative of thiophenic sulfur,
3. a copolymer produced from cyclohexene and 1,2 ethylene dithiol (7), as a representative of aliphatic and alicyclic sulfides, and
4. vulcanized natural rubber as a representative of aliphatic sulfides and disulfides.

All the polymers contained some thiolic sulfur.

The use of sulfur containing polymers can be used to identify the temperature region where each sulfur group is reduced only if two conditions are fulfilled:

1. the rate of the chemical reaction controls the rate of release of H_2S when both coal samples and polymer samples are examined,
2. the rate of the reduction of each sulfur functional group depends only on the hydrocarbon structure in its immediate vicinity.

Table 1 shows the results of tests of the various polymers and the maximum temperature for each group.

4.2 Quantitative Analysis of the Concentrations of Sulfur Groups

4.2.1 Recovery of Organic Sulfur

Quantitative analysis can be accomplished provided that all the sulfur present in the form of each group is reduced to H_2S . It is also assumed that the distribution does not change during the analysis and that all the H_2S released is detected and determined.

Each mole of sulfur, when reduced, produces one mole of H_2S . Therefore, the number of moles of H_2S formed during the reduction of each group is proportional or equal to the number of moles sulfur present in the sample in that form.

The recovery of sulfur from model compounds containing aliphatic thiols, thiophenes and aryl sulfides was 94-99%.

Table 2 shows the results of the quantitation of the kinetogram of three samples of Illinois #6 coal with different particle sizes. The two most important conclusions from these tests are that the recovery of thiophenes and aromatic sulfides depends on the coal particle size used and that to a first order approximation, the recovery of other groups is independent of the coal particle size. 17

is conceivable that during the analysis, in the interior of large coal particles, the sulfur groups can condense and form (graphitized) compounds which are less amenable to reduction. The strong reducing agent used can penetrate into smaller coal particles and inhibit the rate of condensation. While aliphatic thiols and sulfides are reduced at low temperature, before condensation commences, the reduction of thiophenes occur simultaneously with the condensation and therefore in a large particle thiophenic group could form condensed thiophenes which are less amenable to reduction.

4.2.2 Recovery of Pyritic Sulfur

Table 3 shows that a very small fraction of the pyritic sulfur is recoverable when pure crystalline iron pyrite is tested. In all the cases tested, the recovery never exceeded 1-2%. Somewhat larger recovery is obtained when slow heating rates or reducing agents with smaller reducing potential are used. When strong reducing agents are used, a layer of metallic iron is believed to be formed on the surface of the iron sulfide which prevents diffusion of the reducing species.

Small iron pyrite particles, of the order of 1-10 microns are often reduced more effectively than larger particles because they are less crystalline and often contain more impurities than larger particles.

4.3 Resolution

The evolution of H_2S from aliphatic sulfides and from iron pyrites coincides to the extent that it is almost impossible to resolve the two peaks. However, since iron pyrite can be determined independently using ASTM D3131, it was possible to estimate the relative contribution of pyritic sulfur and sulfidic sulfur to the unresolved peaks. Somewhat better resolution was obtainable at slow rates of heating, however in these cases the overall recovery and the signal to noise ratio were reduced.

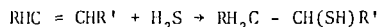
4.4 The Sulfur Distribution in Raw Coals

Table 4 shows the distribution of the various classes of sulfur in five coals and table 5 shows the distribution of the organic sulfur groups in the same five coals. The results shows that the content of thiols is substantially larger in lignites and HVB coals than in LVB coals. The fraction of aliphatic sulfides is approximately the same in coals with different ranks and vary around 20% of the organic sulfur. If it is accepted that all the unrecovered organic sulfur is due to thiophenes (and aromatic sulfides), then the data indicate clearly that larger fractions of the organic sulfur is present as thiophenic sulfur in higher ranked coals than in lower ranked coals. The accepted theory on the hydrocarbon structure of coal is that higher ranked coals are more condensed than lower ranked coals. It should not, therefore, be surprising that the sulfur groups are also more condensed, more thiophenic, in higher ranked coals than in lower ranked coals.

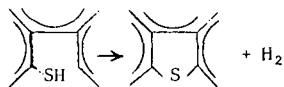
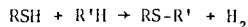
The data on the relative amounts of -SH, R-S-R and thiophenic sulfur can be explained as follows: suppose that most of the organic sulfur is initially trapped by the organic matrix in the form of thiolic sulfur. Typical "trapping reactions" are:



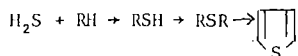
and



During the coalification, thiols can condense to form sulfides and eventually aromatic sulfides and thiophenes:



The sequence of the condensation reactions is therefore:



In other words, the sulfides are an intermediate form which the sulfur may have before it is converted to the thiophenic form. Thus, it should not be surprising that the fractions of sulfidic sulfur is approximately constant since during the coalification, sulfidic groups are formed from thiolic groups and are consumed to produce thiophenes. These processes are condensation processes which are believed to occur in the structure of coal during coalification.

4.5 The Sulfur Distribution in Treated Coals

Various treatments are known to be selective to specific sulfur groups. It was therefore interesting to examine the kinetogram of treated coals. Three treatments are described:

1. oxidation with H_2O or HNO_3 ,
2. removal of the alkaline minerals with HCl , and
3. methylation of the coal with methyl iodide.

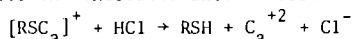
4.5.1 Oxidation

Mild oxidation of coal with acidic solutions of hydrogen peroxide or nitric acid dissolves the iron pyrite and converts the thiols to sulfonic acids. Some organic functional groups oxidize to the corresponding sulfides and sulfones (8). However, in general, the latter process requires strong oxidizing conditions. From the analytical point of view one might think that it is not important whether the organic sulfur groups are oxidized or not, since the reducing agent used converts them back very rapidly to the non-oxidized form. Therefore, the results of the analysis will not differentiate between the reduced and the oxidized form of a sulfur group. In other words, oxidation could have been used to remove the interference from pyrite without much effect on the determination of the other sulfur groups. However, oxidation appears to increase the resistance to mass transport and thus to reduce the resolution. Figure 3 shows the kinetograms of two coal samples analyzed for the U.S. Department of Energy. The first is the original coal, the second is an oxidized sample. The results show that the oxidation did

not remove any organic sulfur although the pyritic sulfur was removed. The signals are however much less resolved in the oxidized sample than in the raw coal. Since the oxidation was conducted in an acidic inorganic solution, and because it is known that sulfonic acids can be hydrolyzed to hydrocarbons and sulfuric acid, some of the thiols seem to disappear as a result of the oxidation.

4.5.2 HCl Treatment

Dilute HCl dissolves the organic and carbonate salts of calcium, magnesium and iron. Since some H₂S can react with basic calcium and iron salts, it was desired to examine the effect of HCl treatment on the kinetogram. Figure 4 shows the kinetograms of raw coal and HCl extracted coal. The most important difference between the kinetograms is that the second peak due to thiophenols disappeared and the thiols peak is increased. It is plausible that some of the sulfur which is determined as thiophenolic is indeed thiolic. Thiols can react with calcium to form calcium thiolates, reduction of which may require larger activation energy than thiols. HCl treatment replaces the calcium with hydrogen and converts the thiolates into thiols:



4.5.3 Treatment with Methyl Iodide

Samples of Illinois #6 were treated with methyl iodide, CH₃I, and the products were analyzed using two methods: The method of Postovski and Harlampovich (9) for thiols and aliphatic sulfides, and using our thermokinetic method. The results of the analysis are described in table 6. The results show that only a very small fraction of the organic sulfur is indeed accounted for by the CH₃I method and therefore the value of this method as an analytical tool is questionable.

The kinetograms of an untreated but demineralized sample and that of a demineralized sample treated with CH₃I are shown in figure 5. The data show that the methyl iodide treatment results in lower recovery of organic sulfur and in a change in its distribution. In particular, some of the sulfur which is originally detected as aromatic thiol is apparently alkylated and becomes aromatic sulfide. However, the alkylation must also reduce the rate of mass transport since the thiophenes and aromatic sulfides are not visible in the kinetogram of the treated coal.

5.0 Implications to Coal Desulfurization

It is widely recognized today that coal desulfurization efficiency depends on the distribution of sulfur in the original coal to pyritic and organic sulfur. Pyritic sulfur can be removed relatively easily while it is more difficult to remove organic sulfur.

Preliminary data show that part of the organic sulfur can be easily desulfurized. In particular, it seems that the thiolic sulfur and part of the sulfidic sulfur can be easily removed. Therefore, the authors suggest coals may be classified into two groups: coals which can be easily desulfurized, (most

of their organic sulfur is thiolic) and coals which can not be easily desulfurized (most sulfur is non-thiolic). Thus, thermokinetic tests can be used to screen coals and to infer which are best used as feeds for precombustion desulfurization.

References

1. Attar, A., "The Fundamental Interactions of Sulfur and Modelling of the Sulfur Distribution in the Products of Coal Pyrolysis." A paper submitted in the 83rd National Meeting of the AIChE held in Houston, TX., March 20-24 (1977). In print in Vol. IV, "Coal Processing Technology," CEP Technical Manual (1978).
2. Attar, A. and Corcoran, W. H., Ind. Eng. Chem., Proc. Res. and Dev., 16 (2), 168 (1977).
3. Attar, A., Fuel, 57, 201 (1978).
4. Attar, A., and Dupuis, F., Prep. Div. Fuel Chem., ACS, 23 (2), 44 (1978). The paper is present in the preprints but is not listed in the table of contents.
5. Jüntgen, H., Erdöl and Kohle, 17, 180 (1964).
6. Jüntgen, H., and Van Heek, K. H., Fuel, 47, 103 (1968).
7. Supplied by Phillips Petroleum whom the authors wish to thank.
8. Attar, A., and Corcoran, W. H., Ind. Eng. Chem., Prod. Res. and Dev., 17 (2) 102 (1978).
9. Postovski, J. J. and Harlampovich, A. B., Fuel, 15, 229 (1936).

Table 2: The Effect of Particle Size on the Analysis of Sulfur Functional Groups

Run #	Coal	Mesh Size	Sample weight mg	-SH mg g coal	ϕ -SH mg g coal	R-S-R FeS ₂ mg/g coal	ϕ -S- ϕ mg g coal	 mg g coal	Total mg g coal	Recovery %
S-111	Illinois #6	-100+120	32.7	1.33	1.44	4.15	1.17	*	8.07	19
S-112	"	-200+270	32.3	1.11	1.58	3.48	*	*	6.16	14.7
S-113	"	-325	32.2	1.69	1.80	3.11	*	67	7.26	17.1

* Not detected

Table 3: The Effect of Pyrite Particle Size on the Recovery of Sulfur

Particle Size	% Recovered	
	mesh	microns
-60+100		0.9
-100+120	149-250	1.9
-120+170	125-149	1.6
-170+200	88-125	1.5
-200+270	77-88	1.5
-270+325	53-74	0.9
-325	44-53	2.1
	< 44	

* The estimated error is \pm 0.4%.

Table 4: Sulfur Class Distribution in Five Coals

Coal	Denote	Total s (wt.%)	Pyritic s (wt.%)	Sulfatic s (wt.%)	Organic s (wt.%)
Illinois	A	4.5	1.23	0.06	3.2
Kentucky	B	6.6	5.05	0.135	1.43
Martinka	C	2.20	1.48	0.12	0.60
Westland	D	2.60	1.05	0.07	1.48
Texas lignite	E	1.20	0.4	—	0.80

Table 5: Distribution of Organic Sulfur Groups in Five Coals

Coal	% Organic s Accounted	Thiolic	Thiophenolic	Alip Sulfide	Aryl Sulfide	Thiophenes*
A	44	7	15	18	2	58
B	46.5	18	6	17	4	55
C	81	10	25	25	8.5	21.5
D	97.5	30	30	25.5	—	14.5
E	99.7	6.5	21	17	24	31.5

* Corrected for "unaccounted for" sulfur

* C and E are calculated on total sulfur content

Table 6: Analysis of Illinois #6 Coal by the CH₃I Method by Thermokinetics

	LECO % mg/gm	ASTM % mg/gm	DSFG % mg/gm	CH ₃ I method % mg/gm	DSG on CH ₃ I treated coal (S-105) % mg/gm
Total Sulfur	4.5	45			
Sulfate Sulfur		0.04	0.4		
Pyritic Sulfur		1.23	12.3	4.81	0.6
Organic Sulfur { -SH φ-SH R-S.R. A-S.A. 				6.1	8.6
				8.5	3.45
				0.96	8.0
Total Organic Recovered		3.23	32.3	85.1	27.5
				7.2	62.1
				2.32	20.05

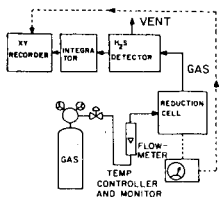


FIGURE 1 SCHEMATIC DIAGRAM OF EXPERIMENTAL SYSTEM

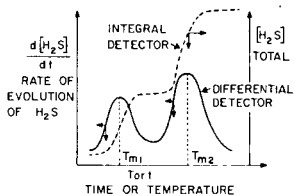


FIGURE 2 ANALYSIS OF A MIXTURE CONTAINING TWO GROUPS USING A DIFFERENTIAL AND AN INTEGRAL DETECTORS

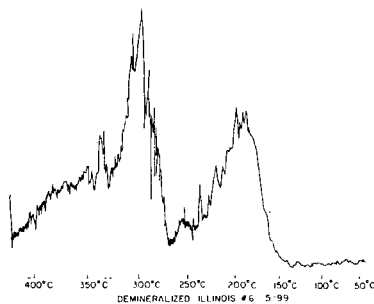
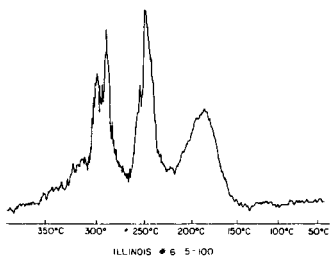


Figure 3

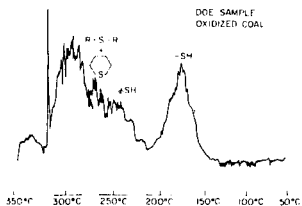
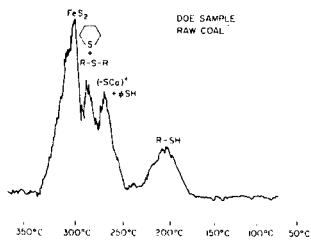


Figure 4

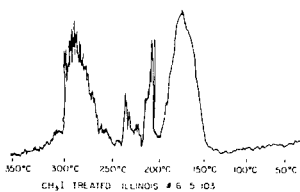
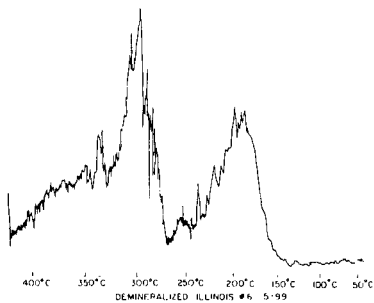


Figure 5

Chemical Structure of Heavy Oils Derived from Coal Hydrogenation by Mass Spectroscopy

S. Yokoyama, N. Tsuzuki, T. Katoh, Y. Sanada,
D. M. Bodily* and W. H. Wiser*

Coal Research Institute, Faculty of Engineering,
Hokkaido University, Sapporo, 060, Japan

*Department of Mining, Fuels Engineering, University of Utah,
Salt Lake City, Utah 84112, U. S. A.

Introduction

Coal hydrogenation heavy oil consists of numerous complicated hydrocarbons and nonhydrocarbon compounds, consequently the elucidation of the chemical structure is extremely complicated and time consuming. Thus, the chemical structure of coal liquids have been investigated mainly to the present by means of ^1H - and ^{13}C -NMR techniques or a combination thereof. In other words the technique of mass spectrometry for structural analyses is advantageous to gain information of the individual compounds regarding molecular weight and compound types [1,2]. A combination of dual-packed adsorption liquid chromatography (LC) and gel permeation chromatography (GPC) developed by the Bureau of Mines API project 60 [3] for separation into compound types and further into their molecular size are appropriate to the sample preparation procedure for mass analyses, because molecular ion coefficient were assumed to be approximately the same for LC-GPC sub-fraction inasmuch as they have characteristic compound types and narrow molecular weight distribution. On the other hand, results of GPC technique which is a very useful method to clarify complicated mixtures of heavy oil derived from coal, was compared to the mass results. It can be concluded that both results from mass and GPC analyses should be used independently to elucidate the chemical structure of coal liquids.

Experimental

Sample preparation of heavy oil

Hydrogenation reaction of Hiawatha, Utah coal (C: 72.0, H: 5.6, N: 1.7, S: 0.90, O: 19.8, d.a.f.%) was performed with the condition of 950°F of reaction temperature and 1800 psi of hydrogen pressure with ZnCl_2 impregnated to coal as catalyst by an entrained-flow tubular coil reactor of the University of Utah process [4]. The reaction products were trapped in three reservoirs connected to the reactor in series and was separated according to their condensability. Heavy oil products collected in the first reservoir nearest to the reactor was subjected to investigation in this work. Separation procedures to characteristic materials prior to gaining acid-base-less neutral compounds were described in our previous reports [5] and also shown in Fig. 1. Neutral heavy oil obtained was separated subsequently into compound types of saturated hydrocarbons (Fr-P), mono-aromatic (Fr-M), diaromatic (Fr-D), three and more large aromatic rings (Fr-T) and polyaromatic-polar compounds by means of dual-packed silica alumina adsorption liquid chromatography modified partially the Bureau of Mines API-60 method, with an additional solvent of 70% benzene-30% cyclohexane system to obtain separately a narrow cut of concentrate of 3 and 4 aromatic ring compounds. Elution curve of liquid chromatography are shown in Fig. 2. Respective type compounds Fr-M, D and T were separated further by GPC packed Bio-beads S-X4 and 8 according to their respective molecular size into 7 fractions. In Fig. 3, GPC elution curves for Fr-M, D and T were shown.

Mass spectra were measured by Hitachi M-52 GC-MS spectrometer. Mass spectra of each series of GPC subfraction for Fr-M, D and T were analyzed with the low resolution and low ionization voltage method by GC-MS technique for Fr-M-3 to 7 and Fr-D-3 to 7 and by direct insert technique for high molecular fraction of

Fr-M-1, 2, Fr-D-1, 2 and Fr-T-1 to 7, respectively.

Mass spectrometry was scanned repeatedly with 6 or 10 sec. interval times during the period of elution from GC column or volatilization of samples introduced into the ionization chamber and multiple mass spectra of about 50 to 800 for respective LC-GPC subfraction were measured to obtain the representative gross mass spectral data for complicated mixtures. Numerous mass spectra were treated by computer (Hitachi, HITAC 10 II) for the summing up of these spectra to calculate them as an integrated mass spectra.

Results and Discussion

Each series of LC-GPC subfractions were investigated previously for chemical characterization by ^1H - and ^{13}C -NMR method [6,7] and were elucidated to have approximately mono-, di- and tri- and/or tetraaromatic derivatives for Fr-M, D and T, respectively, as the average structural unit. It was also confirmed that values of aromaticity for GPC subfractions of individual compound types increase gradually with the increasing GPC fraction number from 1 to 7 and have also the largest fa values for Fr-T and the smallest one for Fr-M at the same elution volume of GPC. From the results described above, the separation effects of LC and GPC according to compound types and molecular size were assumed to be excellent. Considering these characteristics for chemical structure, LC-GPC subfraction are found to be suitable as samples for mass analyses because the molecular ion coefficient is not so large in difference among respective compounds in the same fraction.

Integral mass spectra of LC-GPC subfraction

On the measurement of mass spectra by means of the low energy ionization method, species of ion peaks observed were mostly parent ion and isotopic ion (P+1) and were minor for fragment peaks like (P-1), indicating that the cleavage of molecules are minor. Although, Fr-D-1 and Fr-T-1 which are the highest molecular weight in that they have large aliphatic substitution, were observed in the predominant fragment peak of odd mass number at lower mass range, therefore the data of these fractions were not included in this report. On the integral mass spectra of series of LC-GPC subfraction, the average number molecular weight were calculated from the mass to charge ratios (M/e) for respective parent peaks and those intensities, and are shown in Fig. 4. By increasing the fraction numbers of GPC for each compound type series, the molecular weight diminishes progressively from about 400 or 500 to 200 in proving the satisfactory fractionation of GPC. In Fig. 4, molecular weight results derived from vapor pressure osmometry were compared with the results of mass analyses to ensure the accuracy of conventional methods. The correlation between both are excellent except for a slight deviation from the theoretical line with the increase in molecular weight.

Compound types of LC-GPC subfraction

Deficiency of hydrogen number for M/e of parent peak can be predicted the type of compound by assigning the value of z number. Assuming that molecular ion coefficients are approximately similar, the contents of respective type compound for GPC fraction 1 or 2 to 7 of Fr-M, D and T were estimated semiquantitatively. Consequently, hydrocarbon types for Fr-M-1 to 7 were assigned mainly to alkylbenzenes (Z=-6), alkylmononaphthenobenzenes (Z=-8) and alkylindanaphthenobenzenes (Z=-10) and for Fr-D-2 to 7 to alkyl-naphthalenes (Z=-12), alkylmononaphthenonaphthalenes (Z=-14) and alkylindanaphthenonaphthalenes (Z=-16) and for Fr-T-2 to 7 to alkylphenanthrene or alkylanthracene (Z=-18), alkylpyrene (Z=-22), alkylcrysene (Z=-24) and these naphthenologs (Z=-20, -26). Distribution of various compound types for Fr-M, D and T in summing the contents of respective GPC subfraction 1 to 7 were shown in Fig. 5.

Alkyl carbon distribution

The same Z values in the integrated mass spectra for individual LC-GPC subfraction were selected to obtain the distribution of alkyl carbon in respective hydrocarbon types. In Fig. 6, the content distribution of molecular weight or alkyl carbon number on the same Z values were plotted for Fr-M, D and T series.

These ranges of alkyl carbon numbers move progressively from low to higher ones with 5 to 10 carbon extents in proceeding to GPC fraction 7 to 1 for respective hydrocarbon types. Therefore, separability of GPC for various hydrocarbon types was confirmed further by mass analyses as to be divided satisfactorily according to molecular sized especially by alkyl carbon number on these samples. It can be seen that Fr-M consists of larger alkyl carbon substitution which reaches 35 carbons for Z=-6 series, indicating a lower aromaticity and decreasing of Z values which indicates an increase of naphthene ring, distribution of alkyl carbon decrease. On the other hand, alkyl carbon number of Fr-T have a range of 0 to 10 indicating a lower aromaticity which is in agreement with the results from ¹H-NMR structural analyses.

GPC correlation for molecular weight vs elution volume

To predict the molecular weight distribution and chemical structure from the GPC elution curve, the GPC correlation curve between molecular weight and elution volume for corresponding structural compounds are necessary. However, it was very difficult to gain information of these relations because the supply of reference sample were limited. If the coal liquid itself can be used as a reference compound for calibration, useful GPC correlation of various compound type can be obtained. Molecular weight at maximum distribution by difference of alkyl carbon number for each GPC fraction on respective Z series shown in Fig. 6 were compared with elution volume for corresponding fraction. The correlation between the two were shown in Fig. 7. The relationship between the two for respective Z values on Fr-M, D and T are in fair as GPC correlations.

Molecular weight distribution for whole samples of Fr-M, D and T were constructed by summation of peak intensities for parent peak belonging to the same Z series corresponding to all GPC fractions, and were shown with the solid lines in Fig. 8. On the other hand, GPC elution curves for Fr-M, D and T were cited again in the same figure for comparison. The results from mass analyses for Fr-D and T do not include the data of Fr-D-1 and Fr-T-1 because of uncertain results of mass analyses for these as described previously, therefore a slight discrepancy were recognized in the vicinity of high molecular range. Although, considerable agreement between both derived from different methods are satisfactory.

References

- [1] A. G. Sharkey, Jr., J. L. Shultz, T. Kessler and R. A. Friedel, "Spectrometry of Fuels", Plenum Press, p. 1 (1970)
- [2] H. J. Coleman, J. E. Dooley, D. E. Hirsch and C. J. Thompson, *Anal. Chem.*, **45**, No. 9, 1724 (1973)
- [3] D. F. Hirsch, R. L. Hopkins, H. J. Coleman, F. O. Cotton and C. J. Thompson, *Anal. Chem.*, **44**, 915 (1972)
- [4] R. E. Wood and W. H. Wiser, *Ind. Engng. Chem. -Process Design Dev.*, **15**, 144 (1976)
- [5] S. Yokoyama, D. M. Bodily and W. H. Wiser, 172nd ACS National Meeting, San Francisco, Sep. 1976
- [6] S. Yokoyama, D. M. Bodily and W. H. Wiser, The 36th Annual Meeting of Chem. Soc. Japan, April, 1977
- [7] S. Yokoyama, D. M. Bodily and W. H. Wiser, The 37th Annual Meeting of Chem. Soc. Japan, April, 1978

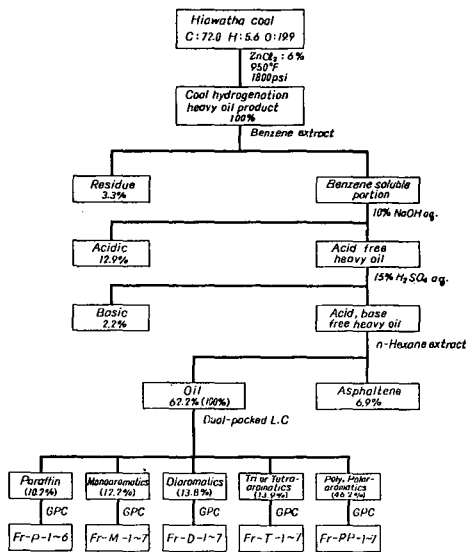


Fig. 1 Separation scheme

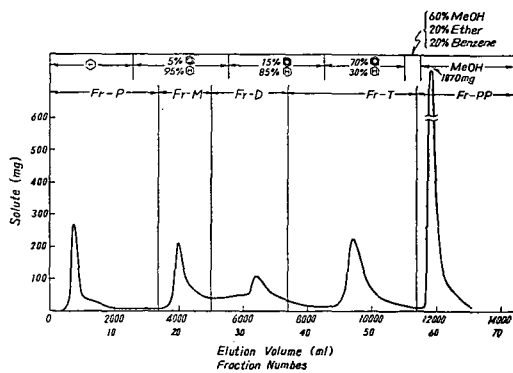


Fig. 2 Elution curve of dual-packed liquid chromatography

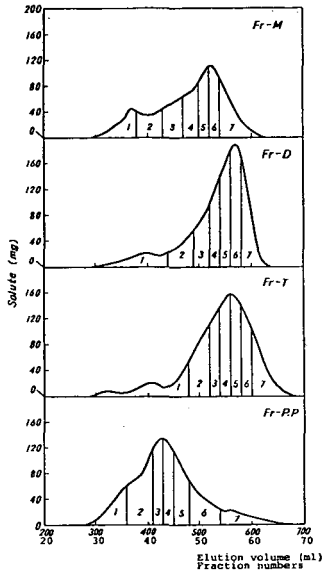


Fig. 3 GPC chromatogram of Fr-M, Fr-D, Fr-T and Fr-PP

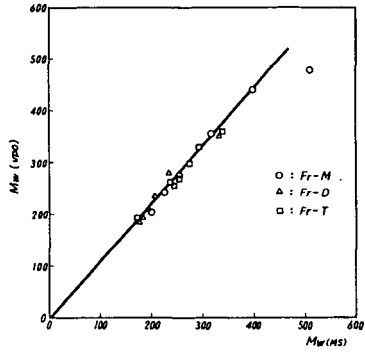


Fig. 4 Molecular weight results from VPO and Mass spectrometry

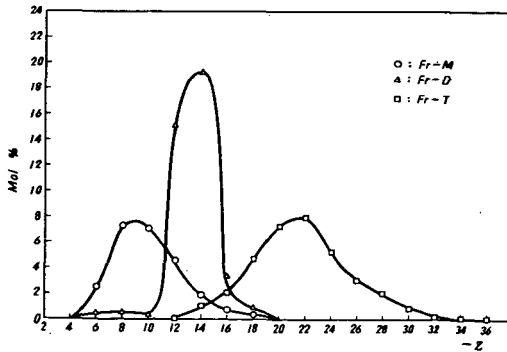


Fig. 5 Distribution of hydrocarbon type compounds for LC-GPC subfractions

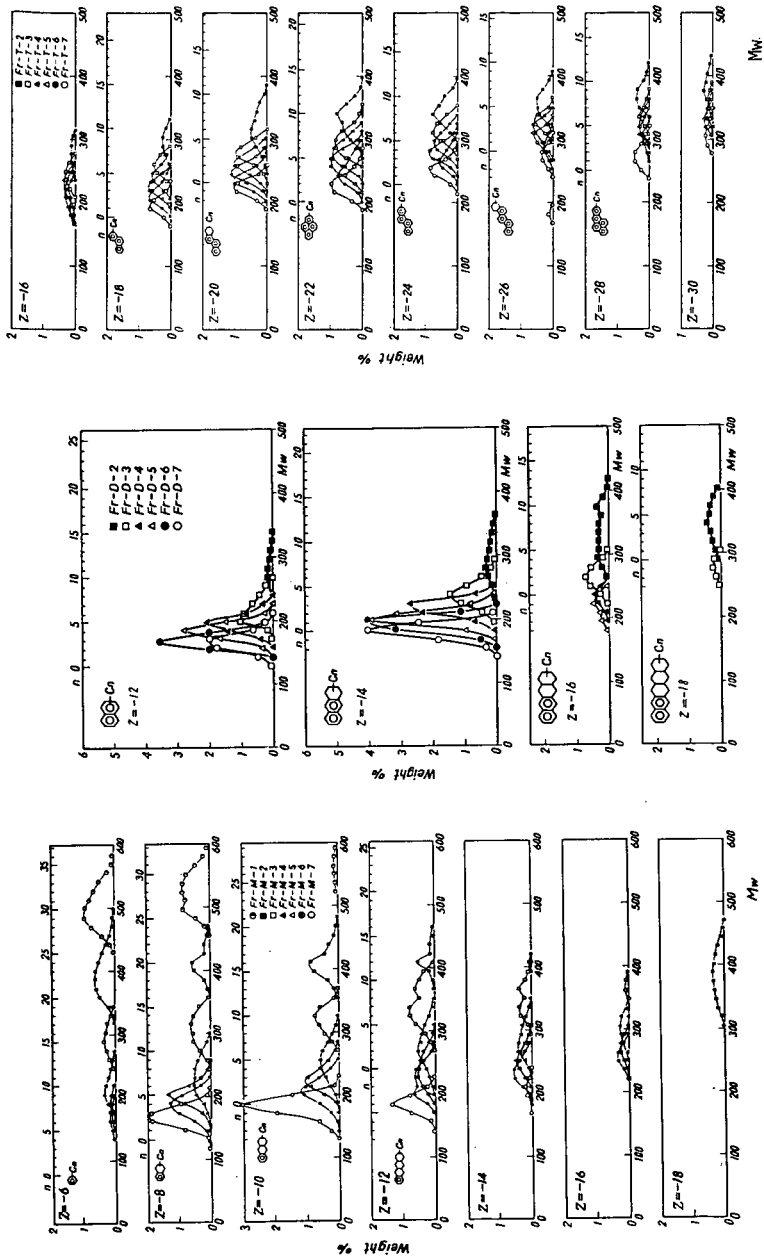


Fig. 6 Distribution of hydrocarbon compound types for Fr-M, Fr-D and Fr-T

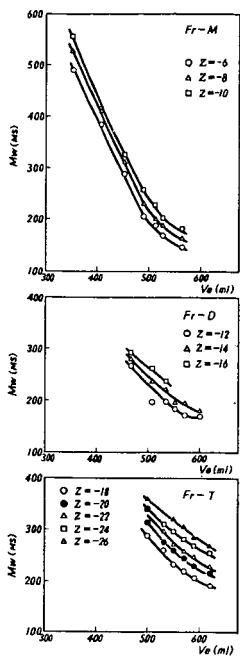


Fig. 7 Relationship between molecular weight and elution volume for various type of compound

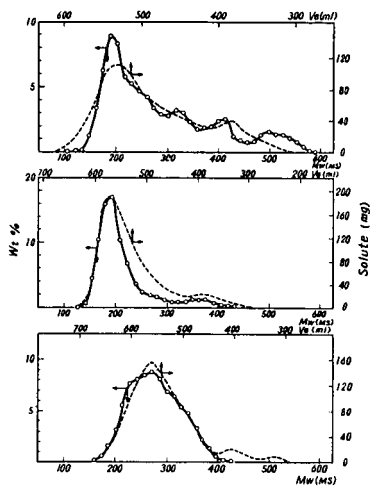


Fig. 8 Comparison with molecular weight distribution and GPC elution curves

STRUCTURAL ANALYSIS OF QUINOLINE EXTRACTS AND HYDROLYSIS PRODUCTS OF COALS

Koji Ouchi, Kazuyuki Iwata, Masataka Makabe, Hironori Itoh

Faculty of Engineering, Hokkaido University, Kita 13, Nishi 8, Sapporo, Japn.060.

The mean structure of coals has been extensively investigated by X-ray, magnetic susceptibility, gases evolved during carbonization, IR spectra etc., and the structural analysis was first developed by van Krevelen(1) using density and refractive index. Among these the method which gives the most precise image appears to be NMR method. However this method is limited in that it can be applied only to soluble material by special solvents. Usually coals can be dissolved only in part, therefore the results do not represent the whole coal.

Thus in the present work we tried to increase the solubility of coals using chemical reaction or strong solvent(quinoline), which would have the smallest change in the unit structure(cluster unit). The results of structural analysis of the products with these two methods are in good agreement, although both methods and their yield are quite different. This means that the structural image obtained here represents the true mean structure of coals.

Experiments

1)Coal sample. Vitritnits of 12 coal samples were concentrated using the sink and float method. Their analytical values are shown in Table 1.

2)Quinoline extraction. 5g of crushed coal under 100 Tyler mesh and 100g of purified quinoline were placed in a 500ml autoclave with a magnetic stirrer and after replacing the atmosphere by nitrogen this was heated at 350-380°C for 1-4 hours. After cooling the products were centrifuged and filtered. The residue was washed with fresh quinoline and methanol. The filtrate was concentrated under vacuum and poured into 500ml of 2N HCl, filtered, washed with hot and cold water and dried.

3)NaOH-alcohol reaction(2). 5g of coal, 5g of sodium hydroxide and 50g of ethyl alcohol were placed in an autoclave of 230ml with a magnetic stirrer and, after replacing the atmosphere by nitrogen, this was heated at 300°C or 350°C for 1 hour. After neutralizing with HCl the precipitate was centrifuged, filtered and dried. The product was then extracted with pyridine by shaking for 10 hours at room temperature.

4)¹H-NMR. ¹H-NMR was recorded in d-quinoline for quinoline extracts and in d-pyridine for pyridine extracts of NaOH-alcohol reaction products, using TMS as an internal standard. The concentration was 5% for d-quinoline and 2% for d-pyridine.

Results and Discussion

First the extraction conditions were examined using Indian Ridge coal and Balmer coal. The results are shown in Table 2. The effect of temperature from 350 to 375°C, of time from 1 hour

to 6 hours and of nitrogen pressure from 0.1 MPa to 10 MPa were examined. The results were in an error range and we adopted a rather higher temperature for older coals.

The extraction or reaction condition, extraction yield, ultimate analysis of extracts and their molecular weight are shown in Table 3. Quinoline extraction yield attains maxima in a range of 81~87 %C, but there is some scattering of results even with the same carbon percent. If we plot the extraction yield vs. H of raw coals a linear relationship was seen in a range of 91.5~81.2%C (Fig 1). In younger coals it decreases linearly. Teshio coal has an extraction yield of 20.4%, but after hydrolysis with NaOH solution (5N) at 250°C for 6 hours, the extraction yield increases to 35.9%. Therefore the ether linkages appear to be a cause of the decrease of extraction yield in the younger coal range. In the hydrolysis reaction associated with partial hydrogenation using NaOH-alcohol the younger the coals are, the easier the products dissolve in alcohol. This also means that the younger coals have an abundance of ether linkages.

The carbon percent of extracts in the younger coal range increases in comparison with that of raw coals. The quinoline extraction of NaOH-alcohol reaction conditions are somewhat severe for the younger coals and some oxygen containing functional groups such as carboxyl or hydroxyl groups decompose at those temperatures, which results in a reduction of oxygen content. In the higher coal rank the analytical values of extracts are nearly the same as those of the raw coals, although the extraction yield is higher, which means that there is no change in their structure except for some splittings of ether linkages and a slight saturation of aromatic rings which took place in the reaction of NaOH-alcohol (3). In short, the unit structure (or structure of cluster unit) in the raw coals may be preserved without change in the quinoline extracts or in the pyridine extracts of NaOH-alcohol except for some changes of functional groups in the younger rank coals.

The results of the structural analysis are shown in Table 4. In bituminous coals in which the extraction yield of both methods is nearly 100%, the results show an amazing coincidence in both methods except for slightly higher values for f_a , σ_{al} , \mathcal{C}_{al} , although the methods are completely different. The higher values for these indices come from a slight hydrogenation in the NaOH-alcohol reaction. In the younger rank of coal the difference is somewhat higher, but in spite of this the coincidence is sufficient to discuss the rough unit structure, although the extraction yield and method are quite different. This small difference comes partly from the difference of extraction yield and partly from the slight hydrogenation of coal in NaOH-alcohol reaction. When we pursue the change of structural indices with time at 260°C for Taiheiyō coal in NaOH-alcohol reaction f_a changes from 0.7 at 1 hour to 0.5 at 22 hours. The extrapolated value of f_a for 0 hour almost corresponds to that of the quinoline extract. The extrapolated value of R_a is 1.4 which also coincides well with 1.5 of quinoline extract. All other indices show the same coincidence. We have shown these extrapolated values in Table 4.

The results show that the aromatic ring number of the younger coals is 1~2 with 0.5 naphthenic ring, that of 80~85°C coal 2~3 with 0.5 naphthene ring and that of 90°C coal 5 with 1 naphthene ring. The molecular weight per unit structure of younger coals is 160~180, that of 80~85°C coal 200~300 and that of 90°C coal 320~340. Oxygen content per unit structure decreases from younger coals

to the older coals, but as described before those values in younger coals do not represent the true ones. If we take the analytical values of raw coals, we can obtain the corrected oxygen number per unit structure, as shown in Table 4.

Referring to the fact that the ether linkages are rich in younger coals, we can say that the unit structures consisting of benzene or naphthalene rings with 0.5 naphthenic ring are linked mainly by the ether linkages and methylene bonds in younger coals. In bituminous coals the unit structure consisting of 2-5 aromatic rings and about 1 naphthene rings are linked with each other mostly by the methylene bonds. The youngest coal has 2.5-2.8 oxygen atoms per unit structure. The bituminous coals have about 1 oxygen atom per unit structure and the highest rank of coal has 0.3.

Appendix

Structural analysis. Hydrogen was divided into the following four types. Aromatic hydrogen H_a : 6-9ppm, hydrogen attaching α carbon H_α : 2-5ppm, hydrogen attaching over β carbon except for terminal methyl H_β : 1.1-2ppm, hydrogen in terminal methyl H_r : 0.3-1.1ppm. First 60% oxygen is assumed to be the hydroxyl group and the hydrogen in this hydroxyl group was subtracted from the total hydrogen. The residual hydrogen was distributed in the above four types.

The structural indices was calculated from the following equations when the molecular weight was not known.

$$\text{aromaticity, } fa = \frac{C/H - 1/2 \cdot (H_\alpha + H_\beta) / H - 1/3 \cdot (H_r / H)}{C/H} \quad (1)4$$

H/C ratio in hypothetical unsubstituted aromatics,

$$H_{a0}/C_{a0} = \frac{H_a/H + 1/2 \cdot (H_\alpha/H) + 0.6O/H + 2 \cdot (0.4O + N)/H}{C/H - 1/2 \cdot (H_\alpha + H_\beta) / H - 1/3 \cdot (H_r / H)} \quad (2)4$$

$$\text{degree of substitution, } \sigma = \frac{1/2 \cdot (H_\alpha/H) + 0.6O/H + 2 \cdot (0.4O + N)/H}{H_a/H + 1/2 \cdot (H_\alpha/H) + 0.6O/H + 2 \cdot (0.4O + N)/H} \quad (3)4$$

degree of aliphatic substitution,

$$\sigma_{al} = \frac{1/2 \cdot (H_\alpha/H)}{H_a/H + 1/2 \cdot (H_\alpha/H) + 0.6O/H + 2 \cdot (0.4O + N)/H} \quad (4)5$$

$$\text{number of aromatic carbon per unit structure, } C_{a0} = \frac{3}{(H_{a0}/C_{a0}) - 1/2} \quad (5)6$$

$$\text{number of total carbon per unit structure } C_{us} = C_{a0}/fa \quad (6)$$

$$\text{number of aliphatic carbon per unit structure, } C_{al} = C_{us} - C_{a0} \quad (7)$$

$$\text{number of hydrogen per unit structure, } H_{us} = 12C_{us} \cdot H\% / C\% \quad (8)$$

$$\text{total ring number per unit structure, } R_{tus} = C_{us} - H_{us}/2 - C_{a0}/2 \quad (9)$$

$$\text{aromatic ring number per unit structure, } R_{aus} = 1/2 \cdot (C_{a0} - H_{aus}) + 1, \quad (10)7$$

$$H_{aus} = (H_{us}/C_{us}) \cdot C_{a0}$$

naphthenic ring number per unit structure, $R_{nus} = R_{tus} - R_{aus}$ (11)

molecular weight per unit structure, $Mol. WT. us = 12 C_{us} / C\%$ (12)

(5) is only valid for cata condensed aromatic nuclei. (9) is approximately valid when the degree of polymerization is large.

The absolute values of the number of each type of atoms were used when the molecular weight was known. In this case (9) was calculated as follows.

degree of polymerization $n = C / C_{us}$ (C is the total number of carbon per molecule) (13)

total number of aromatic carbon per molecule, $C_a = C_{aus} \cdot n$ (14)

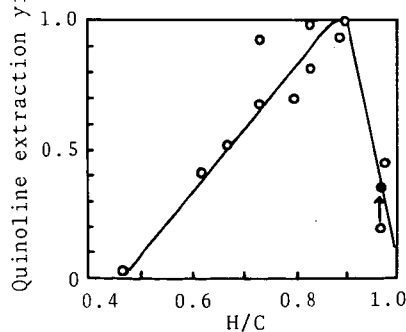
total ring number per molecule, $R_t = C - H / 2 + 1 - C_a / 2$, (H is total number of hydrogen per molecule) (15)¹⁾

total ring number per unit structure, $R_{tus} = R_t / n$. (16)

(Reference)

- 1) J. Schuyer, D. W. van Krevelen, "Coal Science", Elsevier Pub. Co., Amsterdam (1957)
- 2) M. Makabe, Y. Hirano, K. Ouchi, Fuel, 57, 289 (1978)
- 3) M. Makabe, K. Ouchi, Fuel Proc. Tech, in press.
- 4) Modification of equation of J. K. Brown, W. R. Ladner, Fuel, 39, 87 (1960)
- 5) Modification of equation of Y. Maekawa, K. Shimokawa, T. Ishii, G. Takeya, Nenryo Kyokaiishi (J. Fuel Soc. Japan), 46, 927 (1967)
- 6) S. Yokoyama, N. Onishi, G. Takeya, J. Chem. Soc. Jpan, Chem. and Ind. Chem. 10, 1963 (1975)
- 7) D. R. Clutter, L. Petrakis, R. L. Stenger, R. K. Jensen, Anal. Chem. 44, 1395 (1972).

Fig 1. Relation of quinoline extraction yield vs. H/C of raw coals.



● Hydrolysis product

Table 1. Analysis of sample coals.

*S+O

No	Name	Ash %	ultimate analysis(daf) %				Odiff
			C	H	N	S	
1	Teshio	7.0	71.5	5.8	1.8	-	20.9*
2	Taiheiyo	5.3	77.9	6.3	1.1	0.2	14.5
3	Akabira	3.9	81.2	6.0	1.7	-	11.1*
4	Basewater	2.8	83.6	5.6	1.7	0.7	8.4
5	Miike	8.9	83.9	6.3	1.2	2.1	6.5
6	Daiyon	2.4	84.0	5.8	2.0	0.8	7.4
7	New Yubari	2.5	86.7	6.2	1.1	-	6.0*
8	Indian Ridge	1.5	87.4	5.3	0.9	-	6.4*
9	Goonyella	1.5	87.9	5.4	1.9	0.6	4.2
10	Balmer	2.5	89.4	5.0	1.4	0.4	3.9
11	Beatrice	0.8	91.5	4.7	1.3	0.6	1.9
12	Hongei	1.0	93.4	3.7	1.1	0.3	1.5

Table 2. Examination of quinoline extraction yield.

Coal	Indian Ridge				Balmer	
Temperature °C	350	360	370	375	380	380
Time hrs	4	6	1	1	4	4
Pressure MPa	5	0.1	10	0.1	1	10
Extraction yield %	63.0	64.0	61.5	68.0	51.9	50.0

Table 3. Extraction or reaction condition, yield, ultimate analysis and molecular weight of extracts.

No	Reaction ¹⁾	Temperature °C	Time hr	Yield %	ultimate analysis %				molecular weight
					C	H	N	Odiff	
1	Q	350	4	35.9 ²⁾	83.0	6.2	3.6	7.2	-
	N	300	1	97.8 ³⁾	78.4	7.8	1.6	12.2	755
2	Q	350	4	44.9	82.9	7.0	2.1	8.0	-
	N	300	1	98.1 ³⁾	80.8	8.1	1.3	9.8	870
3	Q	350	1	93.8	81.8	5.7	2.4	10.1	-
	N	300	1	96.9 ³⁾	82.6	7.2	1.9	8.3	890
4	Q	350	4	69.0	83.6	5.5	2.2	8.7	-
	Q	350	4	100.0	84.5	6.2	1.4	7.9	-
6	Q	350	4	81.0	82.7	5.8	2.9	8.6	-
	Q	350	4	97.8	85.8	5.7	1.4	7.1	-
7	N	350	1	91.1 ³⁾	86.8	6.4	1.7	5.1	1160
	Q	375	1	68.0	87.2	5.2	1.4	6.2	-
8	N	350	1	52.4 ³⁾	86.9	6.5	1.3	5.3	905
	Q	350	4	93.0	86.7	5.2	3.8	4.3	-
10	Q	380	4	51.9	88.1	5.0	2.4	4.5	-
	Q	370	4	41.6	88.8	4.9	1.7	4.6	-
12	Q	350	4	1.3	-	-	-	-	-

1)Q:quinoline extraction, N:NaOH-alcohol reaction,pyridine extracts.

2)Hydrolysis product with NaOH solution at 200°C,6hrs.

3)Pyridine extraction yield of NaOH-alcohol reaction products.

Table 4. Results of structural analysis.

No	1		2			3		4	5
Reaction)	Q	N	Q	N	N'5)	Q	N	Q	Q
Ha%	0.38	0.11	0.37	0.13	-	0.43	0.22	0.51	0.37
Hx%	0.28	0.36	0.25	0.35	-	0.34	0.39	0.29	0.32
H β %	0.27	0.41	0.32	0.41	-	0.16	0.29	0.16	0.25
H γ %	0.06	0.12	0.06	0.10	-	0.08	0.10	0.05	0.06
fa	0.75	0.53	0.71	0.52	0.70	0.79	0.63	0.82	0.75
Haus/Caus	0.82	1.00	0.88	0.97	0.90	0.81	0.89	0.78	0.75
σ	0.47	0.77	0.43	0.65	0.45	0.48	0.54	0.41	0.46
σ -al	0.20	0.39	0.20	0.40	0.17	0.20	0.34	0.17	0.23
Cus	12.5	11.5	11.1	12.3	11.5	12.3	12.4	13.1	16.0
Caus	9.4	6.0	7.9	6.4	8.0	9.7	7.7	10.7	12.0
Calus	3.1	5.5	3.2	5.9	3.4	2.6	4.6	2.4	4.0
Rtus	2.3	1.9	1.6	1.9	1.8	2.3	2.3	2.5	3.1
Raus	1.8	1.1	1.5	1.1	1.4	1.9	1.4	2.2	2.5
Rnus	0.5	0.9	0.1	0.8	0.4	0.4	0.8	0.4	0.6
Mol. Wtus ²⁾	181	176	161	183	181	180	180	188	227
Ous ³⁾	0.8	1.4	0.8	1.1	2.0	1.1	0.9	1.0	1.1
Ous ⁴⁾	2.8	2.5	1.6	1.7	-	-	-	-	-

No	6	7		8		9	10	11
Reaction)	Q	Q	N	Q	N	Q	Q	Q
Ha%	0.39	0.39	0.26	0.52	0.28	0.48	0.55	0.63
Hx%	0.29	0.28	0.29	0.26	0.36	0.31	0.27	0.24
H β %	0.25	0.25	0.27	0.16	0.27	0.15	0.15	0.09
H γ %	0.06	0.08	0.11	0.05	0.09	0.06	0.02	0.04
fa	0.77	0.80	0.70	0.84	0.70	0.83	0.86	0.89
Haus/Caus	0.76	0.66	0.67	0.65	0.69	0.68	0.64	0.64
σ	0.48	0.43	0.53	0.35	0.45	0.42	0.35	0.29
σ -al	0.20	0.20	0.33	0.16	0.32	0.19	0.16	0.14
Cus	15.0	23.4	25.7	23.8	22.2	20.1	24.9	24.1
Caus	11.5	18.8	17.6	20.0	15.8	16.7	21.4	21.4
Calus	3.5	4.6	7.7	3.8	6.6	3.4	3.5	2.7
Rtus	3.0	4.8	5.7	5.3	4.9	4.6	5.9	5.4
Raus	2.4	4.2	4.0	4.5	3.4	3.7	4.9	4.9
Rnus	0.6	0.6	1.8	0.8	1.5	0.9	1.0	0.5
Mol. Wtus ²⁾	218	328	356	328	307	279	340	326
Ous ³⁾	1.2	1.5	1.1	1.3	1.0	0.1	0.4	0.3
Ous ⁴⁾	-	-	-	-	-	-	-	-

1)Q:quinoline extraction

N:NaOH-alcohol reaction

2)Molecular weight per unit structure

3)Number of (oxygen atom)diff. per unit structure

4)Corrected number of (oxygen atom)diff. per unit structure

5)Extrapolated values to 0 hour in the time variation reaction at 260°C.

Chemical Structures and Reactivities of Coal
as an Organic Natural Product

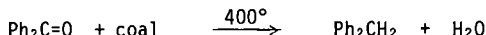
Clair J. Collins, Hans-Peter Hombach, Ben M. Benjamin

W. H. Roark, Brian Maxwell, and Vernon F. Raaen (1)

Contribution from the Chemistry Division
Oak Ridge National Laboratory, Oak Ridge, Tennessee 37830

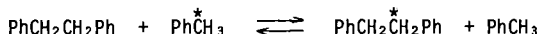
A. The Role of Tetralin in the Pott-Broche Process

It has recently been demonstrated (2) that several bituminous coals and lignites are better hydrogen donors than tetralin, a donor which has been employed, since its use in the Pott-Broche process (3), as the coal chemists' "standard." The better hydrogen-donating abilities of these various coals were tested toward several reactions (4), but that used as the model was the reduction, in a closed tube at 400°, of benzophenone to diphenylmethane:

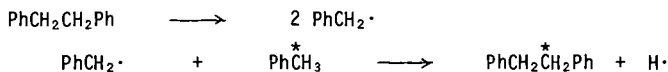


These results naturally raise the question of the role of tetralin, or of the recycle oil used in its place, during many of the solvent-refined coal processes — particularly since the solid product of such processes often contains no more hydrogen than the original coal (5). Neavel (6) examined the liquefaction of coal in tetralin and other solvents, using kinetic techniques, and found that donor and nondonor solvents appear to be equally capable in dispersing the coal after 5 minutes at temperatures of 400-570°C. Upon prolonged heating in nondonor solvents, the free radicals which form in the coal are thought to polymerize to higher molecular weight materials, whereas in the presence of tetralin, these radicals can be trapped by transfer of hydrogen.

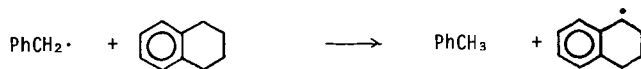
In order to test some of these concepts we carried out several experiments with carbon-14-labeled compounds. In one of these bibenzyl and toluene-¹⁴C were heated at 400° for one hour. There was intermolecular transfer of hydrogen with formation of toluene and other products, but the reisolated bibenzyl had undergone (to a small extent) an exchange reaction with toluene as shown by the fact that the reisolated bibenzyl contained carbon-14:



This exchange reaction must take place through a free-radical mechanism, possibly as follows:



When the two components — bibenzyl and toluene-¹⁴C — were heated in the presence of tetralin, however, there was no exchange between the two as shown by the fact that the reisolated bibenzyl was completely devoid of carbon-14. The reason must lie in the ready ability of tetralin to trap the benzyl radicals before they can react with toluene:



In several other reactions carried out with Illinois No. 6 coal and labeled substrate (e.g. α -naphthol- α - ^{14}C), the mixtures were heated for up to one hour in closed tubes at 400° , and benzene was used as a vehicle to ease material transfer. To our surprise, significant quantities of unlabeled biphenyl were discernible upon subsequent work-up. Although the yields were not determined, sufficient biphenyl was formed in one case to allow its isolation and identification by nmr. Through some as yet unexplained mechanism, a phenyl radical must have been produced, which then reacted with another benzene molecule to form biphenyl:



The presence of tetralin, however, inhibits biphenyl formation.

In an effort to determine whether tetralin does more than act as a radical scavenger during Pott-Broche-like processes, we prepared tetralin-1- ^{14}C (7) and heated it (1.933 g, 15.82 C; per mole) for one hour with 3.06 g of vitrain (from Illinois No. 6 coal). The product was extracted with pyridine, and the residue was treated with THF, plus a mixture of nonradioactive tetralin and naphthalene. The residue still contained carbon-14 which, on a tetralin basis represents 2.6-2.8% by weight of the residue. The pyridine soluble fraction also contained carbon-14 representing 1.6% by weight of that fraction (on a tetralin basis). Thus the tetralin- ^{14}C appears to have undergone a chemical reaction with the coal. We have previously reported (4) that tetralin and Illinois No. 6 coal when heated at 400° yield α - and β -methyl-naphthalenes, in which the methyl groups undoubtedly have their origin in the coal.

The role of tetralin during coal conversion, therefore, is 1) to act as a dispersion vehicle; 2) to supply hydrogen radicals, when needed, to trap coal radicals, and 3) in a very minor way to undergo intermolecular reaction with the coal through making and breaking of C-C (and possibly other) bonds.

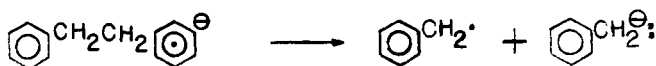
B. Reductions of Coal

Two chemical reactions for solubilizing coals have received much attention in recent years, these are 1) the Friedel Crafts reaction (8-19) and 2) reductions, either with lithium in suitable solvents (20-26), or electrolytically with lithium salts in ethylenediamine (27-32). Part of the interest in these reactions is undoubtedly due to the fact that they can be carried out at low temperatures.

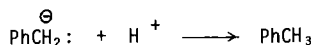
The chemical changes affected during coal reductions are usually considered to be breakage of ether and thioether linkages, as well as reduction of aromatic nuclei. Alkyl groups are not affected (33). The Birch-Hückel reaction (34) of aromatic rings to cyclic olefins is well known. It was recently reported (35) that the use of NaK in mixed ethers as a coal reductant cleaves the alkyl linking groups (e.g. $-\text{CH}_2-\text{CH}_2-$) between aromatic moieties, and results in an increase in the number of methyl groups in the reduced product. Oxidation studies (36, 37) have indicated a high frequency of ethylene connecting links in some bituminous coals, as shown by the isolation of large quantities of succinic acid. We therefore carried out the reduction of three model compounds under the conditions reported (37) by Hombach and Niemann, using glycol ethers as the solvent. The compounds chosen were diphenylmethane, bibenzyl, and 1,3-diphenylpropane. Of the three compounds, diphenylmethane exhibited some, and bibenzyl exhibited considerable C-C splitting in only 20 minutes, whereas 1,3-diphenylpropane was stable except for traces of toluene and ethylbenzene (when quenched with propanol-2). The results can be illustrated for bibenzyl, which was added to the solution (37) of "solvated electrons." The mixture was stirred for 20 minutes, then $^{14}\text{CH}_3\text{I}$ was added to the reaction mixture, followed by water and then pentane. The pentane solution was washed, dried, and subjected to g.c. analyses with an apparatus fitted with a carbon-14 radioactivity monitor (38). The

results are shown in Fig. 1. The products were separated on a preparative g.c. column (39) and identified through their nmr spectra.

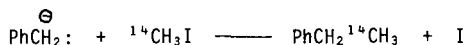
Thus, to the methods previously employed for breaking bonds in coal molecules and thereby lowering their molecular weights, must now be added the use of "solvated-electrons" for breaking -CH₂-CH₂- linkages. The mechanism for cleavage of bibenzyl must be approximately as follows



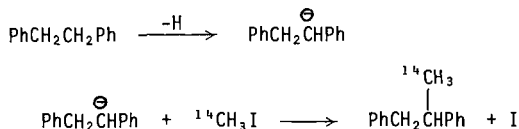
Toluene results by donation of a proton to a benzyl carbanion from the solvent:



The carbon-14-labeled ethylbenzene is formed by reaction of the benzyl carbanion with ¹⁴CH₃I:



The other product, 1,2-diphenylpropane is formed in the conventional manner:



References

1. Research sponsored by the Division of Chemical Sciences, U. S. Department of Energy, under contract W-7405-eng-26 with the Union Carbide Corporation.
2. V. F. Raaen and W. H. Roark, *Fuel*, **57**, in press (1978).
3. See, for example, K. F. Schlupp and H. Wien, *Angew. Chem. Int. Ed. Engl.*, **15**, 341 (1976).
4. C. J. Collins, B. M. Benjamin, V. F. Raaen, P. H. Maupin and W. H. Roark, "Organic Chemistry of Coal," ACS Symposium Series No. 71, J. W. Larsen, Ed., Chapter 12, pp. 165-170 (1978).

5. D. D. Whitehurst, M. Farcasiu and T. O. Mitchell, "The Nature and Origin of Asphaltenes in Processed Coals," EPRI AF-252, pages (1) 2-17 (1976).
6. R. C. Neavel, Fuel, 55, 237 (1976).
7. C. J. Collins, J. Amer. Chem. Soc., 73, 1038 (1951).
8. C. Kröger, H. de Vries, Justus Liebigs Ann. Chem., 652, 35 (1962).
9. C. Kröger, H. G. Rabe, B. Rabe, Brennstoff Chem., 43, 179 (1962).
10. C. Kröger, H. G. Rabe, B. Rabe, Erdöl Kohle Erdgas Petrochem., 16, 21 (1963).
11. C. Kröger, Forschungsber. Nordrhein-Westfalen Nr., 1488 (1965).
12. W. Hodek, F. Meyer, G. Kölling, Amer. Chem. Soc. Symposium Ser., 55, 408 (1977).
13. W. Hodek, 7. Internat. Conf. on Coal Science, Prag 1968.
14. M. S. Iyengar, D. D. Banerjee, D. K. Banerjee, Nature (London), 186, 388 (1960).
15. F. Micheel, D. Laus, Brennstoff Chem., 47, 345 (1966).
16. F. Micheel, L. Rensmann, Makromolekulare Chem., 65, 26 (1963).
17. A. H. Haines, F. Micheel, Makromolekulare Chem., 80, 74 (1964).
18. F. Micheel, H. Licht, Makromolekulare Chem., 103, 91 (1967).
19. W. Hodek, G. Kölling, Fuel, 52, 220 (1973).
20. L. Reggel, R. A. Friedel, I. Wender, J. Org. Chem., 22, 891 (1957).
21. P. H. Given, V. Lupton, M. E. Peover, Nature (London), 181, 1059 (1958).
22. L. Reggel, R. Raymond, S. Friedman, R. A. Friedel, I. Wender, Fuel, 37, 126 (1958).
23. L. Reggel, W. A. Steiner, R. A. Friedel, I. Wender, Fuel, 40, 339 (1961).
24. H. W. Sternberg, C. L. Delle Donne, L. Reggel, I. Wender, Fuel, 43, 143 (1964).
25. L. Reggel, I. Wender, R. Raymond, Fuel, 43, 75 (1964).
26. L. Reggel et al., US Department of Interior, Bureau of Mines, Bulletin No. 615 (1965).
27. P. H. Given, M. E. Peover, Fuel, 39, 463 (1960).
28. R. E. Markby, H. W. Sternberg, I. Wender, Nature (London), 199, 997 (1963).
29. H. W. Sternberg, C. L. Delle Donne, R. E. Markby, I. Wender, Advan. Chem. Ser., 55, 516 (1966).
30. See also J. A. Franz and E. W. Skiens, Fuel, 57, 502 (1978).

31. H. W. Sternberg, R. E. Markby, I. Wender, J. Amer. Chem. Soc., 89, 186 (1967).
32. J. D. Brooks, R. A. Durie, H. Silberman, Australian J. Chem., 17, 55 (1964).
33. See, for example, A. J. Birch, G. Subba Rao, Advances in Organic Chemistry, 8, 1 (1972).
34. H. P. Hombach, K. Nieman, Ergänzungsband der Zeitschrift Erdöl und Kohle, Erdgas, Petrochemie, Compendium 1977/1978, p. 295-310.
35. V. F. Raaen, unpublished work (1975).
36. N. C. Deno, B. A. Greigger, S. G. Stroud, Preprints of Papers Presented at Anaheim Cal., March 12-17, 1978, Division of Fuel Chemistry of the American Chemical Society, 23, No. 2, Pages 54-57.
36. Klaus Niemann, Ph.D. Dissertation, "Reduktion von Kohle mit Hilfe solvatisierter Elektronen," Abteilung für Chemie an der Ruhr-Universität Bochum (1977).
37. A Barber-Coleman Series 5000 g.c. fitted with radioactivity monitor was employed.
38. Varian Aerograph Series 2800.

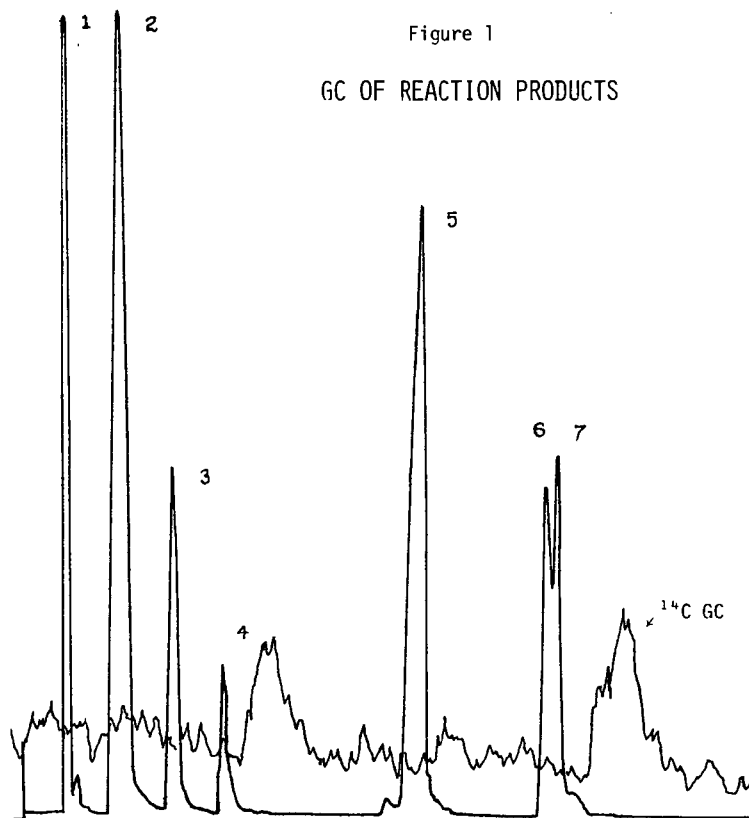


Figure 1
GC OF REACTION PRODUCTS

- 1 pentane
- 2 1,2-dimethoxyethane
- 3 toluene
- 4 ethylbenzene
- 5 2,5,8,11-tetra-oxadodecane
- 6 1,2-diphenylethane
- 7 1,2-diphenylpropane

The Effect of Reagent Access in Coal Reactivity

John W. Larsen^{1a,b}, P. Choudhury^{1a}, Tom Greene^{1a}
and E.W. Kuemmerle^{1a}

Department of Chemistry, University of Tennessee
Knoxville, Tennessee 37916
and Oak Ridge National Laboratory, P.O. Box X
Oak Ridge, Tennessee 37830

Hypothesis: The reactivity of bituminous coals under mild conditions is dominated by the accessibility of the reacting groups in the coal to reagents and not by the intrinsic reactivity of those groups. Evidence for this hypothesis will be presented. It is not conclusive evidence, but it is sufficient to warrant further exploration of this idea.

Bituminous coals contain cross linked, three dimensional macromolecular networks. Perhaps the best evidence for this comes from experiments in which the coal is swollen by solvents (1). The weight increase in several coals which have been exhaustively extracted with pyridine are shown in Table 1. These coals can be swollen to about twice their original volume by absorbing solvent. The solvent-coal interactions responsible for this inhibition are strong enough so that if the coal "molecules" were not covalently linked together, they would dissolve. The observed behavior is characteristic of a cross linked macromolecular network (2,3,4).

Coal is a highly porous, insoluble material. An attacking reagent has access to those parts of the surface of the coal which form the walls of the pores into which it can diffuse. Any solvent which expands the pore structure will enhance a coal's reactivity by increasing the surface area accessible to the reagents. One limitation on coal reactivity is the ability of reagents to penetrate the pore structure.

However, even ready penetration of the pores only gives access to the surface of the coal. For complete reaction, the reagent must diffuse into the coal network and penetrate to the bonds or groups with which it will react. It would seem that this diffusion process is likely to be very slow, and indeed may limit not only the rate of reaction but also the number of groups which ultimately react. Some examples of access limited reactions follow.

Analysis for Phenolic Hydroxyl. Maher and O'Shea (5) measured the phenolic hydroxyl content of Greta coal (DAF 82.4%C, 6.2%H, 1.7%N, 1.0%S) by titration in ethylenediamine solvent. They also extracted the coal with various solvents and measured the OH content of the extract and the residue. The data are shown in Table 2 and it is obvious that the results with the extracted coals are greater than that obtained with the whole coal. Precautions were taken to prevent oxidation and the generation of new phenolic OH groups by depolymerization seems unlikely. An increase in the accessibility of OH groups is the most reasonable explanation.

Friedel-Crafts Acylation. The Friedel-Crafts acylation of coals give products whose "solubility" increases with the size of the acyl group (6). These products are of very high (10^5 - 10^6) molecular weight (7). The proton nmr and ^{13}C nmr of octanoylated Bruceton coal are shown in Figs. 1 and 2. Peaks due to aromatic protons are absent from the proton nmr. The peaks due to the methylene α and β to the carbonyl group are broadened, while the methylene peaks at the terminal end of the chain show normal line widths. These data can be explained if acylation occurred at the coal surface and the resulting substance was solubilized, micelle like, by the interactions of the long chain with the solvent. The aromatic protons would still be in a solid environment, and their absorption would be too broad to detect. The motion of the portion of the acyl chain close to the coal surface would be hindered by close packing, giving rise to broad lines. The other end would have free motion and normal line widths as observed.

Heredy-Neuworth Depolymerization. Using currently accepted models for bituminous coal, it is clear that any reaction which cleaves the bonds between aromatic carbons and methylene groups should result in destruction of the coal and the products of low molecular weight products. The Heredy-Neuworth depolymerization is one such reaction (8,9). When applied to coal it gives mostly high molecular weight products, 80% greater than 3000. The colloidal material from a depolymerization can be further depolymerized if reacted again. The cleavage of these bonds in model compounds is not a slow reaction. These results can be explained by postulating limited access of the necessary reagents to the interior of the coal.

There are reactions which produce low molecular weight products from coals. Heat has ready access to the interior of coal, so pyrolysis would be expected to, and does, rapidly destroy the network and produce low molecular weight products. Vigorous reactions, such as oxidation, can chew their way into the coal by cutting small molecules off of the surface. This requires vigorous, unselective reactions. The attempts to use mild, selective reactions to solubilize coal lead to high molecular weight products.

If the hypothesis stated here is correct, its consequences for coal chemistry and processing will be enormous. Methods for gaining ready, rapid access to the interior of the coal network should be sought. The discovery of such methods will allow rapid, mild processing of coals. If rapid access cannot be obtained, pyrolysis may be the necessary first step of any process rapid enough to be commercially attracted.

Acknowledgement. We are grateful to the Department of Energy for support of this work and to EPRI for support of the acylation studies.

References

1. a) Department of Chemistry, University of Tennessee, b) Chemistry Division, ORNL.
2. This idea was first brought to our attention by Frank Mayo, and we acknowledge this with thanks.
3. P.J. Flory, "Principles of Polymer Chemistry", Cornell University Press, Ithaca, N.Y. 1953.
4. L.R.G. Treloar, "The Physics of Rubber Elasticity", Clarendon Press, Oxford, 1975.
5. T.P. Maher and J.M. O'Shea, *Fuel*, 46, 286 (1967).
6. W. Hodek and G. Kolling, *Fuel*, 52, 220 (1973).
7. H.-P. Hombach, Ph.D. Thesis, Westfalischen Wilhelms-Universitat, Munster, 1972.
8. L.A. Heredy and M.B. Neuworth, *Fuel*, 41, 221 (1962).
9. For a review of the early chemistry of this reaction see J.W. Larsen and E.W. Kuemmerle, *Fuel*, 55, 162 (1976).

Table 1. Swelling^a of Four Pyridine Extracted Coals with A Series of Organic Solvents.

Coal	Toluene	Ethanol	Acetone	1,4 Dioxane	Pyridine
N.D. Lignite	1.20	1.35	1.44	1.49	1.82
Wyodak	1.33	1.43	1.54	1.71	2.16
Ill. No. 6	1.44	1.41	1.54	1.83	2.18
Bruceston	1.43	1.39	1.46	1.78	2.03

a) Ratio: weight of swollen coal at equilibrium; original weight of coal.

Table 2. Sum of phenolic groups in extracts and residues Basis: 100g of d.a.f. coal: 160 milliequivalents (from ref. 5).

Solvent	Extract		Residue		Total milli-equivalents
	Weight (g)	Total acidity (m.equiv./g)	Weight (g)	Total acidity (m.equiv./g) mean	
Iso-amy1 alcohol	2.2	N.D.	97.8	1.99	>195
Dimethyl formamide	22	3.21	78	1.35	176
Diethylamine	4.1	1.73*	95.9	1.86	185
Pyridine	16	2.51	84	1.75	187
Aniline	15	2.82	85	1.53	172
Ethylenediamine	23	2.88	77	1.24	161
Chloroform	4.7	0.92	95.3	3.03	293
Dichloromethane	2.0	0.30	98	2.32	228

* Approximate figure only, obtained from stirred extractor experiment where yield was 3.5 per cent.

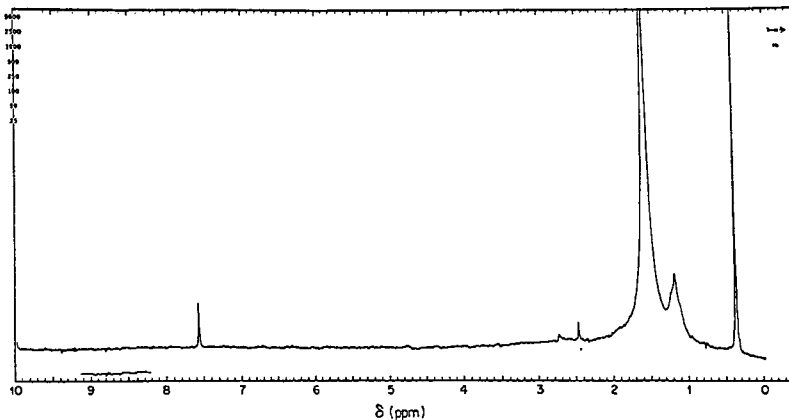


Fig. 1. Proton NMR Spectrum of Octanolyated Bruceton Coal in CCl_3 .

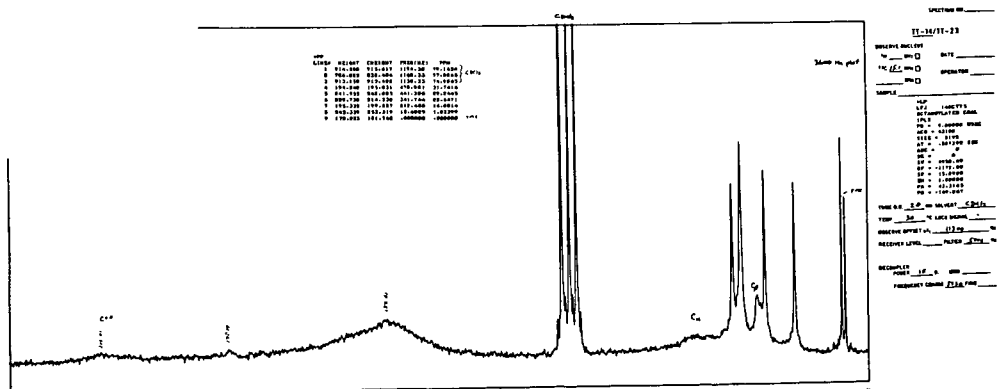
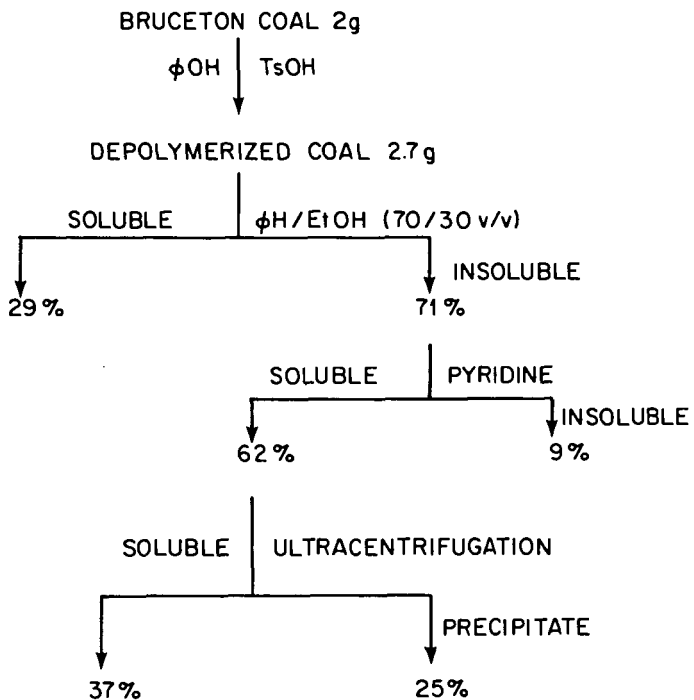
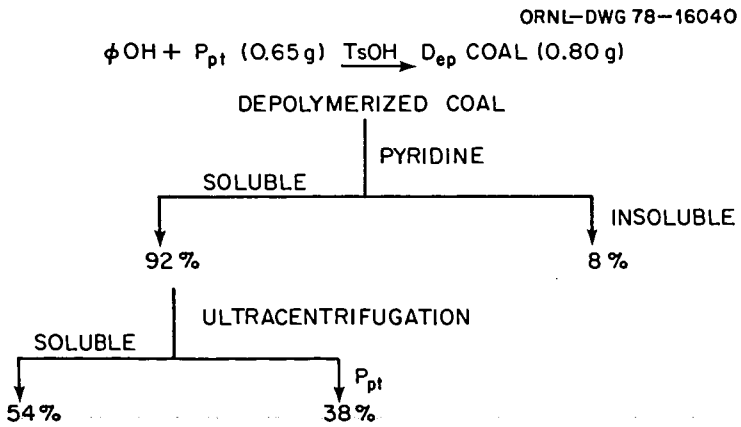
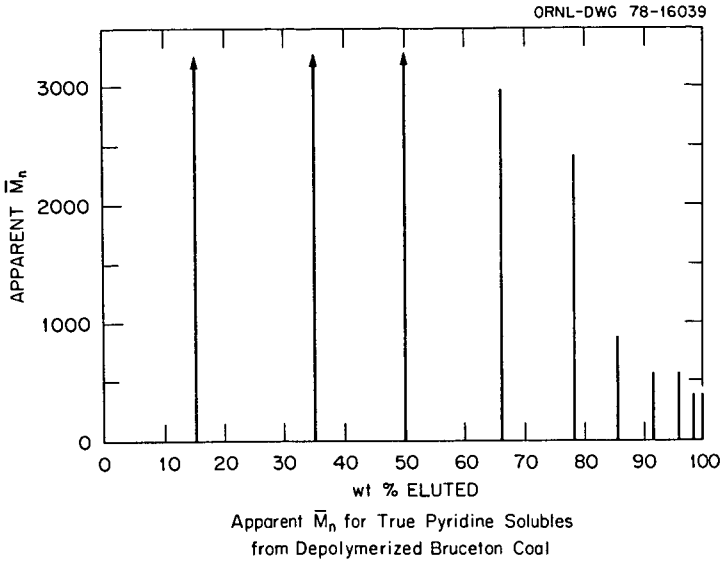


Figure 2. ^{13}C nmr Spectrum of Octanolyated Bruceton Coal (CDCl_3 solvent).





THE PHYSICAL STRUCTURE OF BROWN COAL

R.J. Camier, S.R. Siemon, H.A.J. Battaerd and B.R. Stanmore

Department of Chemical Engineering,
University of Melbourne,
Parkville, Vic. 3052.

Introduction

The behaviour of coal during processing is determined by its physicochemical composition and structure. The examination of the coal "molecule" has been hampered by the inability to find techniques which measure any meaningful properties of such large complex structures. Most attacks on the problem have been by means of breaking down the structure into smaller, more tractable pieces, examining these and inferring the original structure. With bituminous coals the severity of the treatment needed to rupture the molecules raises doubts as to the validity of the method. There is uncertainty even with brown coals which are geologically younger and bear more resemblance to the molecules of classical organic chemistry. This is reflected, for instance, in the diversity of models proposed for basic molecular arrangement (1-5).

Brown coals have the advantage that they can be broken down by the comparatively gentle treatment of alkali digestion (6) into fragments in the micron and submicron range. This results in a soluble fraction of humic acids and an insoluble residue, humins. With Victorian coals it has been found that maximum digestion occurs at pH 13 to give humic acid yields ranging from 15 to 40% of the dry coal mass (7).

This paper reports on a study of digested coal fractions which were subjected to particle size analysis using sedimentation techniques. For the humins fractions a gravitational sedimentation technique was adopted while the more finely divided humic acids required an ultracentrifuge to generate a sufficiently large force field. The nature of the fragments generated by this technique has resulted in a modified hypothesis of coal genesis.

Experimental

The coal examined was a sample of medium-light earthy coal from the Yallourn mine in the Latrobe Valley, Victoria. Its ultimate analysis on a d.a.f. basis was C 65.6%, H 5.18% and oxygen by difference 27.95%. A stock sample was prepared by wet ball milling, followed by further size reduction in a domestic food pulper and was then stored under water in a closed vessel.

For each test a 15 ml quantity of slurry was mixed with 500 ml quantity of 0.1 M NaOH solution to maintain pH at 13. After digesting overnight the slurry was wet-screened on a B.S. 350 mesh screen to remove +43 μm oversize particles. The underflow was then passed through a micropore filter of nominal pore size 1.2 μm . The coal thus been fractionated by particle size into humins (the +43 μm and the -43 μm + 1.2 μm fractions) and humic acids (-1.2 μm fraction).

Some of each of the fractions was acid washed to remove sodium and reprecipitate the humic acids. A yellow supernatant liquid remained after precipitation of the humic acids, due to small quantities of fulvic acid. An elemental analysis was then carried out on the dried solids of each fraction.

Other samples of alkaline slurry were subjected to particle size analysis by sedimentation. With the -43 μm + 1.2 μm fraction this was done in a 50 mm diameter settling column with a tared pan at the base to continuously record the mass of sedimented solid. The data was analysed by the method of Odén (8) and the particle size distribution (Stokesian diameter) expressed on a mass % basis was calculated.

The humic acid fraction (-1.2 μm) which was a dark brown suspension containing 4.7 mg/l of coal did not settle even after standing for six months. This slurry was

spun in a Beckmann ultracentrifuge with special long tubes to generate high g values. Alkali-resistant polyallomer tubes were used so that the solids which collected in the base could be removed in a special guillotine, then dried and weighed. The heights of suspension charged varied from 10 to 80 mm and rotational speeds up to 40 000 rpm were used. The data was again analysed by Odén's method, modified according to Brown (9).

Results

A typical output from the sedimentation balance for $-43 \mu\text{m} + 1.2 \mu\text{m}$ material so shown in Fig. 1. The occurrence of distinct peaks indicates that groups of closely-sized particles are present, the smallest being about $6 \mu\text{m}$ in effective (Stokesian) diameter. The persistent appearance of the same size groups in all tests at different pH and with different coal types suggested that some fundamental unit was present. A microscopic examination of the material revealed that cylindrical rods about $0.9 \mu\text{m}$ in diameter and $6-8 \mu\text{m}$ long were common. When the drag coefficient for such particles was calculated from Lamb's formula for cylinders at low Reynolds' number (see Prandtl (10)), the terminal setting velocity was the same as for a spherical particle of about $6 \mu\text{m}$ diameter.

The larger particle sizes could thus be accretions of these basic units and a number of such agglomerations were noted. The rods were arranged side by side, close packed in bundles. It appears that the alkali peels these rods from the coal mass and they subsequently agglomerate in solution, doubling in volume at each coalescence.

Elemental analyses of the fractions showed the 'rod' fraction ($-43 \mu\text{m} + 1.2 \mu\text{m}$) is rich in both hydrogen and carbon compared with the original coal, Fig. 2 although the effect is partly obscured by the oxidation which takes place in alkaline solution. The same trends appeared in all coal samples tested.

The particle size distribution for the humic acid fraction is depicted in Fig. 3. No material sedimented out until the most extreme conditions were applied (40 000 rpm for 24 h), when some lightening of colour at the top of the solution was observed. The sedimented particles had a Stokesian diameter of around $2 \mu\text{m}$, which means that a particle size gap of three orders of magnitude exists between these and the next largest particles detected ($5 \mu\text{m}$). Taking the density of coal substance to be 1.43 g/cm^3 , a solid sphere of diameter $2 \mu\text{m}$ would have a molecular mass of 4,000. If the molecules were rod-shaped, even smaller molecular masses would be predicted. Literature values of the molecular mass of regenerated humic acids range between 800 and 20 000 with the values clustering around 1,000 and 10,000 (11,12,13).

Since the humic acid fraction constitutes 30% of the dry coal mass, about one third of the coal is in the form of small macromolecules, and bound to the coal structure with bonds weak enough to be disrupted by dilute alkali.

It is of interest to note that the particle size gap supplies a rational basis to the traditional German classification scheme of defining humic acid and humins on the basis of a particle size separation (filtration).

Discussion

The presence of geometrically uniform rods and the absence of particles over such a wide particle size range have implications for our understanding of coal chemistry and genesis. The following discussion attempts to harmonise these observations.

Three explanations have been considered to explain the rods found during this work. These are that they are:-

- i) bacterial remains
 - ii) plant cell remains
 - iii) artifacts formed during phase separation in the coalification process.
- Since bacteria, including rod-like bacilli are active during the biological digestion

stage of coalification, remnants of their protoplasm may have been incorporated into the coal matrix. If this were so, their protein content should result in a high nitrogen content and the results are listed in Table 1.

TABLE 1.
Nitrogen content (d.a.f.) of Coal Size Fraction

Material	original coal	+43 μ m	-43 μ m+1.2 μ m	-1.2 μ m
Nitrogen content (% daf)	0.75	0.63	0.78	0.70

Although the nitrogen content of the rod fraction is higher than the others, it can only be significant if the rods constitute less than about 2% of the total mass of the -43 μ m + 1.2 μ m fraction. Since their concentration appears to be much greater than this, the hypothesis is unattractive.

The abundance of identifiable cell fragments observed under the microscope lends weight to the second hypothesis. Cell sizes vary with location in the plant and remains of coniferous tracheids or other cells would be of the correct size. The composition of the rod fraction is close to that of lignin and the rods have been observed peeling off larger woody fragments. The cell remains explanation must therefore be considered as a possibility in the absence of other information.

The third hypothesis is more speculative and far-reaching in its implications. It is generally accepted (14) that the first step in the genesis of coal is the destruction of cellulose and the degradation of lignin to monomer which either is a humic acid or polymerises to give humic acids. The polymerisation of these acids takes place by condensation as indicated by the decrease in acidity with increase in molecular mass. As the concentration of monomer decreases, a gel point is reached and a giant network is formed, swollen by the solvent water. As the polymerisation proceeds further, the network will become cross-linked, resulting in shrinkage and water exclusion.

Considering macromolecules in surface energy terms, the solubility parameter has been defined as

$$\delta = \left[\frac{E}{V} \right]^{1/2}$$

where E is the molar cohesive energy and V is the molar volume. For two polymers A and B, the materials are compatible if (15),

$$(\delta_A - \delta_B)^2 < 4.2 \text{ kJ/l}$$

If this inequality does not hold phase separation of polymers will occur. The solubility parameter of coal over a wide range of coal ranks has been measured (15,17,18) and is plotted in Fig. 4. The value of δ falls nearly linearly from 32 to 23 as the carbon content rises from 70 to 89% and rises slowly thereafter. At 89% carbon, polar groups are largely absent and aromatisation has commenced. By extrapolation back to the 65-70% carbon range occupied by brown coals, the line is steep enough such that a difference of only 1% in carbon content is sufficient to create incompatibility between coal molecules.

A large polymer molecule is able to exist with different parts of the chain in different phases and an increase in the concentration of the species will concentrate solvated parts together as well as concentrating the precipitated parts. With two different polymers e.g. polystyrene and polybutadiene blocks of one will form within a continuous phase of the other, with domain sizes between 10 and 100 nm usual. This segregation into phases will be enhanced by the swelling effect of the remaining polymer.

In the case of coal formation, woody residues intermingle with condensation polymers which are swollen by the water-soluble products from the degradation of

cellulose and lignin. The local changes in carbon content brought about by condensation polymerisation may be sufficiently large for phase separation to occur and the rods may be formed from local high-carbon regions, compare Fig. 2. Rod-shaped inclusions are known to form in materials like polyethylene oxide/polypropylene oxide copolymers within certain concentration limits as listed below.

high concentration of A	spheres of B dispersed in A
↓	rods " " " " "
↓	alternate layers of A and B
low concentration of A	rods of A dispersed in B
	spheres " " " "

In this view rods are precipitates formed from the humic acid groundmass and represent a further step in the coalification chain.

The revised model of coal structure which emerges from this study envisages a gel of humic acid molecules swollen by water and incorporating particulates. These include rods and detrital matter like pollen, cell remains, exinite material etc. which are held together by the humic acid "glue". The bonds linking this mass together must be of a homopolar non-regenerable type as rheological studies of Victorian coals have shown that the bonds are broken by shear action during mechanical working and do not remake on standing (19). This excludes the hydrogen bond commonly regarded as the major bond type for brown coal gels, as hydrogen bonds are known to remake after rupture. It appears that van der Waals type bonds may hold the structure together. On rupture the water which is liberated on shearing would be able to attach at the vacant sites and thus prevent the remaking of the original stronger bonds.

Conclusions

1. Particle size analysis of alkali-digested brown coal provides a useful insight into coal structure.
2. Victorian coals contain significant quantities of cylindrical rod-shaped particles, 1 μm in diameter and 6-8 μm long, which are high in carbon and hydrogen.
3. No particles exist in alkali-digested coal solutions between 6 μm and 2nm Stokesian diameter.
4. Brown coal can be regarded as a gel of humic acids which incorporates larger particles bound by non-regenerable bonds.

References

1. AGROSKIN A.A., "Chemistry and Technology of Coal", English translation from Russian, Israel Program for Scientific Translations, Jerusalem (1966)
2. FUCHS W., "Die chemie der Kohle", Springer, Berlin (1931)
3. DURIE R., in "Chemistry of Brown Coals", Coal Research in C.S.I.R.O., 6, 12, (1959)
4. BREGER, I.A., "Chemical and Structural Relationship of Lignin to Humic Substances", Fuel, 9, 204 (1951)
5. DRAGUNOV, S.S., in "Soil Organic Matter", Ed. Konova, M.M., Pergamon, London (1961) p. 65
6. MUKHERJEE, P.N., BHOWMIK, J.N. and LAHIRI, A., Fuel, 36, 417 (1957)
7. CAMIER, R.J., Ph.D. Thesis, Uni. of Melbourne, (1977)
8. ODÉN, S., Soil Science, 19, 1 (1925)
9. BROWN, C., "Particle Size Distribution by Centrifugal Sedimentation", J. Phys. Chem, 48, 246 (1844)
10. PRANDTL, L., "The Essentials of Fluid Dynamics", Blackie, London (1960) p. 190

11. BROOKS, J.D., "Advances in Coal Chemistry 1950 - 1970, Coal Research in C.S.I.R.O. 45, 20 (1971)
12. SAMEC, M., and PIRKMAIER, B., Kolloid - Z., 51, 96 (1930)
13. FUCHS, W., Brennstoff - Chem., 9, 178 (1928)
14. FLAIG, W., "The use of Isotopes in Soil Organic Matter Studies", Pergamon, New York (1966)
15. BRANDRUP, J., and IMMERGUT, E.H., "Polymer Handbook", Wiley, New York (1966)
16. VAN KREVELEN, D.W., Fuel, 44, 229 (1965)
17. KIROV, N.Y., O'SHEA, J.M. and SERGEANT, G.D., Fuel, 46, 415 (1967)
18. SANADA, Y., and HONDA, H., Fuel 45, 451 (1966)
19. COVEY, G.H., and STANMORE, B.R., "The Rheological Behaviour of Victorian Brown Coal", to be published, Fuel.

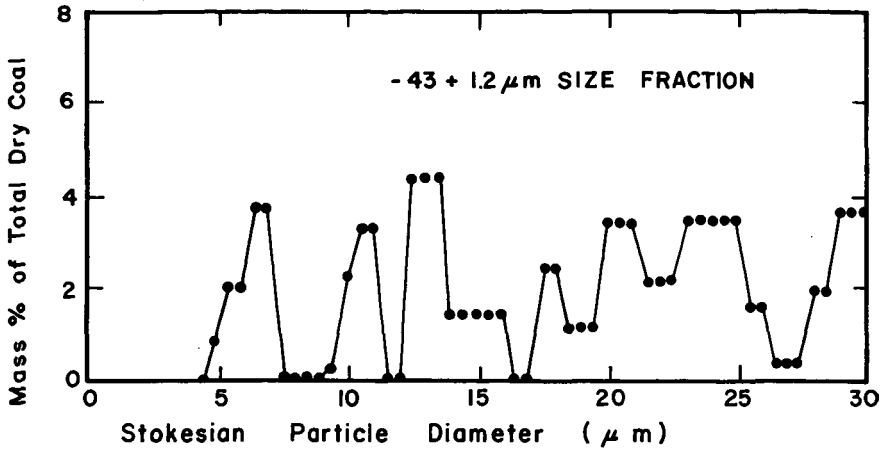


FIG. 1 PARTICLE SIZE DISTRIBUTION

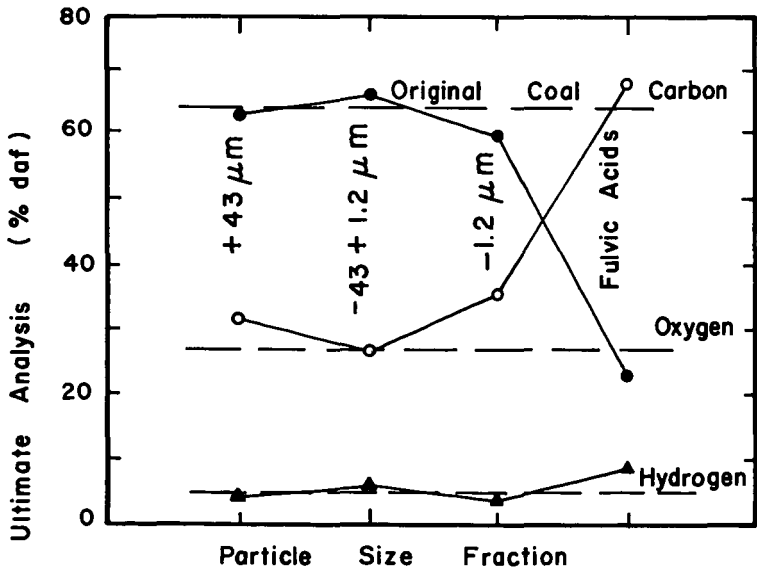


FIG. 2 ULTIMATE ANALYSIS OF FRACTIONS

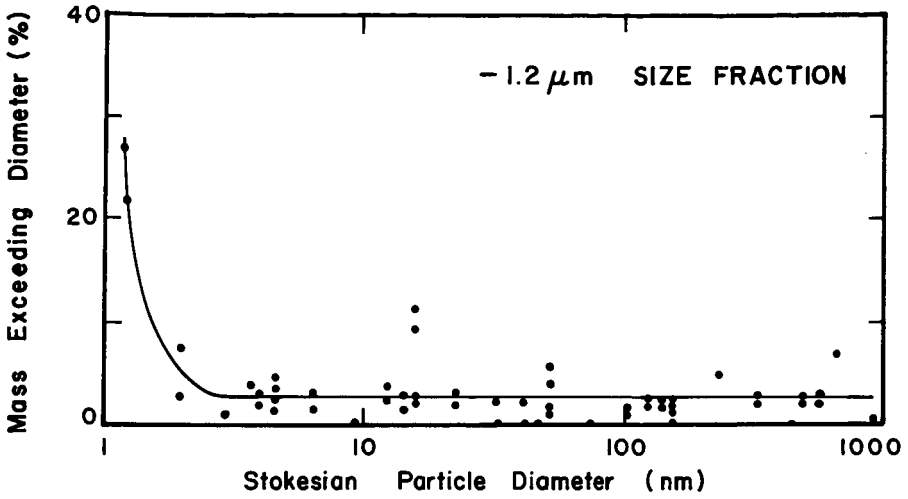


FIG. 3 PARTICLE SIZE DISTRIBUTION

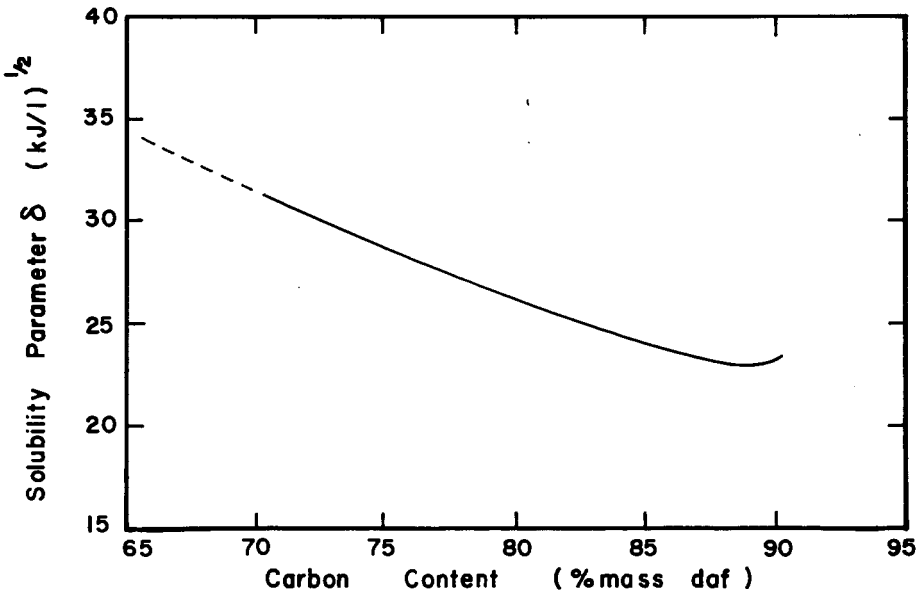


FIG. 4 SOLUBILITY PARAMETER vs % CARBON

THE ULTRAFINE STRUCTURE OF COAL DETERMINED BY ELECTRON MICROSCOPY

L. A. Harris and C. S. Yust

Metals and Ceramics Division
Oak Ridge National Laboratory
Oak Ridge, Tennessee 37830 USA

INTRODUCTION

The technological utilization of coal is dependent upon its physical characteristics as well as its chemistry. The size and spatial distribution of pores; and the size, distribution, and identity of the submicron size minerals are physical attributes of particular interest because of their influence in coal conversion processes such as liquefaction and gasification.

The present paper is one of a series in which electron microscope analyses including transmission, scanning transmission, and scanning reflection methods have been employed in examining bituminous coals (1, 2). These techniques have the advantage of revealing the microstructures of coal at magnifications substantially greater than that available with light microscopy. Consequently, a more detailed direct observation of the pores and submicron minerals within the coal may be obtained.

EXPERIMENTAL

Sample Selection and Preparation

Samples were selected from two high volatile bituminous coals, namely, Illinois No. 6 and Eastern Kentucky splint coal from Perry County. The selection of the above coals was based on the fact that both are of equal rank but of different lithotypes (i.e. maceral contents), microstructures, and geographically separated. Consequently some evaluation could be made of the variation in microscale features which could be significant in coal utilization or diagenesis.

Specimens were prepared from the above samples by slicing sections normal to the bedding and subsequently grinding them into optical thin sections approximately 10-15 μm thick. The optical sections were removed from the glass slide by acetone and thinned to electron transparency by ion bombardment (ion milled). The ion milling process was performed on fragments approximately 3 mm on edge using argon gas and a liquid nitrogen cold stage in order to ensure a sample free from thermal damage. The ion milled samples were fixed to electron microscope grids using silver conductive paint.

Analytical Methods

Both a high voltage transmission electron microscope (TEM) (1 Mv) and a scanning transmission electron microscope (STEM) (120 Kv) were used in this study. The STEM was fitted with an energy dispersion system utilizing a Si(Li) detector. Microchemical analyses of particles as small as 20 nm for elements of atomic number 11 or greater could be attained by use of the STEM and EDX.

* Research sponsored by the Division of Basic Energy Science, U.S. Department of Energy under contract W-7405-eng-26 with the Union Carbide Corporation.

RESULTS AND DISCUSSION

Figures 1 and 2 are TEM photomicrographs of specimens from the splint coal and the Illinois No. 6, respectively. The photomicrographs serve to illustrate the differences in microstructures between coals of the same rank. In general, the splint coal contains fragments of exinite, inertinite, and vitrinite closely compacted together, with the former two macerals making up over 70 volume percent of the total material. On the other hand, the Illinois No. 6 coal contains large bands of vitrinite interbedded with inertinite and exinite, where the latter two macerals combined comprise between 10 and 20 volume percent of the total macerals.

EASTERN KENTUCKY SPLINT COAL

Examination of the microstructure in Figure 1 reveals that the exinitic material (E) is essentially featureless in electron transmission. This material however, frequently contains relatively large and irregularly shaped pores (P). Immediately adjacent to the exinite is a region of vitrinite (V), containing a nearly uniform distribution of fine porosity. The boundary between the exinite and the vitrinite contains opaque fragments of mineral bearing inertinite as well as more finely divided inertinitic matter. The coarse porosity associated with the granular inertinite at the boundary is seen by detailed study to be continuous with the finer porosity that is observed in the vitrinite. This gradation of porosity from the inertinite to the vitrinite may be indicative of a transitional zone between the two macerals. The vitrinite bands observed in this field are relatively porous and as would be expected in a low density body, the porosity is highly interconnected.

The porosity associated with the exinitic maceral of the splint coal can be seen more clearly in Figure 3. The large, irregularly shaped pores often form distinct tubular channels which extend from the apparent center of the spore exinite to the boundary between the spore and the surrounding inertinite. Commonly, the channels contain spherical mineral particles, which appear to be associated with the formation of the channels. Other studies (3) on the interaction of fine metal particles on graphite surfaces have demonstrated that particulates can catalyze surface reaction and lead to generation of elongated pores of the type shown here. The particles in the exinite were identified by means of EDX analyses and selected area diffraction (see inserts in Figure 3) as the mineral aragonite (calcium carbonate) which presumably enters the exinite from the granular inertinite that typically surrounds the spore exines. Usually, the granular inertinite contains an appreciable amount of mineral matter, primarily as clays.

Previous porosity studies of coal by gas absorption methods (4) reveal a direct relationship between the fine porosity and the vitrinite content of a coal. These observations are confirmed by this study for both the splint and Illinois No. 6 coals in as much as all the vitrinite observed by TEM was found to contain large regions of fine porosity. In Figure 4, a TEM photomicrograph of a vitrinite fragment in the splint coal, the pore sizes range from approximately 2 nm, to greater than 20 nm. The smallest pores, some of which may even be less than 2 nm, appear to be related to connecting channels or irregularly shaped pores that cannot be described as spherical. Stereo pairs of these vitrinite fragments indicate a connecting network of pores suggesting high permeability.

ILLINOIS NO. 6 COAL

The granular constituent shown in the Illinois No. 6 microstructure (Fig. 2) contains a broad range of interconnecting pores (~40–50 nm in dia.) which may be classified as predominantly macropores (<50 μm). The exact identity of this constituent is not clear, however, it is thought to be a mixture of inertinite and exinite. The microstructure of this coal is dominated by large vitrinite bands

(V) which are separated by the highly porous regions. Areas of apparently interconnected fine porosity can be observed in both vitrinite bands (see arrows). Also noteworthy in this microstructure are the opaque (OP) fragments that have been found to contain minerals. The opacity of the mineral regions may be due to a greater thickness of the face caused by the greater resistance minerals have to ion milling.

Figure 5 is a TEM photomicrograph of a region of vitrinite in the Illinois No. 6 coal obtained at higher magnification (50K) in order to perform a more detailed analysis of the porosity associated with this maceral. Pore dimensions range from approximately 1 to 10 nm which classifies them as a mixture of micropores (<2 μm) and mesopores (2–50 μm). The detection of porosity in the 2 dimensional image becomes more difficult as the specimen thickens. However, when viewed in 3 dimensions via a stereo pair, the porosity in the thicker regions remains clear. Three dimensional viewing also reveals that the porosity is irregularly shaped, and is often present as volumes of highly interconnecting pores. In regions of locally high porosity as is observed in the center of Fig. 5, the degree of interconnectivity is relatively great whereas in the surrounding region the pore volumes are largely isolated.

Several vitrinite fragments were found to contain bands of minerals, aligned parallel to the bedding plane of the coal (Fig. 6). Many of the minerals exhibit well developed growth habits. A size analysis of the minerals (5) by direct measurement from the TEM photomicrographs reveals that the majority of minerals were under 30 nm in diameter with the average diameter being approximately 10 nm. Larger mineral fragments up to 300 nm on an edge were recorded but comprised only a small fraction of the total observable mineral matter. Subsequent analyses of small angle x-ray scattering (6) (SAXS) from a similar sample of Illinois No. 6 coal showed a multimodal size distribution (Fig. 7) which essentially confirms the TEM observations. For example, the peak at 3 nm relates to the fine pores observed in the vitrinite component whereas the peak at 10 nm fits the average mineral diameter, and finally the peak at 25 nm accounts for the larger mineral fragment plus the larger pores observed in the granular constituent.

In addition to the microstructural studies of these two bituminous coals an effort was also made to do EDX analyses via STEM on microareas of the macerals in order to obtain data related to the composition of the coal macromolecule. However, typically, the observation of detectable elements (i.e., of atomic number 11, Na or greater) always correlated with the presence of minerals, except for sulfur. These observations, though limited, do suggest that chemical analyses of coal which report the existence of heavy metals (>Na) in coal macerals as part of the organic constituent may be suspect. As witnessed in Fig. 6, the size range for minerals can be exceedingly small, e.g. less than 2 nm in diameter thus their detection by standard techniques very improbable.

CONCLUSIONS

The shape and size of pores in two high volatile bituminous coals of differing lithotypes have been directly observed by means of transmission electron microscope (TEM). The distribution of the porosity with respect to their maceral associations were ascertained as were the sizes and distributions of the micro minerals. The use of stereo pairs reveals the interconnectivity of the pores in micro volumes of the macerals indicating a high degree of permeability within those regions.

The finest porosity was observed in vitrinite fragments of both coals and ranged in size from under 2 nm to 20 nm in diameter, with the majority in the smaller end of the size range. On the other hand, inertinite appears to be the most porous maceral and typically contains a broad range of pores from 5 through 50 nm. Much

of the inertinite is granular material varying from fine to coarse grained particles with the former corresponding to micrinite.

Finally, the least porous maceral is exinite which generally appears as a featureless material except for the presence of irregular and tubular pores thought to be initiated by the catalytic action of minerals. The intimate relationship between exinite and inertinite such as exists in durains, where the inertinite contains large amounts of fine mineral matter, may therefore promote the generation of porosity in exinites.

REFERENCES

1. L. A. Harris and C. S. Yust, *Fuel*, 55, 233 (1976).
2. L. A. Harris, D. N. Braski, and C. S. Yust, *Microstructural Science*, 5, 351 (1977).
3. G. R. Hennig, *J. Inorg. Nucl. Chem.*, 24, 1129 (1962).
4. S. P. Gan. H. Nandi and P. L. Walker, *Fuel*, 51, 272 (1972).
5. R. A. Strehlow, L. A. Harris and C. S. Yust, *Fuel*, 57, 185 (1978).
6. J. S. Lin, R. W. Hendricks, L. A. Harris, and C. S. Yust, *J. Appl. Cryst.*, in press, (1978).

By acceptance of this article, the publisher or recipient acknowledges the U.S. Government's right to retain a nonexclusive, royalty-free license in and to any copyright covering the article.

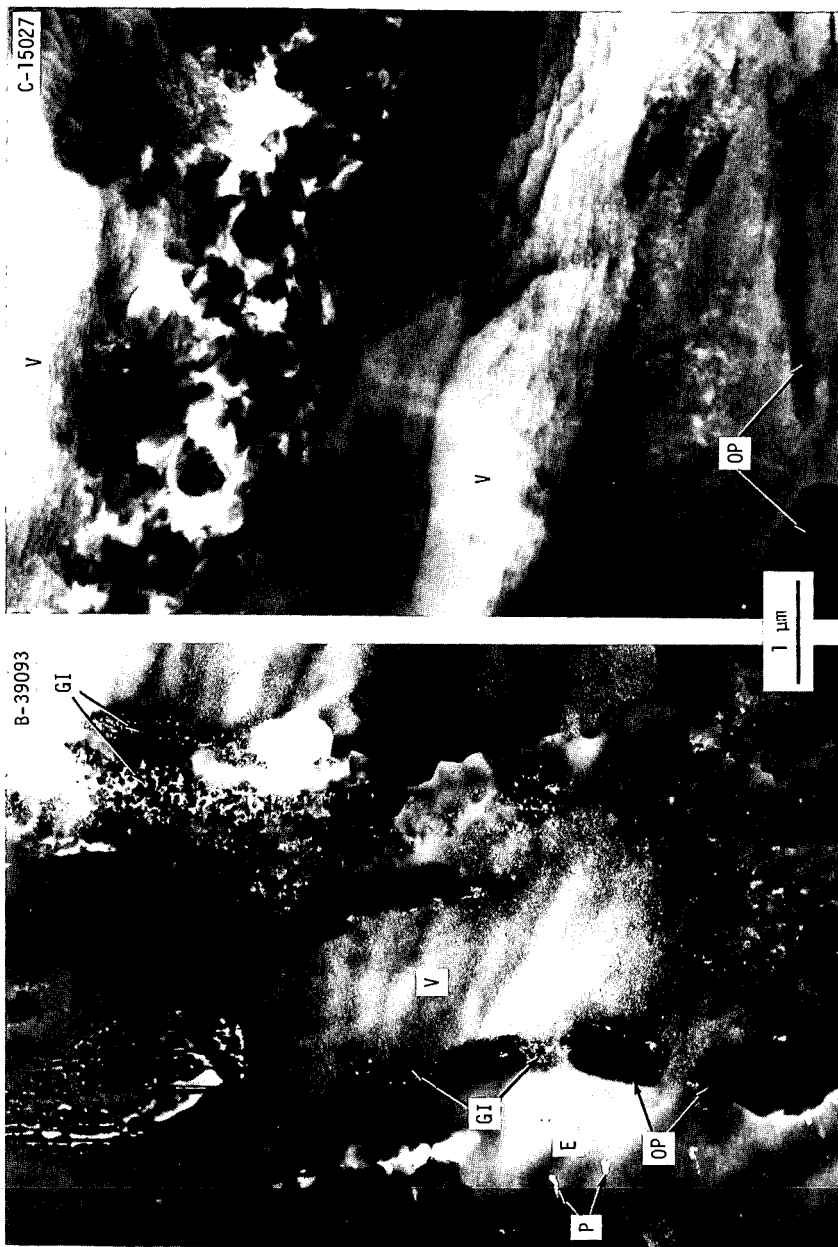


Fig. 1. TEM Splint Coal (Where E = Exinite, V = Vitrinite, GI = Granular Inertinite, OP = Opaque Particles, and P = Pores in Exinites).

Fig. 2. TEM of Illinois No. 6 Coal (Where V = Vitrinite and OP = Opaque Particles).

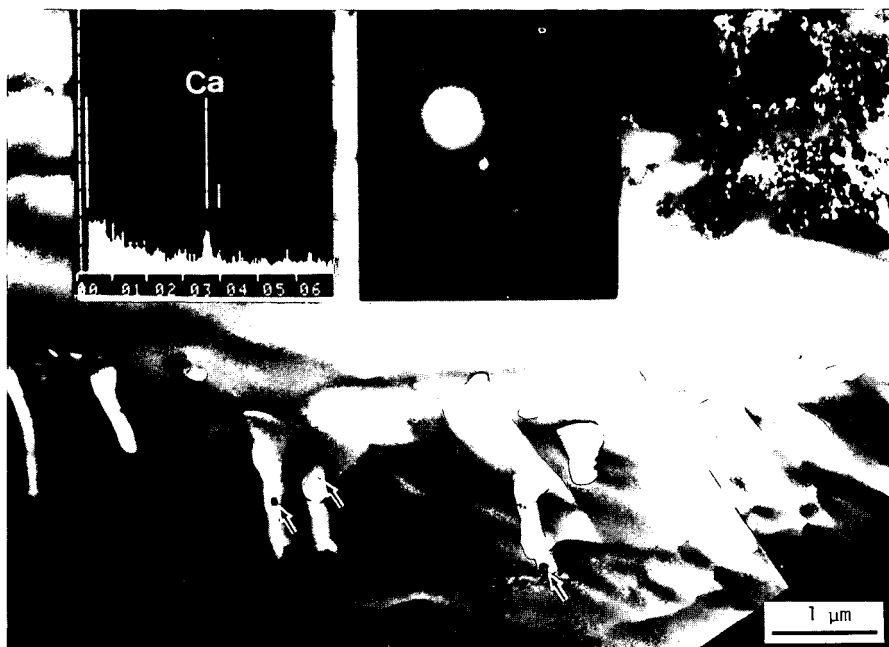


Fig. 3. TEM of Tubular and Irregular Pores in Exinite Showing the Location (See Arrows) and Identity (See Insets) of Spherical Particles.



Fig. 4. Fine Porosity Observed in Vitrinite Fragment in Splint Coal by TEM.

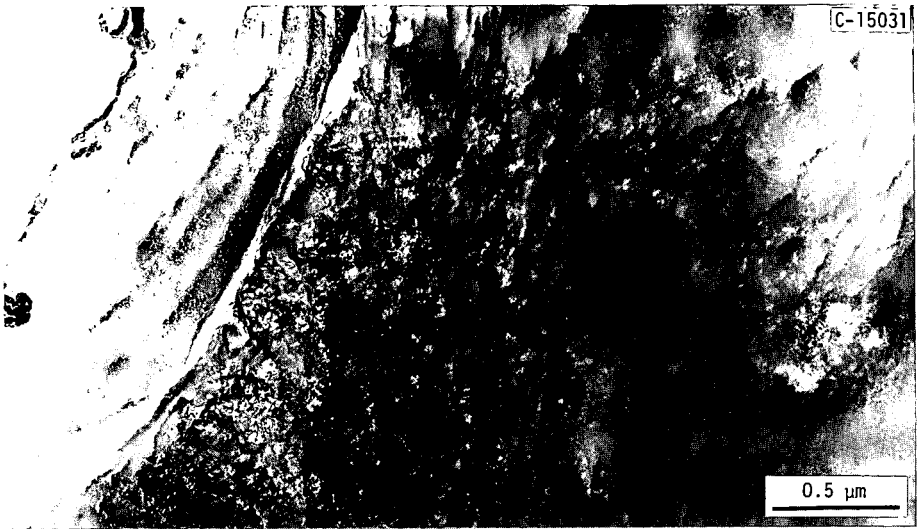


Fig. 5. Fine Porosity Observed in Vitrinite Fragment of Illinois No. 6 Coal by TEM.



Fig. 6. TEM of Vitrinite of Illinois No. 6 Showing Bands of Minerals.

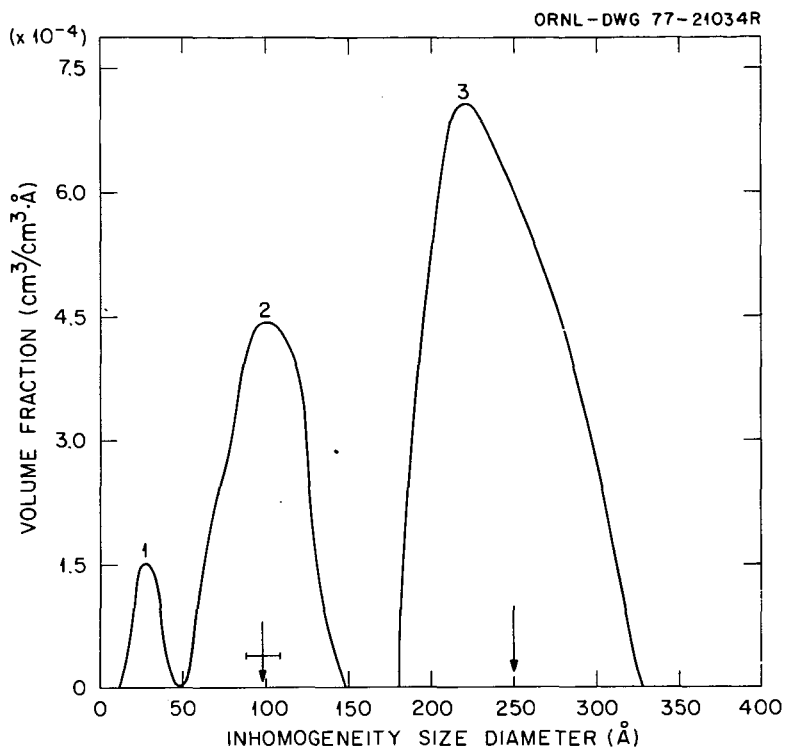


Fig. 7. The Size Distribution of Pores and Minerals from Vitrinite (Illinois No. 6) Obtained by Small Angle X-Ray Scattering (SAXS).

CHARACTERIZATION OF IRON BEARING MINERALS IN COAL

Pedro A. Montano

Department of Physics, West Virginia University, Morgantown, WV 26506

Introduction

Due to the importance of coal as a major source of energy and the environmental hazards involved in its use, considerable research has become necessary in order to a) fully understand the different compounds appearing in the coal and their transformation during processing; and b) know how those compounds contribute to the pollution of the environment, i.e., acidity of water streams near the coal mines and pollution by power plants. Some positive properties can be associated with the mineral matter in coal. For example, recently several researchers have shown that the mineral matter in the coal may play an important role in the liquefaction process (1). Of all the minerals in the coal, the iron bearing minerals seem to be the most important. In most coal utilization techniques the coal is used as raw material, and as a result both the organic and inorganic components may be critical in the acceptance or rejection of a coal for a particular process. Owing to the great importance of iron as a major constituent of the mineral matter in many coals the Moessbauer effect becomes a powerful tool in the characterization of the iron bearing minerals.

The most common use of the Moessbauer effect in mineralogy and geology has been the determination of the oxidation states of iron in various minerals (2). The study of the Moessbauer spectral area also gives valuable information on the concentration of the different minerals in rocks (2). Recently the Moessbauer effect was applied to the study of iron bearing minerals in coal and to determine the amount of pyritic sulfur (3,4,5).

In what follows the application of Moessbauer spectroscopy (^{57}Fe) to determine the iron bearing minerals will be described and a critical view of the advantages and disadvantages of the technique will be presented. In this study more than 200 coal samples were investigated and more than 2000 Moessbauer runs were carried out on those samples. Before going into the experimental results, a brief description of the Moessbauer parameters which give the necessary information to determine the compounds seems appropriate.

Moessbauer Parameters

Isomer Shift (IS): The shift observed in the Moessbauer lines with respect to zero velocity is produced by the electrostatic interaction of the nuclear and s-electrons charge distributions. It is given in the non-relativistic approximation by (6)

$$IS = \frac{2\pi}{5} ze^2 (R_{ex}^{-2} - R_{gd}^{-2}) \{ |\psi_{\text{abs}}(0)|^2 - |\psi_{\text{source}}(0)|^2 \} \quad 1)$$

The IS gives valuable and unique information on the valence states of iron, in special for high spin Fe^{2+} and Fe^{3+} .

Besides the IS there exists a shift of the Moessbauer lines due to the second order Doppler effect (7). This shift is given by

$$\delta E_{\text{SODS}} = \frac{E_0}{2} \frac{\langle v^2 \rangle_T}{c^2} \quad 2)$$

where $\langle v^2 \rangle_T$ is the thermal average of the square of the velocity of the Moessbauer atom in the solid. It is a parameter that strongly depends on the lattice dynamical properties of the solid.

The hyperfine interactions affecting the Moessbauer effect are the quadrupole and magnetic interactions (2). The quadrupole interaction exists when the electrons and/or the neighboring atoms produce an inhomogeneous electric field at the nucleus, and when the nucleus possesses a quadrupole moment, Q . This interaction produces a splitting of the Moessbauer lines for ^{57}Fe given by (2)

$$\Delta E_Q = \frac{1}{2} e^2 q Q (1 + \eta^2/3)^{1/2} \quad 3)$$

where q is the electric field gradient, and η the asymmetry parameter. When q arises from the electrons of the Moessbauer atom, the temperature dependence of the QS is very pronounced, like in high spin Fe^{2+} compounds. This temperature dependence is very useful in the identification of the electronic ground state of the ion.

The hyperfine magnetic interaction arises from the interaction of the nuclear magnetic dipole moment with a magnetic field due to the atom's own electrons. In many cases Moessbauer studies at low temperatures are necessary to fully characterize a compound. In such cases one usually applies an external magnetic field. This technique is particularly useful for the study of the electronic ground state of iron ions in minerals (8,9).

A very important Moessbauer parameter is the Debye-Waller factor (DWF). The DWF depends on the temperature and is given in the harmonic approximation by (2)

$$\text{DWF} = \exp(-k^2 \langle x^2 \rangle_T) \quad 4)$$

where $\langle x^2 \rangle_T$ is the mean square displacement of the atom along the direction of the γ -ray emission. The DWF is frequently evaluated in Moessbauer spectroscopy using an effective Debye model. The DWF can be different for the same compound if the particle size is very small. One has to be aware of this problem when using the Moessbauer effect as a quantitative analytical tool.

The Moessbauer effect can be used not only for the identification of mineral species, but also for a quantitative analysis of the mineral contents. The Moessbauer spectral area is given for a single line source and absorber by (10)

$$A = p^{-1} f_s \Gamma_a \frac{\pi}{2} \sum_{n=1}^{\infty} \frac{(-1)^{n+1}}{n!} \frac{(2n-3)}{(2n-2)!} t^n \quad 5)$$

$p = 1 - B/N(\infty)$

$t = n \frac{\sigma_a f_a}{\Gamma_a}$

where B = background (non-Moessbauer radiation); $N(\infty)$ = counting rate at infinity velocity; Γ_a = full width of half-height of the absorption line; $f_s f_a$ = DWF of absorber and source; σ_a = absorption cross-section at resonance; n_a = number of Moessbauer atoms per square centimeter. The above formula has to be corrected for lines splitted by hyperfine interactions (11). When using the Moessbauer effect as a quantitative analytical tool, care must be taken that B , f_s and f_a are known. A discussion on the quantitative method of analysis will be given at the end of the paper.

Experimental Procedures

The coal samples used in this work were collected following strictly ASTM procedure D2013-72. The samples were mounted in lucite containers that were hermetically sealed. Pressed pellets of the grinded coal were also used as samples. The average surface densities of the samples used were between 150 to 300 mg/cm². Several samples from the same seam were analyzed in order to check for consistency of the results. Some runs were carried out on raw coals (not grinded) as well, for testing purposes. The bulk of the samples used in this study were from West Virginia coals. The Moessbauer spectrometer used in this work was a conventional constant acceleration spectrometer. A 50mC ⁵⁷Co:Pd source was used. The Moessbauer spectra were analyzed using a non-linear least-square fit program and assuming Lorentzian lineshapes. The measurements covered a wide temperature range. Many runs were carried out at low temperatures (4.2 K) and in the presence of an external magnetic field (40 kOe). The velocity calibration is given with respect to α -Fe at room temperature (RT).

Experimental Results and Discussion

The different iron bearing minerals detected in coal using Moessbauer spectroscopy are classified below according to their major groups, i.e., sulfides, clays, carbonates, and sulfates.

Sulfides: Iron disulfide (pyrite) is the most important of the iron bearing minerals in coal. In pyrite the iron ion is in the low spin configuration, Fe^{II}. The six d-electrons are occupying the T_{2g} ground state and no magnetic moment is present at the iron site (8). In pyrite^{2g} each cation has a distorted octahedral coordination of six nearest neighbors sulfur, the octahedron being slightly compressed along one of the axis. Consequently, the crystalline field at the iron site is lower than cubic and an electric field gradient exists at the ⁵⁷Fe nucleus, producing a characteristic QS in the Moessbauer spectrum.

There is a metastable phase of FeS₂, marcasite, which is the orthorhombic dimorph of pyrite and appears also in several coals. Marcasite has slightly different IS and QS (Table 1). When the amount of marcasite in coal is more than 20% of the total iron disulfide content its detection using Moessbauer spectroscopy is possible. In general, petrographical techniques seem to be more appropriate for identification of marcasite (at least for qualitative measurements). In table 1 a list of the different iron sulfides and their respective Moessbauer parameters is given.

A typical spectrum of a coal is given in figure 1. The sample has been treated with HCl (following ASTM standard D-2492) to get rid of the non-pyritic iron (sulfates). The spectrum is typical of pyrite. All the ca. 2000 spectra run in this work show the presence of pyrite (contents ranging between 7 to 0.1%). While studying several coal macerals a new Moessbauer spectrum associated with pyrite was observed in three different samples (9) rich in frambooidal pyrite. The extra Moessbauer doublet showed the same magnetic behavior as pyrite (low spin). However, its Moessbauer parameters are different and the IS suggests a smaller electronic density at the nucleus than for FeS₂. The low temperature measurements indicate that the spectrum cannot be associated with any of the other minerals. It is possible that this phase is highly disordered (or "amorphous") FeS₂.

Other iron sulfides are produced during coal processing. They are mainly pyrrhotites. For compositions varying between FeS (troilite) and Fe₇S₈ (monoclinic pyrrhotite), the compounds are referred to generally as pyrrhotites (12). The Moessbauer spectrum of iron pyrrhotites can be observed in the coal liquefaction

mineral residue. The study of these pyrrhotites is of considerable importance due to their potential use as disposable catalysts in coal liquefaction (1). It is to be noted that the presence of pyrrhotites was observed in some severely "weathered" coal. In studies carried out under a reducing hydrogen atmosphere (between RT and 400°C) the conversion of all the pyrite to pyrrhotites was observed.

Clay minerals: Clay minerals represent a large percentage of the inorganic mineral content in coal. Illite, kaolinite and mixed clays are the major clay minerals present in coal. The crystal structures of the clay minerals are basically derived from two types of sheets. A tetrahedral sheet typically made of SiO_4 units, and an octahedral sheet typically made of $\text{Al}(\text{O}, \text{OH})_6$ units (13). The ideal formula, i.e., for kaolinite is $\text{Al}_2^{3+}\text{Si}_2^4\text{O}_5^{2-}(\text{OH})_4$, but as in all clay minerals, a certain amount of cation substitution is possible. In mica and its derived clay minerals, illites, the octahedral sheet contains only Al^{3+} , but in the tetrahedral sites one quarter of the Si^{4+} is replaced by Al^{3+} . The net negative charge of the layer is balanced by interlayer alkali cations which also bond the layers together. The interlayer in montmorillonite or vermiculite is occupied by H_2O and/or cations, whereas in chlorite there is a complete sheet of aluminum (magnesium) hydroxide, the brucite sheet. Continuous ranges of chemical composition are often possible between the different clays and there is a great variety of mixed layer structures. Iron can be substituted in the octahedral layer in its high-spin ferrous and ferric forms, and occasionally in the tetrahedral layer. However, the iron concentration in clays is relatively small (a few % by weight) for kaolinite and illite, the most frequently found clays in coal (14).

In general the clays appearing in the coal show slightly different Moessbauer parameters than pure clays. The usual method utilized to identify the clay minerals in coal is X-ray diffraction of the LTA, but due to the poor crystallinity of the clays in the coal the technique cannot be used for quantitative measurements. The Moessbauer effect is not much of an improvement due to the small iron content of the clays. A coal rich in clays is shown in figure 2 (about 10% mineral matter). The appearance of two peaks at higher velocity is not due to the presence of two sites in the clay or to two different clays, it is produced by szomolnokite. By treating the sample with HCl, the sulfate was washed away and the clay (possibly illite) could be clearly seen (Figure 3). Treating the coal with HNO_3 dissolves the pyritic iron and the spectrum of the clays can be detected more clearly. Figure 4 shows the Pittsburgh coal (230 mesh) shown in Fig. 1 after treatment with HNO_3 . The spectrum (notice the smaller effect) is identified as that of kaolinite (a small QS is detectable).

In general, to study the clays in coal one should treat the samples as described above, or run the experiments at low temperatures in order to resolve the overlapping lines (measurements in an external magnetic field become necessary) (8,9). Moessbauer parameters for the principal clay minerals, pure and as they appear in coal, are given in table 1.

Sulfates: The iron sulfates were detected in more than 90% of the coal samples studied. The sulfates are considered to be produced by "weathering" of the coal. The amounts detected in this study ranged from 0.2 to 0.005% of total weight.

The standard technique used for detection of sulfates is X-ray diffraction of the LTA. Nevertheless, we have observed that in some cases sulfates are present in the coal and the X-ray does not show any line attributable to them (15). The most abundant divalent iron sulfate observed in the coals studied is $\text{FeSO}_4 \cdot \text{H}_2\text{O}$ (szomolnokite), a monoclinic crystal with a tetramolecular unit cell (16). This compound

orders antiferromagnetically around 10K with an effective interval field of 359 kOe (9). Other sulfate minerals found less frequently are $\text{FeSO}_4 \cdot 4\text{H}_2\text{O}$ (rozenite), and $\text{FeSO}_4 \cdot 7\text{H}_2\text{O}$ (melanterite); anhydrous ferrous sulfate was detected when the coal was stored under vacuum. The ferric sulfates commonly observed in several coals are coquimbite and jarosites.

A word of caution concerning the presence of trivalent sulfates in the coal is appropriate here. These sulfates have in general lines which overlap with the Moessbauer pyrite lines. The result is the detection of a slightly asymmetric pyrite spectrum. If one treats the samples with HCl it will appear as if some of the pyrite has dissolved in HCl, but this is of course not true, and is the result of the presence of the iron sulfates. The ferric sulfates are easily distinguishable from pyrite. When Moessbauer measurements are carried out at 4.2K in the presence of a large external field, the characteristic hyperfine field of Fe^{3+} is detected (about 500 kOe). It was observed also that many of the ferric sulfates are formed during LTA (3).

In figure 5 a Moessbauer spectrum for a mixture of szomolnokite (A) and rozenite (B) is shown. The sample was characterized by X-ray diffraction as well as Moessbauer spectroscopy. After LTA (17) the Moessbauer spectrum shows the presence of szomolnokite (no rozenite) and ferric sulfate. This was observed for all the runs carried on the coal samples studied. In table 1 a list of the iron sulfates and their respective Moessbauer parameters is given.

Carbonates: The Moessbauer spectra of some of the coal samples show the presence of FeCO_3 (siderite). Siderite has a rhombohedral structure with an octahedron of oxygens around the iron with a small trigonal distortion along the c-axis. Siderite is magnetically ordered at low temperatures ($T_N = 38\text{K}$) with a very distinctive Moessbauer spectrum (18). During the study it was observed on several occasions that a Moessbauer spectrum appeared to be that of FeCO_3 ; however, by carrying out low temperature measurements the presence of either clay or ankerite was inferred. Ankerite $[\text{Ca}(\text{FeMg})(\text{CO}_3)_2]$ is another carbonate that appears in some coals. It is nearly impossible to distinguish ankerite from siderite using Moessbauer spectroscopy at room temperature (RT). One has to carry out low temperature measurements. In table 1 the relevant Moessbauer parameters are given for the iron carbonates observed in coal. In all the measurements no more than 0.1% siderite by weight was detected.

Other minerals: In this work no other minerals were detected using Moessbauer spectroscopy, except the ones mentioned above. However, in heavily weathered coals and coal refuse the presence of iron oxides (hematite and to a lesser extent magnetite) were observed. Pyrrhotite was also detectable in some of the heavily weathered coals. Other minerals like spharelite, chalcopyrite and arsenopyrite were not detectable in these experiments. Some of the latter minerals have been identified using scanning electron microscopy, but their presence in the coal is too small to make their contribution to the Moessbauer spectrum significant. Other sulfides like Fe_3S_4 or Fe_2S_3 (19) were not detectable in any of the samples at RT or 4.2K. No evidence of organically bound iron in coal was found for all the studied samples (20).

Moessbauer Spectroscopy as a Tool for Quantitative Determination of Pyritic Sulfur

The use of Moessbauer spectroscopy to determine the amount of iron in a sample presents several serious problems to the experimentalist. One has to know the Debye-Waller factor of pyrite and the background radiation accurately. The DWF of FeS_2 can be determined from the temperature dependence of the spectral area for pure crystals of known thicknesses. However, in many coals pyrite is highly dispersed

and form very small particles which have low crystallinity; consequently, the DWF might differ considerably from that of large FeS_2 crystals. Also, a very important source of error is the determination of the non-resonant radiation background. In all the runs carried out in this study it was observed that variations of 10 to 30% occur in background counting rates for samples of coals with the same weight per unit area. The differences are due to the heterogeneity of the mineral composition of the coals. Both photoelectric scattering (mainly by the 14.4 keV) and Compton scattering of the high energy γ -rays contribute to the background radiation. This, of course, indicates that a full analysis of the γ -ray spectrum for each sample is necessary. Any use of standards to determine the amount of pyritic sulfur will have to take into consideration the problems mentioned above (5). The use of Moessbauer spectroscopy for quantitative analysis has to go hand in hand with the standard chemical procedures (ASTM D 2492-68), as a *complementary technique and not as a substitute*. In general, the most accurate Moessbauer quantitative measurement will give an error of about 10%.

Conclusions

The Moessbauer effect has been used as an analytical tool to characterize the different iron bearing minerals in coal. It has been pointed out that by the use of low temperature measurements (in the presence of a large external magnetic field) and treatment of the coal samples all the iron bearing minerals can be correctly identified. The use of Moessbauer spectroscopy as a quantitative analytical tool presents several experimental difficulties. It is recommended that this spectroscopy be used as a *complement* to and not as a substitute for the standard techniques.

Acknowledgements

The author thanks Drs. A.H. Stiller and J.J. Renton of the West Virginia Geological Survey for their invaluable help in carrying out this investigation. The technical assistant of William Dyson in some of the measurements is gratefully acknowledged.

References

1. Thomas, M.G., Granoff, B., Baca, P.M., and Noles G.T., 1978. Division of Fuel Chemistry, American Chemical Society, 23(1):23.
2. Bancroft, G.M., 1973. Moessbauer Spectroscopy: An Introduction for Inorganic Chemists and Geochemists. New York: John Wiley.
3. Montano, P.A., 1977. Fuel 56:397.
4. Levinson, L.M., and Jacobs, I.S., 1977. Fuel 56:453.
5. Huffman, G.P., and Higgins, F.E., in press. Fuel.
6. Kistner, O.C., and Sunyar, A.W., 1960. Phys. Rev. Letters 4:412.
7. Pound, R.V., and Rebka, G.A., Jr., 1960. Phys. Rev. Letters 4:274; Josephson, B.D., 1960. Phys. Rev. Letters 4:342.
8. Montano, P.A., and Seehra, M.S., 1976. Solid State Communications 20:897.

9. Russell, P., and Montano, P.A., 1978. *Journal of Applied Physics*. 49(3):1573; 49(8):4615.
10. Lang, G., 1963. *Nucl. Instr. Methods* 24:425.
11. Housley, R.M., Grant, R.W., and Gonser, V., 1969. *Phys. Rev.* 178:514.
12. Power, L.F., and Fine, H.A., 1976. *Minerals Sci. Engng.* 8:106.
13. Millot, G., 1970. *Geologie des Argiles*. Paris: Masson.
14. Rao, C. Prasada, and Gluskoter, J. Harold, 1973. *Illinois State Geological Survey, Circular* 476.
15. Stiller, A.H., Renton, J.J., Montano, P.A., and Russell, P.E., 1978. *Fuel* 57:447.
16. Pistorius, C.W.F.T., 1960. *Bull. Soc. Chim. Belg.* 69:570.
17. The LTA was carried out by J.J. Renton at the West Virginia Geological Survey.
18. Ono, K., and Ito, A., 1964. *Journal of the Phys. Soc. of Japan* 19:899.
19. Schrader, R., and Pietzsch C., 1969. *Kristall und Technik* 4:385; Stiller, A.H., McCormick, B., Jack, Russell P., and Montano, P.A., 1978. *Journal of the American Chem. Soc.* 100:2553.
20. Lefelhocz, J.F., Friedel R.A., and Kohman, T.P., 1967. *Geochim. Cosmochim. Acta* 31:2261.
21. Thiel, R.C., and van den Berg, C.B., 1968. *Phys. Stat. Sol.* 29:837.
22. Goncharov, G.N., Ostonevich, Yu. M., Tomilov, S.B., and Cser, L., 1970. *Phys. Stat. Sol.* 37:141; Novikov, G.V., Egorov, V.K., Popov, V.I., and Sipavina, L.V., 1977. *Phys. Chem. Minerals* 1:1; Gosselin, J.R., Townsend, M.G., Tremblay, R.J., and Webster, A.H., 1976. *Solid State Chem.* 17:43.
23. Vaughan, D.J., and Ridout, M.S., 1971. *J. Inorg. Nucl. Chem.* 33:741.
24. Jefferson, D.A., Tricker, M.J., and Winterbottom, A.P., 1975. *Clays and Clay Minerals* 23:355.
25. Coey, J.M.D., 1975. *Proc. Int. Conf. on Moessbauer Spectroscopy* 333, Cracow.
26. Vertes, A., and Zsoldos, B., 1970. *Acta Chim. Acad. Sci. Hung.* 65:261.
27. Greenwood, N.N., and Gibb, T.C., 1971. *Moessbauer Spectroscopy*. London: Chapman and Hall, Ltd.
28. Hryniewicz, A.Z., Kubisz, J., and Kulgawczuk, D.S., 1965. *J. Inorg. Nucl. Chem.* 27:2513.

TABLE 1. MOESSBAUER PARAMETERS OF MAJOR IRON BEARING MINERALS AT RT.

Name	IS (mm/sec)	QS (mm/sec)	Magnetic Hyperfine Field (kOe)	Ref.
SULFIDES:				
Pyrite (FeS ₂)	0.32(2)	0.63(2)	0	*
Marcasite (FeS)	0.28(2)	0.59(2)	0	*
Troilite (FeS)	0.77(4)	0.28	310	(21)
Pyrrhotite (FeS _{1+x}) (1<x<0.143)	0.64 - 0.69	-0.14 - 0.32	243 - 310	(22)
	0.70	0.30	322	
Greigite (Fe ₃ S ₄)	0.40 (4.2K)	0	486 (4.2K)	(23)
	0.45	0.4	465	
Fe ₂ S ₃	0.35(6)	0.82(6)		
	0.51(12)	0.88(12)	253 (4.2K)	(19)
Sphalerite (Zn, Fe)S	0.30(2)	0.61(2)	0	*
CLAYS:				
Kaolinite	0.30	0.59	492 (4.2K)	(22)
Chamosite	0.38(5)	0.78(8)		(25)
	1.14(6)	2.57(8)		
Fayalite	1.17(6)	2.85(8)		*
	0.99(7)	1.72(10)		
Montmorillonite	0.38(8)	0.50(13)		(25)
	1.15(6)	2.81(6)		
Muskovite	0.37(5)	0.75(8)	40 (4.2K)	*
	1.17(3)	3.08(7)	500	
	0.36(5)	0.52(12)		
Glaucanite	0.38(3)	1.21(5)		(25)
	1.14(6)	2.30(6)		
Chlorite	0.17(6)	0.78(8)	505 (4.2K)	*
	1.13(4)	2.67(6)	20	
	0.34(3)	0.43(4)	0	
Illite #36 (Morris)	1.24(5)	2.60(6)	20 - 30 (4.2K)	*
	1.27(3)	1.92(4)	0	
	0.28(6)	0.60(8)		
Illite #35 (Fitchian)	1.14(7)	2.77(7)	20 - 30 (4.2K)	*
	1.25(8)	2.54(8)		
	0.25(4)	0.58(6)		
Illite #35 (Fitchian) after treatment with HNO ₃	1.05(4)	2.73(6)		*
	1.20(5)	2.51(6)		

TABLE 1. (Cont.)

Name	IS (mm/sec)	QS (mm/sec)	Magnetic Hyperfine Field (kOe)	Ref.
Illite (Coal)	0.3 - 0.4	0.4 - 0.5	≈ 0	*
	1.1 - 1.2	2.6 - 2.8	15	
SULFATES:				
FeSO ₄	1.28(2)	2.90(2)	185 (4.2K)	*
Szomolnokite (FeSO ₄ ·H ₂ O)	1.18(2)	2.69(2)	359 (4.2K)	(9)
Rozenite (FeSO ₄ ·4H ₂ O)	1.32(4)	3.17(4)		* (26)
Melanterite (FeSO ₄ ·7H ₂ O)	1.31	3.20		(26)
Coquimbite	0.39(3)	0.60(5)	550 (4.2K)	* (27)
Jarosites	0.43(2)	1.1 - 1.2	470 - 480 (4.2K)	* (28)
CARBONATES:				
Siderite (FeCO ₃)	1.24(2)	1.87(10)	184 (4.2K)	(18)

(*) This work

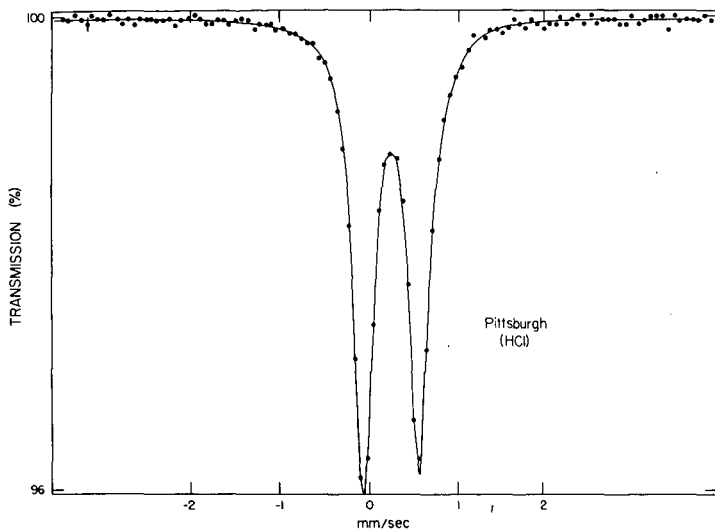


FIGURE 1. Moessbauer spectrum of a Pittsburgh coal (RT) after treatment with HCl.

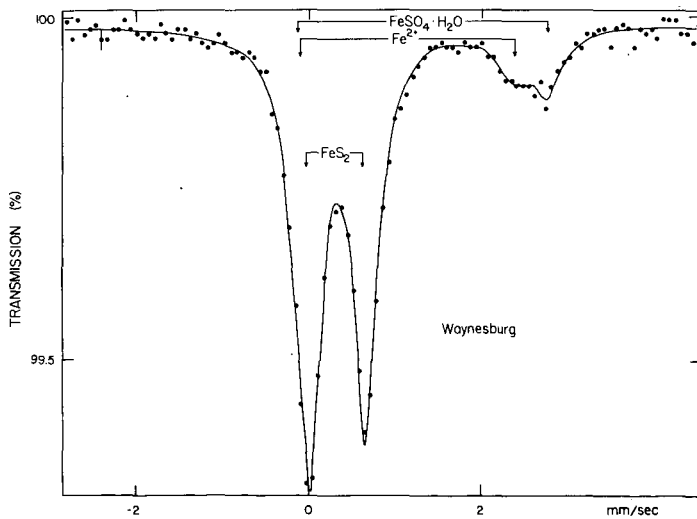


FIGURE 2. Moessbauer spectrum of a Waynesburg coal

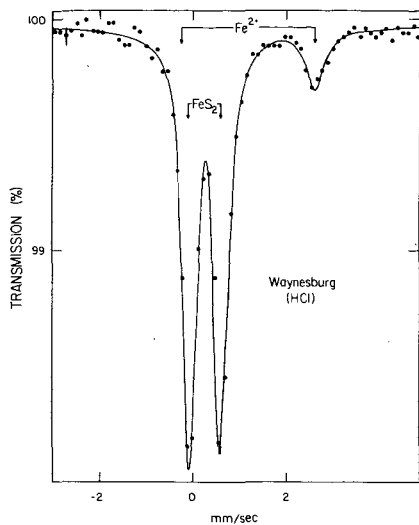


FIGURE 3. Waynesburg coal after treatment with HCl (RT).

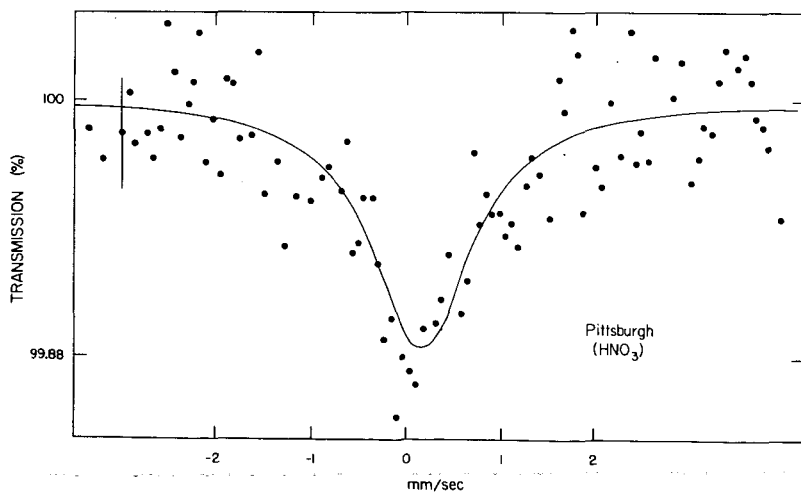


FIGURE 4. Pittsburgh coal (Fig. 1) after treatment with HNO₃

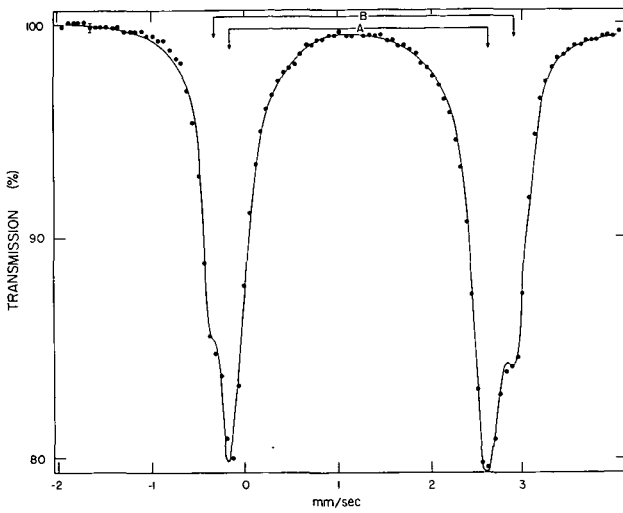


FIGURE 5. Moessbauer spectrum of szomolnokite and rozenite (RT).

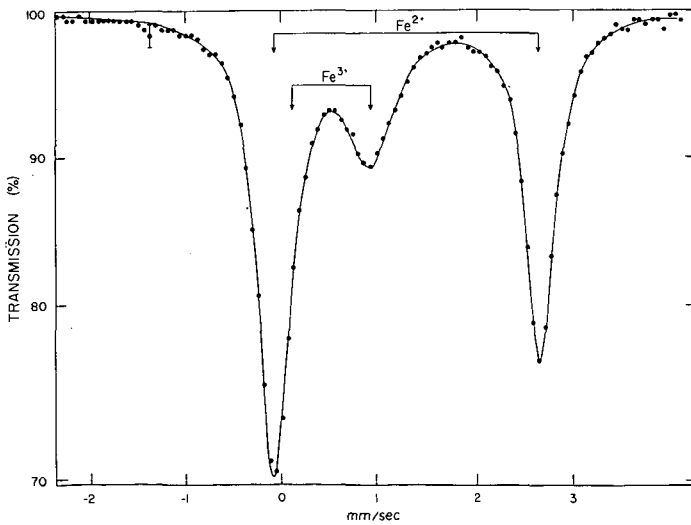


FIGURE 6. Moessbauer spectrum after LTA.

Geologic controls on element concentrations
in
the Upper Freeport coal bed

C. B. Cecil, R. W. Stanton, S. D. Allshouse, R. B. Finkelman,
and L. P. Greenland

U.S. Geological Survey, National Center, Reston, VA 22092

Introduction

The primary objective of this investigation was to determine the geologic controls on variations of mineral matter in the Upper Freeport coal bed near Homer City, Pa. (fig. 1). Mineral matter consists of the inorganic constituents of coal, including mineral phases and elements other than organically bound hydrogen, oxygen, nitrogen, and sulfur [1]. By this definition, organic sulfur is not part of the mineral matter; however, variations of all sulfur forms including organic sulfur were considered in this study.

The concentrations of 70 elements were determined on 75 bench-channel and 21 complete bed-channel samples from two deep mines in the study area (fig. 2). Ultimate, proximate, sulfur forms, maceral, and pyrite morphological analyses were also conducted on these samples. Scanning electron microscope [2] and electron microprobe [3] analyses were conducted on selected channel and column samples to determine element-mineral and maceral associations.

Results

The Upper Freeport coal bed of the Homer City study area is divisible in the field into five zones (fig. 3). In the northern part of the area where all five zones are present, the coal bed averages 83 inches (211 cm) in thickness; in the southern part where only three zones are present, the coal bed averages 48 inches (122 cm) in thickness. Laboratory analyses show that each of the five zones consists of distinct mineral matter-maceral associations. Elements that tend to be concentrated in the upper and/or basal zones of the bed include As, Cd, Cl, Fe, Hg, Mn, Pb, Se, S, and Zn.

Linear regression analysis was used to determine relationships among elements, sulfur (total, pyritic, and organic), ash, and maceral concentrations on the 75 bench-channel samples. On the basis of this statistical analysis, element concentrations in the coal can be related to three variables: ash, pyritic sulfur, and calcium (reported as CaO). The elements (some of which are reported as oxides) that positively correlate with each of the three variables are shown in figure 4. Only manganese is positively correlated with all three variables. The fusinite-semifusinite maceral concentrations correlate with the ash content.

Discussion

The mineral-matter content of the Upper Freeport coal bed of the Homer City area was controlled by interrelated geologic, geochemical, and paleobotanical variables. The elements that positively correlate with the ash (fig. 4) probably accumulated contemporaneously with the peat. Possible sources include: 1) mineral matter incorporated by plants, or 2) detrital minerals and dissolved elements incorporated during the peat stage of coal formation. Element concentrations resulting from mixed sources such as deposition of detrital minerals, sorption of dissolved ionic species, and mineral matter of plant origin would not lead to a strongly interrelated assemblage. Fusinite and semifusinite are generally believed to be the coalified products of partially oxidized peat and plant material. Oxidation results in a loss of organic matter and a concentration of residual mineral matter;

therefore, as the fusinite-semifusinite content of the coal increases, the ash and statistically related element contents also increase. Plant inorganic matter must be the major source of the ash-related elements. This interpretation is consistent with 1) the moderate ash content (8-15%), 2) the positive correlation between ash and fusinite-semifusinite content, and 3) the element-ash correlations illustrated in figure 4.

The calcium in the coal bed is primarily in authigenic calcite. Fixation of the calcium in the peat by ion exchange and/or as calcium salts of humic acids with subsequent liberation of CO₂ and organically bound calcium during coalification may have resulted in the formation of calcite in macerals and cleats. The buffering effect of calcium carbonate species supplied to the ancestral peat partially controlled the pH. Sulfate-reducing bacterial activity is greatest at neutral pH and minimal or nonexistent at pH 4.0 or less [4]. Therefore, pH values near neutral favor 1) bacterial generation of sulfide species if sulfate ions are present, 2) bacterial degradation of peat that could result in the concentration of mineral matter, and 3) retention of mineral matter because of decreasing solubilities as pH increases.

Low pH (<4.0) would favor a low-ash (<8%), low-sulfur (<1%) coal. Partial neutralization of waters of the ancestral peat of the Upper Freeport coal is indirectly indicated by the presence of 1) calcite in coal macerals and cleats and 2) mixed carbonate and clastic sediments directly under the coal bed. The Upper Freeport coal studied is a medium ash (8-15%), medium sulfur (1-3%) coal that is consistent with partial neutralization of peat waters.

The pyrite in the Upper Freeport coal is usually concentrated in the upper and/or basal zones of the bed throughout the area. Genetically, pyrite and the associated trace elements As and Hg appear unrelated to the bulk of the coal ash. Although pH conditions were suitable for pyrite deposition, pyrite concentrations were controlled by the availability of ferrous iron and appropriate sulfur species.

Summary

The elements in the Upper Freeport coal bed of the area can be genetically related to three variables (i.e., ash content, pyritic sulfur content, and calcium content). The buffering effect of dissolved calcium carbonate species may have been sufficient to maintain a pH of 4 or greater. Under these pH conditions, sulfate-reducing bacteria generated sulfide species, which reacted to form minerals such as pyrite, sphalerite, chalcocopyrite, and galena. During coalification, the calcium salts of humic acids decomposed to form calcite and carbon compounds that may account for the calcite in coal macerals and cleats. The pH conditions that existed during peat formation were conducive to the retention of mineral matter, the bulk of which was of plant origin.

References

- [1] C. P. Rao, and H. J. Gluskoter, Occurrence and distribution of minerals in Illinois coals. Illinois Geol. Survey Cir. 476 (1973).
- [2] R. B. Finkelman, R. W. Stanton, C. B. Cecil and J. A. Minkin, Modes of occurrence of selected trace elements in several Appalachian coals, (1979), this session.
- [3] J. A. Minkin, E. C. T. Chao and C. T. Thompson, Distribution of elements in coal macerals and minerals: determination by electron microprobe, (1979), this session.
- [4] J. E. Zajic, Microbial biogeochemistry, Academic Press (1969).

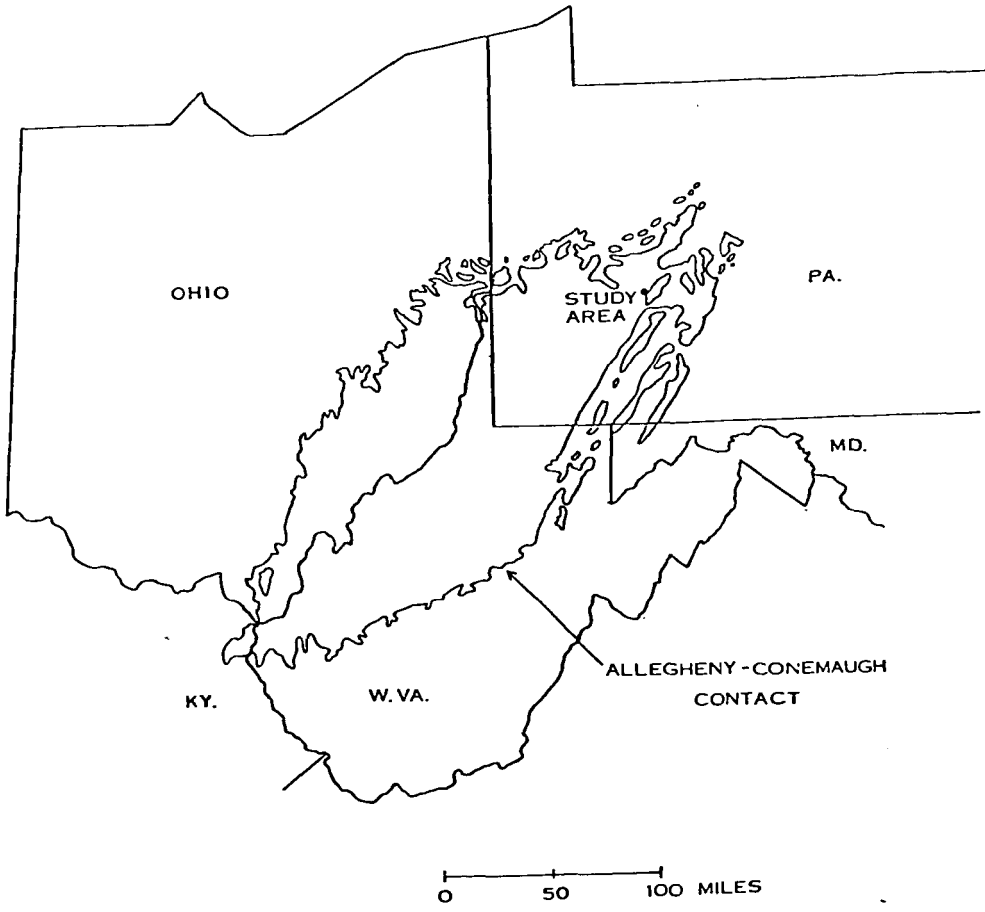
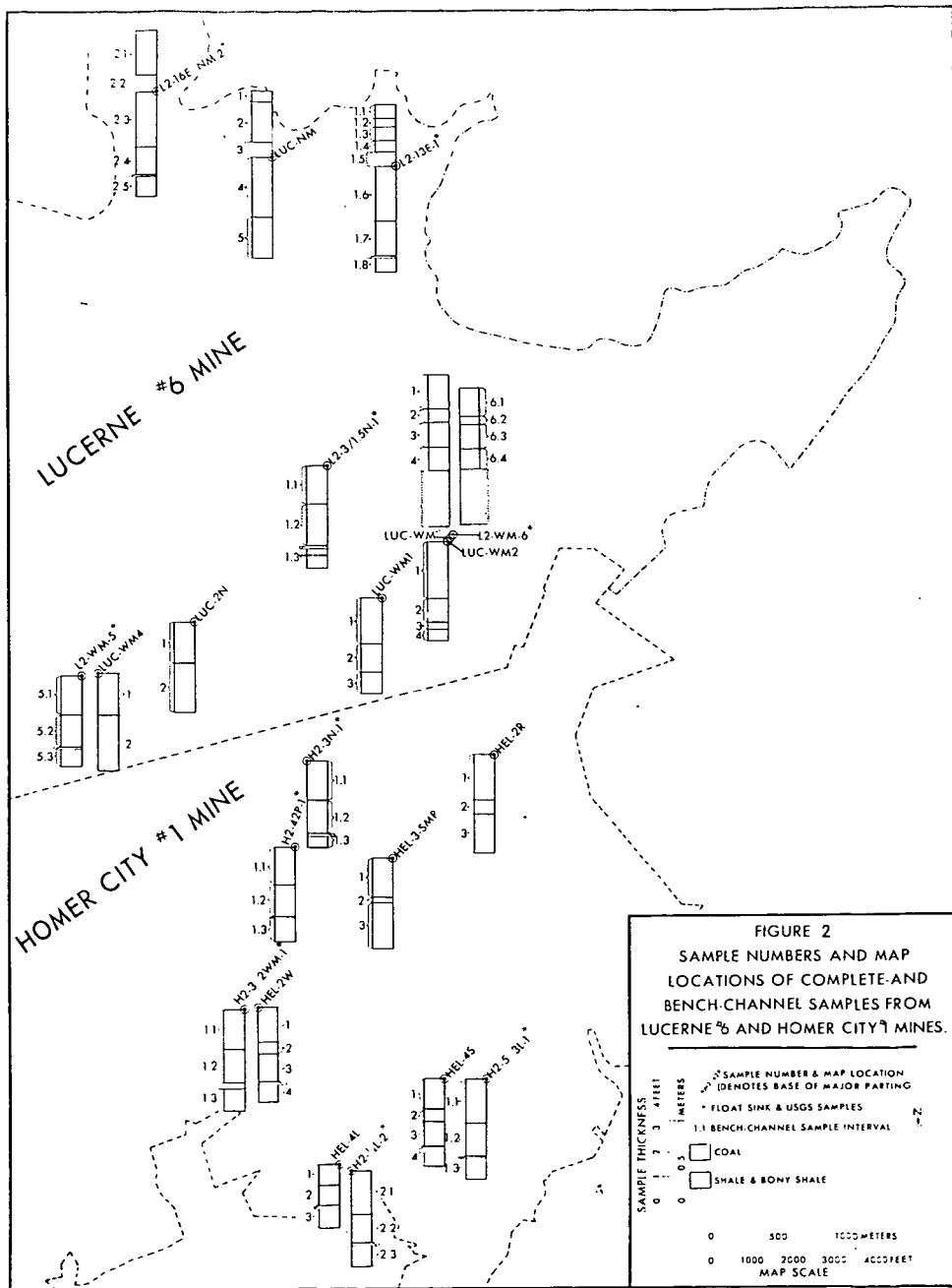
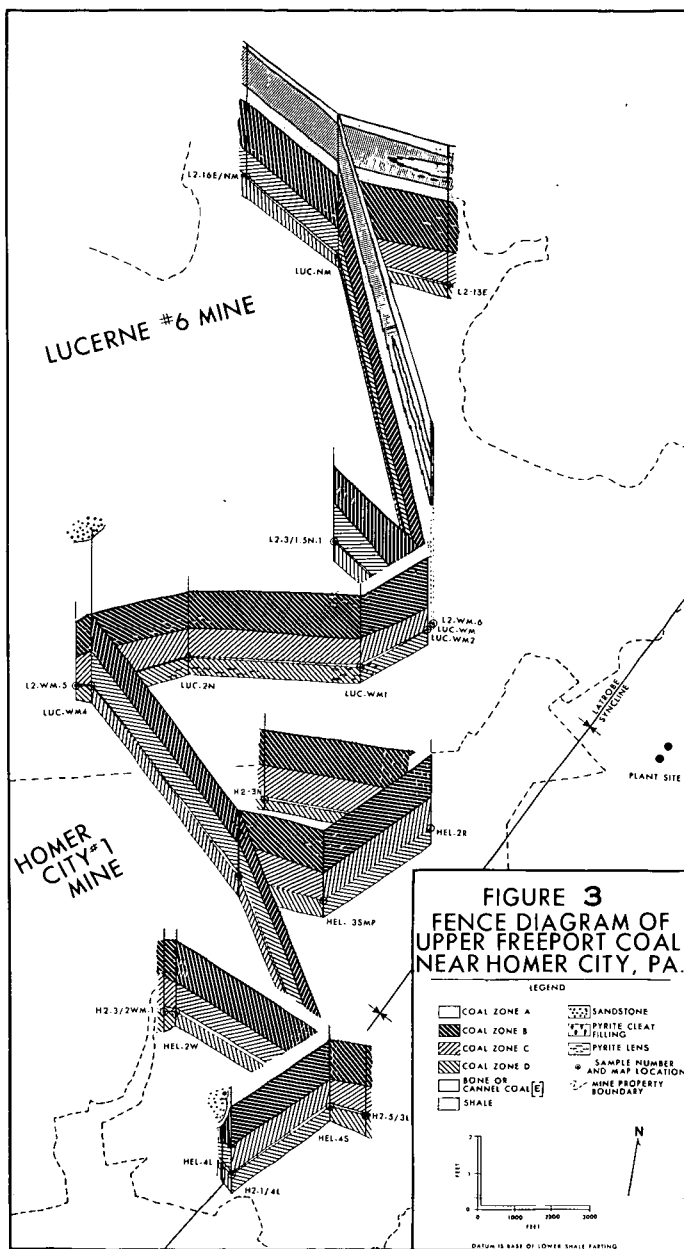


Figure 1. - Index map of Homer City, Pa., study area and Allegheny Group-Conemaugh Group contact.





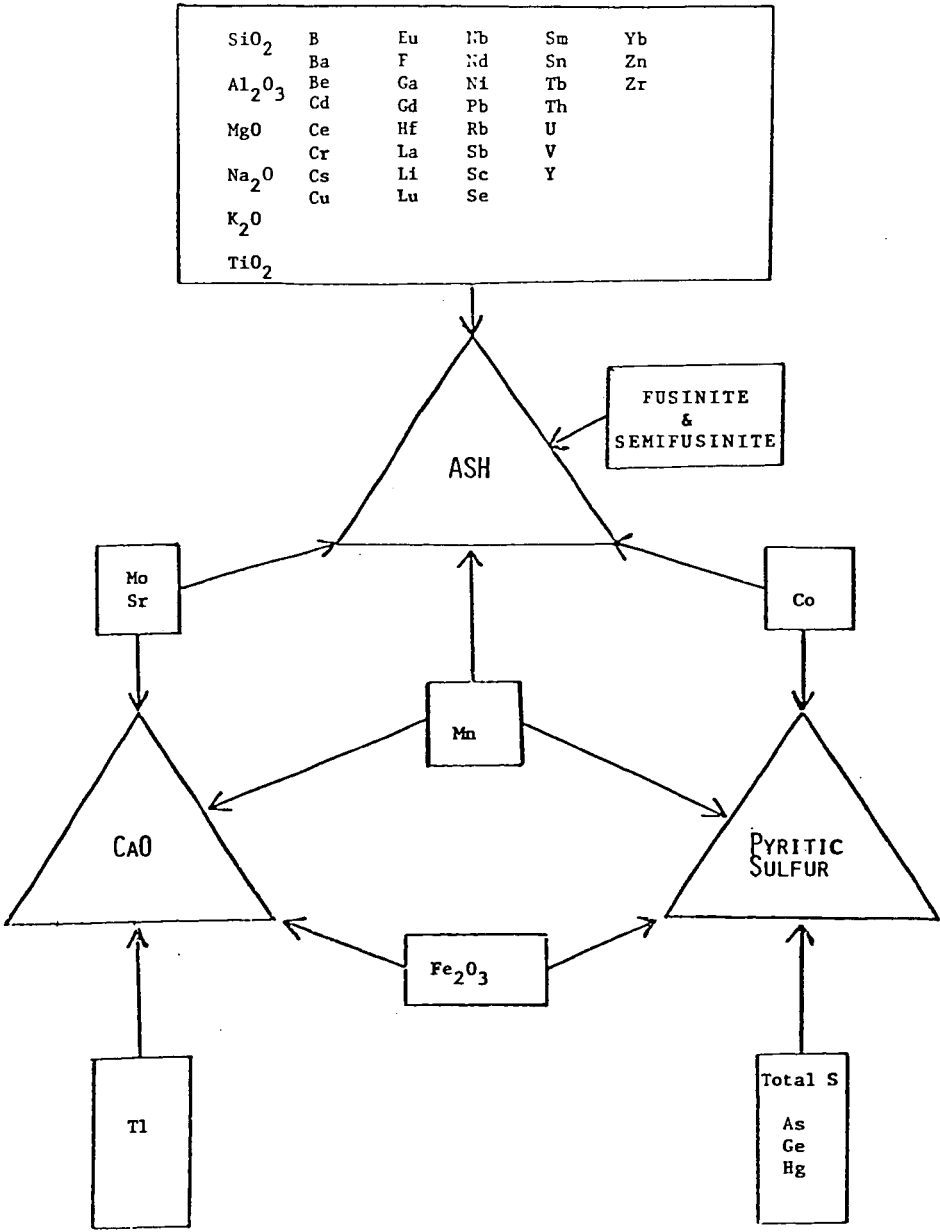


Figure 4. Mineral matter constituents and macerals of the Upper Freeport coal that statistically positively correlate with ash, pyritic sulfur, and calcium.

Modes of Occurrence of Selected Trace Elements
in
Several Appalachian Coals

Robert B. Finkelman, Ronald W. Stanton,
C. Blaine Cecil and Jean A. Minkin

U.S. Geological Survey, National Center, Reston, VA 22092

Most coal-cleaning processes are predicated on differences in physical properties between the coal and the included mineral matter believed to contain the undesirable elements. However, as the mode of occurrence of most elements in coal (particularly the trace elements) is not clearly understood, the effectiveness of the coal-cleaning procedures in removing these trace elements is uncertain. By combining detailed chemical, mineralogical, and petrographic techniques we have determined how various trace elements, particularly those of environmental interest occur in several Appalachian bituminous coals.

This study was conducted primarily on polished blocks of coal using a scanning electron microscope (SEM) with an energy dispersive X-ray detector. With this system individual *in situ* mineral grains as small as 0.5 μm can be observed and analyzed for all elements of atomic number 11 (Na) and greater that are present in concentrations as low as about 0.5 weight percent [Finkelman (1), and Finkelman and Stanton (2)].

On the basis of the abundance of the accessory minerals in the Waynesbury coal, Finkelman (1) calculated the concentrations for 10-15 trace elements. The calculated values for many of these elements, including Zn and Cu, correlated well with their analytical values. These data suggest that the trace elements occur in this coal predominantly as specific accessory minerals. For example, zinc occurs as zinc sulfide (sphalerite; Figure 1) and copper as copper iron sulfide (chalcopyrite; Figure 2). SEM analysis of other coals from the Appalachian Basin appears to substantiate this conclusion. Preliminary estimates based on the new data suggest that most of the selenium in these coals and much of the lead occur as 1 to 3 μm particles of lead selenide (clausthalite?), which are often associated with cadmium-bearing sphalerite and chalcopyrite, (Figure 3). These fine-grained mineral intergrowths occur exclusively within the organic constituents and in all probability formed in place. Experiments by Bethke and Barton (3) on the chemical partitioning of selenium between sphalerite, galena (PbS) and chalcopyrite suggest that the sphalerite-chalcopyrite-clausthalite assemblage would be the expected assemblage at low temperature (300°C).

If all the selenium in these coals occurred as lead selenide this would tie up about half the available lead. Although galena is not found associated with sphalerite or chalcopyrite it does occur as micrometer-sized particles on the edges of pyrite grains (Figure 4). This mode of occurrence may account for the lead in excess of that tied up by the selenium.

Because substantial amounts of Zn, Cu, Pb, Cd, and Se occur as finely dispersed mineral grains in the organic matrix, considerable amounts of these elements can be retained in the lighter specific gravity fractions of cleaned coal (4).

Figure 5 illustrates the concentration of Zn in a size-gravity separation of the Upper Freeport coal. Similar results have been obtained for Cd, Cu, and Pb on six samples of this coal. The divergence of these curves in the high specific gravity range is consistent with the observation that these elements occur as fine-grained minerals which are increasingly released from their organic matrix with fine grinding.

It is evident from Figure 5 that the concentrations, on a whole coal basis, of Zn (this would apply to Cu, Cd, and Pb as well) are much greater for the higher specific gravity (Sp. G.) fractions. However, the bulk of the coal generally floats at the lower Sp. G. levels. Recalculating these data to show the proportion of each element in each Sp. G. fraction reveals that substantial amounts of these

elements are retained in the lighter (<1.50) fractions (Table 1). Similar results were obtained in a washability study of these coals by Cavallaro and others (5). Not all the Upper Freeport samples demonstrated this type of behavior. In several samples more than 50 weight percent of the coal sank in Sp. G. 1.60 liquids, carrying with it as much as 85 percent of these trace elements.

Figure 6 illustrates the concentration of Zn in the high-temperature ash of one of the size-gravity fractions. Similar results have been obtained for Cd, Cu, and Zn in many of the Upper Freeport samples. The highest concentrations of these elements commonly occur in the ash of the lightest fraction of the coal. This reflects the association of fine-grained sphalerite, chalcopyrite, and clausthalite (?) with the organic matrix. The high concentrations in the sink 1.8 fractions are probably due to the release of some of these minerals during grinding.

Many of the trace elements of environmental interest (e.g. As, Cd, Cu, Hg, Pb, Tl, Se, Zn) occur as sulfides. In coal the most prominent sulfide mineral is pyrite (FeS₂). The crystal chemistry of pyrite allows for only a small amount of solid solution with most of the above mentioned elements (6). Indeed, preliminary electron microprobe and ion microprobe analyses of pyrite and its dimorph marcasite from several coals suggest that most pyrite is free of trace constituents to concentrations as low as 100 ppm.

Arsenic is one chalcophile element whose mode of occurrence and behavior differs from that of Zn, Cd, Pb, Cu, and Se. Although arsenic sulfide has been observed in coals, the bulk of the As in the Upper Freeport coal appears to be associated with pyrite. The distribution of As in the Upper Freeport coal appears to be controlled, to a large extent, by the fractures within the coal and within the pyrite. Thus far, arsenic has been found only in pyrite horizons that are associated with fractured coal, although not all such pyrite occurrences had detectable arsenic. Within these favorable sites As was found only along the outer rims of pyrite grains or along fractures within the pyrite. Optically, the As-bearing pyrite always appears "dirty" due to abundant microfractures, perhaps caused by reactions with epigenetic As-bearing solutions. Pyrite without microfractures did not have detectable arsenic (>0.01 weight percent).

In the size-gravity separations, As was found to concentrate in the sink 1.8 fraction along with pyrite.

Correlation coefficients based on statistical analyses of analytical data from 96 Upper Freeport coal samples indicate that As and pyrite correlate well with each other (7). Mercury, the only other element with which arsenic and pyrite have a strong positive correlation, behaves similarly to arsenic in the size-gravity separations (Table 1). In all probability the mode of occurrence of mercury is similar to that of arsenic.

With this type of information on mode of occurrence, coal-cleaning procedures can be devised to effectively remove the undesirable trace elements.

References

- (1) R. B. Finkelman, Scanning Electron Microscopy/1978/vol. 1, 143, (1978).
- (2) R. B. Finkelman and R. W. Stanton, Identification and significance of accessory minerals from a bituminous coal. Fuel (in press).
- (3) P. M. Bethke and P. B. Barton, Jr. Econ. Geol., 66, 140, (1971).
- (4) C. B. Cecil, R. W. Stanton, S. D. Allshouse and R. B. Finkelman, Preparation characteristics of the Upper Freeport coal, Homer City, PA. R & D Program Report (in press).
- (5) J. A. Cavallaro, A. W. Deurbrouck, H. Schults, G. A. Gibbon, and E. A. Hattman. A washability and analytical evaluation of potential pollution from trace elements in coal. EPA interagency Energy/ Environmental R & D Program Report EPA-60017-78-038, (1978).
- (6) W. A. Deer, R. A. Howie and J. Zussman; Rock Forming Minerals, vol. 5, non-silicates, 1962, J. Wiley and Sons Inc.
- (7) C. B. Cecil, R. W. Stanton, S. D. Allshouse, R. B. Finkelman and L. P. Greenland. Mineral matter in the Upper Freeport Coal Bed, Homer City, Pa., EPA, Inter-agency Energy/Environmental R & D Program Report (in press).

Table 1. Trace element concentrations in size-gravity splits of two Appalachian coals. Values are in percentages of the element in each Sp. G. fraction of a size split.

Upper Freeport (H2-42P-1.1)

Mesh size	Cd		Cu		Pb		Zn		Hg		As	
	+1/4"	8x100	+1/4"	8x100	+1/4"	8x100	+1/4"	8x100	+1/4"	8x100	+1/4"	8x100
Float 1.275	36	9	20	10	19	13	5	28	21	0.5	8	tr
1.300	17	16.5	33	30	18	9	12.5	27	13	3.5	10.5	6
1.325	10	0.5	18	12	16	2	11	4	2	3.5	7	1
1.400	6	6.5	13	12	18	9	7.5	4.5	4	5	8	2.5
Cumulative percent	(69)	(42.5)	(67)	(45)	(71)	(33)	(35)	(63.5)	(40)	(12.5)	(33.5)	(15.5)
1.600	9	4	11	8.5	14	10	5	7	10	4	4	6
1.80	9	14.5	32	5	5	4	65	9	15	10	10	2.5
Sink 1.80	12.5	49.5	42	10	10	53	21	40	4	87	46.5	75
Cumulative percent												99
												69.5
												78

Waynesburg

Mesh size	Cu		Pb		Zn		As*	
	>10	10-20	>10	10-20	>10	10-20	>10	10-20
Sp. G.								
1.30	33	18	34	15.5	28.5	27	15	34.5
1.50	65.5	79	53	60.5	41.5	59.5	62.5	33
Cumulative percent	(98.5)	(97)	(91)	(94.5)	(85)	(70)	(86.5)	(77.5)
								(67.5)
1.70	0.5	1.5	3	1.5	4.5	9	2.5	6
Sink 1.70	0.5	1.5	6	4	10	21	11	17
Cumulative percent								25
								<150
								<150
								990
								610

*ppm
tr = trace

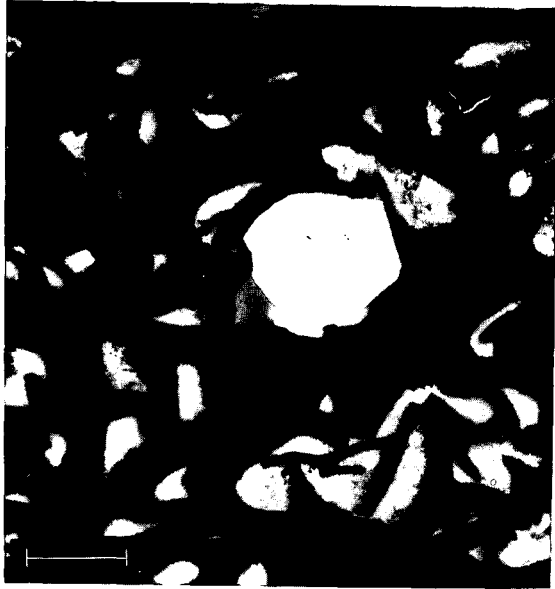


Figure 1. SEM photomicrograph of a sphalerite crystal in semifusinite.
Scale bar = 10 μm .

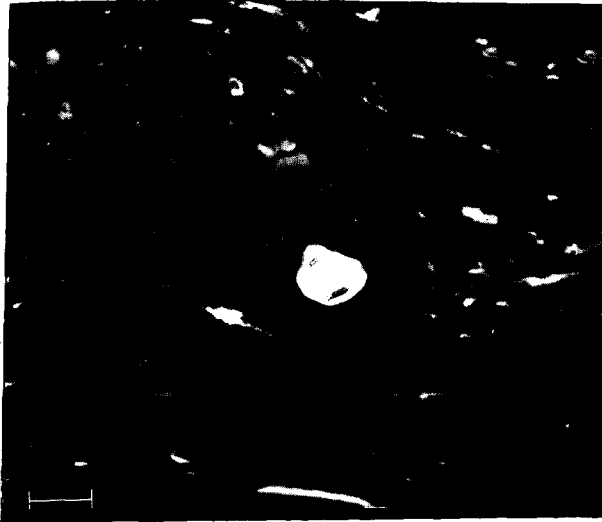


Figure 2. SEM photomicrograph of a chalcopyrite grain.
Scale bar = 10 μm .



Figure 3. SEM photomicrograph of a grain consisting of sphalerite (right rim), chalcopyrite (left rim), and lead selenide (bright cap).
Scale bar = 10 μm .



Figure 4. SEM photomicrograph of galena (light gray) on pyrite (medium gray). Backscattered electron image.
Scale bar = 1 μm .

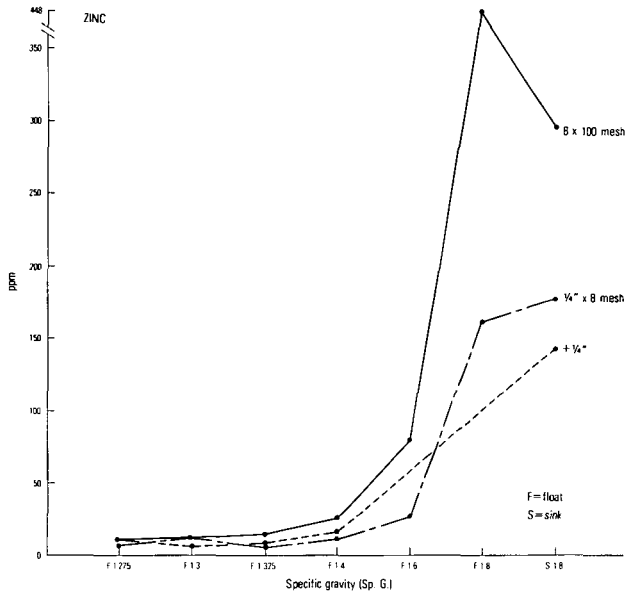


Figure 5. Concentration of zinc (whole-coal basis) in size-gravity separates of the Upper Freeport coal sample H2-42P-1.1.

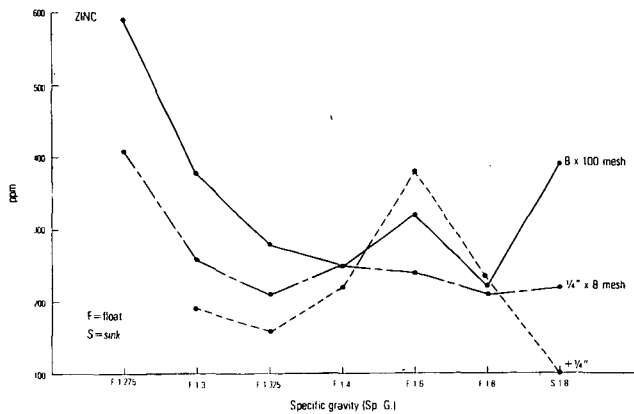


Figure 6. Concentration of zinc in the ash of size-gravity separates of Upper Freeport coal sample H2-53L-1.0.

Distribution of Elements in Coal Macerals and Minerals:
Determination by Electron Microprobe

Jean A. Minkin, E. C. T. Chao and Carolyn L. Thompson

U. S. Geological Survey, National Center, Reston, Va. 22092

Systematic study of elemental abundances in coal macerals and minerals is vital to understanding the genetic history and geological significance of particular coal beds, in correlating coal beds for coal mine planning, in assessing the environmental impact of utilization of coal from a particular source, and in evaluating the potential for recovery of waste by-products and for catalytic action in coal conversion. In-situ determinations of elemental concentrations in macerals and in clays, sulfides and other mineral constituents may help to establish the primary vs. secondary emplacement of particular elements, i.e. elements which were fixed when the coal precursors were deposited vs. mobile elements which may have been introduced and/or redistributed by ground water circulation and other diagenetic processes. Furthermore, determination of the distribution of elements between macerals and minerals is essential in evaluating the possibility of removal of contaminants by grinding and washing, because elements in macerals cannot be effectively removed by these procedures.

Application of electron microprobe analysis to coal-related studies is still in the developmental stage (1). We report here preliminary results of intensive study of one columnar coal sample to indicate the nature of the data on elemental distribution that are readily obtainable through use of the electron microprobe. In order to preserve the stratigraphic relationships of the different coal facies, polished blocks (Figure 1) and polished thin sections were prepared to represent the total thickness of the coal bed. These blocks and thin sections were first studied petrographically with the optical microscope, and areas representative of the principal lithologic units (Figure 2) were designated for analysis by the electron microprobe. A 118-cm thick columnar sample of medium volatile bituminous Upper Freeport coal used for this study was collected in the Helen Mine, Indiana County, Pa. Petrographic analysis (E. C. T. Chao et al., unpublished data) indicates that the coal bed is composed of two cycles of organic-matter deposition and five major lithologic coal types (Figure 3). The division between the two cycles of deposition is the base of one major lithologic unit, a carbonaceous shale parting with bands of vitrite between depths 85 and 92.5 cm. This carbonaceous shale, characterized by water-transported depositional features, may be a key stratigraphic marker. Above the shale parting three major lithologic coal types are discernible: one from the top of the coal to 30 cm depth, another from 30 to 50 cm, and a third from 50 to 85 cm. The fifth is the column interval from 92.5 to 118 cm.

The electron microprobe has been used for in-situ determinations of abundances of 23 elements in the macerals and for analyses of discrete mineral grains present at representative depths of the column. The instrument at the Reston laboratories of the U. S. Geological Survey is routinely capable of wavelength dispersive analysis of all elements stable in vacuum and of atomic number 9 (fluorine) and greater. Limit of detectability for most elements is about 100 ppm, and the minimum target area which can be analyzed is approximately $3 \times 3 \mu\text{m}$. Penetration depth of the electron beam into the target is from 1 to $5 \mu\text{m}$.

Table 1 summarizes the range of abundance of the 23 elements analyzed in macerals of the five major lithologic coal types of the column. At the sites where these elements were detected by probe analysis, discrete minerals were not observed optically down to the limit of resolution (about $0.5 \mu\text{m}$). Strehlow et al. (2), in a transmission electron microscope study of Illinois No. 6 coal, reported a profusion of mineral particles in vitrinite in the size range from 30nm to approximately $0.2 \mu\text{m}$. Thus it is probable that some of the elements detected in our electron microprobe maceral analyses are associated with submicron-sized mineral

matter. In particular, silicon and aluminum, which vary in abundance in a parallel manner are probably associated with extremely finely dispersed clay minerals.

Two elements, sulfur and chlorine, clearly seem organically associated in the macerals of this coal. Sulfur appears to be homogeneously distributed throughout a given maceral, implying an association on the molecular level. Furthermore, a comparable amount of iron is not present, as would be true if this were submicron-sized pyrite or marcasite. The amounts of organic sulfur determined by electron microprobe analysis (Table 1) tend to be greater in the lower depositional unit and are in good agreement with analyses of this coal by conventional methods (3,4). The amount of sulfur in inertinite tends to be about half that in vitrinite, while the sulfur content of the exinites analyzed (this coal contains very little exinite (Figure 3)), more closely approaches the level in vitrinite. Harris et al. in a suite of coals they studied (5) found that exinites always have more sulfur than do vitrinites but determinations by Raymond and Gooley (1) generally agree with our results. In the Upper Freeport sample, chlorine like sulfur, seems homogeneously distributed in a given maceral. In addition, comparable levels of cations such as sodium or potassium were not detected (Table 1), as would be expected if the chlorine were associated with mineral inclusions. Gluskoter and Ruch (6) also concluded that in coals from the Illinois Basin weakly bound chlorine in organic combination was a likely mode of occurrence. Chlorine concentrations in the Upper Freeport sample tend to be higher for the upper cycle of deposition (Table 1). X-ray fluorescence data on ash from this coal show a similar trend (3). This trend perhaps implies greater salinity of the swamp water during the period of growth and deposition of the coal precursors of the upper depositional cycle, compared with the lower.

A systematic study has also been made of the composition of the clays over the full 118-cm depth of the column (Table 2). Identification of the clay minerals is based on their chemical compositions. Those with $K_2O > 2.5$ wt. % are tentatively designated as illites, those with $Al_2O_3 > 30$ wt. %, $SiO_2 > 40$ wt. % and $K_2O \leq 1.5$ wt. % are labeled kaolinites, and "mixed layer" clays are those with K_2O between 1.6 and 2.5 wt. %. In the upper unit of deposition, illites are distinctly dominant and kaolinites occur mostly in shale. "Mixed layer" clays are found only below 92.5 cm depth. Clays in the shales are generally lower in silicon and higher in iron than those in the rest of the coal column. Illites tend to be higher in titanium and lower in aluminum than the other two clay types.

Electron microprobe analyses of iron sulfides determined that arsenic is present in pyrite only from depth 5 to 20 cm in this coal column. The mode of arsenic occurrence is discussed by Finkelman et al. (7).

Because much of this sample of Upper Freeport coal is vitrinite-rich (Figure 3), even small amounts of non-volatile elements in the vitrinite (Table 1) will contribute significantly to the coal ash. The clay and quartz optically observed in vitrinite generally is less than $30\mu m$ in grain size; thus, the elements shown in the analyses of Table 2 will also probably remain in the coal even after fine grinding and washing.

These preliminary elemental studies using the electron microprobe have documented variations in sulfur and chlorine abundance in macerals, clay compositions, and presence of arsenic in pyrite which clearly indicate differences in the depositional and subsequent environmental characteristics of the upper and lower depositional units of this coal. It is hoped that after refinement of our methods of study, more complete evaluation of the abundance of particular elements in a given coal bed will be possible through correlation of modal analyses of maceral-mineral composition (E. C. T. Chao et al., unpublished data) with in-situ chemical data for macerals and minerals obtained by electron microprobe and proton-induced X-ray emission (the latter for elements at concentrations less than 100 ppm) techniques.

References

- (1) R. Raymond and R. Gooley, Scanning Electron Microscopy, 1978/1, p. 93-108 (1978), Scanning Electron Microscopy, Inc. AMF O'Hare, Ill. 60666.
- (2) R. A. Strehlow, L. A. Harris, and C. S. Yust, Fuel 57, 185 (1978).

- (3) C. B. Cecil, R. W. Stanton, S. D. Allshouse, R. B. Finkelman, and L. P. Greenland, "Mineral matter in the Upper Freeport Coal Bed, Homer City, Pa.", EPA Interagency Energy/Environment R & D Program Report (1979). In press.
- (4) ASTM (1977). Annual Book of ASTM Standards. Designation D2492-77. Amer. Soc. Testing and Materials, Phila., Pa., p. 322-326.
- (5) L. A. Harris, C. S. Yust, and R. S. Crouse, Fuel 56, 456 (1977).
- (6) H. J. Gluskoter and R. R. Ruch, Fuel 50, 65 (1971).
- (7) R. B. Finkelman, R. W. Stanton, C. B. Cecil, and J. A. Minkin, "Modes of Occurrence of Selected Trace Elements in Several Appalachian Coals" (1979), this session.

Table 1. Electron Microprobe Determinations of Minor and Trace Element Concentrations (Wt. %) in Macerals of the Five Major Lithologic Coal Types, Upper Freeport Column Sample H2-42P-1.

	0 - 30 cm		30 - 50 cm		50 - 85 cm	
	V	E and I	V	E and I	V	E and I
Al	0-0.11	0-0.14	0.03-0.05	0.09-8.3	0-0.48	0-8.0
Ba	n.d.	n.d.	0	0	0-0.03	0-0.10
Bi	0	0	0-0.07	0-0.06	0	0-0.07
Ca	0.02-0.07	0-0.11	0-0.05	0-2.6	0-0.07	0-6.2
Cl	0.25-0.28	0-0.15	0.24-0.32	0.09-0.48	0.15-0.31	0-2.2
Co	0	0	0-0.05	0-0.08	0-0.04	0-0.04
Cr	0-0.02	0	0-0.05	0-0.05	0-0.03	0-0.08
Cu	0-0.06	0-0.03	0	0	0-0.08	0-0.10
F	0	0-0.08	0	0-0.02	0-0.05	0-0.12
Fe	0-0.05	0-0.41	0-0.04	0-0.20	0	0-0.09
K	0	0-0.36	0	0-0.12	0-0.06	0-0.92 (I) 0-0.05 (E)
Mg	0	0-0.11	0	0-0.04	0	0-0.79 (I) 0-0.06 (E)
Mn	0	0	0	0-0.09	0-0.03	0-0.07
Na	0	0-0.07	0	0-0.07	0-0.03	0-0.35
Ni	0	0	0-0.04	0-0.04	0	0-0.08
P	0	0-0.11	0	0	0	0-0.09
Pb	0	0-0.03	0	0-0.02	0-0.04	0
S	0.46-0.57	0.09-0.40 (I) 0.45-0.48 (E)	0.37-0.49	0.16-0.29 (I) 0.34-0.43 (E)	0.43-0.63	0.13-0.29 (I) 0.23-0.42 (E)
Si	0-0.29	0-0.25	0.04-0.07	0.15-10.9	0-0.30	0-1.80 (I) 0-9.4 (E)
Sr	0	0	0	0	0	0
Ti	0-0.03	0	0.02-0.05	0-0.02	0.02-0.25	0-0.02
V	0-0.02	0-0.03	0	0	0-0.04	0-0.03
Zn	n.d.	n.d.	0	0-0.02	0	0-0.07

V: Vitrinite E: Exinite I: Inertinite
n.d. = not determined

"0" = < 0.01 wt. %.

Table 1. continued

	85 - 92.5 cm		92.5 - 118 cm	
	V	E and I	V	E and I
Al	0.09-0.30	0.14-3.3	0-0.47	0-8.9 (I) 0-0.03 (E)
Ba	0	0	0-0.07	0-0.16
Bi	0	0	0-0.08	0-0.07
Ca	0-0.07	0-0.09	0-0.10	0-0.89
Cl	0.02-0.24	0	0.21-0.27	0.02-0.12
Co	0	0	0	0-0.03
Cr	0-0.02	0-0.04	0-0.02	0-0.04
Cu	0	0-0.02	0	0
F	0-0.04	0-0.02	0-0.05	0-0.78
Fe	0.04-0.13	0.05-0.34	0-0.07	0-1.78 (I) 0-0.14 (E)
K	0-0.06	0-0.04	0	0-0.03
Mg	0	0-0.06	0-0.02	0-0.17
Mn	0-0.03	0-0.04	0-0.04	0-0.08
Na	0	0-0.71 (I) 0-0.03 (E)	0-0.02	0-0.34 (I) 0-0.05 (E)
Ni	0-0.05	0	0-0.02	0
P	0	0	0	0-0.30
Pb	0	0	0-0.02	0-0.06
S	0.63-0.66	0.28-0.38 (I) 0.41 (E)	0.59-0.69	0.18-0.42 (I) 0.44-0.56 (E)
Si	0-0.26	0.20-0.48	0.04-0.77	0.03-10.7 (I) 0-0.09 (E)
Sr	0	0	0	0
Ti	0.22-0.39	0-0.02	0.02-0.17	0 (I) 0-0.42 (E)
V	0-0.05	0	0-0.03	0
Zn	0	0-0.03	0-0.03	0-0.05

V: Vitritinite E: Exinite I: Inertinite "0" = < 0.01 wt. %.
n.d. = not determined

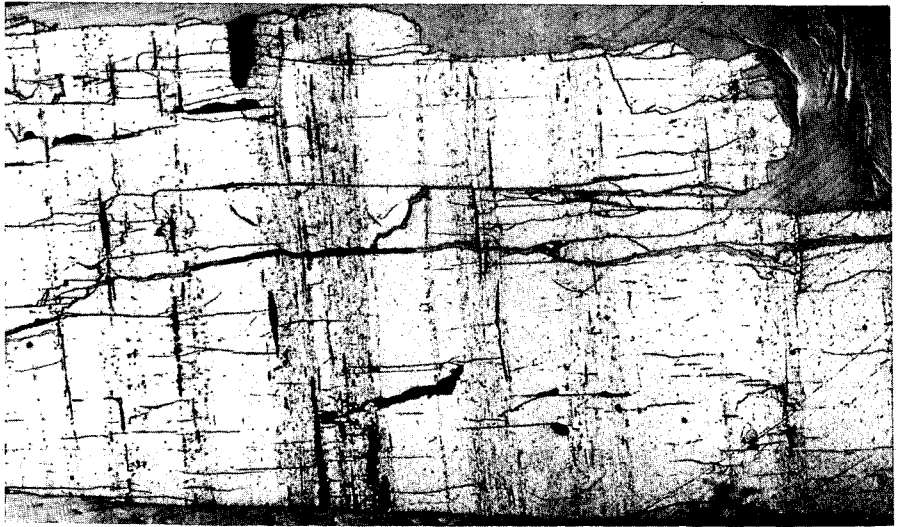
Table 2. Electron Microprobe Analyses of Clay Minerals in Upper Freeport Coal Column Sample HZ-42P-1

Depth (cm.)	ILLITES		KAOLINITES		"MIXED LAYER" CLAYS	
	56	88	88	112	96	112
SiO ₂	48.9	45.2	44.6	44.6	47.2	47.6
Al ₂ O ₃	32.4	35.4	36.0	38.1	36.9	36.2
FeO*	1.42	2.69	3.2	0.63	1.22	1.73
MgO	1.70	0.43	0.85	0.15	0.60	0.87
CuO	0	0	0	0	0.05	0.05
K ₂ O	6.6	8.2	0.16	0.10	1.71	1.83
Na ₂ O	0.23	0.69	0.09	0.07	0.18	0.55
TiO ₂	0.49	0.18	0.03	0	0.07	0.03
MnO	0	0	0	0	n.d.	0
Total Oxide Wt. %	91.7	92.8	84.9	83.6	87.9	88.9

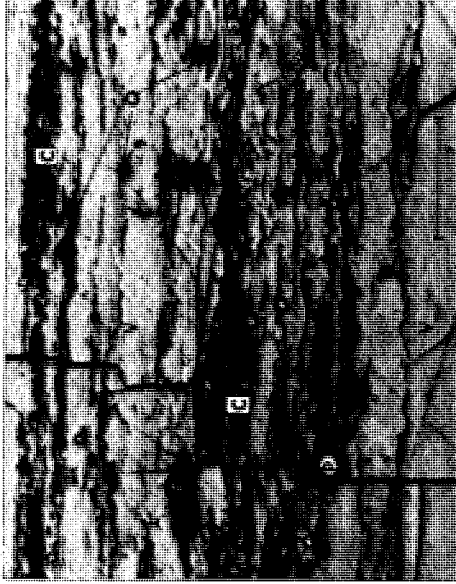
*O = < 0.01 wt. %.

n.d. = not determined.

*Total Fe as FeO.



(left) Figure 1. Vertical-illumination photograph of a polished block from depths 27-30.5 cm, Upper Freeport column sample H2-42P-1. Light gray bands are vitrinite; darker bands are assemblages containing 90-95 volume % vitrinite, 5% exinite and lesser amounts of inertinite and mineral matter. Very dark lenses at depth 28-28.5 cm are inertinites (fusinite and semifusinite). Bar scale 0.5 cm.



(Above) Figure 2. Photomicrograph of an area at depth 96.5 cm, same column, showing mineral matter dispersed in vitrinite. Vitrinite is labeled V, quartz Q, clay C, pyrite P, and inertinite I. Taken in reflected light using an oil-immersion contrast objective lens. Bar scale 0.1 mm.

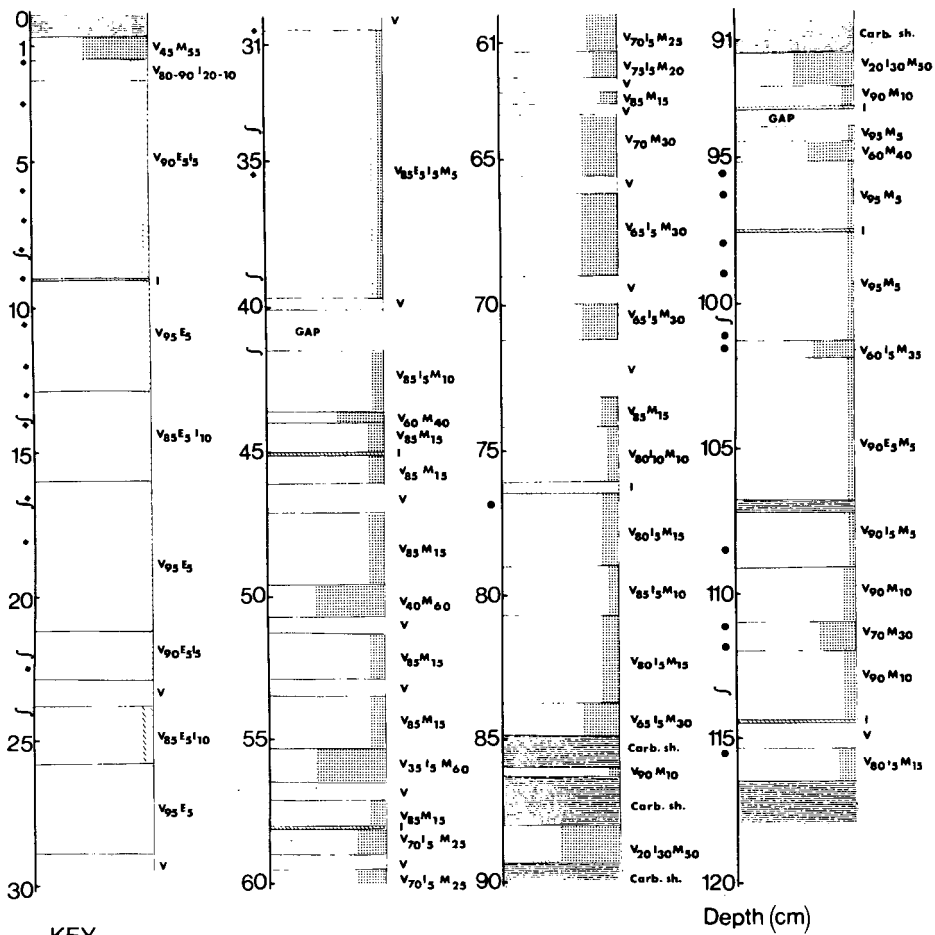


Figure 3. Generalized columnar profile of H2-42P-1. Volume percentages of macerals and mineral matter are plotted across the column according to the amount of each present, and indicated numerically by the label at the right side of the column for a particular depth interval.

RAPID, EASY MULTIELEMENT ANALYSIS OF WHOLE COAL VIA SLURRY-INJECTION ATOMIC ABSORPTION SPECTROPHOTOMETRY

James E. O'Reilly and Donald G. Hicks

Department of Chemistry, University of Kentucky, Lexington, Ky., 40506; and The Institute for Mining & Minerals Research, Kentucky Center for Energy Research Laboratory, P.O. Box 13015, Lexington, Ky., 40583.

INTRODUCTION

In recent years, a few laboratories have reported on the use of flame atomic absorption/emission methods for the analysis of solids directly, bypassing normal ashing and dissolution steps(1-5). However, not all these workers made attempts to achieve quantitative results. For example, although the early paper by Harrison(4) and the recent one by Willis(5) are quite significant, neither reported any quantitative analyses of standard or non-standard analyzed samples! Furthermore, no efforts have been made thus far to determine functional limits of detection and analysis for a wide variety of elements in any one particularly significant solid matrix such as coal. Atomic absorption(AA) procedures involving non-flame furnace atomization techniques seem to have been more widely investigated(6-13).

The need to analyze coal for major, minor, and trace-level elements has been underscored by the Clean Air Act of 1970(14) and the Toxic Substances Control Act of 1976(15,16). Concentrations of trace elements are of great interest in the geological characterization of coals(17), and Hook(18) has emphasized the significance of metals content of coal in determining the quality of industrial products such as coke, iron, and steel. Moreover, the U.S. National Bureau of Standards has recently introduced bituminous and sub-bituminous coal Standard Reference Materials (19,20) having certified concentration values for 14 trace metals. A survey has shown that 70 % of the millions of geochemical exploration samples collected annually have been analyzed by AA procedures(21). But conventional AA analysis procedures are plagued by lengthy sample preparation steps, usually involving a high or low-temperature ashing for many hours, followed by a prolonged dissolution in mixed acids. Even for a "rush" analysis, the turnaround time is nearly 2 days from receipt of samples.

Therefore, we have developed an atomic absorption method for the direct analysis of whole coal by injection of powdered coal slurries into either flames or graphite furnaces. This paper greatly expands the preliminary observations of O'Reilly(22) on the slurry-injection approach to flame AA analysis of coal. Our work is oriented toward a comprehensive exploration of the capabilities of this general approach for determining a wide variety of elements in some difficult-to-digest solid matrices such as coal, coal ash, oil shale, limestone, pigments, glasses, and selected ores. That is, solid matrices with "relatively" constant major component compositions.

EXPERIMENTAL

Apparatus and Reagents: All absorption and emission signals were measured using a non-modified Varian Model AA-6 atomic absorption spectrophotometer equipped with a Model BC-6 H₂-lamp background corrector, Model CRA-90 graphite tube/cup atomizer system, and a high quality strip chart recorder capable of expanding the 100 mv output absorbance signal by 100x in several steps. A standard Varian premix

burner with single-slot "high solids" heads was used throughout for flame atomization studies. As supplied, nebulizer intake capillaries had quite variable I.D. values. To minimize clogging, only those with I.D. greater than 35 μ m were utilized. To decrease the frequency of removing solid particles constantly collecting therein, a large conical suction flask was filled with water and used as a burner "drain trap" at floor level. A length of 8 mm glass tubing was inserted through a one-hole rubber stopper to a point about 5 inches below the water surface, and also connected to the burner chamber. A plastic tube ran from the flask side arm to a drain in the floor. The critical, final comminution of analytical samples was accomplished by use of a swing-mill (Spex Model 8510 Shatterbox) with 3.7 x 2.5 inch hardened steel or tungsten carbide(WC) grinding containers.

Certified atomic absorption standard solutions (Fisher Scientific) were used to prepare aqueous standards. A 10 % by weight stock solution of Triton X-100(Rohm & Haas scintillation grade) wetting agent was prepared and diluted daily as needed to 0.2 % or 0.5 % with distilled and doubly deionized water. Other materials were reagent grade.

Reference standard coals of nominal sub-60 mesh(-250 μ m) particle size were prepared from several eastern Kentucky bituminous coal samples. Ten to twenty pounds of each of these raw coals was put through (a) a standard jaw crusher, (b) a roller-mill, and (c) a Holmes Model 500 rotor-beater type of pulverizer equipped with a screen allowing output particles of 60-mesh or smaller. After tumbling each total sample 2 hrs, they were dried briefly at 110°C to remove surface moisture. The reference standard coals were then analyzed for content of several elements by conventional AA procedures involving 24-hr low-temperature oxygen-plasma ashing(23,24) and dissolution of the ash after treatment with aqua regia/HF in a teflon bomb(25,26) or fusion with lithium tetraborate (27,28). Analysis of NBS-SRM coal as an unknown and studies on the linearity of AA signals versus concentration made use of these samples.

Analysis Procedure: The grinding chamber of the Spex swing-mill was "dry-cleaned" initially, and also between samples, by a 2-min milling of about 6 mL of the new coal sample to be analyzed. After discarding the resulting powder, the chamber was quickly wiped with laboratory tissue and blown out with a jet of dry air. Roughly 10 mL of the new coal sample was then added to the container and pulverized for 10 minutes. The majority of the powdered sample was dumped into a 325-mesh(44 μ m) metal screen sieve with a 3-inch brass body, then shaken and bumped by hand for 1.5 minutes. Two-thirds or more of the solid typically passed the screen. The -44 μ m powder which collected in the bottom pan was covered with a snug-fitting lid, shaken vigorously for about 10 sec, and tumbled 10-12 times. Analytical samples in the range of 0.1 to 2.5 g were placed in 150-mL beakers. Using graduated cylinders or repipets, 30 to 100 mL of 0.5 % Triton X-100 slurring solution was gently added to produce slurries containing 0.1 to 8.0 grams coal per 100 mL slurring liquid(0.1 % to 8 % wt/vol solids). Actually, with the burner slot parallel to the light beam, most elements in most coal samples could be determined using slurries of 0.3 %, 5 %, or 8 % solids. Slurries of reference standard coals and unknowns were always prepared to contain approximately the same % solids. Samples were then stirred magnetically for about 30 minutes prior to aspiration into the burner. Absorbance measurements, made while stirring the slurries gently, were corrected for non-atomic "background" absorption using broad-band emission from an H₂-arc lamp. Absorbances of standard and unknown

coal slurries were normalized to the same % solids value which was chosen to be near the solids level of the slurries actually prepared. Element concentrations in the unknowns were determined from best-fit calibration curves constructed from standards, or from simple ratios of absorbances of standards and unknowns with subsequent averaging.

When analyzing coal by non-flame graphite furnace atomization techniques, suspensions containing 0.2 to 8.0 g of unsieved powdered coal per 100 mL total slurry volume were prepared by dilution in volumetric containers. After brief mixing, slurries were transferred to wide mouth containers and stirred a few minutes. Adding 5 to 25 μ L of the slurries to the graphite tube or cup provides a functionally accurate and rapid method to measure 10 to 2000 μ g of powdered coal sample.

RESULTS AND DISCUSSION

Sample Comminution Studies: Of several types of grinding devices examined, a swing-mill (Spex "Shatterbox") was found to be generally superior after considering such factors as (a) production of a very high percentage of really fine (-325 mesh) particles, (b) grinding 7 to 45 grams of sample, (c) short milling time, (d) number of samples milled simultaneously, and (e) general ease of operation and reproducibility. Table I illustrates that absorbances of samples ball-milled 60 min are significantly lower than those for samples pulverized 12 min in any swing-mill container. Usually, slurries made from unsieved coal ground in the swing-mill WC chamber did not clog burner capillaries. But clogging did occur often enough for us to recommend a brief partial sieving in the analytical procedure. The optimum time (Fig. 1) to grind 12 mL of coal having a 44-250 μ m starting range of particle sizes was found to be 12-15 minutes, although grinding times as short as 5 min will produce suitable samples when sieved. Since absorption has been shown to increase with decreasing particle size(5), 12 min in a swing-mill WC dish apparently results in a maximum state of subdivision of particles. Prior to this maximum absorbance grinding time, the -325 mesh powder exhibits a signal slightly greater than that of the unsieved samples. But after 12 minutes, the two types of samples show no difference in signal. To minimize clogging, 30-min of intermittent stirring is recommended after first mixing the slurry, particularly for water-based slurries of higher solids content. However, analytically useful slurries are obtainable after only 5-10 min stirring of either water-based suspensions with lower % solids or organic solvent mixtures of any solids level. Slurries having 8 % solids in a water base or 20 % solids in organic solvents have been aspirated a few minutes without clogging a 0.4 mm I.D. burner capillary. Regardless of the % solids, the rate of slurry aspiration is essentially the same as the uptake rate of the particular slurrying liquid (within 1 % to 2 %). Although clogging factors are discussed here, it is emphasized that it rarely happened when following routine analysis procedures.

Analysis By Flame Atomization: Best-fit calibration curves, obtained at some particular % solids level, are generally linear over a reasonable concentration range---as illustrated by Figures 2 and 3. Individual points resulting from different standard coals show a small, but highly reproducible, scatter about the line. We interpret this to be caused by relatively small matrix variation effects. For elements tested, slurry calibration curves have the same general shape. That is, they exhibit the same relative positioning of data points whether obtained (a) in $N_2O-C_2H_2$ or air- C_2H_2 flames, (b) from unsieved or partially sieved powders, (c) after 15 min milling in a swing-mill or 2 hr in a

rolling-jar ball-mill, or (d) after 20 min or 3 hrs stirring. Strong emission signals for several elements were obtained from coal slurries. In the case of sodium, the AA calibration curve had the same shape as one obtained from atomic emission measurements. Precisions attainable by this slurry-injection AA approach are quite good as seen in Table II, and are similar to those observed for replicate determinations on purely aqueous standards. Relative standard deviations (RSD) are typically 1 % of the mean for elements with strong signals, and 3-4 % when scale expansion is required.

For some elements whose coal slurry AA signals are quite small, considerable scale expansion is necessary and non-atomic "background" absorbance becomes significant (Fig. 3). Experimental observations shown in Table III suggest that this apparent absorption is primarily caused by light scattering from the solid particles. This "background" signal increases linearly with increasing solids level, is relatively constant from one coal to another, is greater when measured near the top of the burner, is much greater when the slurry is aspirated by non-burning gases (Table III), decreases gradually as wavelength changes from 200 nm to 600 nm (Table III), has the same magnitude whether measured with line or broadband light sources (Table III), increases with increasing slurry aspiration rate, is greater for coal sieved through a screen with larger openings (i.e. larger particles), is much less in the $N_2O-C_2H_2$ flame than in the air- C_2H_2 flame, and has a maximum observed absorbance of 0.002/1 % solids---this latter data in accord with Willis⁵ (5) value for pulverized rocks.

Figure 4 indicates that conventional atomic absorption sensitivities (ppm at which $Abs. = 0.0044$) for elements in the NBS-1632 coal matrix increase in the same general order as AA sensitivities determined in aqueous solution. Atomization efficiencies relative to water media were determined as $\% \text{ atomization} = (100)(\text{slurry absorbance})/(\text{aqueous solution absorbance})$ at equal effective concentrations of the test element. These efficiencies for coal ranged between 16 % and 24 % of those obtainable from aqueous solution. Apparently, the NBS-1632 coal matrix (and perhaps others) does not drastically affect the signal of one element relative to another.

Flame response profile studies have shown that elements generally exhibit a maximum absorbance at a point higher in a flame when slurries are fed in than when aqueous solutions are aspirated (Fig. 5). As can be seen in Figure 6, the relative atomization efficiency in a flame also increases with increasing height above the burner. The % atomization of slurries increases more rapidly with increasing height in the $N_2O-C_2H_2$ vs air- C_2H_2 flame, and, the height of maximum absorbance is nearer the top of the burner in the $N_2O-C_2H_2$ vs air- C_2H_2 flame; both observations being in contrast with the greater aspiration rate of the $N_2O-C_2H_2$ burner. Along with the fact of lower non-atomic background absorbance therein, these data indicate that the $N_2O-C_2H_2$ flame is more efficient than the air- C_2H_2 flame in decomposing solid particles.

Of 33 elements studied, 23 were found to have sufficient sensitivity to be determined by flame atomization at levels normally encountered in coal (Al, Si, Fe, K, Ca, Mg, Na, Ti---Ba, Be, Cu, Cr, Co, Eu, Li, Mn, Ni, Pb, Rb, Sr, V, Yb, and Zn). Eu and Yb were detected by their emission signals from $N_2O-C_2H_2$ flames. Ag, As, Bi, Cd, Mo, P, Pd, Se, Sn, and Te were not detected with sufficient sensitivity. Utilizing

flame atomization, concentrations of 16 elements have been determined in NBS-1632 SRM coal with moderate accuracies of ± 5 to 25% error (Table IV). Although NBS-1632 is a relatively uniform blend of several coals, it is to be noted that the eastern Kentucky coals used as standards were not uniform. When considering sample-to-sample variations, it has been observed that slurry absorbances of Si and Al increase as ash content of the coal increases. But, correlations are not linear. Some other elements tested (Fe, Ti, Mg, Ca, K, Na, Ba, Sr) do not consistently show a similar correlation. Analysis of high speed photographs of flames has shown that the rise velocity of the larger of the $-44 \mu\text{m}$ coal particles near the top of the burner is essentially the same as the streaming velocity of the gases through the burner slot.

SUMMARY AND CONCLUSIONS

Most of our work has concerned flame atomization AA procedures, which are generally faster and more convenient than non-flame electrothermal atomization techniques. A recent brief report by Gladney(10) showed that Be in coal could be accurately determined by graphite furnace techniques, with observed precisions around 7.5 % RSD. Our work confirms determination of this particular element, and also shows that injection of μL amounts of slurries into a graphite cup/tube is a rapid and very reproducible way to circumvent microbalance weighings! In general, it appears that powdered coal slurries may be analyzed (in these devices) for elements which allow higher ashing and atomization cycle temperatures. Using a 2.5 mm I.D. graphite cup for atomization, 8 replicate determinations on 10- μL aliquots from a 1 % solids slurry ($-44 \mu\text{m}$ coal) resulted in a relative standard deviation of 3.2%.

Ease of sample preparation plus greatly increased speed of analysis using a commonly available instrument are the main advantages of this slurry injection AA method for coal analysis. As an example, the turnaround time for determining the concentrations of 4 elements in 6 samples can be reduced to 2 hrs from the current 2 days required by conventional AA procedures! Some operator time is also saved. The technique is useful for extremely fast single element scanning, which would allow more frequent and widespread sampling of coal shipped in large vessels. Although multielement scanning is a sequential process, it is rapid and does compete in total analysis time with X-ray fluorescence techniques, for instance. Assuming 10-12 min XRF instrument time per sample count period, and high and low energy counting on each sample, the XRF and slurry-injection AA methods both need about $\frac{1}{2}$ day to determine 12 elements in 6 samples. The price paid for this speed is the achievement of only modest accuracy. However, slurry-injection AA accuracies might be improved over those implied by the data in Table IV if standards and unknowns are matched somewhat better with respect to approximate ash content or general type of coal. Accuracies are certainly good enough for geochemical explorations, and are actually in the range of values reported(17) for conventional AA determinations.

ACKNOWLEDGEMENTS

We are grateful to Henry E. Francis, Karen Moore, and Sayra Russell for selected analyses, and to Dennis Sparks for initial preparation of some coal samples. Financial support for this project was provided by the Kentucky Center for Energy Research and the Institute for Mining and Minerals Research, and by Georgia State University (sabbatical leave for DGH).

REFERENCES

1. P. T. Gilbert, Anal. Chem., **34**, 1025 (1962).
2. J. L. Mason, Anal. Chem., **35**, 874 (1963).
3. V. I. Lebedev, Zh. Anal. Khim., **24**, 337 (1969).
4. W. W. Harrison and P. O. Juliano, Anal. Chem., **43**, 248 (1971).
5. J. B. Willis, Anal. Chem., **47**, 1752 (1975).
6. F. J. Langmyhr, J. R. Stubergh, Y. Thomassen, J. E. Hanssen, and J. Dolezal, Anal. Chim. Acta, **71**, 35 (1974).
7. F. J. Langmyhr, R. Solberg, and L. T. Wold, Anal. Chim. Acta, **69**, 267 (1974).
8. E. L. Henn, Anal. Chim. Acta, **73**, 273 (1974).
9. D. A. Lord, J. W. McLaren, and R. C. Wheeler, Anal. Chem., **49**, 257 (1977).
10. E. S. Gladney, At. Absorpt. Newsl., **16**, 42 (1977).
11. D. D. Siemer and H. Wei, Anal. Chem., **50**, 147 (1978).
12. B. V. L'vov, Talanta, **23**, 109 (1976).
13. F. J. Langmyhr, Talanta, **24**, 277 (1977).
14. U. S. Clean Air Act of 1970, Public Law 91-604, Dec 31, 1970.
15. U. S. Toxic Substances Control Act of 1976, Public Law 94-469, Sec. 4, 10, 27.
16. R. M. Druley and G. L. Ordway, Eds., "The Toxic Substances Control Act," Bureau of National Affairs, Washington, D.C., 1977.
17. H. J. Gluskoter, R. R. Ruch, W. G. Miller, R. A. Cahill, G. B. Dreher, and J. K. Kuhn, "Trace Elements in Coal: Occurrence and Distribution," Illinois State Geological Survey Circular 499, 154 pp., 1977.
18. W. Hook, Pure Appl. Chem., **49**, 1465 (1976).
19. NBS-1632a and NBS-1635 SRM Data sheets, National Bureau of Standards, U. S. Department of Commerce, Washington, D.C., 1978.
20. J. M. Ondov, W. H. Zoller, L. Olmez, N. K. Aras, G. E. Gordon, L. A. Rancitelli, K. H. Abel, R. H. Filby, K. R. Shah, and R. C. Ragaini, Anal. Chem., **47**, 1102 (1975).
21. J. S. Webb and M. Thompson, Pure Appl. Chem., **49**, 1507 (1976).
22. J. E. O'Reilly and M. A. Hale, Anal. Lett., **10**, 1095 (1977).
23. H. J. Gluskoter, Fuel, **44**, 285 (1965).
24. C. E. Gleit and W. D. Holland, Anal. Chem., **34**, 1454 (1962).
25. B. Bernas, Anal. Chem., **40**, 1683 (1968).
26. B. Bernas, Amer. Lab., **5** (8), 41 (1973).
27. R. B. Muter and L. L. Nice, in "Trace Elements in Fuel," S. P. Babu, Ed., American Chemical Society, Washington, D.C., 1975.
28. J. H. Medlin, N. H. Suhr, and J. B. Bodkin, At. Absorpt. Newsl., **8**, 25 (1969).

FIGURE CAPTIONS

- Figure 1. Effect of grinding time in a Spex Shatterbox (tungsten-carbide container) on the atomic absorbance of several elements in one coal sample that was originally 60/325 mesh (44-250 μ m particle diameters). The solid circles are for unsieved final samples, the open circles for a final sample partially screened through a 325-mesh sieve. Conditions: nitrous oxide-acetylene flame; 1% wt/vol coal slurry; wavelengths = 285.2, 248.3, and 213.9 nm for Mg, Fe, and Zn.
- Figure 2. Calibration curve for analysis of zinc in whole coal. Conditions: air-acetylene flame, 0.4% wt/vol coal slurry in 0.2% Triton X-100, coal ground in a tungsten-carbide swing-mill.
- Figure 3. Calibration curve for analysis of manganese in whole coal illustrating correction for background absorbance. A: Absorbance of coal slurries without correction for background absorbance. B: Flame background absorption (particulate scattering) of aspirated coal slurries at 380 nm measured separately with a hydrogen-arc lamp mounted in place of a hollow-cathode lamp. C: The resultant background-corrected calibration curve. Conditions: air-acetylene flame, 3% wt/vol coal slurry in 0.2% Triton X-100, coal samples ball-milled, -325-mesh fraction.

Figure 4. Atomic absorption sensitivities ($A = 0.0044$) for a number of elements in NBS-1632 coal slurry versus the experimental sensitivity for those elements in purely aqueous standard solutions. The two lines represent effective atomization efficiencies of an element in a coal slurry of 16 and 24% that in aqueous solution. Conditions: nitrous oxide-acetylene flame except for Rb; coal slurries were of different solids levels in 0.2% Triton X-100; coal ground in a tungsten-carbide swing-mill.

Figure 5. Effect of measurement height in the flame on the atomic absorbance of iron in aqueous solution and in a coal matrix. Circles--in an air/acetylene flame; triangles--in a nitrous oxide-acetylene flame. Solid points--0.50% coal slurry in 0.5% Triton X-100; open points--aqueous 5 ppm iron solution. Conditions: The coal (1.07% Fe content) was ground 15 min in a steel swing-mill and sieved through a 200-mesh (75 μ m) screen.

Figure 6. Effect of measurement height in the flame on the relative atomization efficiency ($\epsilon_{rel} \times 100$) of iron in a coal matrix. Conditions same as in Figure 5.

Table I. Atomic Absorbance of Certain Elements vs. Grinding-Preparation Method^a

Grinding-Preparation Method	Grinding Time, min	Sieving ^b	Element ^c				
			Mg(NA)	Al(NA)	Si(NA)	Fe(NA)	Fe(AA)
Ball mill	60	yes	0.661	0.299	0.212	0.148	0.290
Swing-mill (steel)	12	yes	0.831	0.533	0.301	0.188	0.468
Swing-mill (WC)	12	yes	0.860	0.575	0.314	0.198	0.504
Swing-mill (WC)	12	no	0.862	0.577	0.317	0.195	0.504

^aThe same sample of coal was used in all grinding tests. ^bAfter grinding, the subsample was partially sieved through a 325-mesh screen (44 μ m diameter particles). Conditions: 2% wt/vol coal slurries in 0.2% Triton X-100. ^cAbsorbances are the average of at least three measurements; AA = air-acetylene, NA = nitrous oxide-acetylene flame. The normal atomic absorption wavelengths were used for the four elements studied. WC = tungsten carbide grinding chamber.

Table II. Precision of Atomic-Absorption Signal Intensities^a

Element	Series A RSD ^b	Series B RSD	Series C RSD
Fe	1.1	0.90	0.95
Zn	2.5	2.7	2.3
Mg	0.72	-	0.76
K	-	-	0.93

^aIn the A series of replicate analyses, nine 15-mL subsamples of a particular -60 mesh coal were milled 15 min in the swing-mill hardened-steel container and sieved 1.5 min by hand through a 200-mesh (75 μ m) screen. Series B was 10 subsamples of the same coal pulverized 2 hr in a rolling-jar ball-mill, and then sieved 2 min by hand through a 400-mesh (38 μ m) screen. Series C consisted of nine 12-mL subsamples of a different coal milled 10 min in the Shatterbox WC container, and then sieved 1.5 min by hand through a 325-mesh (44 μ m) screen. Series A and C employed an air-C₂H₂ flame while series B used the N₂O-C₂H₂ flame.

^bRSD = relative standard deviation as percent of the average.

Table III. Background Absorbance of a Coal Slurry at Several Wavelengths^a

Wavelength, nm	Lamp ^b	Absorbance, $\times 10^3$		
		N ₂ O-C ₂ H ₂ Flame	Air-C ₂ H ₂ Flame	Air-C ₂ H ₂ No Flame ^c
207.5	HC	1.5	4.7	12.4
214	H ₂	---	4.8	---
231.7	HC	1.3	4.9	12.9
267.3	HC	1.1	3.3	11.9
280	H ₂	---	3.2	---
326.1	HC	---	2.9	---
358	H ₂	---	2.2	---
391.0	HC	0.6	2.6	9.5
450	H ₂	---	1.8	---
459.3	HC	---	2.0	---
610.4	HC	---	1.6	---

^a5% wt/vol slurry in 0.5% Triton X-100. Coal was ground 15 min in a steel swing-mill, and sieved through a 200-mesh sieve. Dash means measurement not made. ^bHC = isolated line from a hollow-cathode lamp; H₂ = Hydrogen arc lamp. ^cFlame not lit, but gases flowing on the air-C₂H₂ burner head; zero absorbance set with 0.5% Triton X-100 aspirating.

Table IV. Analysis of NBS-1632 Bituminous Coal SRM by Slurry-Injection
Atomic Absorption Spectrophotometry^a

Element	NBS	Slurry-AA	Error, % of NBS
	Concentration, ^b µg/g	Concentration, µg/g	
Si	<u>32000</u>	26000	19
Al	17300*	15700	9
Fe	8700	9200	6
Ca	4340*	4950	14
K	2790*	2570	8
Ti	<u>800</u>	690	13
Na	396*	480	21
Sr	128*	99	22
Cu	18	20	11
Zn	37	34	8
Mn	40	38	5
Ni	15	14	7
Cr	20.2	23	14
Pb	30	24	20
V	35	43	23
Co	5.6*	4.4	21

^aVarious analyzed Kentucky coals were used as standards.

^bUnmarked values are NBS certified, underlined values are NBS provisional;

*values are averages of several reported in the 1977 Illinois State Geological Survey Circular 499 (17).

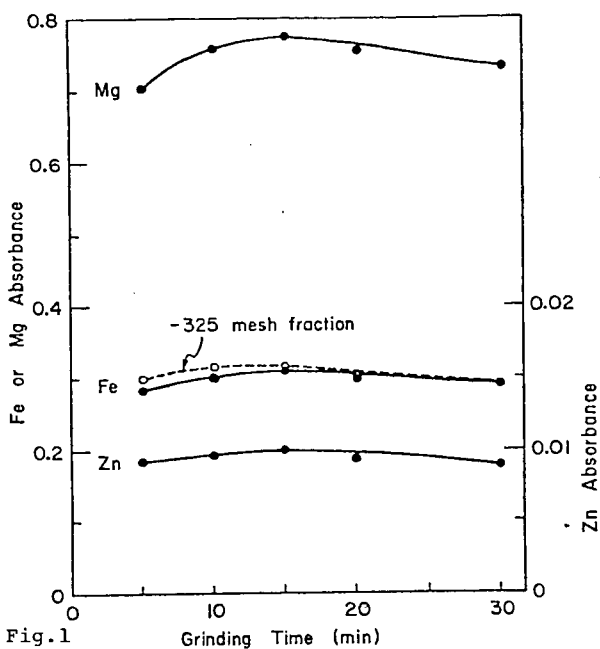


Fig. 1

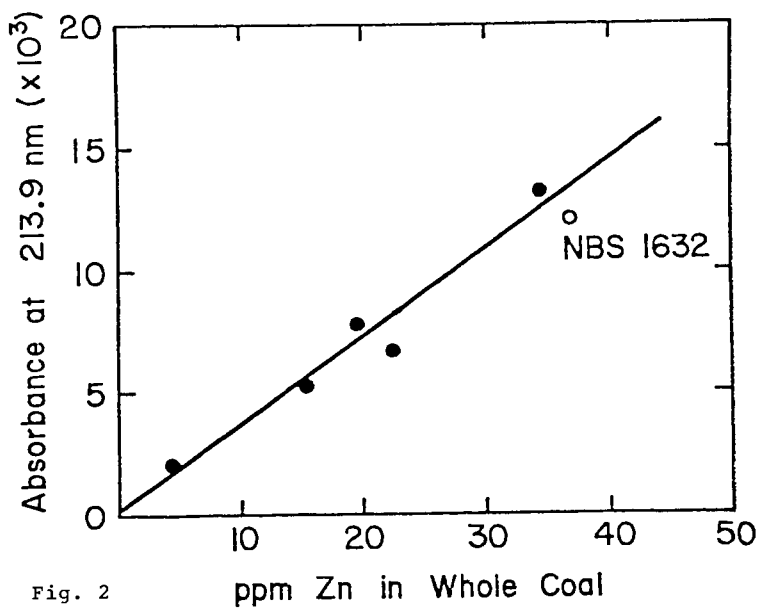
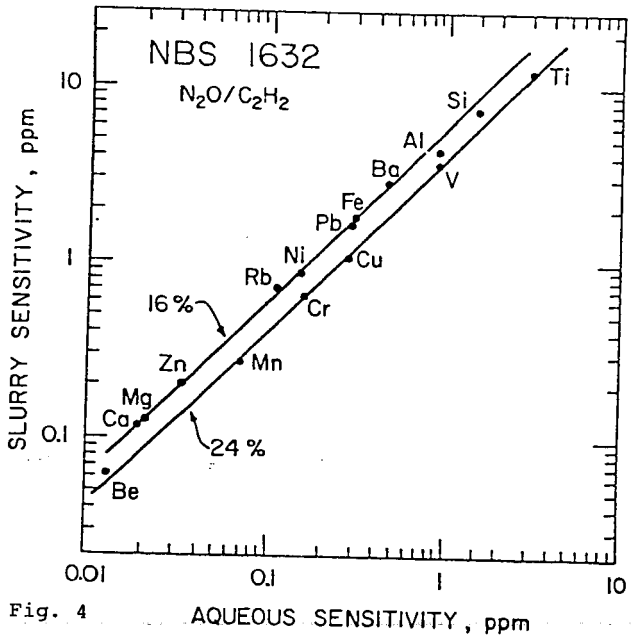
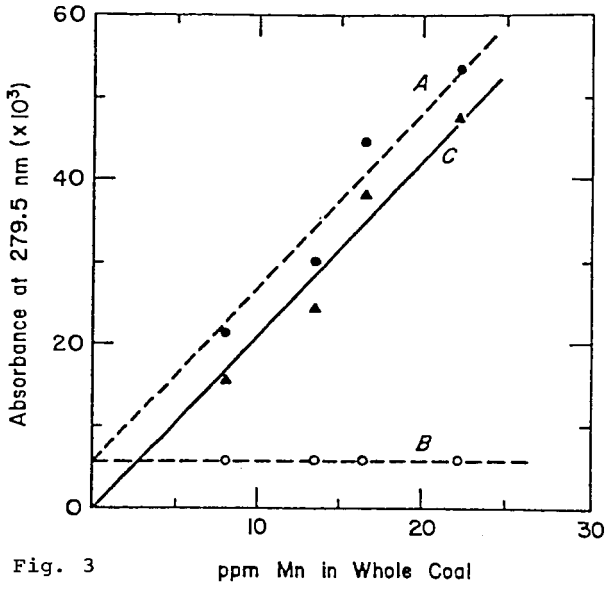


Fig. 2



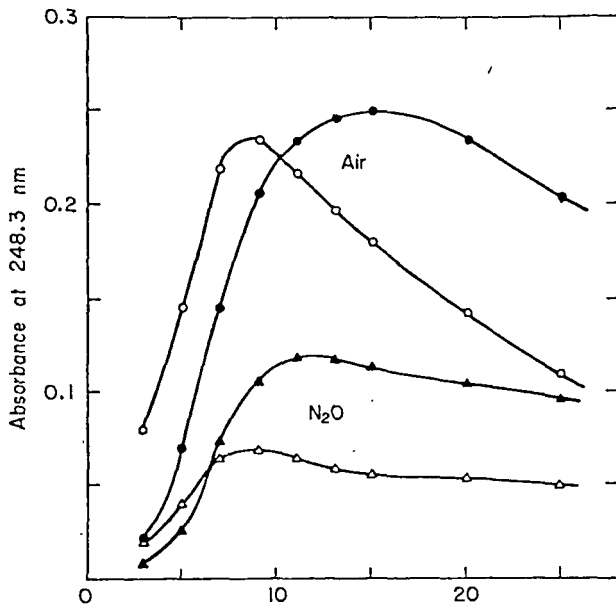


Fig. 5 Height of Measurement, mm above Burner Top

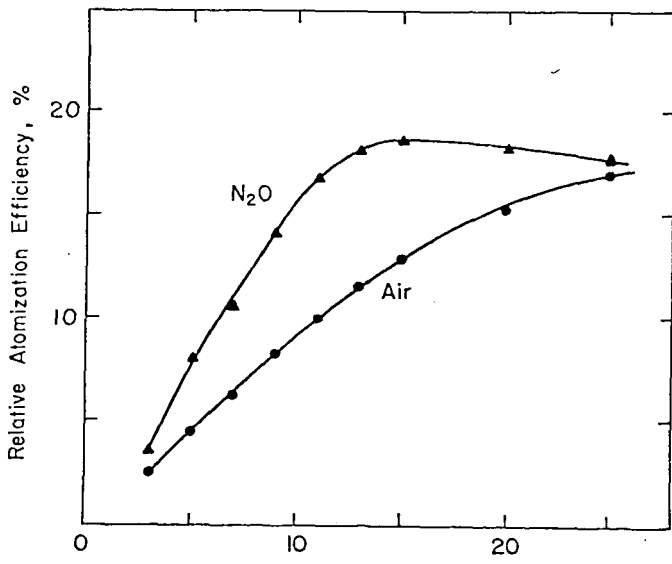


Fig. 6 Height of Measurement, mm above Burner Top

Precision on the Determination of Trace Elements in Coal

Mutsumi Ihida, Teruaki Ishii, Rieko Ohnishi

Nippon Kokan K.K., Chemical Analysis Laboratory, Technical Research Center
1-1, Minamiwatarida-cho, Kawasaki-ku, Kawasaki, 210 Japan

1 Introduction

The quantity of mineral matter contained in coal is generally 5 to 25 per cent of the total contents. Most of the mineral matter are contained in the form of silicate, while the rest of a few per cent are trace elements with more than 20 kinds including zinc, cadmium, lead, nickel, chromium, copper, and vanadium etc..

At the present moment, it would not be so important to find out the quantity of these trace elements in coal for the purpose of recovering raw materials except certain materials such as germanium and gold, however to know the quantity of trace elements in coal is becoming more important for the purpose of the environmental chemistry.

There are following problems in conducting the determination of trace elements;

- 1) Concentration of the elements are slight.
- 2) Coal is composed of organic matter.
- 3) Difficulty in obtaining a standard sample required for the determination.

To cope with these problems, the Sample Research Committee, JUSE, has conducted a Round-Robin study with cooperation of seven laboratories and tried to evaluate the precision of the determination of trace elements in coal and coke. Besides, it was considered that volatility loss at the stage of pretreatment of sample might have occurred for the elements with inferior reproducibility such as zinc.

The result of the study is described hereinafter.

2 Experimental

2-1 Design of Experiment

Three kind of test samples crushed under 250 μ m, shown in Table 1, were analyzed at seven laboratories by the analytical method described below. Each kind of sample was analyzed two times and the measurement by the atomic absorption method was performed twice respectively.

Analytical procedure was as follows;

Transfer 1g of the sample, weighed to the nearest 0.1mg, to a platinum dish. Add 5ml of HF and 10ml of HNO₃. Evaporate to white fumes to expel all HF. Transfer the sample to 200ml beaker, add 30ml of HNO₃, and 10ml of HClO₄. Cover the beaker, and heat until the solution becomes clear. Evaporate to dense white fumes. Cool, and approximately 50ml of water. Filter through a texture paper, and wash the residue with warm HCl (2+100). Transfer the residue to a platinum crucible, ignite, fuse with 2g of Na₂S₂O₇, and then add to the original solution. Transfer to a 100ml volumetric flask, and dilute exactly to the mark with water. Measure the absorption of an aliquat by an atomic absorption apparatus.

2-2 Result of Experiment

Original data obtained are shown in Table 2. About 600 data obtained are statistically analyzed, and the precision calculated by using ANOVA (nested design) are summarized in Fig. 1, Fig. 2, and Fig. 3 respectively. (See formulas (1), (2)

and (3)).

Repeatability (Error due to A.A. method only),

$$\sigma_E = \sqrt{v_E}, \quad \text{C.V.} \cdot \sigma_E = \sigma_E / \bar{x} \times 100 \quad \dots\dots\dots (1)$$

Repeatability (Error due to pretreatment),

$$\sigma_P = \sqrt{(v_L - v_P) / 4}, \quad \text{C.V.} \cdot \sigma_P = \sigma_P / \bar{x} \times 100 \quad \dots\dots\dots (2)$$

Reproducibility (Error among different laboratories),

$$\sigma_{\bar{x}} = \sqrt{\sigma_L^2 + \sigma_E^2 / 2 + \sigma_P^2 / 2}, \quad \text{C.V.} \cdot \sigma_{\bar{x}} = \sigma_{\bar{x}} / \bar{x} \times 100 \quad \dots (3)$$

2-3 Discussion

2-3-1 Repeatability within same laboratory

As is evident from Fig. 3, C.V. of repeatabilities (C.V. σ_E) are less than 10% except cadmium and lead. These inferior repeatability of the above two elements may be due to the contents of them closing to the detection limit of the A.A. method as shown in Table 3.(1) In such a case, pre-extraction procedure may be effective to improve the precision.(2)

2-3-2 Error due to pretreatment

As is evident from Fig. 1, C.V. of pretreatment (C.V. σ_P) for zinc is inferior than that of other elements. It suggests that volatility loss of zinc may be occurred during decomposition.

The supplemental experiment using seven samples, therefore, has been carried out to study the effect of pretreatment for the determination of zinc. The following three pretreatments have been compared on the zinc. In addition, nickel has also been determined from the same solution as a reference, because it has higher boiling point than that of zinc.

- 1) Low temperature ashing method.
- 2) High temperature ashing method.
- 3) Wet oxidation method employed on the above Round-Robin Study.

As is evident from Fig. 4 showing the effect of pretreatments, significant loss during incineration was observed technically compared to the wet oxidation method in case of zinc. On the other hand, no significant bias was observed among the three methods in case of nickel. Anyway, the volatility loss of zinc during pretreatment should be studied more precisely because it may results the inferior precision.

2-3-3 Reproducibility between different laboratories

As is evident from Fig. 2, the C.V. of reproducibilities (C.V. $\sigma_{\bar{x}}$) calculated using all of the data including outliers, were almost more than 20%. Even if the outliers are excluded, most of the elements still show inferior reproducibility.

3 Conclusion

- 1) The precisions (repeatability and reproducibility) on the determination of trace elements in coal and coke (zinc, nickel, chromium, copper, lead, cadmium, and vanadium) are insufficient on the viewpoint of coefficient of variance ($\sigma_x / \bar{x} \times 100$) on the most elements are more than 20% when outliers are not rejected.
- 2) C.V. of cadmium and lead are inferior because of substantial difficulties on the

A.A.method. That is, the contents of cadmium are close to the detection limit, and the lack of sensitivity for the determination of lead may cause these inferior precision respectively.

- 3) In case of the determination of zinc, the more precise studies on the pre-treatment should be carried out in the future.

Afterwords

These studies were carried out in Japan prior to the first international Round-Robin Study of ISO/TC 27/WG 14 (Trace elements). A part of the statistical analysis on the above experiment was reported in a document ISO/TC 27/WG 14, No. 6 (Japan-6).

Literature cited

- (1) "Atomic Absorption Spectrophotometry in the Steel Industry", The Iron and Steel Institute of Japan, (1975) P. 52 - P. 53.
- (2) "Round-Robin Studies for the Estimation of Accuracy and Precision of Pollution and Environment Control Analysis", The fourth SAC Conference (1977).

Table 1 Proximate Analysis of the Samples

% of the Air-Dried Coal and Coke

Samples	Moisture	Ash	*V.M.	**F.C.
U.S. Massey H.V. Coal	1.4	13.2	32.4	52.6
Japanese Miike Coal	9.9	6.5	38.3	54.2
Metallurgical Coke	0.1	11.6	0.5	87.8

* Volatile Matter ** Fixed Carbon

Table 2 Trace Elements in Coal and Coke

PPM in Air-Dried Whole Coal and Coke

(1) Sample ; U.S. Massey H.V. Coal

Lab.	Zn		Cd		Pb		Ni		Cr		Cu		V		
	P ₁	P ₂													
A	m ₁	29.0	17.2	0.26	0.26	5.15	3.83	11.2	11.9	15.2	17.2	16.9	16.5	34.3	30.4
	m ₂	27.7	17.2	0.13	0.26	6.47	5.15	10.6	10.6	17.2	17.2	15.3	15.3	29.0	27.1
B	m ₁	27.1	26.0	0.34	0.45	8.58	8.32	12.5	12.5	20.5	19.4	17.2	19.3	32.1	30.8
	m ₂	27.3	26.4	0.34	0.43	8.05	8.05	12.5	12.5	20.7	19.4	17.2	18.3	32.1	30.8
C	m ₁	11.6	23.0	<u>0.95</u>	<u>2.09</u>	4.22	0.26	18.6	12.7	14.7	22.7	16.6	26.6	30.6	33.4
	m ₂	12.0	20.7	<u>0.66</u>	<u>1.25</u>	5.15	8.18	9.6	12.4	19.5	23.4	17.2	14.5	23.2	26.0
D	m ₁	16.9	22.0	0.95	0.40	7.52	7.26	12.3	12.3	19.7	19.7	20.5	20.5	32.7	31.9
	m ₂	17.0	20.7	0.75	0.63	11.9	9.50	15.0	13.2	16.5	16.9	19.8	20.7	30.6	30.5
E	m ₁	23.9	18.6	0.48	0	10.6	11.9	<u>20.6</u>	<u>20.9</u>	<u>7.5</u>	<u>8.6</u>	21.6	23.5	25.2	28.1
	m ₂	21.6	18.6	0.48	0	10.6	11.9	<u>20.6</u>	<u>20.9</u>	<u>7.7</u>	<u>8.3</u>	20.9	21.9	25.2	29.1
F	m ₁	19.7	12.2	0.21	0.21	5.15	4.49	10.4	10.0	21.3	19.1	17.4	18.2	29.6	26.4
	m ₂	18.7	22.0	0.17	0.17	5.02	4.49	10.3	9.8	21.3	19.3	17.4	18.2	28.5	26.4
G	m ₁	21.8	18.1	0.32	0.18	3.34	5.41	11.9	11.5	17.7	18.9	19.0	16.8	31.2	31.9
	m ₂	21.6	18.2	0.26	0.22	2.38	5.68	12.1	11.7	17.4	18.5	18.5	16.4	31.2	31.7

p ; pretreatment , m ; measurement

— Outliers

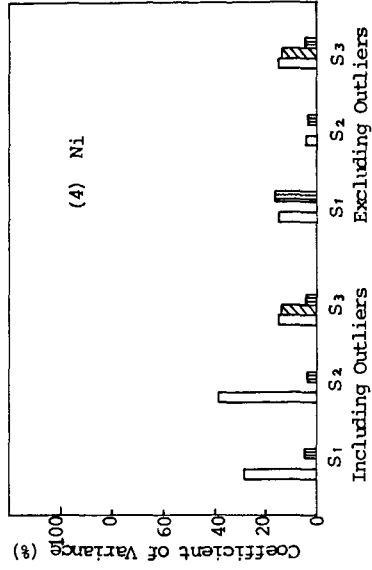
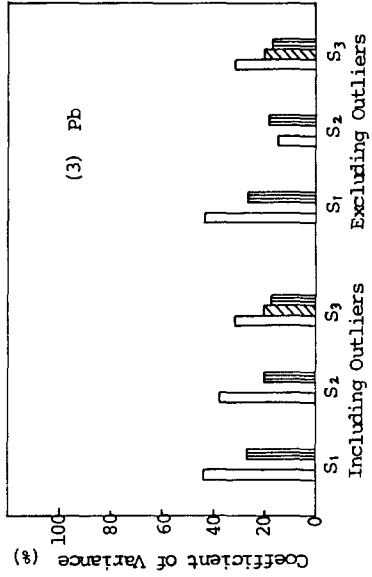
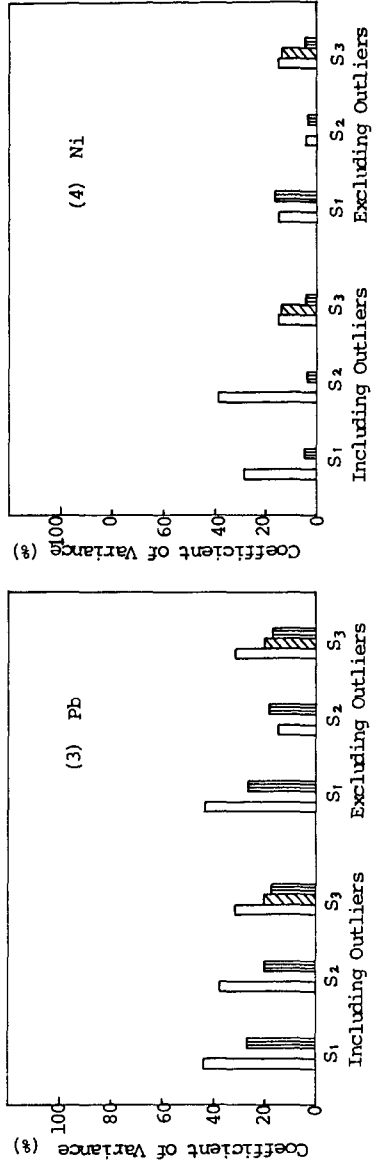
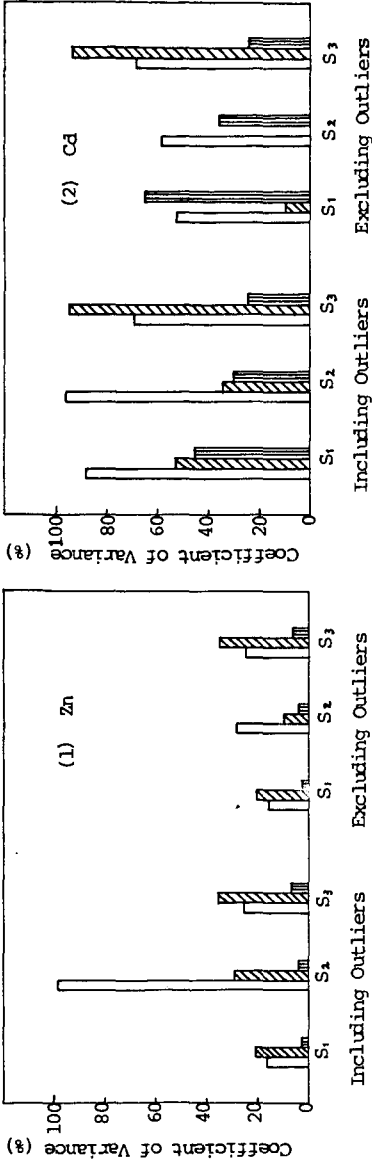
Table 2 Concluded

(2) Sample ; Japanese Miike Coal

Lab.	Zn		Cd		Pb		Ni		Cr		Cu		V	
	P ₁	P ₂	P ₁	P ₂	P ₁	P ₂	P ₁	P ₂	P ₁	P ₂	P ₁	P ₂	P ₁	P ₂
A	m ₁	3.58 3.90	0.13 0.13	3.19 1.89	18.9 18.5	8.45 8.45	5.72 5.59	<u>4.55</u> <u>4.55</u>						
	m ₂	2.93 3.58	0.07 0	3.19 3.19	18.5 18.5	8.45 8.45	5.07 5.07	<u>4.55</u> <u>4.55</u>						
B	m ₁	<u>27.0</u> <u>26.7</u>	0.20 0.21	2.99 3.51	20.3 20.6	10.4 9.62	6.24 6.50	7.15 7.15						
	m ₂	<u>27.1</u> <u>26.8</u>	0.20 0.21	3.06 3.45	20.2 20.5	10.4 9.55	6.24 6.31	7.22 7.02						
C	m ₁	<u>35.4</u> <u>21.5</u>	<u>0.56</u> <u>0.81</u>	3.25 3.45	49.4 7.5	8.13 11.0	5.59 5.46	4.62 6.96						
	m ₂	<u>23.8</u> <u>23.1</u>	<u>0.39</u> <u>0.73</u>	2.21 1.56	22.8 13.0	9.75 11.4	5.72 6.24	4.75 10.9						
D	m ₁	4.29 4.36	0.18 0.20	<u>4.42</u> <u>4.03</u>	19.9 19.8	9.43 10.9	6.50 6.63	5.92 6.57						
	m ₂	4.42 4.36	0.31 0.34	<u>5.33</u> <u>5.33</u>	22.1 21.4	8.84 9.10	6.37 6.37	4.75 5.92						
E	m ₁	5.20 4.10	0.12 0.12	3.90 3.25	25.3 23.7	<u>2.86</u> <u>2.86</u>	6.70 6.70	4.68 8.00						
	m ₂	4.75 4.23	0.12 0.12	3.90 3.25	25.3 25.3	<u>2.86</u> <u>2.86</u>	6.70 6.63	8.00 4.86						
F	m ₁	4.55 4.42	0.07 0.07	3.25 2.80	19.3 19.0	9.62 10.7	5.59 5.72	<u>4.23</u> <u>4.23</u>						
	m ₂	4.55 4.36	0.07 0.07	3.38 2.80	19.2 19.2	9.69 10.5	5.66 5.86	<u>4.42</u> <u>4.23</u>						
G	m ₁	9.00 6.50	0.10 0.10	<u>0.78</u> <u>1.56</u>	13.7 14.0	9.62 9.69	5.66 6.11	5.98 6.50						
	m ₂	7.67 6.50	0.11 0.11	<u>1.56</u> <u>1.76</u>	14.0 13.3	8.71 8.58	8.85 6.11	5.98 6.50						

(3) Sample ; Metallurgical Coke

Lab.	Zn		Cd		Pb		Ni		Cr		Cu		V	
	P ₁	P ₂												
A	m ₁	24.4 14.5	0.23 1.16	4.52 5.68	41.8 43.5	22.6 19.1	24.4 24.4	47.6 46.4						
	m ₂	24.4 13.3	0 1.16	6.73 7.89	40.6 42.3	22.6 20.9	21.8 22.9	55.1 51.0						
B	m ₁	16.2 16.0	0.25 0.34	5.92 6.38	44.7 44.7	24.9 24.0	24.9 25.8	55.3 54.9						
	m ₂	16.2 16.2	0.24 0.34	6.03 6.38	44.4 45.2	25.1 24.0	24.9 25.8	55.1 54.3						
C	m ₁	10.2 12.1	0.37 1.30	4.41 2.20	78.3 7.0	19.7 34.8	24.2 21.5	30.2 45.8						
	m ₂	10.3 17.6	0.41 1.31	6.73 4.87	41.8 23.2	20.3 24.4	24.8 24.0	36.0 48.7						
D	m ₁	15.2 13.5	0.43 0.38	9.05 9.63	44.3 44.3	22.9 21.9	26.8 26.9	56.0 53.2						
	m ₂	14.6 13.9	0.58 0.57	10.4 8.70	50.6 50.2	18.7 21.7	25.8 25.8	55.3 55.0						
E	m ₁	16.7 15.3	0.42 0	9.28 5.92	48.4 50.7	7.5 7.5	28.8 28.8	41.8 42.8						
	m ₂	16.1 15.3	0.42 0.21	6.96 5.92	51.2 54.8	7.5 7.5	28.8 29.0	33.4 34.1						
F	m ₁	14.0 13.9	0.14 0.14	4.99 4.64	47.8 71.3	27.8 25.3	25.9 25.3	50.8 51.3						
	m ₂	14.0 13.9	0.21 0.21	4.99 4.87	48.0 71.6	27.5 24.9	25.9 25.5	49.9 52.0						
G	m ₁	15.3 15.5	0.17 0.21	6.26 2.09	39.9 40.4	23.3 23.9	24.8 24.1	61.2 49.2						
	m ₂	15.5 15.1	0.15 0.19	5.92 1.74	39.4 39.4	23.0 23.9	26.4 26.0	55.2 58.0						



□ Repeatability C.V. σ_r , ▨ Repeatability C.V. σ_p , ▩ Repeatability C.V. σ_w
 Sample: S₁; U.S. Massey H.V. Coal, S₂; Japanese Miike Coal, S₃; Metallurgical Coke

Fig. 1 Precision on the Determination of Trace Elements

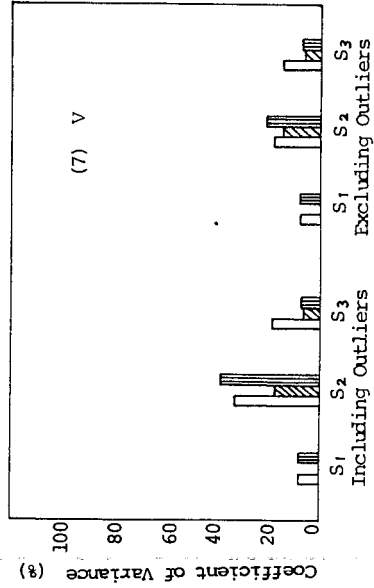
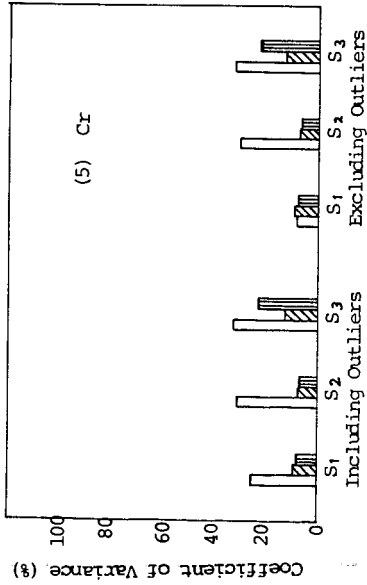
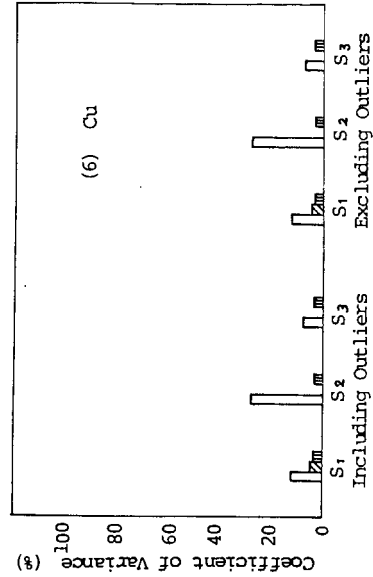


Fig. 1 Concluded

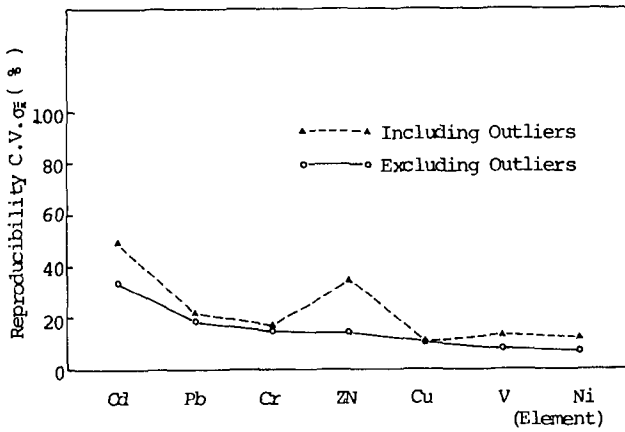


Fig. 2 Error among Different Laboratories

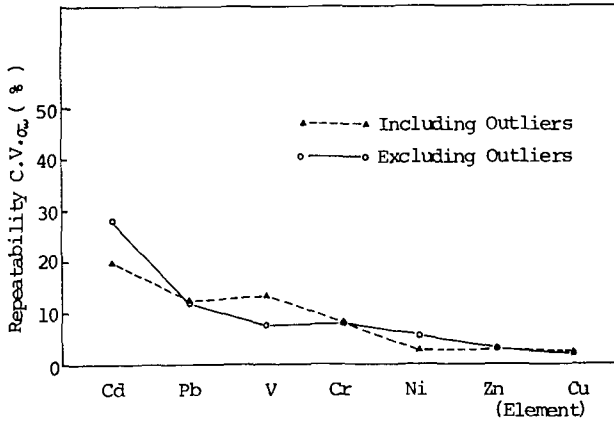
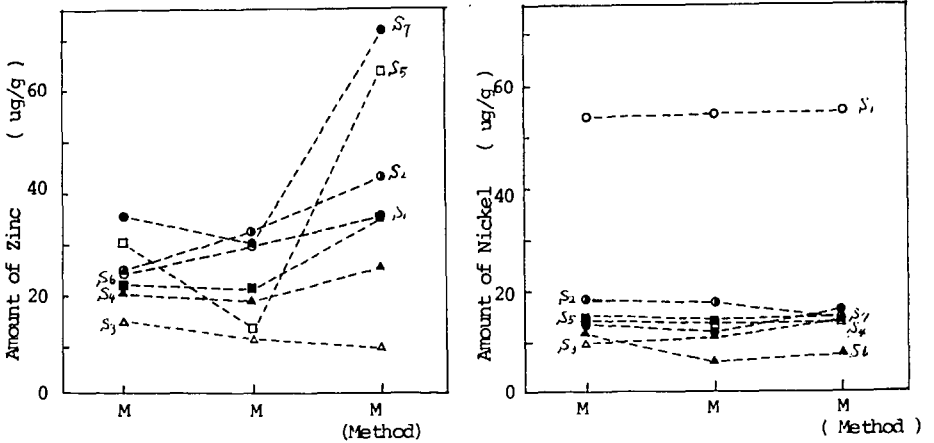


Fig. 3 Error due to Atomic Absorption Analysis

Table 3 Detection Limit and Sensitivity of the Atomic Absorption Method

Element	Line Å	Detection Limit µg/ml	Sensitivity 1% Absorption µg/ml	Analytical Rang of Sample µg/ml
Zn	2138	0.02	0.04	0.1~0.2
Cd	2288	0.002	0.02	0.02~0.04
Pb	2833	0.03	0.5	0.03~0.07
Ni	2320	0.005	0.1	0.06~0.2
Cr	3579	0.003	0.08	0.03~0.2
Cu	3247	0.005	0.1	0.06~0.2
V	3514	0.04	1.3	0.06~0.3



M₁: Low temperature ashing method, M₂: High temperature ashing method
M₃: Wet oxidation method
S₁: Metallurgical coke, S₂: Hongeil coal, S₃: Beatrice coal, S₄: Vicary coal
S₅: Pittoston coal, S₆: Black water coal, S₇: Yutoku coal

Fig. 4 Comparison of Analytical Values of Zinc and Nickel in Coal and Coke by Three Decomposition Method

Trace Element Variations in an
Oil-Shale Retorting Operation

Thomas R. Wildeman
Department of Chemistry/Geochemistry
Colorado School of Mines
Golden, Colorado 80401

and

Robert N. Heistand
Development Engineering Inc.
Box A, Anvil Points
Rifle, Colorado 81650

Experiments were conducted jointly between Colorado School of Mines (CSM) and Development Engineering, Inc. (DEI) using raw shale feed to the Paraho Semi-Works retort. (1,2) A schematic diagram of the 10-1/2 foot O.D. Semi-Works retort is shown in Figure 1. The Direct Mode operation, where combustion occurs within the retort to provide necessary heat, is portrayed in this schematic diagram. Operations are continuous and flows are countercurrent. Gases flow upward. The downward flow of shale is controlled by a hydraulically-operated grate mechanism. Shale is distributed evenly across the top of the bed by a rotating distributor. Here, the shale is preheated by rising hot gases in the mist formation zone. Next, the preheated shale passes through the retorting zone where the organic kerogen is decomposed into oil, gas, and coke. The coke remaining on the retorted shale serves as fuel in the combustion zone. Air is distributed evenly across the bed in an air-gas mixture in this zone. In the lower section of the retort, the shale is cooled by bottom recycle gas and this gas, in turn, is preheated before entering the combustion zone. The oil, as a stable mist, is carried out the top of the retort through the off-gas collector and is separated from the gas in a coalescer-electrostatic precipitator system.

In the Indirect Mode operation, the gas blower is replaced by an external heater. The middle and upper recycle gas is passed through this heater to provide heat needed for retorting. In this mode, the product gas is not diluted with products of combustion and nitrogen from the air, and the carbon remaining on the retorted shale is not utilized.

Uniform flow of solids and gases within the retort is essential in order to maintain a continuous operation and a high efficiency. In the Paraho Semi-Works retort, the bottom grate, the air-gas distributors, and the rotating shale distributor are designed to assure uniform flows. In addition, the raw shale feed is carefully screened and handled to a uniform feed. Feedstock for the retort consists of + 1/2 inch to - 3 inch nominal size. Fines and non-uniform shale size can result in gas channeling, high pressure drops, and uneven bed temperatures. These problems cause low oil yields and could, eventually, result in a retort shutdown. In addition to providing good operations and high efficiencies within the retort, the resulting lump-size retorted shale reduces considerably the environmental impact caused by dusting.

Although lump-size feed improves retort operation, minimizes environmental impacts, and reduces crushing costs, this feed creates problems in securing a representative sample for laboratory analysis. A raw

shale sampling system was designed to meet the accepted criteria for sampling this lump-size, non-homogeneous material. (3) A diagram of the Paraho sampling system is shown in Figure 2. A motorized gate diverts flow from the retort at preset intervals (usually 30-50 minutes). Approximately 200 pounds of material is taken in a single cut. The sample is crushed to -3/4 inch and passed through a four-stage splitter. The retained sample is crushed to - 1/4 inch and passed through a second four-stage splitter. This system provides a 24-hour composite laboratory sample (20-30 lbs, - 1/4 inch) from the 2 1/2-4 tons of the lump material sampled from the raw shale feed. An examination of the Paraho raw shale sampling system showed it to be unbiased. (4) Careful analyses of the grade (gallons oil/ton shale) indicated no significant differences between reject streams A and B and the laboratory sample. This laboratory sample was used in the studies presented in this paper.

Sampling Program

The objective of this research is to determine the concentrations of trace elements in the Paraho oil-shale feedstock and to study the fate of those trace elements during retorting. Elements of particular interest are B, F, As, Se, and Mo (5). In this regard, sampling the Paraho feedstock presents a problem. Lumps of rock -3 inches to +1/2 inch in size is not an ideal size of sample. One or two lumps is all that would be needed for most analyses, but that can hardly be considered representative. However, if the Paraho sampler were used to secure a sample, the amount would be about 6 kg. The sample is obviously physically heterogeneous. Does this also mean that it will be chemically heterogeneous? In addition, mining, hauling, crushing and retorting are a continuous operation at Anvil Points, little stockpiling is done. Does this mean that feedstock sampled on one day will differ significantly from that used in the retort on another day? Fundamental sampling questions such as this require a sampling program that is based on a strong foundation of statistical theory.

The statistical model followed in the sampling was a hierarchical or nested analysis of variance (6,7). In this case, one month of 30 days in which the retort was operating was subdivided or nested into 24 hour, 8 hour, and 1 hour periods. Of these 30 days, 6 were chosen as test days. Samples were taken on each of the three 8 hour periods. Then, on one randomly chosen 8 hour shift, eight 1 hour samples of oil shale feedstock were taken. This nested sampling design is shown in Figure 3. Now, for some constituent, such as iron, if all the samples were the same then

$$\text{concentration of Fe}_i = \mu_{\text{Fe}} \quad (1)$$

where μ_{Fe} is the mean of Fe concentrations and i designates the i^{th} sample. This is not the case. There can be a deviation or error due to the time in which the sample was taken and the imprecision of the analysis. So the equation 1 becomes

$$\% \text{Fe}_{ijkm} = \mu_{\text{Fe}} + \alpha_i + \beta_{ij} + \gamma_{ijk} + \delta_{ijkm} \quad (2)$$

Mean + 24 hr + 8 hr + 1 hr + analysis

where i designates the retort day and α_i is the deviation from the mean due to the sample being taken on that day. Similarly, β_{ij} represents the deviation due to the sample being taken in the j^{th} 8 hr shift of the i^{th} day, γ_{ijk} means the same for the 1 hr period; and δ_{ijkm} is the error for the analysis. By carefully setting up a nested sampling design and randomly selecting the sampling periods, an estimate of magnitude of the error or deviation for each time

period can be obtained. Certainly, if more periods were sampled, the estimates of error would be better, but the design choice is such that a minimum of samples yields meaningful estimates on all the error parameters.

One can not actually determine the errors and deviations; but if the sampling design is properly constructed, estimates of the errors can be estimated (6,7). Such an estimate is called a variance, the variance equation corresponding to equation 2 is

$$s_{Fe}^2 = s_{\alpha}^2 + s_{\beta}^2 + s_{\gamma}^2 + s_{\delta}^2 \quad (3)$$

These variances are similar to estimates of the standard deviation but in this case, the variance is partitioned among several components. The partitioning of the variance allows the following questions to be answered:

1. Is the mean of all the samples representative of the whole retort month or is there a trend over the month?
2. Is there significant scatter in any one of the 24 hr; 8 hr; or 1 hr time periods?
3. Are the analytical procedures precise enough or do they contribute to most of the scatter in the concentration values?

Analysis Program

DEI performed the Fischer assay analyses by a procedure that has been described previously (4). The precision of the analyses has been determined to be 2% relative standard deviation for the oil yield and 15% and 20% relative standard deviation for the water yield and gas plus loss yield. All 70 oil shale feedstock samples that were collected were analyzed for oil yield.

The elemental analyses were done by energy dispersive x-ray fluorescence (EXRF) analysis. The details of the analytical procedure have been previously published (8,9). In this procedure, four samples were chosen for analysis in each of the six hourly sample sections and three of the eight hour shift samples were analyzed for each day for a total of 37 samples. Also, duplicates of eight samples were analyzed to determine the variance of the analysis procedure. The relative standard deviation for the analysis for each element is listed in Table I. They range from above 10% for light elements to below 5% for heavier elements. These results are typical of the precision of the EXRF method. Comparison of analyses of NBS standard coal (SRM 1632) and round robin analyses done on oil shales show the accuracy of the analyses to be within $\pm 10\%$ (10,11). K and Se concentrations do not compare well with other analytical methods; the results are aberrant by about 30%.

Results and Conclusions

In Table I, the results for the Fischer assays and EXRF analyses are listed. The average, mean, range, standard deviation of the mean, and relative standard deviation of the mean are based on all samples. The average analysis relative standard deviation is based on the variations found in the eight samples for which multiple analyses were performed. The percent of variance for 24 hr, 8 hr, 1 hr and analysis level is determined from the analysis of variance program. The meaning of the variances requires an explanation.

For each level (i) analytical, 1 hour, 8 hour, 24 hour, and analysis,

a variance S_i^2 is determined for each element. Then, the percent of total variance for the level for the concentration of Fe is:

$$\% (S_{Fe})_i^2 = \left(\frac{(S_{Fe})_i^2}{\sum_{i,j,k,m} (S_{Fe})_n^2} \right) \times 100$$

This parameter measures where the majority of the variation lies for each concentration in the 4 level sampling scheme design. For example, for oil yield, the % variance is greatest on the 24 hr level, the value being 63%. This implies that the samples taken on the 1 hr and 8 hr periods each day did not change significantly with respect to the day-to-day changes. Thus, the samples taken on one day are appreciably different from the samples taken on other days. The 24 hr averages for oil yield for the 6 days were 23.8, 25.8, 30.4, 24.5, 31.2, and 26.9 gallons per ton respectively. The daily variation is readily apparent. For day 3 where the 24 hr average is 25.8, the 8 hr oil yields are 25.2, 26.7, and 25.4 gpt and the 1 hr oil yields are 25.5, 22.4, 27.8, 21.2, 26.7, 27.4, 25.3, and 25.0 gpt. These results are about typical. The tight range of the 8 hr samples is obvious; the 1 hr samples range a bit more but not as much as the daily averages. The percent of variance for the 1 hr level is 37%. Thus, the percent of variance is a measure of how much scatter there is in the concentration of a substance at each level.

The first conclusion that appears from the results in Table I is that the oil yield measurably changed from day to day. The percent of variance is 63% for the daily level, 0% for the 8 hr level, and 37% for the 1 hr level. The oil yield is a reasonable measure of the organic content of the shale. So, this implies that for the retort month there were measurable differences from day to day in the organic content. This also implies that an average organic content for the month is probably not meaningful, but that a daily average for organic content can be reasonably estimated.

The elemental concentration results show these samples to be quite interesting. A geochemist would expect concentration ranges for trace elements to range by about a factor of 10 over a section of a formation. Here the range is only a factor of 2. For some elements like Rb and Sr, the relative standard deviation over all the samples is less than 10%. For most of the elements, the analytical precision is at 10% or less. This can be considered to be quite respectable for a multi-element analytical technique. Nevertheless, for Ca, Mn, Fe, Cu, and Se the analytical precision contributions most of the error as can be seen by the percent of variance for the analysis for these elements. This implies that more precise techniques should be used to obtain the concentrations of these elements in oil shale. Finding techniques with uniform precision significantly below 10% is difficult. For none of the elements does the daily or 8 hr percent of variance exceed 33%. This implies that a representative sample for the retort month for the inorganic elements can be calculated. The grand mean for each element represents a reasonable average for the whole month. For the elements listed, the results are not statistically different from those of other laboratories who were conducting other experiments at Anvil Points at the same time. So thus, the mean concentration values for the elements represent an accurate estimate of the feedstock that month within the constraints of the analytical scheme and the sampling design.

The contrast in conclusions for the organic and inorganic portions of the oil shale feedstock is obvious. Since great care was taken in the consideration of the sampling design, one has to conclude that this difference is real. To test this further, the concentration of all the substances listed in Table I for all the samples analyzed were tested by a linear correlation program. The results for the correlation coefficients are listed in Table II. None of the coefficients relating the oil yield to the elements rises above 0.5. This also shows the basic dissimilarity between organic and inorganic portions of this oil shale.

Several implications arise from this organic and inorganic difference. The primary conclusion is that on a production level none of the above elements vary in the same general way as the organic content of the oil shale. This conclusion allows the situation of variability in layers in the formation; but if there is mining, then hauling and crushing blend out any variations. This conclusion also will allow the possibility of some minor amount of an element such as As or Pb to be associated with the organic portion of the shale but the majority of amount of that element cannot be associated with organics in the shale. Another implication of this dicotomy is that the results of analyses on the organic content which would typically be performed by an oil analysis laboratory will not yield information about the inorganic elements. This implication means that specific analyses for the inorganic elements will have to be made if their concentrations are of interest. Fortunately, the results shown for Table I for the inorganic elements show the feedstock to be quite uniform. This means that careful analysis of a sample taken once a week will yield more information on elemental concentrations than less accurate analyses taken on samples collected every hour or every shift.

References

1. Jones, J. B., Jr. (1977) Technical Evaluation of the Paraho Process, 11th Israel Conf. on Mechanical Engineering, Technion, Haifa, Israel.
2. Jones, J. B., Jr. (1976) The Paraho oil-shale retort. Quart. Colo. School of Mines, vol. 71, No. 4, pp. 39-48.
3. Taggart, A. F. (ed.) (1967) Handbook of Mineral Dressing, J. F. Wiley & Sons, New York,
4. Heistand, R. N. (1976) The Fischer Assay: Standard for the oil shale industry. Energy Sources, vol. 2, pp. 397-405.
5. Chappell, W. R. (1978) Toxic trace elements and shale oil production. Proc. 11th Oil Shale Symp. Colo. School of Mines, Golden, CO., In Press.
6. Miesch, A. T. (1976) Sampling designs for geochemical surveys-syllabus for a short course. U. S. Geol. Survey, Open-File Report 70-772, 132 pp.
7. Miesch, A. T. (1976) Geochemical survey of Missouri - Methods of sampling, laboratory analysis, and statistical reduction of data. U. S. Geol. Survey Prof. Paper 954-A, 39 pp.

8. Alfrey, A. C., Nunnelley, L. L., Rudolph, H., and Smythe, W. R. (1976) Medical Applications of small x-ray Fluourescence System. In: Adv. in X-ray Analysis, vol. 19, Kendall/Hunt, Dubuque, Iowa, pp 497-509.
9. Kubo, H., Bernthal, R. and T. R. Wildeman (1978) Energy dispersive x-ray fluourescence spectrometric determination of trace elements in oil samples. Anal. Chem., vol. 50, pp 899-903.
10. Wildeman, T. R., and Meglen, R. R., (1978) The analysis of oil-shale materials for element balance studies. In. Analytical Chemistry of oil shale and tar sands, Adv. in Chem. Series.
11. Fox, J. P., Fruchter, J. S., and T. R. Wildeman (1979) Inter-laboratory study of elemental abundances in raw and spent oil shales. Oil shale sampling, analysis and quality assurance symposium. March 26-28, 1979, Denver, Colorado.

Table I. Concentration parameters of Paraho oil shale. The sampling period is from August 23, 1977 through September 20, 1977.

Substance	Conc. Unit	Grand Mean	Grand Standard Deviation	Grand Rel. Std. Dev. %	Range	Avg. Analysis Rel. Dev. %	% OF VARIANCE			
							24 hr Level	8 hr Level	1 hr Level	
Oil	gpt	27.0	3.2	11.9	22-39	2	63	0	37	-
Water	gpt	4.4	1.7	39	1.6-11.4	15	0	93	7	-
Gas & Loss	gpt	2.2	0.6	28	1.0-3.7	20	0	26	74	-
Ca	%	12.3	1.5	12	7.2-15	13	3	0	0	97
Mn	ppm	313	34	11	191-380	10	12	0	0	88
Fe	%	2.13	0.21	10	12.2-25	9.2	6	0	0	94
Ni	ppm	32	3	9.5	18-36	6.6	0	0	55	45
Cu	ppm	35	4	10.1	20-40	6.6	8	22	2	68
Zn	ppm	83	24	29	40-180	9.8	14	0	68	18
Ga	ppm	7.0	0.8	12	4-8	7.6	18	0	32	50
As	ppm	44	5.6	13	26-58	8.7	25	0	23	52
Se	ppm	1.5	0.26	17	1.0-2.3	15	7	0	0	93
Rb	ppm	80	6	7.4	45-85	1.7	24	0	73	3
Sr	ppm	770	66	8.6	410-830	2.2	32	0	62	6
Y	ppm	12	1.2	10.6	6.2-14	4.9	8	0	49	43
Zr	ppm	56	14	25	26-120	8.3	10	0	80	10
Nb	ppm	5.7	0.5	9.7	3.3-6.6	2.4	19	0	72	9
Mo	ppm	23	2.5	10.8	13-28	2.3	0	0	89	11
Ba	ppm	480	67	14	240-670	1.7	14	0	84	2
Pb	ppm	24	3.1	13	15-35	3.2	0	26	65	9

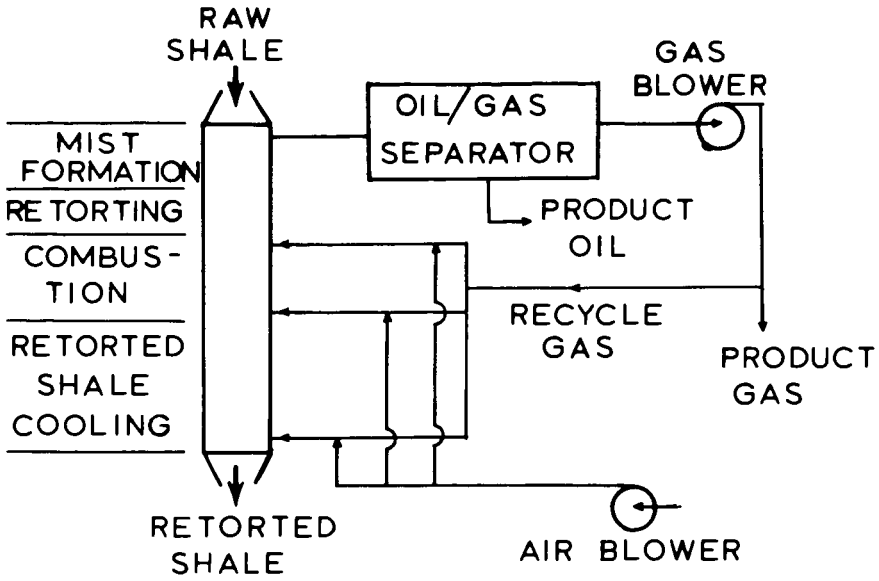


FIGURE 1. SCHEMATIC OF PARAHO RETORT FOR THE DIRECT HEATED MODE.

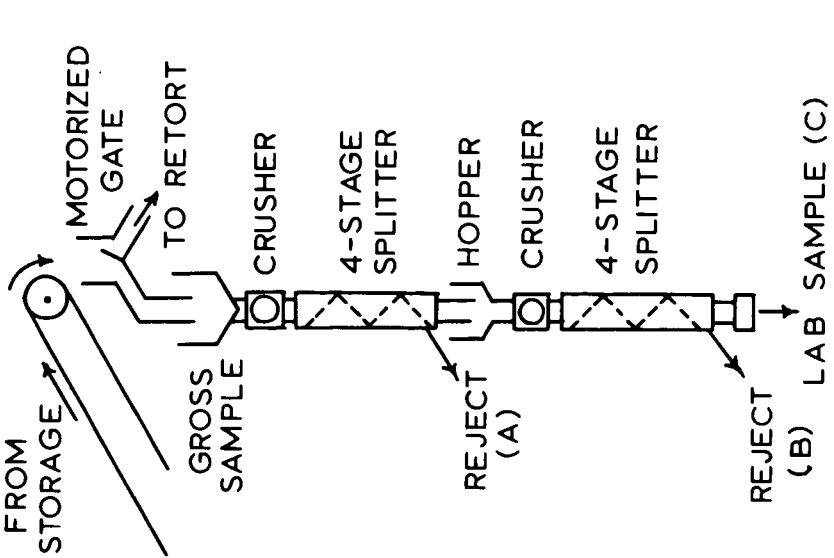


FIGURE 2. FEEDSTOCK SAMPLING SYSTEM FOR THE PARAHO RETORT.

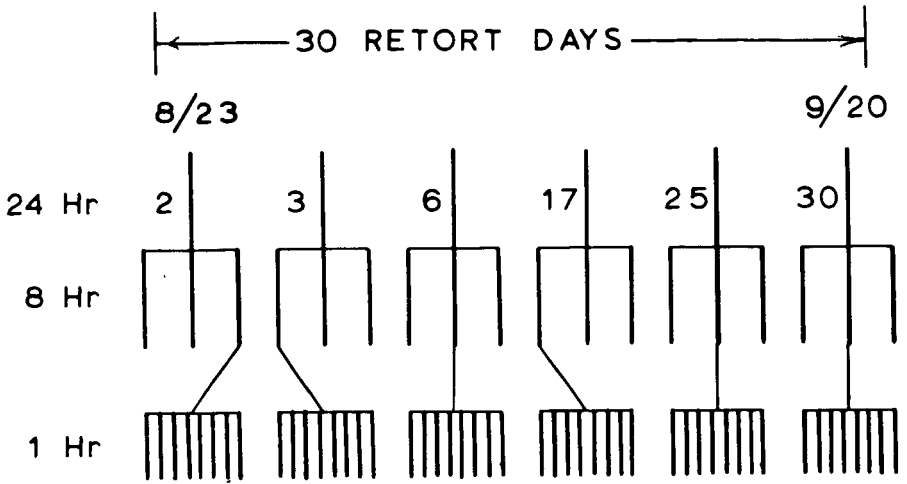


FIGURE 3 TIME NESTED PARAHO SAMPLING DESIGN.

Aromatic Nitrogen Compounds in Fossil Fuels - A Potential Hazard?

C.-h. Ho, B. R. Clark, M. R. Guerin, C. Y. Ma,¹ and T. K. Rao*

Analytical Chemistry and Biology Divisions*
Oak Ridge National Laboratory, Oak Ridge, TN 37830

Introduction

To achieve energy independence in the United States, converting coal to oil or extracting oil from shale will be required. Before commercial scale fossil fuel conversion facilities become a reality, chemical and biological studies of currently available synfuel samples derived from coal or shale are urgently needed in order to determine what the potential health problems, such as from occupational exposure, might be.

The nitrogen content either of shale oil (1-2%) (1) or coal derived oil (1-1.5%) (2) is far higher than that in petroleum (average N-content in petroleum is 0.05-0.1%) (3). This means enormous amounts of nitrogen containing species will be produced and found in crude synfuels, and this could lead to significant health or environmental impact. Clearly, a thorough characterization of nitrogen compounds in synfuels is an important pursuit.

Aromatic nitrogen compounds such as basic aza-arenes, neutral aza-arenes, and aromatic amines are considered environmentally important and several members of these classes of compounds possess biological activity. For example, dibenz(a,h)acridine, 7 H-dibenzo(c,g)carbazole, and 2-naphthylamine (4), are well known as carcinogens. In this paper, the methods used to isolate the basic aromatic nitrogen compounds and neutral aza-arenes from one shale oil and one coal-derived oil will be discussed. The mutagenic activities of these fractions, based on the Ames Salmonella typhimurium test, will be compared.

Experimental

Samples

A shale oil was obtained from the Laramie Energy Research Center's 150-ton retort operated for above ground simulation of *in-situ* retorting. The raw oil from the retort was an intimate emulsion of solids, water and oil; the emulsion was collapsed by centrifugation at 2500 RPM for about 20 min. at room temperature. Three phases were produced: an oily top phase (~50% vol.), a gelatinous intermediate phase (~20% vol.), and an aqueous phase (~30% vol.). The oil phase has been studied in this laboratory (5,6) and similar samples from other retort runs have been examined by others, principally by workers at the Laramie Energy Research Center (1,7,8).

A crude coal liquid (not necessarily representative of any final production scale product) was obtained from the Pittsburgh Energy Research Center. This material was very viscous, contained no water, and had a small amount of filterable solids (>5 μ m range).

Separation Procedures

Neutral aza-arenes. Figure 1 shows the separation scheme for isolation of neutral aza-arenes from synfuels. After removing acidic and basic components from the whole sample, the neutral fraction was loaded onto a Sephadex LH-20 gel column. The column was eluted sequentially with 250 ml of isopropanol (Fraction AP) and 600 ml of acetone (Fraction AROM). Pentadecane and naphthalene were used to indicate the appropriate cut between elution of aliphatic compounds and 2-ring aromatic compounds.

¹Faculty Research Member, University of Mississippi.

Acetone was removed from Fraction AROM and the residue was separated into three sub-fractions on a silicic acid column: Fraction I (PAH), eluate from 1200 ml benzene/hexane (1/3); Fraction II (neutral aza-arenes), eluate from 600 ml benzene/hexane (2/1); and Fraction III (polar), eluate from 600 ml ethanol. A mixture of a number of PAH compounds (pyrene, C¹⁴-carbazole and 7 H-dibenzo(c,g)carbazole) were chromatographed in establishing this procedure.

Basic components. Basic fractions of the oils were produced by first dissolving the oils in diethyl ether and extracting the acids with a 1 M NaOH solution. A second extraction with 1 M HCl removed the basic components which were further partitioned between an aqueous/ether phase at pH 11. The basic fractions are contained in this ether phase. Further details of this procedure are reported elsewhere (9). Figure 2 shows the subfractionation scheme used to further separate basic fraction constituents. The basic fraction was placed onto a basic alumina column. The column was eluted with 500 ml benzene (benzene subfraction) followed by 700 ml ethanol. Ethanol was removed and the residue was separated further on a Sephadex LH-20 gel column. The column was eluted sequentially with 250 ml of isopropanol (isopropanol subfraction) and 600 ml of acetone (acetone subfraction).

Column packings and reagents. Basic alumina (100-200 mesh, AG-10, Bio-Rad Laboratories), Sephadex LH-20 gel (25-100 μ , Pharmacia Fine Chemicals) and silicic acid (100 mesh, Mallinckrodt, washed successively with hexane, acetone, and methanol; activated in 150°C oven for 16 hours) were used for column packings. Forty grams of alumina were added to 75 ml of benzene in a modified 50 ml buret column. A Sephadex column was prepared by swelling 75 g of the gel in isopropanol with sufficient excess to form a pourable slurry. The slurry was poured into the 250 ml buret column and allowed to compact by the gravity elution of 50-100 ml of isopropanol. A silicic acid column was made by pouring a slurry of 100 g of silicic acid in hexane into a 2.5 cm (O.D.) x 50 cm glass column.

All solvents were reagent grade and were freshly distilled except for the absolute ethanol. Reagents prepared for the microbial mutagenesis bioassay are described elsewhere (10,11).

GC/MS

GC/MS data were obtained using a Perkin-Elmer Model 3920 gas chromatograph interfaced to a DuPont 21-490B mass spectrometer via a glass jet separator. An effluent splitter provided about a 2:1 split between the mass spectrometer and a flame ionization detector, respectively. A Hewlett-Packard 21-094B data system interfaced to the mass spectrometer provided for the generation of mass spectra, mass chromatograms, library searches, etc. A glass GC column of 20 ft. x 1/8-in. O.D. was packed with 3% Dextsil 400 on 100/120 mesh Chromosorb 750 and installed with graphite ferrules. GC temperature programming was from 100°C (8 minutes hold) to 320°C at a linear rate of increase of 1°/min. Injector and detector temperatures were set at 320°C, helium gas inlet pressure at 100 psig, MS ionization voltage at 70 eV, mass scan rate at 2 seconds/decade and the MS resolution at about 600.

Microbial Mutagenesis Assay. Salmonella typhimurium bacteria, strain TA98, were generally employed. The experimental procedures are described by Ames et al. (10). Briefly, the bacteria are added to a soft agar containing nutrients and in some cases, enzyme activation preparations along with the substance being tested. The essential condition is that the amino acid, histidine, is absent. The suspension, containing approximately 2×10^8 bacteria, is overlaid on minimal agar plates and incubated. If the test substance is a mutagenic agent in this system, then large colonies (which have reverted to the wild type) are evident on the plate and can be counted, i.e., by mutation they can produce their own histidine and grow in a

histidine-free medium. If no colonies form except for a control background level, then no mutations have occurred. A test consists of assays at several concentrations of test substance in order to obtain a dose-response curve. Some potential mutagens require metabolic activation with liver homogenate preparations.

Results and Discussion

Neutral Aza-arenes

The procedures used for the isolation of neutral aza-arenes from synthetic crude oils evolved in part from an extraction scheme and a gel filtration chromatographic scheme (5, 12) developed in this laboratory. The silicic acid adsorption chromatography step was developed by Snook et al. (13) to isolate indole/carbazole from cigarette smoke condensate. But the silicic acid chromatography has been evaluated and some modifications have been made to make the system compatible with a gravity flow column. A good separation between PAHs and neutral aza-arenes was achieved by eluting the column with 1/3 (benzene/hexane) followed by 2/1 (benzene/hexane). However when large quantities of aliphatic compounds are present in the sample, these contaminate all the eluate fractions. It is necessary to remove major portions of aliphatic components prior to the silicic acid step. Gel filtration chromatography with a Sephadex LH-20 column eluted with isopropanol is effective for removing a major portion of aliphatic and polymeric compounds while retaining aromatic compounds of two rings and higher. Further elution of the column with acetone results in the quantitative recovery of aromatic components in order of increasing aromaticity (5). Silicic acid chromatography produced a relatively pure neutral aza-arene fraction (Fraction II), suitable for GC/MS analysis and bioassay. The separation of PAH and neutral aza-arene fractions was further confirmed by a chromatographic study of oil samples spiked with large excesses of benzo(a)pyrene along with carbazole. Tracer studies of oil samples spiked with C^{14} -carbazole showed that carbazole was not eluted from the column with even as much as 1600 ml 1/3 (benzene/hexane). The recovery of C^{14} -carbazole from the silicic acid column with 2/1 (benzene/hexane) was 97% for the coal derived oil and 75% for the shale oil. This agrees well with data on cigarette smoke condensate (13).

The presence of indole/carbazole analogues in Fraction II from both oil samples is also supported by their IR spectra. These fractions have a sharp band at 3430 cm^{-1} which is normally found in the IR spectrum of carbazole and is characteristic of the N-H group in these compounds.

In a peak by peak comparison of GC profiles of Fraction II obtained with an FID and an NPD, we found the majority of the GC peaks were nitrogen containing compounds.

The proton NMR spectrum of Fraction II gave a ratio of aliphatic protons to aromatic protons close to unity (1.06) indicating that only a few alkyl groups are contained in Fraction II. This result seems to be consistent with the observation from GC/MS analysis in which the biggest alkyl substituent was six carbons.

The odd m/e values of molecular ions obtained from GC/MS data confirmed the predominant presence of nitrogen compounds in Fraction II. Tentatively identified components are C_1 - C_3 phenylpyrroles, indole, C_1 - C_6 indoles, C_1 - C_3 phenylindoles, carbazole, C_1 - C_5 carbazoles, benzocarbazoles, and C_1 - C_3 benzocarbazoles.

The weight distribution of aliphatic and aromatic subfractions are listed in Table 1. N-heterocyclic material is much less than aromatic hydrocarbon material in the shale oil. The quantities of carbazole in the original oil samples were estimated by external standard calibration based on GC peak height. They

are 147 ppm for the shale oil and 268 ppm for the coal-derived oil. Because of lack of standard neutral nitrogen-heterocyclic compounds, the quantitative data, except for carbazole, are not available at this time.

Table 2 summarizes the mutagenicity test data on the four neutral subfractions of coal-derived oil and several commercially available neutral aza-arenes. Indole and carbazole, exhibit no mutagenicity. Highly carcinogenic 7 H-dibenzo(c,g)-carbazole gave a slight but definite positive mutagenic activity at a low dose range (below 25 µg/plate). Specific activity could not be determined for this compound due to the toxic effect at a higher dose range. Benzocarbazoles and their alkyl-substituted compounds were not available for this study. Despite the incompleteness of this study, the correlation between chemical structure and mutagenic activity is expected to be in general agreement with that observed with PAH (14). Fraction AP which contains mostly aliphatic and polymeric constituents shows no mutagenic activity as expected. PAH subfractions exhibit the lowest specific activity among the three subfractions. The neutral aza-arene fractions, which are normally isolated with PAH fractions, have more than two times the specific activity of the PAH fraction. This indicates that the analysis of neutral aza-arene fractions of synfuels are as important as PAH analysis. The higher specific activity of the neutral aza-arene fraction may contain substantial quantities of multi-ring compounds. The further sub-fractionation of the neutral aza-arene fractions into fractions with aza-arenes of approximately the same ring sizes is presently being undertaken.

Basic nitrogen compounds. To further understand what classes or types of basic nitrogen compounds are the most bioactive among compounds in the basic fraction, we recently developed a separation method which isolates the mutagenically active compounds from the bulk of the base fraction (15). The subfractionation scheme is shown in Figure 2. This separation method was devised using a microbial mutagenesis bioassay as a liquid chromatographic detector in the development of the chromatographic subfractionation procedure. Table 3 summarizes the mutagenicity test data on the three basic subfractions of the synfuels. The bioactivities of several commercially available compounds and three that were synthesized in this laboratory are listed in Table 4 for comparison. About 90% of the basic mutagenic activity is recovered in the acetone subfraction which comprises about 10% of the basic fraction. That suggests that the method can be used for isolation of basic mutagenic components from samples of different origins (in this case oil shale or coal). To demonstrate the utility of the method, 3 different kinds of cigarette smoke condensates were fractionated using this scheme and the mutagenic compounds were also concentrated in the acetone subfraction. GC/MS data indicate that the major compound type of the benzene subfractions is C₃-C₁₃ alkyl substituted pyridines. Mutagenic activities of some commercially available pure pyridines (such as pyridine and C₁-C₃ pyridines) and one specially synthesized C₉-pyridine are essentially zero in agreement with these results. The major compounds in the isopropanol fractions are partially hydrogenated 1-2 ring aza-arenes. Biological data on compounds of this type are not available for comparison.

The acetone subfraction of shale oil was about half as mutagenic as benzo(a)pyrene while the coal-derived oil subfraction was about four times more active. GC/MS data indicate multi-ring aza-arenes comprised a large portion of the acetone subfraction, e.g. aza-benzoperylene, aza-indenopyrene, and aza-coronene have been identified. This finding is consistent with bioactivity data from a few multi-ring aza-arene compounds such as dibenz(a,j)acridine (13,000 rev/mg), 9-methyl-10-aza-benzo(a)pyrene (30,000 rev/mg) and 10-azabenz(a)pyrene (130,000 rev/mg). The purposes in synthesizing two nitrogen isologs of benzo(a)pyrene was, first, to confirm the higher mutagenic activity of multi-ring aza-arenes, which comprise a large portion of the acetone subfraction, and to compare their activities with the mutagenic activity of benzo(a)pyrene. 10-azabenz(a)pyrene is two times more active than benzo(a)pyrene. A methyl group on the 9 position of azabenz(a)pyrene, decreases the mutagenic activity. This might be explained by steric hindrance toward the forming of an epoxide at the 7 and 8 position.

The presence of aromatic amines in the active subfraction from both oil samples was first suggested from their IR spectra. Bands at 3220 cm^{-1} and 3370 cm^{-1} , which are normally found in the IR spectra of aromatic amines, are characteristic of the amino compounds in the fraction. By acetylation of the acetone subfraction, we isolated large amounts of primary aromatic amides from the acetone subfraction. A mixture of ten compounds consisting of 4 aza-arenes and 6 aromatic amines (2,4,6-trimethylpyridine, quinoline, acridine, dibenz(a,h)acridine, N, N-dimethylaniline, N-methylaniline, N-phenyl-2-naphthylamine, aniline, 2-naphthylamine, and 1-aminopyrene) was separated on a basic alumina column followed with a Sephadex LH-20 column. All primary amines (1,2, and 4-ring compounds), quinoline and dibenz(a,h)acridine were concentrated in the acetone subfraction. This finding may mean that the primary aromatic amines as well as multi-ring aza-arenes are producing the mutagenic activities of the acetone subfractions. A logical extension of this work is to further separate the acetone subfraction into primary amines and multi-ring aza-arenes. This should lead to some important conclusions regarding the mutagenic effects of these classes of compounds.

References

1. J. R. Morandi and R. E. Poulson, A.C.S. Prepr., Div. Petrol. Chem., **20**(2), 162 (1975).
2. Unpublished results, I.B. Rubin, Oak Ridge National Laboratory, Oak Ridge, TN.
3. H. L. Lochte and E. R. Littmann, "The Petroleum Acids and Bases," Chemical Publishing Co., Inc., New York, NY, 291 (1955).
4. C. E. Searle, Ed., "Chemical Carcinogens," ACS Monograph 173, ACS, Washington, DC (1976).
5. A. R. Jones, M. R. Guerin and B. R. Clark, Anal. Chem. **49**, 1766 (1977).
6. B. R. Clark, "Oil Shale and Shale Oil-Organic Characterization," presented at the 2nd Workshop on Oil Shale Environmental Research, Nov. 2, 1977, Richland, WA.
7. R. E. Poulson, C. M. Frost and H. B. Jensen, in Advances in Chemistry Series, T. F. Yen, Ed., **1** (1978).
8. R. E. Poulson, H. B. Jensen, and G. L. Cook, A.C.S. Prepr., Div. Petrol. Chem. **16**(1), A49 (1971).
9. A. P. Swain, J. E. Cooper, and R. L. Stedman, Cancer Res. **29**, 579 (1969).
10. B. N. Ames, J. McCann and E. Yamasaki, Mutat. Res. **31**, 347 (1975).
11. T. K. Rao, A. A. Hardigree, J. A. Young, W. Lijinsky and J. L. Epler, Mutat. Res. **56**, 131 (1977).
12. I. B. Rubin, M. R. Guerin, A. A. Hardigree, and J. L. Epler, Environ. Res. **12**, 358 (1976).
13. M. E. Snook, R. F. Arrendale, H. C. Higman and O. T. Chortyk, Anal. Chem. **50**, 88 (1978).
14. M. R. Guerin, J. L. Epler, W. H. Griest, B. R. Clark, and T. K. Rao, in Carcinogenesis, Vol. 3: Polynuclear Aromatic Hydrocarbons, edited by P. W. Jones and R. I. Freudenthal, Raven Press, New York (1978).

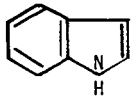
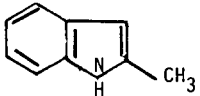
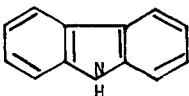
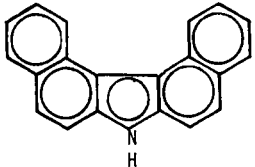
15. M. R. Guerin, B. R. Clark, C.-h. Ho, J. L. Epler, and T. K. Rao, "Short-Term Bioassay of Complex Organic Mixtures, Part I. Chemistry," Symposium on Application of Short-Term Bioassays in the Fractionation and Analysis of Complex Environmental Mixtures, Williamsburg, VA, February 21-23, 1978.

Table 1. Weight Distribution of Neutral Fractions*

	Weight % Distribution	
	<u>Shale Oil</u>	<u>Coal-Derived Oil</u>
Aliphatic and Polymeric (AP)	85.1	35.1
Aromatic (AROM)	14.9	62.9
PAH (I)	10.1	35.9
Neutral Aza-arene (II)	1.4	9.5
Polar (III)	4.3	17.7

* Acid-base extraction yield 89.6% by weight of neutral fraction from shale oil and 56% from coal-derived oil.

Table 2. Mutagenic Activities of the Neutral Subfractions of a Coal-Derived Oil and Some Neutral Aza-arene Compounds

<u>Fraction/Compound</u>	<u>Specific Activity (rev/mg)*</u>
Aliphatic and Polymeric Fraction (AP)	0
PAH Fraction (I)	1390
Neutral Aza-arene Fraction (II)	3250
Polar Fraction (III)	3380
	0
	0
	0
	0
	**

*Tested on TA98 with Aroclor S-9.

** Four-fold increase over spontaneous reversion at dose below 25 μ g/plate. Toxic effect developed at higher dose.

Table 3. Distribution of Mutagenic Activity in Basic Subfractions

Subfraction	Shale Oil Base Fraction			Coal-Derived Oil Base Fraction		
	Average ¹ Weight (%)	Average Specific Activity (rev/mg)	Average ² Relative Activity (%)	Average ¹ Weight (%)	Average Specific Activity (rev/mg)	Average ² Relative Activity (%)
Benzene	78	0	0	76	850	2
Isopropanol	13	277	1	12	0	0
Acetone	9	25,000	92	12	220,000	88
TOTAL	100		93	100		90

¹ Percentage by weight of the basic fraction.

² Percentage of mutagenic activity (TA98, S9, Aroclor 1254) of the basic fraction accounted for in the sub-fraction.

Table 4. Mutagenicity of Basic Aromatic Compounds*

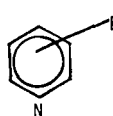
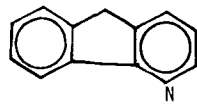
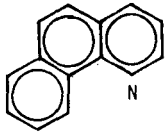
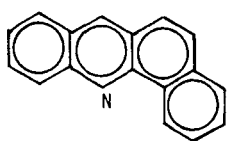
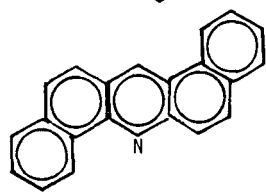
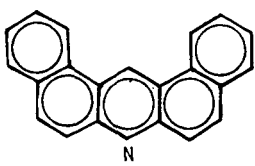
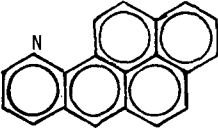
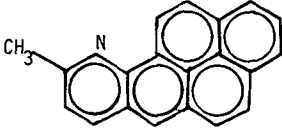
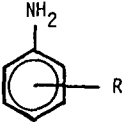
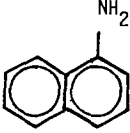
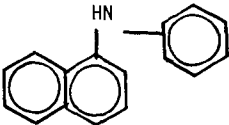
Compound Type - Basic Aza-arene	Specific Activity (rev/mg)
 <p>R = H, CH₃, C₂H₅, C₃H₇, C₉H₁₉</p>	0
	340
	0
	0
	0
	6,000
	13,000

Table 4. Continued

Compound Type - Basic Aza-arene (cont'd)	Specific Activity (rev/mg)
	130,000
	30,000
Aromatic Amine	
	R = H, CH ₃ , C ₂ H ₅
	4,660
	0

*Aroclor induced.

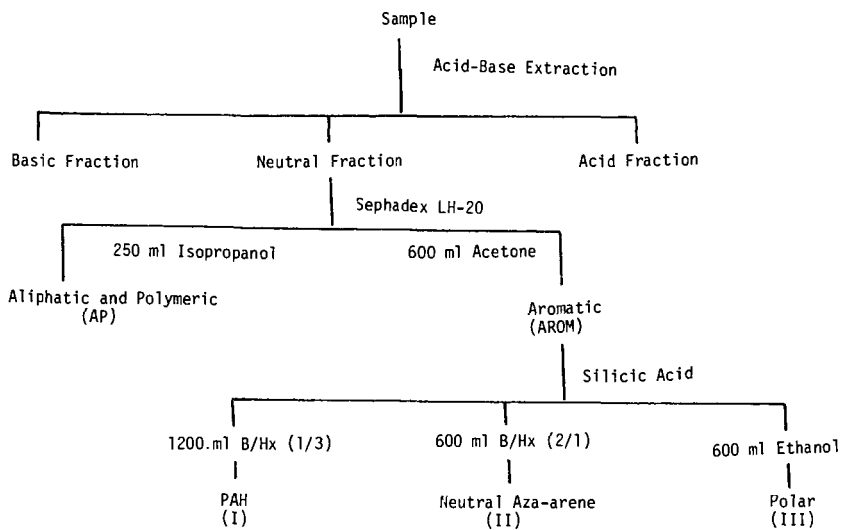


Figure 1. Isolation of Neutral Aza-arenes from Synfuels.

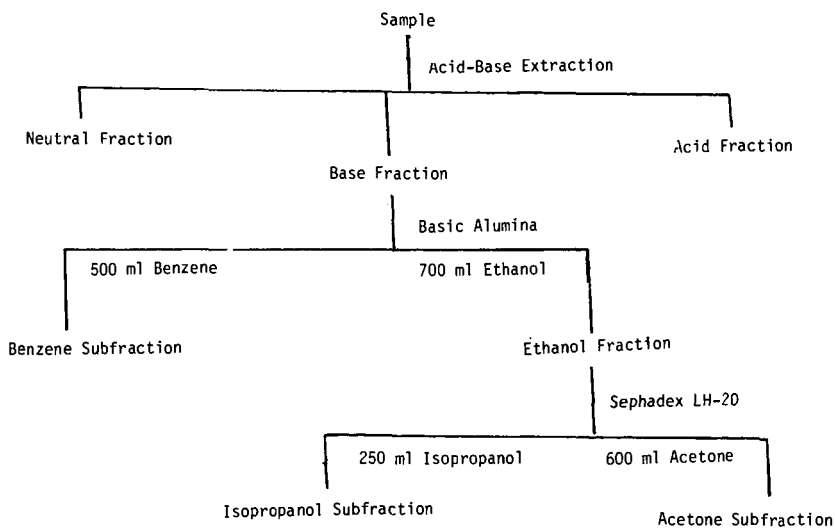


Figure 2. Subfractionation of the Basic Fraction of Synfuels.

MICRO-ANALYSIS of POLYNUCLEAR AROMATIC HYDROCARBONS in PETROLEUM

Hidetsuru Matsushita

Department of Community Environmental Sciences, National Institute of Public Health, 4-6-1, Shirogane-dai, Minato-ku, Tokyo, Japan, 108

It is well known that petroleum and related oils are largely used in our communities and that these oils contain many kinds of polynuclear aromatic hydrocarbons (PAH) in trace amounts. Some PAH are carcinogenic to experimental animals and are suspected to be carcinogenic to man. In fact, occupational cancer has been observed in various types of worker groups having an occupational contact with petroleum and related products such as fuel oil, lubricating oil, paraffin oil, waxes and so on (1). These indicate the need of a reliable method for determining PAH in petroleum and related oils. We have devised dual band thin-layer chromatography (TLC). This TLC has been proved to be useful as a tool for routine microanalysis of PAH in various samples such as heavy oil (2), kerosene (2), gasoline (3), air-borne particulates (4,5), cigarette smoke (6), asbestos (7), coal tar (8,9), pitch (9) and so on.

This paper describes two analytical methods for analysing PAH in petroleum and related oils. The first method, multiple PAH analysis, is useful for analysing many kinds of PAH. The second method, major component analysis, is useful for determining 5 - 10 PAH which are prevalent in petroleum and related oils.

1. Multiple PAH Analysis

Multiple PAH analysis consists of the following 3 procedures; selective extraction of PAH by a series of liquid - liquid partition, separation of the extract into each component by two dimensional dual band TLC, and identification and quantitative determination of the separated compounds by spectrofluorometry.

A known amount of petroleum are dissolved in cyclohexane. PAH in this solution is selectively extracted by a series of liquid - liquid partition of the cyclohexane solution - dimethyl sulfoxide (DMSO), [DMSO + (1 + 4) Hydrochloric acid, 1:1,v/v] - cyclohexane, 70% sulfuric acid - cyclohexane, and 5% sodium hydroxide aqueous solution - cyclohexane.

At the first partition, aromatic fraction in the sample is extracted to DMSO phase, remaining aliphatic fraction in cyclohexane phase. The aromatic fraction contain PAH, aromatic quinones, acidic and basic aromatic compounds. At the 2nd partition, PAH, aromatic quinones and some of acidic compounds are extracted to cyclohexane phase, and separated from basic aromatic compounds and water soluble acidic compounds. Aromatic quinones and trace amounts of basic aromatic compounds in the cyclohexane phase are removed by the 3rd liquid - liquid partition. Acidic aromatic compounds are removed by the 4th partition. The final cyclohexane solution thus obtained contains PAH selectively. Table 1 shows the partition coefficients for 30 aromatic compounds in these liquid - liquid partitions, and also shows the number of times required for extracting 99% or more of these compounds.

The cyclohexane solution which contains very rich PAH is washed with water. After removing the residual water in the solution by adding small amounts of sodium sulfate anhydride, the solution is dried up at a low temperature (40°C) under a reduced pressure. The residue is dissolved in a known amount of benzene (0.5 to 1.0 ml).

PAH in this benzene extract are separated into each component by two dimensional dual band TLC. The TLC plate consists of an aluminum oxide layer (4 x 20, cm) and a 26% acetylated cellulose layer (16 x 20,cm). The acetylated cellulose was prepared by acetylation of microcrystalline cellulose for TLC (Avicel SF) using the method of Wieland et al (10). After the application of a few microliters of the benzene extract onto the aluminum oxide layer, the first development is

carried out with n-hexane - ether (19:1,v/v) to the 15 cm mark on the aluminum oxide layer. This is done at about 20% relative humidity, easily achievable by placing a container of saturated aqueous solution of potassium acetate in a developing chamber. Developing time is about 35 min.

PAH on the aluminum oxide layer are then separated into each component on the acetylated cellulose layer by the second development with methanol - ether - water (4:4:1,v/v). It requires about 60 min. for the developer to reach 10 cm from the layer boundary.

PAH separated on the acetylated cellulose layer are detected as small spots by their fluorescence under UV ray (253 & 365 nm). Detection limit is very low and nanogram order of PAH are usually detectable. Most of PAH are stable on the acetylated cellulose layer. Fig. 1 shows two dimensional dual band thin-layer chromatograms of the benzene extracts from a heavy oil C and an ethylene bottom oil. Heavy oil C, which is widely used as a fuel oil, contained 42 PAH and the ethylene bottom oil contained 69 PAH. PAH in each spot can be analysed by spectrofluorometry. At the present time, 10 PAH in the heavy oil C and 21 PAH in the ethylene bottom oil have been identified as shown in Fig.1. Many PAH in the spots on the chromatograms are left for future identification mainly due to the difficulty in getting the reference substances.

This multiple PAH analysis has revealed that various kinds of PAH are contained in petroleum and related oils such as kerosenes (22 - 39 PAH), heavy oils (32 - 42 PAH), paraffin oil (66 PAH) and gasoline (76 PAH).

2. Major Component Analysis

It is often necessary to analyse 5 - 10 PAH which are abundant in petroleum and related oils. These PAH can be analysed by the major component analysis. This method differs from the multiple PAH analysis only in separation procedure. That is, a one dimensional dual band TLC is used instead of the two dimensional dual band TLC mentioned above. The one dimensional dual band TLC has the following advantages as compared with the usual one dimensional TLC: 1) It has a higher separation efficiency. 2) Separation efficiency is not affected by the spot size at the origin. 3) Sample solution up to a few milliliters can be tested. 4) Quantitative sample application is easily achievable. 5) Detectability of PAH is very high. Therefore, this method is especially useful for the analysis of a sample which contains very low amounts of PAH.

The dual band TLC plate used consists of a kieselguhr layer (4 x 20,cm) and a 26% acetylated cellulose layer (16 x 20,cm). The former layer is used for the application of a sample and the latter layer for separating the sample. Fig. 2 shows a one dimensional dual band thin-layer chromatogram of PAH in a gasoline. In this case, gasoline sample was applied to the kieselguhr layer without any purification by liquid-liquid partition, because gasoline sample evaporated rapidly leaving PAH and related compounds on the layer. Development was carried out with methanol - ether - water (4:4:1,v/v) until the developer reach 10 cm from the layer boundary. It required about 60 min. PAH and related compounds in a gasoline are usually separated into 21 - 24 rectangular spots on the acetylated cellulose layer.

After extraction with 4 ml of DMSO, PAH in each spot is identified by spectrofluorometry in due consideration of its R_f value. Spectrofluorometry is useful for the identification of PAH in a spot containing several kinds of PAH and related compounds. For example, PAH in the spot C in the chromatogram in Fig. 2 were easily identified as pyrene and fluoanthene. In this method, 10 PAH are usually identified from a gasoline sample. They are benzo(a)pyrene, chrysene, benzo(b)fluoranthene, benz(a)anthracene, anthanthrene, benzo(k)fluoranthene, perylene, pyrene, fluoanthene, and benzo(ghi)perylene. The first 4 PAH are carcinogen and the last 3 PAH are cocarcinogen.

The identified PAH except benzo(b)fluoranthene can be determined quantitatively by a narrow base line method (6). Benzo(b)fluoranthene can be analysed after complete separation with benzo(a)pyrene by repeat development with methanol

- ether - water (4:4:1,v/v). The narrow base line method has been proved to be very effective in eliminating interference from other PAH and related compounds coexisting in a test solution. For example, pyrene in a solution which also contained fluoranthene, perylene and benzo(e)pyrene was analysed by this method. Observed value of pyrene differed by only 3% from the theoretical values, even when the concentrations of the latter 3 PAH (100 ng/ml) were 5 times higher than pyrene (20 ng/ml). It was also found that observed value of benzo(a)pyrene in a mixed PAH solution differed only 0.8% from the theoretical value, even when the solution contained benzo(b)fluoranthene, chrysene, anthanthrene and dibenzo(a,h)pyrene in 10 times higher concentration than benzo(a)pyrene.

Table 2 shows contents of 9 PAH in regular and premium gasolines as well as coefficient of variation for each PAH obtained in this analysis. The coefficient of variation is low for all PAH analysed. Furthermore, this method is so sensitive that it can analyse PAH quantitatively at a concentration of 1 ng/ml or less.

Another major component analysis is achievable by high speed liquid chromatography instead of one dimensional dual band TLC. A spectrofluorometer is used as a detector of a high speed liquid chromatograph. Fig. 3 demonstrates an example in which a liquid-liquid partition extract from a gasoline is separated and detected at the spectrofluorometric condition for analysing benzo(a)pyrene, benzo(k)fluoranthene, benzo(ghi)perylene and anthracene. The other PAH in the extract can also be analysed in a suitable spectrofluorometric condition. It has been proved that this major component analysis is useful for analysing several kinds of PAH in petroleum and related oils as well as combustion products of these oils.

These analytical methods described in this paper have a wide range of uses, producing reliable data on PAH in petroleum and related oils. These methods will be useful for analysing PAH in various kinds of samples in the environment.

References

1. W.C. Hueper: Occupational and Environmental Cancers of the Respiratory System, pp.118 - 125, Springer-Verlag, Berlin Heidelberg New York (1966).
2. H. Matsushita, Y. Esumi, A. Suzuki: Japan Analyst, 21, 331 (1972).
3. H. Matsushita, K. Arashidani, M. Koyano, T. Handa: J. Jap. Soc. Air Pollution, 11, 44 (1976).
4. H. Matsushita, Y. Esumi, K. Yamada: Japan Analyst, 19, 951 (1970).
5. H. Matsushita, K. Arashidani, T. Handa: Japan Analyst, 25, 263 (1976).
6. H. Matsushita, K. Kawai, K. Arashidani: Proceedings of the 29th annual meeting of Chem. Soc. Japan, I, p.142 (1973).
7. H. Matsushita, K. Arashidani: Proceedings of the 46th annual meeting of Jap. Assoc. Ind. Health, p.172 (1973).
8. H. Matsushita, Y. Esumi, S. Suzuki, T. Handa: Japan Analyst, 21, 1471 (1972).
9. H. Matsushita, K. Arashidani: Japan Analyst, 25, 76 (1976).
10. Th. Wieland, G. Lüben, H. Determan: Experientia, 18, 432 (1962).

Table 1. Partition Coefficients of Aromatic Compounds

Substance		A Phase		DMSO		Cyclohexane		Cyclohexane		Cyclohexane	
		B Phase		Cyclohexane		DMSO + (1+4)		70% H ₂ SO ₄		5% NaOH	
		K	N	K	N	K	N	K	N	K	N
Hydrocarbon	Anthracene	3.9	3	>100	1	>100	1	>100	1	>100	1
	Phenanthrene	3.9	3	40	2	>100	1	14	2		
	Fluorene	7.9	3	>100	1	>100	1	>100	1		
	Pyrene	4.6	3	>100	1	>100	1	>100	1		
	Chrysene	9.8	2	>100	1	>100	1	>100	1		
	Benzo(a)pyrene	13	2	>100	1	>100	1	>100	1		
	Fluoranthene	5.3	3	>100	1	>100	1	>100	1		
	Benzo(b)fluoranthene	10	2	>100	1	>100	1	>100	1		
	Benzo(ghi)perylene	14	2	66	2	>100	1	>100	1		
	Coronene	14	2	40	2	>100	1	>100	1		
Quinone	Anthraquinone	12	2	49	2	0.77	9	>100	1		
	Benzanthrone	20	2	30	2	0.017	270	>100	1		
	Benz(a)anthraquinone	13	2	>100	1	19	2	>100	1		
	p-Benzoquinone	—	—	0.26	7	0.010	460	0.0035	1300		
	1,2-Naphthoquinone	>100	1	0.13	38	0.052	91	—	—		
	1,4-Naphthoquinone	22	2	2.9	4	0.078	62	0.0015	3100		
	Nicotinic Acid	—	—	0.051	92	—	—	0.027	180		
Acid	o-Hydroxybenzoic Acid	—	—	0.115	43	0.086	56	0.001	4600		
	Terephthalic Acid	—	—	0.032	150	—	—	0.031	150		
	Phenazine	4.0	3	4.6	3	—	—	14.5	2		
Base	Carbazole	>100	1	0.83	8	0.14	36	>100	1		
	Lepidine	6.2	3	0.047	100	—	—	—	—		
	Benzo(h)quinoline	7.0	3	0.019	240	—	—	—	—		
	Benzo(f)quinoline	12	2	<0.001	>4600	—	—	—	—		
	Acridine	8.8	3	<0.001	>4600	0.016	290	—	—		
	1-Naphthylamine	55	2	0.007	660	0.001	4600	—	—		
	2-Aminoanthracene	>100	1	0.077	63	—	—	—	—		
	2-Naphthylamine	>100	1	<0.001	>4600	—	—	—	—		
	2-Aminofluorene	>100	1	<0.001	>4600	—	—	—	—		
	2-Aminochrysene	>100	1	0.001	4600	0.055	87	—	—		

K: Partition Coefficient (Concentration in A/Concentration in B)

N: Number of times required for extracting 99% or more of a compound from B phase to A phase

Table 2. Contents of polynuclear aromatic hydrocarbons in gasoline

Sample No.	Pyrene Mean C.V.	Fluoran- thene Mean C.V.	Chrysene Mean C.V.	Benz(a)- anthracene Mean C.V.	Benzo(a)- pyrene Mean C.V.	Benzo(k)fl- uoranthene Mean C.V.	Perylene Mean C.V.	Anth- anthrene Mean C.V.	Benzo(ghi)- perylene Mean C.V.
1	2.9*	1.4*	0.24	0.20	0.05*	0.04	0.02	0.02	0.25
2	5.8*	2.2*	0.75	0.40	0.18*	0.09	0.06	0.04	0.74
3	14.6*	2.6*	0.58	0.20	0.16*	0.02	0.01	0.04	1.09
4	4.8	1.3	0.38	0.28	0.19**	0.05	0.02	0.05**	0.52
5	11.4	2.8	0.93	0.64	0.32	0.09	0.06	0.05	1.07
6	2.5	1.0	0.34	0.22	0.12	0.06	0.03	0.03	0.28
7	16.4	0.6	0.56	0.25	0.22	0.03	0.02	0.05	1.36
8	1.3	2.3	0.11	0.10	0.05	0.03	0.01	0.02	0.13
1	4.6*	1.8*	0.54	0.34	0.06*	0.07	0.03	0.03	0.38
2	10.6*	4.1*	1.07	0.46	0.25*	0.11	0.08	0.08	0.80
3	17.1*	2.9*	0.79	0.26	0.17*	0.02	0.01	0.04	1.65
4	3.4	3.5	0.45	0.39	0.15*	0.04	0.01	0.03**	0.39
5	16.9	1.7	1.31	1.14	0.50	0.15	0.10	0.11	1.22
6	3.4	0.5	0.50	0.29	0.18	0.09	0.03	0.05	0.43
7	20.0	0.8	0.86	0.35	0.35	0.04	0.02	0.09	2.00
8	14.3	3.7	1.28	1.00	0.56	0.23	0.11	0.22	1.64

Mean of 4 determinations, * Mean of 3 determinations, ** Mean of 7 determinations,

C.V.: Coefficient of variation (%)

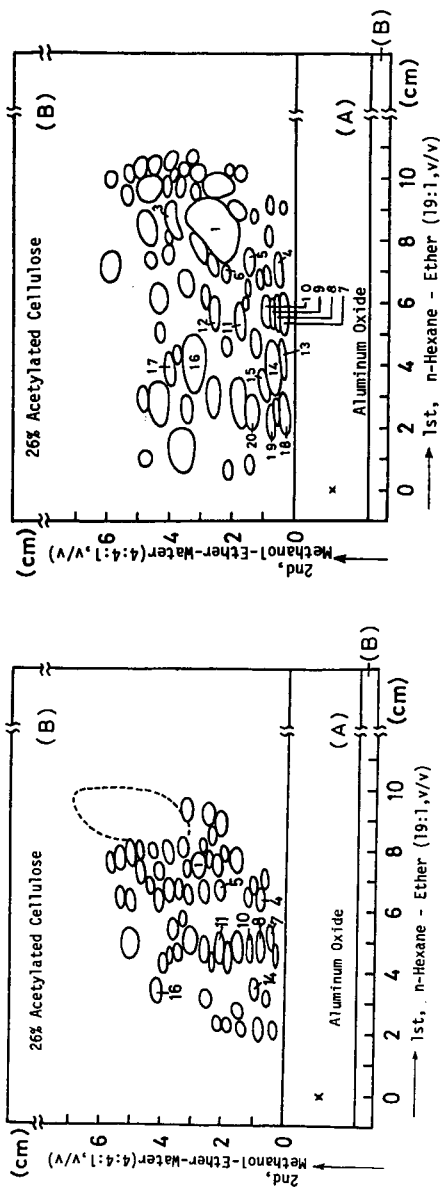


Fig. 1. Two dimensional dual band thin-layer chromatograms of the benzene extracts from heavy oil C (left) and ethylene bottom oil (right)

Identified polynuclear aromatic hydrocarbons and their spot numbers: pyrene and fluoranthene (spot 1), methyl derivatives of pyrene and fluoranthene (3), chrysene (4), benz(a)anthracene (5), benzo(b)fluorene (6), benzo(a)pyrene (7), benzo(b)fluoranthene (8), benzo(j)fluoranthene (9), benzo(k)fluoranthene (10), perylene (11), benzo(e)pyrene (12), anthanthrene (13), indeno(1,2,3-cd)pyrene (14), benzo(b)chrysene (15), benzo(ghi)perylene (16), coronene (17), dibenzo(a,h)pyrene (18), dibenzo(a,i)pyrene (19), and tribenzo(a,e,i)pyrene (20).

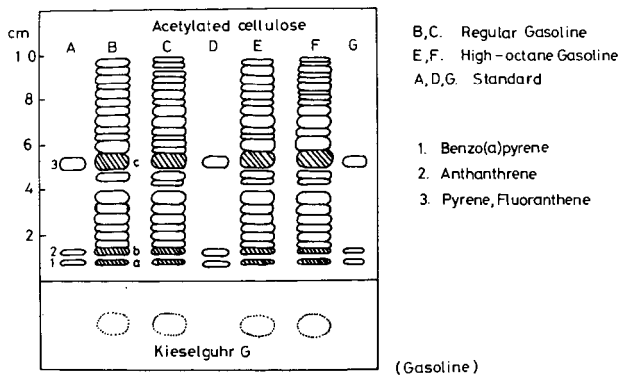


Fig. 2. One dimensional dual band thin-layer chromatogram of gasoline

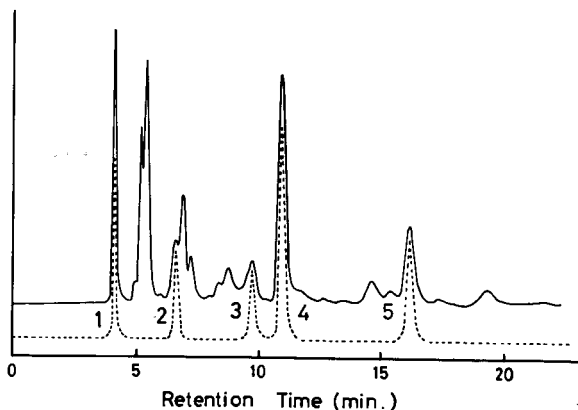


Fig. 3. High speed liquid chromatograms of the liquid-liquid partition extract from gasoline (—) and standard solution having 16 PAH

Column: Zorbax ODS (4.6mm x 25cm), Mobile phase: Methanol-Water (85:15,v/v), Detector: Spectrofluorometer (excitation 370nm, emission 410nm), 65°C, 1100psi.
 1. anthracene, 2. 9-phenylanthracene, 3. benzo(k)fluoranthene, 4. benzo(a)pyrene, 5. benzo(ghi)perylene
 Standard solution is a mixture of 1 - 5 PAH, naphthalene, fluorene, 3,4-benzofluorene, fluoranthene, chrysene, 7-ethylchrysene, benz(a)anthracene, 7-methylbenz(a)anthracene, perylene, benzo(b)fluoranthene and benzo(e)pyrene.

TRACE ELEMENT DISTRIBUTIONS IN COAL GASIFICATION PRODUCTS

D.W. Koppelaar*, H. Schultz, R.G. Lett, F.R. Brown, H.B. Booher, and E.A. Hattman

Pittsburgh Energy Technology Center
U.S. Department of Energy
Pittsburgh, PA 15213

and

S.E. Manahan

Department of Chemistry
University of Missouri
Columbia, MO 15201

INTRODUCTION

The determination of the fate and distribution of trace elements during coal conversion is an important and prerequisite task if such an industry is to be implemented on a massive scale. Considering the overwhelming abundance of native coal resources, an implementation of this magnitude is a distinct possibility in the near future. Coal gasification is currently under investigation by many organizations in the U.S. as an alternative source of environmentally acceptable fuels. In conjunction with ongoing coal gasification studies at this laboratory, trace element investigations have been performed to help assess potential environmental impacts of coal gasification processes. This work presents preliminary findings of trace and minor element distributions in the process streams of the SYNTHANE Gasifier Process Development Unit located at this laboratory.

EXPERIMENTAL

Three separate gasification runs were made with the SYNTHANE Gasifier PDU using Montana sub-bituminous 'C' coal. The SYNTHANE Gasifier characteristics and operating conditions have been described previously (1-3). Maximum average temperatures attained in this unit are typically 950-1000°C. A schematic diagram of the PDU is presented in Figure 1.

An integral part of this study was the sampling of the process streams of the gasification unit. Samples collected for subsequent analysis included the feed coal and feed water (major input streams) and gasifier char, filter fines, and condensable water and tars (major output streams). Sampling points in the PDU are illustrated in Figure 1. The feed coal was systematically thieved during the loading of the gasifier hopper in order to obtain representative samples of this process stream. Feed water (for generation of process steam) was also periodically sampled during the gasification runs. The gasifier char, condensable tars and water, and particulate matter from the gas product stream were collected after each run. The weights of the process streams sampled are reported in Table 1. Also shown are the weight percentages that the samples represent relative to the total amount of the process stream consumed or produced. In most cases, the entire process stream was collected. This procedure ensured representative sampling of these process streams.

Considerable efforts were required to homogenize these samples. The solid process streams were riffled, ground and further comminuted to manageable sizes. In some cases, further grinding to -325 mesh was required. Condensate water analytical samples were taken while vigorously stirring the bulk sample. The con-

*Present address: Institute for Mining and Minerals Research, Kentucky Center for Energy Research Laboratory, University of Kentucky, Lexington, Kentucky 40583

densate tar process stream presented unique sampling problems. This process stream consists of organic and aqueous phases, in addition to a considerable amount of solid material. Due to the immiscibility of these phases, it was not possible to withdraw homogenous samples by merely mixing the process stream. This problem was overcome by adding tetrahydrofuran to the sample to render the various phases miscible.

Samples were analyzed by spark-source mass spectrometry (SSMS) and atomic absorption spectrophotometry (AAS). Approximately 65 elements were semi-quantitatively determined in each process stream by SSMS 'survey' analyses. The feed coal, char, and filtered particular matter process streams were low-temperature ashed, mixed with high purity graphite, and formed into electrodes. Unashed samples were also analyzed for the determination of volatile elements. Aqueous and wet-ashed samples were mixed with graphite and gently dried under an infrared lamp. Photoplate detection was utilized with computer assisted quantitation by means of the Hull equation (4). Figure 2 illustrates a typical SSMS 'survey' analysis of the feed coal process stream. Such analyses are generally accurate to within a factor of three and are especially valuable for the complete inorganic characterization of these process streams.

Isotope dilution spark-source mass spectrometric (ID-SSMS) determinations were also performed. Samples were solubilized by means of Parr acid digestion bombs (5-7) after addition of enriched isotopes. Elements of high environmental interest (Ni, Cu, Se, Cd, Pb, and Tl) were preconcentrated by means of electrodeposition onto high-purity gold electrodes. These electrodes were then sparked in the spectrometer. Quantitation was accomplished using the isotope dilution equation of Paulsen (8-10). Results of ID-SSMS measurements on the three solid process streams are presented in Table 2. Quadruplicate analyses were made, with the precision of such measurements ranging from 2-15% (relative standard deviation).

Atomic absorption determinations of seven elements (Mn, Ni, Cu, Cr, As, Pb, and Cd) were also made. Samples were solubilized by means of high temperature ashing and lithium metaborate fusion for the determination of Mn, Ni, Cu, and Cr (11). Digested sample solutions were aspirated into the atomic absorption spectrometer and quantitated by the method of standard additions. Pb and Cd were preconcentrated by extracting their iodide complexes into methyl isobutyl ketone (MIBK) prior to aspiration into the spectrometer. Arsenic was determined using hydride evolution AAS after wet-ashing of the samples. Results of the AAS determinations of the solid process streams are shown in Table 3. The precision of these determinations ranged from 2-20% r.s.d.

DISCUSSION

All process streams were surveyed for approximately 65 elements by conventional SSMS analyses. Such analyses, although semi-quantitative, provide quick multi-element analyses that are valuable when the inorganic composition of the process streams are unknown and/or unsuspected. This type of analysis is especially useful for process monitoring applications, resulting in an almost complete inorganic characterization of process streams from such a conversion unit. This kind of characterization is especially useful in delineating potential problems and pointing out the need for more accurate analyses of specific elements. As an example of the kind of information that can be extracted from such data, an enrichment ratio can be calculated for various elements based on their concentrations in the filter fines process stream relative to their concentrations in the feed coal (after correcting for the varying ash contents in the two process streams). Table 4 presents the enrichment ratios for a number of elements. An enrichment ratio of unity indicates no enrichment, while ratios greater than unity indicate enrichment in the filter fines process stream. If an enrichment ratio of three or greater is assumed to be significant (to take into account the uncertainty limitations of the technique), then elements can be classified as either enriched or not enriched. Table 4 shows that many elements are shown to be enriched to a great degree. Presumably, such enrichment is due to a volatilization of these elements in the

high temperature zone of the reactor and subsequent condensation of these volatilized elements in the cooler sections of the gasification unit. Although such a mechanism has been shown to be operative in high temperature coal combustion (12-13), this may be the first work showing such a mechanism to be operative during coal gasification. Preliminary SSMS analyses of size-separated filter fines fractions substantiates this finding.

Both the SSMS survey results and the more accurate, precise results obtained by ID-SSMS and AAS show the gasifier char to be the major elemental 'sink' for most elements. This has important environmental ramifications in that this material may be utilized as a combustion material for production of process steam. The fate of the environmentally important elements during this combustion will need to be determined. On the other hand, if the char is disposed of as an alternative to its by-product utilization, significant solid waste problems will almost certainly occur.

Selenium, as determined by ID-SSMS, showed a distribution among the process streams that was markedly different from the bulk of the other elements studied. The major elemental sink for Se was the condensate water process stream. Significant quantities of this element were also found in the condensate tar. This finding can be rationalized in terms of the high volatility of this element. Arsenic, as determined by AAS, does not exhibit such behavior, in contrast to what one might expect for this element. The major sink for this element is the gasifier char. This fact seems to indicate that the arsenic is present in the coal in a non-volatile form and that it is not converted to a volatile form during the gasification process.

Mass balances of elements across a conversion unit may be valuable in predicting the release rates of certain elements to the environment. Such balances can be calculated knowing the concentration of the element in each process stream and the mass of the respective process stream. Mass balances of 100% at the trace level are generally exceedingly difficult to obtain in such complex, open systems as a gasification reactor. Results of such mass balances are shown in Table 5. The data were calculated using the AAS and/or the ID-SSMS concentration values for the elements in the major process streams. The data indicate that the bulk of most elements (Cu, Ni, Mn, Pb, Cr) are being retained within the unit. However, other elements cannot be fully recovered (i.e., Cd and Se) and careful considerations of the fate of these elements must be made in view of their environmental and toxicological hazards.

ACKNOWLEDGMENT

One of the authors (D.W.K.) gratefully acknowledges support from Oak Ridge Associated Universities in the form of a Laboratory Graduate Participantship at the Pittsburgh Energy Technology Center.

REFERENCES

1. Gasior, S.J., R.G. Lett, J.P. Strakey, W.P. Haynes. ACS Div. Fuel Chem. Preprints, 23, (2), 88 (1978).
2. Gasior, S.J., A.J. Forney, W.P. Haynes, R.F. Kenny. Chem. Eng. Prog., 71 89 (1975).
3. McMichael, W.J., et. al. "Synthane Gasifier Effluent Streams", PERC/RI-77/4, 1977.
4. Hull, C.W. Proc. 10th Ann. Conf. Mass Spectrom. Allied Topics, New Orleans, LA, 1962.
5. Bernas, B. Anal. Chem., 40, 1682 (1968).

6. Hartstein, A.M., R.W. Friedman, D.W. Platter. Anal. Chem., 45, 611 (1975).
7. Bulletin No. 4745. Parr Instrument Co., Moline, Ill., 1976.
8. Paulsen, P.J., R. Alvarez, D.E. Kelleher. Spectrochim. Acta, 24B, 535 (1969).
9. Alvarez, R., P.J. Paulsen, D.E. Kelleher. Anal. Chem., 41, 955 (1969).
10. Paulsen, P.J. In: NBS Special Publication 492, U.S. Gov't. Printing Office, Washington, D.C., 1977, p. 33-47.
11. Schultz, H., et. al. "The Distribution of Some Trace Elements in the 1/2 Ton Per Day Synthoil Process Development Unit". PERC/RI-77/2, Pittsburgh Energy Research Center, Pittsburgh, PA, 1977.
12. Davison, R.L., D.F.S. Natusch, J.R. Wallace, C.A. Evans, Jr. Env. Sci. Tech., 8, 1107 (1974).
13. Campbell, J.A., J.C. Laul, K.K. Nielsen, R.D. Smith. Anal. Chem., 50, 1033 (1978).

Table 1

Description of Sample Sizes Taken from SYNTHANE Process Development Unit
for Trace Element Studies

<u>Sample</u>	<u>Run Number</u>		
	<u>293</u>	<u>294</u>	<u>295</u>
Feed Coal, kg	7.7 (11.0) ¹	5.9 (8.0)	6.1 (8.6)
Feed Water, kg	4.9 (5.4)	4.2 (4.8)	4.2 (4.4)
Gasifier Char, kg	17.0 (100)	16.9 (100)	17.0 (100)
Condensate Tar/Water, kg	14.6 (100)	15.5 (100)	15.2 (100)
Condensate Water, kg	52.8 (100)	53.1 (100)	53.5 (100)
Filter Fines, kg	0.4 (100)	0.4 (100)	0.5 (100)
Product Gas, kl	1.7 (1.5)	1.7 (1.4)	1.6 (1.4)

¹Data in parentheses indicate the percentage of the process stream that was taken for preparation and analysis.

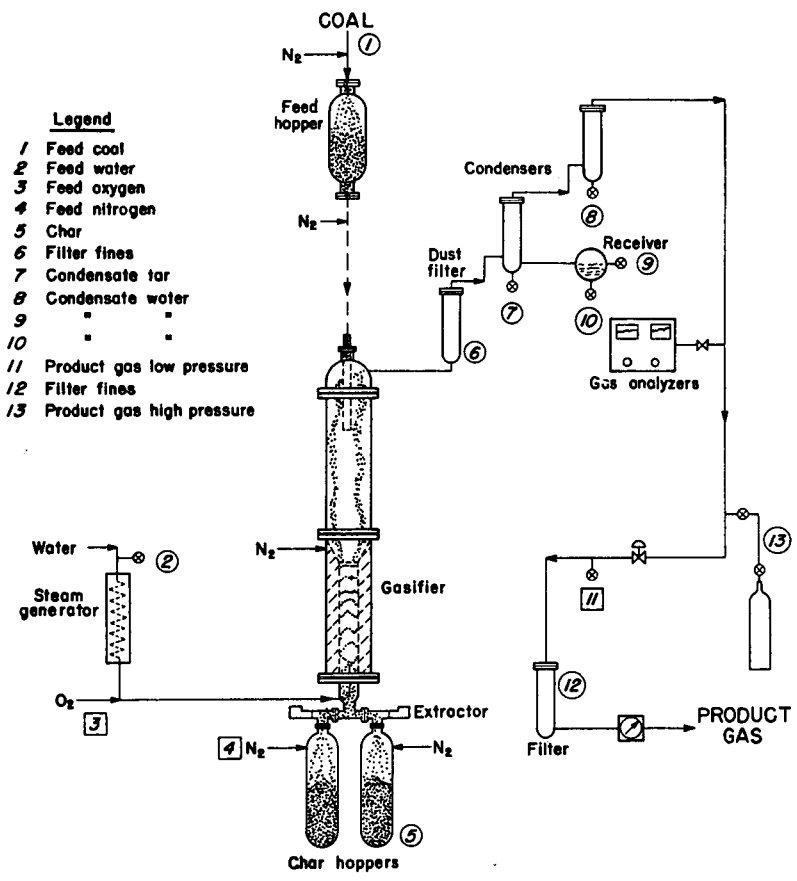


Figure 1 Sampling points on the PETC SYNTHANE Process Development Unit.

Table 2 - Element Concentrations (ppm, wt.) in Gasifier Samples by ID-SSMS Analysis

<u>Sample</u>	<u>Element</u>	<u>Run Number</u>		
		<u>293</u>	<u>294</u>	<u>295</u>
Feed Coal	Ni	2.83	2.56	2.39
	Cu	7.50	7.52	7.24
	Se	0.56	0.54	0.54
	Cd	0.12	0.12	0.14
	Tl	0.05	0.04	0.04
	Pb	5.14	4.80	4.77
Gasifier Char	Ni	11.6	9.06	11.6
	Cu	25.5	24.2	27.8
	Se	0.14	0.21	0.19
	Cd	0.10	0.12	0.13
	Tl	0.11	0.12	0.15
	Pb	21.2	17.1	19.3
Filter Fines	Ni	10.3	11.5	10.0
	Cu	105	150	131
	Se	0.65	0.94	0.74
	Cd	2.16	2.88	1.81
	Tl	0.09	0.11	0.10
	Pb	13.7	13.5	12.47

Table 3 - Element Concentrations (ppm, wt.) in Gasifier Process Streams by AAS Analysis

<u>Sample</u>	<u>Element</u>	<u>Run Number</u>			
		<u>293</u>	<u>294</u>	<u>295</u>	
Feed Coal	Cr	7.1	6.6	7.9	
	Mn	547	512	646	
	Ni	2.2	2.7	2.4	
	Cu	10.2	9.7	10.4	
	As	1.6	1.5	2.0	
	Cd	0.07	0.07	0.09	
	Pb	5.5	4.6	5.3	
	Gasifier Char	Cr	32.4	33.5	30.3
Gasifier Char	Mn	2510	2350	2430	
	Ni	10.8	8.5	8.0	
	Cu	33.0	23.8	27.0	
	As	6.3	6.0	5.7	
	Cd	0.06	0.05	0.05	
	Pb	19.6	18.2	18.9	
	Filter Fines	Cr	12.4	18.5	20.7
	Filter Fines	Mn	519	530	503
Ni		10.0	12.5	10.6	
Cu		114	154	142	
As		9.1	7.9	11.0	
Cd		1.86	2.25	1.75	
Pb		14.1	13.8	15.6	

Table 4 - Enrichment Ratios (E_r) for Various Elements

<u>Non-Enriched Elements</u>		<u>Enriched Elements</u>	
<u>Element</u>	<u>E_r</u>	<u>Element</u>	<u>E_r</u>
Na	2.0	K	3.1
Mg	2.7	Rb	6.5
Al	1.0	Co	4.1
Si	1.2	Ni	3.0
Ca	0.8	Zn	7.0
Ti	1.1	Cu	9.3
Zr	2.9	Ga	4.7
Fe	0.8	Ge	11.0
Cr	1.6	As	6.2
Be	2.4	Br	11.0
Sr	1.2	Sn	3.3
Ba	1.1	Sb	5.7
Hf	1.5	I	14.0
Gd	0.8	Mo	7.3
		Pb	3.8
		Cd	6.5

Table 5 - Elemental Mass Balances

<u>Element</u>	<u>Mass Balance, %</u>		
	<u>293</u>	<u>294</u>	<u>295</u>
Cu (ID-SSMS)	103	92	110
Cr (AAS)	112	118	96
Ni (AAS)	122	75	85
Se (ID-SSMS)	45	44	46
Cd (AAS)	36	35	27
Cd (ID-SSMS)	36	46	33
Pb (ID-SSMS)	102	84	101
Pb (AAS)	88	92	89
As (AAS)	99	95	74

The Effect of Trace Element Associations and
Mineral Phases on the Pyrolysis Products from Coal

J. K. Kuhn, R. A. Cahill, R. H. Shiley, D. R. Dickerson and C. W. Kruse

Illinois State Geological Survey
Urbana, IL 61801

The initial mode of occurrence of trace and minor elements in coal influences their ultimate fate during the processing and/or utilization of coal materials. A float-sink procedure and an acid-leaching procedure have been developed independently and used to estimate the trace and minor element associations with the organic and mineral phases in coal. Values obtained by the two methods were in agreement within the limits of analytical error. Ion exchange studies and internal surface area studies indicated that major differences that were observed could be explained in terms of exchangeable and/or chelated elements on the exposed surfaces of the coal. When these two factors were considered, results from these two methods were sufficiently reliable to allow their values to be used as indicators of an element's organic association.

Representative data for 50 elements from 9 coals are presented for both methods. The mean values for the same elements determined in the acid demineralized coals are given for 27 coals from 3 geographical areas. These values were compared to elemental values for crustal abundance and plant material; only S, Se, and Te had concentrations of organically associated elements significantly in excess of Clarke values (by factors of 20 to 50). Other elements, such as Pb, varied from virtually no organic association, to those, such as Ga, which averaged about 40 to 50 percent organic association.

Although many elements had some organic association, the major amounts of accessory elements in coal were present in the mineral phases. Semiquantitative mineral analysis of the low-temperature ashes (plasma ashing at $<150^{\circ}\text{C}$) was performed on the coals; clay, ranging from 20 to 80 percent and a mean of about 50 percent, was the predominant mineral phase in the inorganic fractions. The sulfide minerals were second and carbonates generally were the third most abundant mineral phase. In any particular coal, however, this order may be mixed or even inverted. Also frequently present in the coals is quartz and many other minerals in lesser amounts.

The mobilities during pyrolysis of the various elements were determined at 450°C , 600°C , and 700°C through the use of both batch and continuous-feed processes. This range in temperature was selected in order to produce chars with minimum sulfur content and with both maximum and minimum surface areas. The coals reached their most plastic (fluid?) state within this temperature range.

The concentrations of 50 elements were determined in 6 whole coals, also their corresponding char residues and condensed volatile products. For most of the coals studied, the data showed significant increase in mobility (volatilization) during pyrolysis for P, Cl, S, As, Br, I, Se, Te, and Zn. Elements that exhibited less significant mobility included Cd, Cr, Cu, Dy, Ga, Hf, La, Li, Pb, Sb, Sc, Sm, U, and Y. Those elements that generally exhibited no mobility during pyrolysis included Si, Al, K, V, Mg, Ca, Fe, Na, Ti, Ba, Ce, Co, Cs, Eu, Lu, Mn, Ni, Rb, Sr, Ta, Tb, and Th. Because of their extremely low concentrations, elements such as Ag, Au, In, Mo, W, and Sn were generally not detected at levels where any reasonable conclusions could be drawn.

Correlation of element mobility and organic association showed that elements associated with the organic material were the same elements that showed losses during pyrolysis. Two exceptions to this general rule were: (1) The alkali and alkaline earth elements generally were not lost during pyrolysis. These same elements were usually present to some extent in an exchangeable ion form and often showed a very high organic association. (2) The group of primarily sulfide elements, which include Pb, Zn and As, normally showed little or no organic association. The mechanism for mobility probably involved a thermal breakdown of the mineral itself. Iron usually occurred as the predominant sulfide mineral, but it was immobile.

The dissociation of pyrite when heated in a reducing atmosphere is well known. In coal, however, this reduction of pyrite to pyrrhotite takes place at relatively low temperatures, occurring at less than 450°C. During this process, two types of pyrrhotite were produced, one of which had magnetic properties. The material formed was susceptible to either chemical or magnetic cleaning. Mössbauer spectroscopy was used to identify four species of Fe^{+2} in the chars, only two species have been identified similarly in the raw coal.

The condensed volatile components from the pyrolysis of the coal were analyzed further to determine the organic composition of the products. Separation of the condensed organics into acid, base, and neutral fractions indicated that the components in the acid fraction predominated at the lower pyrolysis temperatures, and the components contained in the base fraction predominated at the higher temperatures. The distribution of constituents making up the organic fractions were shown to be strongly influenced by the temperature at which the pyrolysis was conducted. Furthermore, removal of virtually all of the mineral phases from the coal prior to heating significantly altered the proportion of tar to light fractions in the product; much less tar was produced when mineral phases were absent.

Correlations of mineral-phase content and the distribution of organic fractions at a given temperature indicated that the temperature at which the process was operated had a dominant effect on the product composition; nevertheless, the composition also was affected significantly by the kinds of mineral phases present. Individual effects of minerals on the distribution of organic constituents in condensed pyrolysis products are still being studied, but it is evident that knowledge of the organic associations and mineral phases present in an individual coal is necessary before a satisfactory evaluation of coal performance during utilization can be made.

Chemical and Mineralogical Characterization of Coal Liquefaction Residues

G. B. Dreher, Suzanne, J. Russell, and R. R. Ruch

Illinois State Geological Survey, Natural Resources Bldg., Urbana, Illinois 61801

The Illinois State Geological Survey, with support from the U.S. Department of Energy, is characterizing the residues from several advanced-stage coal liquefaction processes. Coal liquefaction in plants of commercial size, if developed on a large scale, will eventually result in the production of large tonnages of waste materials. It is desirable to know the compositions of these residues for possible evaluation as sources of valuable metals and also to know whether they are potential environmental hazards. A major objective of this project is to determine whether the residues from several coal liquefaction processes consistently contain recoverable amounts of valuable elements and can, therefore, be reliably classified as potential secondary source reserves for these elements. In this study the concentration levels of some 70 major, minor, and trace constituents have been determined and, where possible, the mineralogy for certain elements has been ascertained. An economic evaluation of the data will be made. The chemical and mineralogical data will aid in predicting the behavior of various elements during certain liquefaction processes.

Sampling and pretreatment. The processes from which samples were obtained are Clean Coke at United States Steel Research, Monroeville, PA; H-Coal, Hydrocarbon Research, Inc., Trenton, NJ; Lignite Project, University of North Dakota, Grand Forks, ND; Solvent Refined Coal, Southern Company Services, Wilsonville, AL (SRC-Ala); Solvent Refined Coal, Pittsburgh and Midway Coal Company, Ft. Lewis, Wash. (SRC-Wash); and Synthoil, Pittsburgh Energy Research Center, Bruceton, PA. In addition, one residue sample from the COED process has been obtained and analyzed. Each of these processes has been described elsewhere (1). Seventy constituents have been determined in 18 sample sets consisting of feed coal, corresponding residue, and where available, product material. The residues as we have received them are not envisioned to be the ultimate waste products; further processing of the materials beyond that which was being conducted when the samples were taken is anticipated for most processes.

The following coals have been used in the sample sets studied: feed coals from the Herrin (No. 6) coal of Illinois; composite samples of No. 9 and No. 14 coal beds and No. 9, No. 11, No. 12, and No. 13 coal beds of western Kentucky; the Pittsburgh No. 8 coal; Wyodak seam from Wyoming; and a lignite from North Dakota.

Residue samples from the liquefaction processes are often intractable mixtures of product oil, partially reacted coal, and unreacted coal. To produce samples that are more easily handled, more homogeneous, and convenient to use in low-temperature ashing procedures, the product oil portion was separated from the mineral matter portion by extraction with tetrahydrofuran (THF). The unextracted residues, however, have been found to be generally homogeneous, and the extracted residues have primarily been used in producing low-temperature (150°C) ashes for mineralogical analyses. The high temperature ash contents of the unextracted ash samples compare favorably with those recovered from the THF soluble and insoluble portions for most samples, indicating that the samples are fairly homogeneous with respect to ash content.

Methods of analysis. The analytical techniques used (shown in Table 1) are atomic absorption spectrometry (AA), instrumental neutron activation analysis (INAA), direct-reading optical emission spectrometry (OED), photographic optical emission spectrography (OEP), energy dispersive X-ray fluorescence spectrometry (XES), wavelength dispersive X-ray fluorescence spectrometry (XRF), radio-chemical separation followed by neutron activation analysis (RC), ion selective electrode (ISE), and standard ASTM methods (ASTM). Mineralogical studies were made by X-ray diffraction analysis and scanning electron microscopy using low-temperature ash samples prepared in an activated oxygen plasma asher. These methods have been described elsewhere (2). Sample pretreatment is summarized in Figure 1.

Results and discussion. All results on "as received" feed coal and residue samples were corrected for moisture and calculated to the 500°C ash basis. It was assumed that (a) the oxidized inorganic material (the 500°C ash) from a feed coal is comparable to that from the corresponding residue, and (b) that the feed coal sample is representative of the coal used to generate a particular residue. When the ash-basis data for a residue is compared to that for the feed coal, an indication is given as to whether an element is lost, retained, or possibly increased during the liquefaction processes. The "ash-basis" data are used to calculate the percentage of change of each element for which data are available.

Ranges for estimating whether an element was retained were calculated by taking into account an average sampling error and the random error of the particular analytical method used for that element. The "retention range" for an element is arbitrarily defined as twice the overall standard deviation of possible errors in analysis of the feed coal and residue. An element is indicated as having undergone a gain if results for that element exhibit a percentage of change (residue, concentration relative to feed coal concentration on the ash-basis in a given process) which is greater than the upper limit of the retention range. Elements undergoing losses exhibit the opposite tendency. All other elements are said to have been "retained" during the liquefaction process. Figures 2 and 3 are bar graphs showing representative gain-loss data for mercury and manganese in the 18 sample sets, and Figure 4 summarizes the gain-loss data obtained for most elements detected in a SRC(Wash) set.

Some general conclusions can be drawn about the mobilities of various elements in the liquefaction processes studied. In many cases only limited conclusions are possible because of a combination of low elemental concentrations coupled with a moderate-to-high analytical uncertainty of measurement. In addition it should be emphasized that these sample sets, in most cases, represent one-time, short-interval sampling under equilibrium conditions, where possible, and may not be fully representative of long-term continuous operation.

1. Ca, S, Ti, As, B, F, Hg, La, Sc, and Zn are generally ($\geq 51\%$ of the sample sets in which the element was determined) lost during the liquefaction process. Dy, Eu, Tb, and Yb are lost or retained in the liquefaction processes in approximately equal numbers.
2. Most of the elements determined show general retention during the liquefaction processes. These are: Fe, K, Si, Ba, Be, Br, Ce, Cl, Co, Cr, Cs, Cu, Ga, Ge, Hf, Li, Lu, Mn, Mo, Ni, Pb, Rb, Sb, Se, Sm, Sn, Sr, Ta, Th, Tl, U, V, W, and Zr.
3. Four elements, Al, Mg, Na, and P behave randomly, exhibiting no clear pattern.
4. Observed gains, where present, most probably reflect contamination or degradation of equipment.
5. Some elements generally occur at concentrations too low to be accurately measured by the methods used and, thus are too low to be considered in the gain-loss data evaluation. These include Ag, Bi, Cd, In, Nd, Pt, Te, Au, and Pd.

In particular, three sample sets from the SRC-Ala process and two sets from the SRC-Wash process exhibit the greatest apparent losses. Elements which exhibit apparent losses in three or more of these sample sets are Al, Fe, Mg, S, Ti, As, B, Be, Br, Co, Dy, Eu, F, Hg, La, Lu, Mn, Mo, Sc, Se, Sm, Ta, Tb, Th, Yb, and Zn. Elements which exhibit increases in concentration in two or more of these five liquefaction processes are Na, P, Si, Cr, and Cs. Filtering aid materials were used in conjunction with all five SRC-Ala sample sets (Johns-Manville 7A, consisting of 92.5 percent diatomaceous earth and 7.5 percent asbestos) and the first two SRC-Wash sample sets. It is probable that at least Na, P, Si, and Cr increases are due to the filtering aids. Diatomaceous earth consists primarily of silicon dioxide and

asbestos minerals which contain the elements Na and Si among others. These materials have been detected by scanning electron microscope analysis of the SRC-Ala residues.

Mineralogical analysis. In addition to the chemical analyses, mineralogical analyses have comprised a major portion of this study. They have yielded information about the modes of occurrence of some elements and may shed some light on the behavior of certain chemical elements during the liquefaction processes.

The major mineralogical change which takes place in the liquefaction processes is the transformation of pyrite (FeS_2) in the feed coal to pyrrhotite (Fe_{1-x}S , where $x = 0. \text{ to } 0.2$) in the residue by the reaction $2\text{FeS}_2 \rightarrow 2\text{Fe}_{1-x}\text{S} + 2\text{S}$. Sulfur probably is evolved as H_2S . Pyrrhotite occurs in the residues primarily as fine-grained (crystal size about $1 \mu\text{m}$) aggregates sometimes incorporating other mineral matter. It also occurs as a fine granular layer on mineral particles.

A small amount of wollastonite, CaSiO_3 , formed by the reaction $\text{CaCO}_3 + \text{SiO}_2 \rightarrow \text{CaSiO}_3 + \text{CO}_2$, was detected by scanning electron microscopy in one residue from an H-Coal set. Some calcite particles found in the residue have a spongy texture similar to that seen in calcined carbonates (3). It appears that some dissociation of the calcite occurred, enabling a small amount of CaO to combine with SiO_2 . In a closed system, calcite, quartz, and wollastonite are stable together under the pressures and temperatures present in liquefaction process preheaters and reactors, if the CO_2 partial pressure is not appreciable (4).

A qualitative summary of mineral matter detected by X-ray diffraction analysis in feed coals and residues is presented in Table 2. An "X" indicates the presence of a mineral in a sample. A question mark indicates uncertainty in the presence of a mineral as determined from the diffraction patterns. Marcasite, a dimorph of pyrite, has been observed in only one feed coal sample. It is also transformed to pyrrhotite during liquefaction. Other minerals may be present in the samples in quantities below the detection limits.

Semi-quantitative X-ray diffraction data for quartz, calcite, pyrite, and pyrrhotite in the low temperature ash samples of several feed coals and their corresponding residues are shown in Table 3. Inclusion of quartz and calcite in pyrrhotite aggregates contributes to an apparent decrease in quartz and calcite from the feed coals to the residues. A decrease in the pyrrhotite concentration in the residue with respect to the pyrite concentration in the feed coals is due to the loss of sulfur from pyrite in the transformation to pyrrhotite. In samples which show the presence of calcite in the residues but not in the corresponding coal, calcite and some pyrite have broken down to form sulfate minerals during storage of the coal. This is a common reaction in coals exposed to moisture (5).

Conclusions. Data from the limited number of sample sets covering several liquefaction processes indicate that relatively few elements (e.g. Hg, S, As, Br, and B) are consistently lost to any significant degree from the resultant residues. Only a few mineralogical changes occur during the processes in which the transformation of pyrite to pyrrhotite most consistently occurs. These experimental observations, including the general range of elemental concentrations found in the residues, along with extensive trace element distribution data now available (2,6) from analyses of many coals from the various U.S. coal fields, will be used for an economic evaluation for many metals. Trace element concentrations for such economically significant metals such as Au, Ag, Pt, Pd, Ta, etc. in most cases will probably be too low for consideration as resources. In some cases, however, such as Zn, there are areas (7) where concentrations are high enough for serious consideration. The more abundant metals in coal--such as Al, Fe, Si, and possibly Ti--although perhaps currently not economical to extract may require attention in the future.

Acknowledgment. This work is supported in part by the U.S. Department of Energy under Contract EY-76-C-21-8004, in which Mrs. Patricia Barnes is Technical Project Officer.

References.

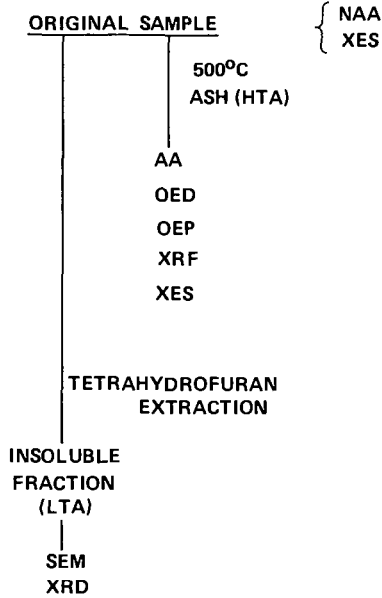
1. Energy Research and Development Administration, "Coal Liquefaction," Quarterly Report, April-June, 1976, ERDA 76-95/2 (1976).
2. Gluskoter, H. J., R. R. Ruch, W. G. Miller, R. A. Cahill, G. B. Dreher, and J. K. Kuhn: Trace Elements in Coal: Occurrence and Distribution, Illinois State Geological Survey Circular 499 (1977).
3. Harvey, R. D.: Petrographic and Mineralogical Characteristics of Carbonate Rocks Related to Sorption of Sulfur Oxides in Flue Gases, An Interim Report to the National Air Pollution Control Administration, Contract No. CPA 22-69-65, (1970).
4. Harker, R. I. and Tuttle, O. F.: Experimental Data on the P_{CO_2} -T Curve for the Reaction: Calcite + Quartz \rightleftharpoons Wollastonite + Carbon Dioxide, American Journal of Science, 254 (4), 239-256 (1956).
5. Rao, C. P. and Gluskoter, H. J.: Occurrence and Distribution of Minerals in Illinois Coals, Illinois State Geological Survey Circular 476 (1973).
6. Swanson, V. E., J. H. Medlin, J. R. Hatch, S. L. Coleman, G. H. Wood, S. D. Woodruff, and R. T. Hildebrand: Collection, Chemical Analysis, and Evaluation of Coal Samples in 1975, USGS Open File Report 76-468 (1976).
7. Cobb, J. C., J. D. Steele, C. G. Treworgy, J. F. Ashby, and S. J. Russell: The Geology of Zinc in Coals of the Illinois Basin, Final Report U.S. Department of Interior Grant 14-08-0001-G-249, August (1978).

Table 1
 Selection of Methods for Determining Various Elements
 In Coal Liquefaction Feed Coals and Residues

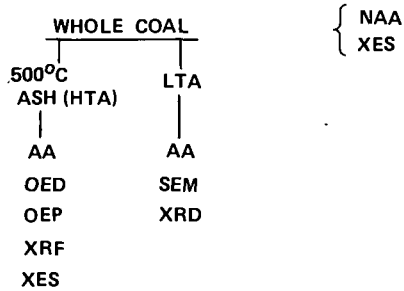
Element	AA	INAA	OED	OEP	XES	XRF	ASTM	ISE	RC	Element	AA	INAA	OED	OEP	XES	XRF	ASTM	ISE	RC
Al					X					Hf		X							
C						X				Hg									X
Ca					X					Ho									X
Fe	X	X			X					I					X				
H						X				In		X							
K		X			X					La		X							
Mg					X					Li			X						
N						X				Lu		X							
Na		X								Mn		X			X				
O					X					Mo			X						
P					X					Nd		X							
S						X				Ni	X	X	X	X	X				
Si					X					Pb		X							
Ti					X					Pd									X
Ag		X		X						Pt									X
As		X								Rb			X						
Au		X						X		Sb		X							
B			X							Sc		X							
Ba					X					Se		X							
Be				X						Sm		X							
Bi				X						Sn			X		X				
Br		X								Sr		X*	X						
Cd		X								Ta		X							
Ce		X								Tb		X							
Cl		X								Te					X				
Co		X	X	X						Th		X							
Cr		X	X							Tl			X						
Cs		X								Tm									X
Cu		X	X	X						U		X							
Dy			X							V			X	X					
Er								X		W		X							
Eu		X								Y					X				
F								X		Yb		X							
Ga		X								Zn		X							
Ge			X							Zr					X				

*Strontium results by INAA are satisfactory above 10 ppm.

A. FLOW SHEET OF RESIDUE SAMPLE PRETREATMENT



B. FLOW SHEET OF WHOLE COAL SAMPLE PRETREATMENT



ISGS 1978

Figure 1 - Flow sheets of sample pretreatments.

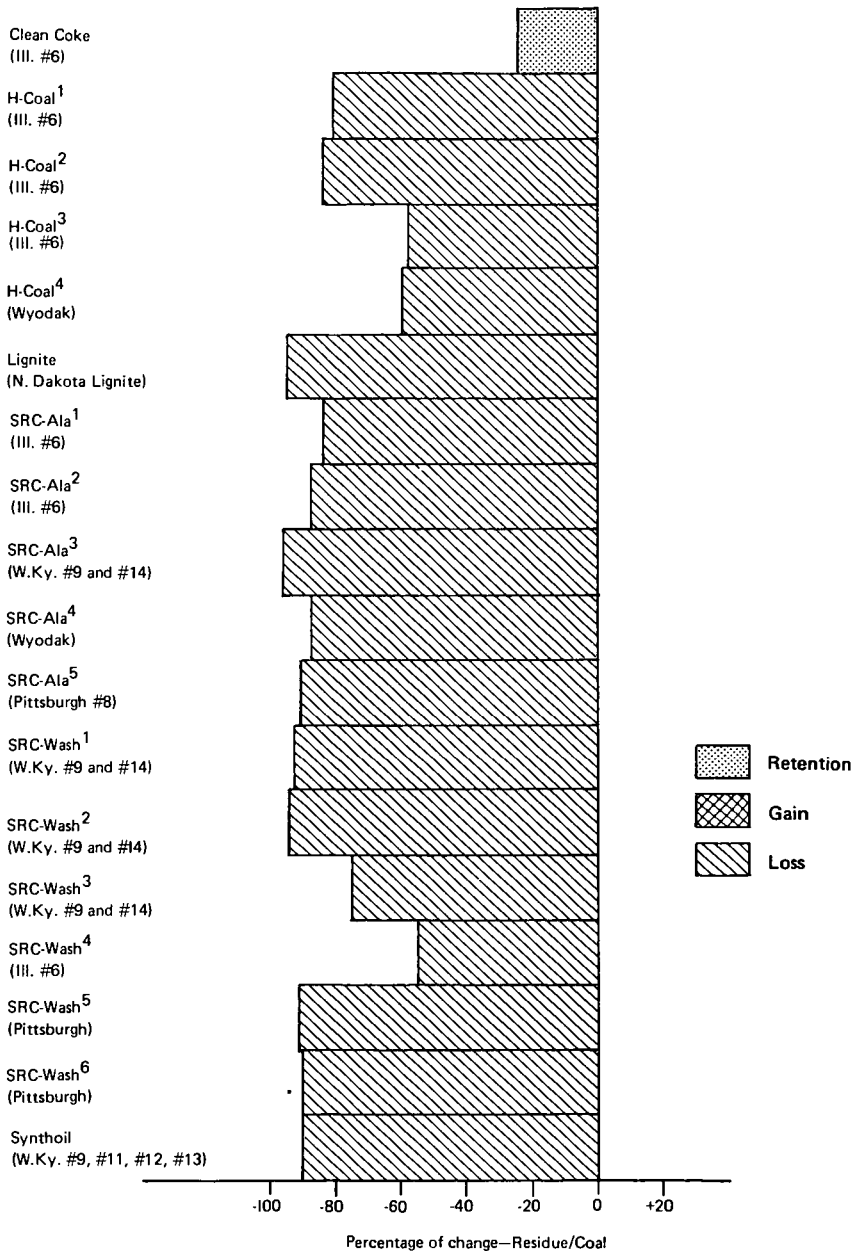


Figure 2 - Summary of percentage of change in elemental composition (500°C ash basis) for Hg in several liquefaction processes from feed coal to residue.

ISGS 1978

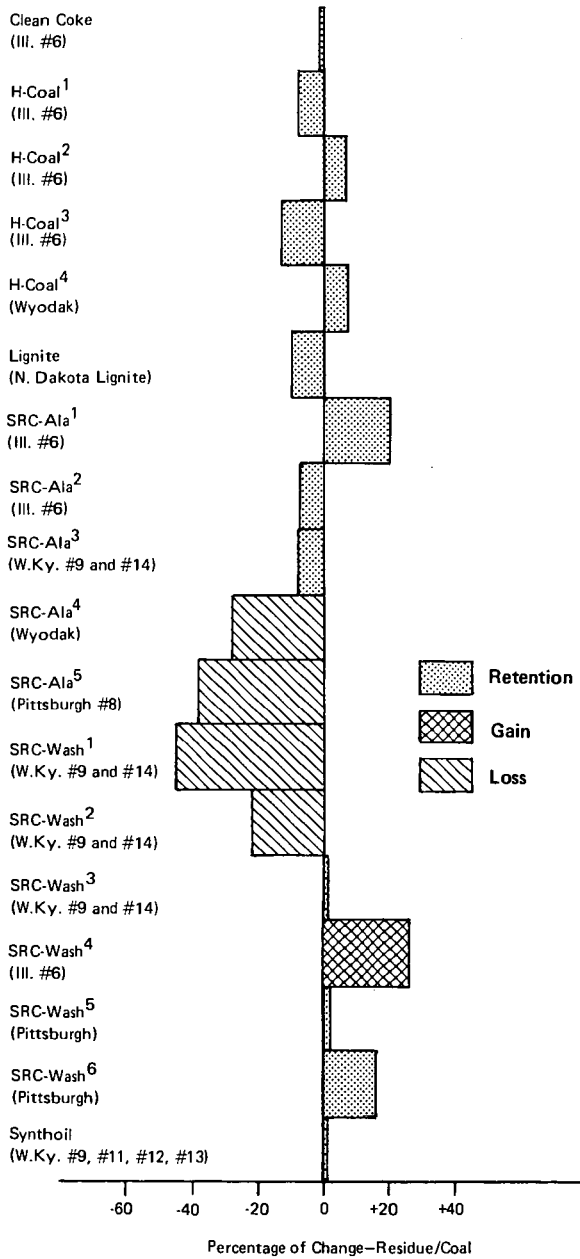


Figure 3 - Summary of percentage of change in elemental composition (500°C ash basis) for Mn in several liquefaction processes from feed coal to residue.

ISGS 1978

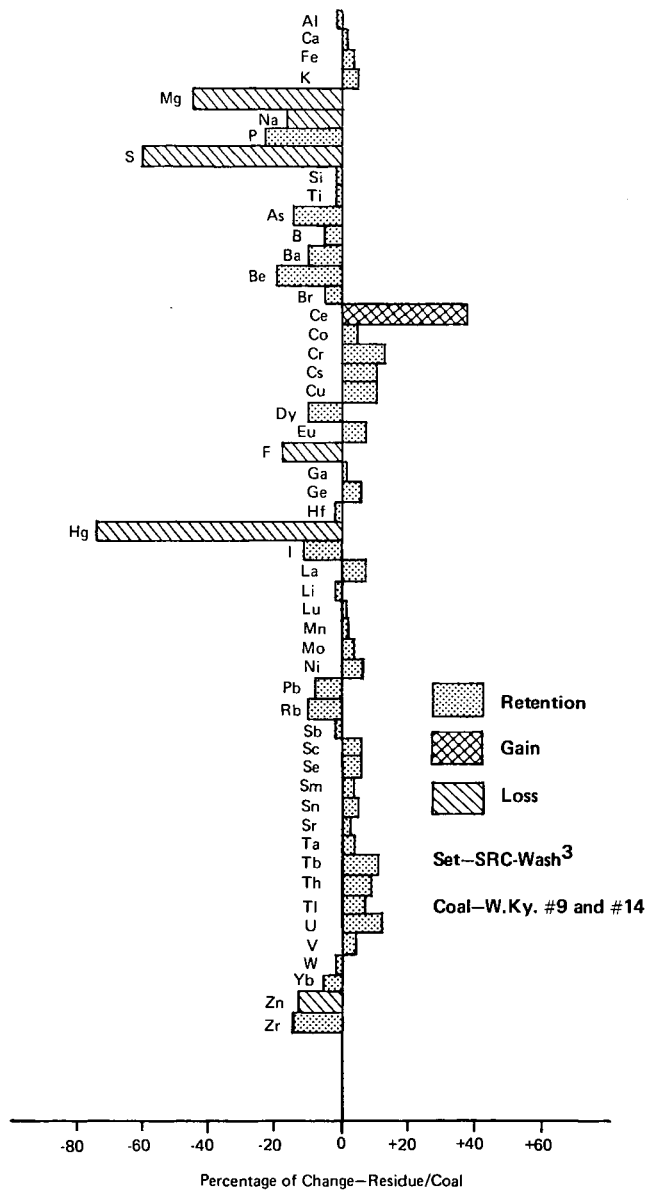


Figure 4 - Summary of percentage of change in elemental composition (500°C ash basis) from feed coal to residue.

ISGS 1978

Table 2

Mineral Matter Detected in Low Temperature Ash
of Liquefaction Samples by X-ray Diffraction Analysis

Lab No.	Sample Set	Anhydrite	Bassanite	Calcite	Coquimbite	Feldspar	Gypsum	Illite	Jarosite	Kaolinite	Marcasite	Pyrite	Pyrrhotite	Quartz
C-19660	Clean Coke			X				X		X		X		X
C-19661A		X	X	X		X		X		X			X	X
C-18903	H-Coal 1	X		X	X			X		X		X		X
C-18941A		X		X				X		X			X	X
C-19194	H-Coal 2	?		X	X			X		X		X		X
C-19196A		?		X		X		X		X			X	X
C-19916	H-Coal 3			X	?					X		X		X
C-19917A		X		X				X	?	X			X	X
C-20021	H-Coal 4		X	X						X		X		X
C-20022A			X	X		X		X		X			X	X
C-19590	Lignite		X	X								X		X
C-19591			?	X		X							?	X
C-19702	SRC-Ala 1			X				X		X		X		X
C-19703				X			X	X		X		?	X	X
C-19705	SRC-Ala 2	X			X	?		X	X	X				X
C-19706		?		X						X		X	X	X
C-19708	SRC-Ala 3				X					X		X		X
C-19709						X		X	X	X		X	X	X
C-19711	SRC-Ala 4	X	X							X		X		X
C-19712				X			X			X				X
C-19714	SRC-Ala 5		X	X		X		X		X		X		X
C-19715						X	X			X			X	X
C-19141	SRC-Wash 1				X					X	X	X		X
C-19142A								X		X			X	X
C-19488	SRC-Wash 2			?				X	X	X		X		X
C-19487		X						X	?	X			X	X
C-19899	SRC-Wash 3	X		X	X			X		X		X		X
C-19902A		X		X		X		X	X	X			X	X
C-20014	SRC-Wash 4			X				X		X		X		X
C-20015A				X				X		X			X	X
C-20016	SRC-Wash 5	X	X	X		X		X	X	X		X		X
C-20017A				X		X		X		X			X	X
C-20019	SRC-Wash 6	?					?	X	X	X		X		X
C-20020A				X				X	?	X			X	X
C-19276	Synthoil			X	X			X		X		X		X
C-19349A				X		X		X		X		X	X	X

Table 3

Average Percentage of Principal Minerals by X-Ray Diffraction
in Low Temperature Ash of Liquefaction Samples

Lab No.	Sample Set	Sample Type	Average Mineral Percentages, by weight, ± 7.5%, absolute			
			Quartz	Calcite	Pyrite	Pyrrhotite
C-19660	Clean Coke	Coal	21	11	19	N.D.
C-19661A		Residue	15	3	N.D.	16
C-18903	H-Coal 1	Coal	22	13	22	N.D.
C-18941A		Residue	17	8	N.D.	15
C-19194	H-Coal 2	Coal	22	9	25	N.D.
C-19196A		Residue	16	4	N.D.	18
C-19916	H-Coal 3	Coal	15	4	22	N.D.
C-19917A		Residue	14	5	N.D.	20
C-20021	H-Coal 4	Coal	11	*	9	N.D.
C-20022A		Residue	10	12	N.D.	*
C-19590	Lignite	Coal	7	*	10	N.D.
C-19591		Residue	12	28	N.D.	*
C-19702	SRC-Ala 1	Coal	22	3	21	N.D.
C-19703		Residue	15	<1	N.D.	13
C-19705	SRC-Ala 2	Coal	18	N.D.	N.D.	N.D.
C-19706		Residue	12	5	N.D.	12
C-19708	SRC-Ala 3	Coal	13	N.D.	23	N.D.
C-19709		Residue	13	N.D.	7	7
C-19711	SRC-Ala 4	Coal	16	*	6	N.D.
C-19712		Residue	16	12	N.D.	N.D.
C-19714	SRC-Ala 5	Coal	12	6	16	N.D.
C-19715		Residue	9	1	N.D.	10
C-19141	SRC-Wash 1	Coal	8	N.D.	39	N.D.
C-19142A		Residue	7	N.D.	N.D.	27
C-19488	SRC-Wash 2	Coal	9	N.D.	37	N.D.
C-19487		Residue	7	N.D.	N.D.	17
C-19899	SRC-Wash 3	Coal	18	2	29	N.D.
C-19902A		Residue	16	1	N.D.	20
C-20014	SRC-Wash 4	Coal	18	4	26	N.D.
C-20015A		Residue	15	3	N.D.	17
C-20016	SRC-Wash 5	Coal	16	5	21	N.D.
C-20017A		Residue	14	3	N.D.	19
C-20019	SRC-Wash 6	Coal	15	N.D.	22	N.D.
C-20020A		Residue	11	3	N.D.	14
C-19276	Synthoil	Coal	15	7	27	N.D.
C-19349A		Residue	13	6	N.D.	22

*Mineral present, but cannot be quantified due to the interference of other mineral peaks.

N.D. = Not Detected

The Development and Application of a Non-Dispersive X-ray Sulfur Analyzer with Mechanisms for Non-linear Approximation and for All Other Matrix Effect Corrections

Akiyoshi Masuko*, Fumio Imai* and Toyotsugu Yamano**

*Nippon Oil Company Ltd., Central Technical Research Laboratory
8, Chidoricho, Nakaku, Yokohama 231, Japan

**Rigaku Corporation, Osaka
14-8, Akaouji, Takatsuki 569, Japan

Introduction

Precise determination of sulfur contents in fuel oils has become more important for quality control by refineries and quality monitoring by environmental agencies.

Of the many test methods used for determining sulfur contents in fuel oils, the bomb method (ASTM D 129) is considered to be the world-wide standard. However, this method requires several hours running time, and the results can vary greatly depending upon the skill of the analyst running the test.

A rapid and exact method is required to routinely analyze sulfur contents in fuel oils, and the method should be easy to operate and to maintain. To meet these requirements, non-dispersive x-ray sulfur analyzers which utilize either a radioisotope such as ^{55}Fe or a small x-ray tube as the fluorescent x-ray generator have been developed by many manufacturers. This kind of analyzer is reportedly superior in terms of speed, accuracy, economy and ease of operation and maintenance as compared to a combustion method such as the bomb method (1). However, the accuracy of the results in the x-ray method cannot be better than that of the standards with which the unknowns are compared. Also, it was found during our research that fairly large errors can arise from the following items. (It should be noted, however, that these errors, though large, rarely exceed the allowable errors cited in ASTM methods):

- (i) Peak overlapping between the S-KX spectrum and Cl-KX spectrum,
- (ii) The use of a linear approximation for the working curve, and
- (iii) Differences in composition between the standards and the unknowns, especially in the carbon-hydrogen weight ratio (C/H) of the hydrocarbon portion of these oils.

With respect to item (i), most manufacturers have already solved the problem. The most straightforward way of doing this is by inserting a sulfur-containing film between the sample and the x-ray detector, since the Cl-KX spectrum is filtered out by such film. However, other methods have also been successful.

The error due to item (ii), can be reduced by narrowing the interpolation range of the standards to be used for the calibration. In fact, many laboratories where sulfur contents of the samples to be analyzed are limited to a certain range can apply the linear approximation without noticeable loss of accuracy. However, in analyzing samples which spread over a wide range of sulfur contents, recalibrations should be made several times a day so that the working range of the approximation is small enough to insure the accuracy desired. The recalibration itself is very troublesome for analysts in routine analysis.

With respect to item (iii), the error can be corrected either theoretically or experimentally if the compositions of both the standards and the samples are known. However, it is tedious to determine these compositions.

To correct these errors automatically, a new type of analyzer was developed. In this paper, the improvements in this analyzer compared to the prototype (Rigaku Sulfur-X) will be reported. In addition to this, the results of tests on a variety of samples will also be described.

Instrument

The non-dispersive x-ray sulfur analyzer discussed in this paper consists of the prototype plus additional components as described below. Figure 1 is a schematic diagram of the apparatus with the broken lines denoting newly installed components, i.e. '9', '10', '13' and '16'. Component '10' calculates the ratio between the S-KX spectrum intensity ('8') and the scattered radiation intensity ('9'). Since the factors influencing the absolute intensity of the S-KX spectrum (e.g., differences in composition, instrumental variables, and atmospheric changes) also influence the scattered radiation intensity to the same degree, using the ratio instead of the absolute intensity corrects for these factors.

Block '17' calculates the values of the constants in the calibration equation shown below (Eq.1).

$$S = a I^2 + b I + c \quad 1)$$

where S is the sulfur content, I is the x-ray intensity ratio between the S-KX spectrum and the scattered radiation, and a, b and c are constants. To determine these constants, three standard samples whose sulfur contents are exactly known are sequentially measured with the analyzer set on mode 'C' (see Fig.1). These constants, once determined and stored in the memory of the calculator, can be used for about one year without loss of accuracy, since the ratio calculator '10' seems to be also effective in correcting the long term drift of the analyzer.

Preliminary Tests

To compare the performance of the modified analyzer to that of the prototype, analyses were made on prepared samples. The samples consisted of white oil plus di-butyl di-sulfide (DBDS). Di-butyl di-sulfide has recently been officially certified by the Japanese government as the sulfur compound for x-ray calibration purposes and is now widely used in Japan.

As can be seen in Fig.2, the relationship between the content and the intensity is not linear. Thus, if the working curve is approximated with a straight line, for example, ranging from 0 wt% to 6 wt%, the maximum error reaches 0.31 wt% at the mid point of the curve, as illustrated in Fig.3(b). It was recognized that the relationship shown in Fig.2 can be more accurately expressed by a quadratic equation rather than a linear equation. Thus, a quadratic approximation was set up using calibration standards containing 0, 3 and 6 wt% sulfur. The results shown in Fig.3(b) clearly indicate that the use of this quadratic approximation greatly reduced the difference between the measured value and actual value of the sulfur content. The maximum error observed was 0.01 wt%.

As shown in Fig.4(a), fairly large errors were observed when samples of high C/H were analyzed by using calibration standards of low C/H. In this case, the standards were prepared from decalin (C/H=6.7) plus DBDS, while the unknowns were prepared from tetralin (C/H=10.0) plus DBDS.

It was previously reported by one of the authors (2) that this error could be corrected by using the following empirical equation,

$$\Delta S = -0.013 S \left(\frac{C/H}{\text{std}} - \frac{C/H}{\text{unkn}} \right) \quad 2)$$

where S is the observed sulfur content and ΔS the value to be added to the observed sulfur content. In the above-referenced study, the factor 0.013 was determined experimentally by using the prototype x-ray analyzer. To use Eq.2, one must know C/H values for both the standards and the unknowns. An alternative expression can also be obtained by using the specific gravity ρ instead of C/H, since it was found that C/H is roughly related to ρ as follows:

$$C/H = 8.82 \rho - 1.06 \quad 3)$$

$$\text{thus, } \Delta S = 0.115 S \Delta \rho \quad 4)$$

where $\Delta\rho = \rho_{\text{std}} - \rho_{\text{unkn}}$

5)

It has been reported(3) that the error due to the C/H difference in the standards and the unknowns can be effectively eliminated by using the scattering intensity of the sample as an internal standard. In the modified analyzer, the effect of the compositional differences between the standards and the unknowns are automatically compensated by installing a scaler for the scattered radiation('9') and a ratio calculator ('10'). Figure 4(b) shows the results obtained by using the modified analyzer for testing the same combination of standards and unknowns tested on the prototype. Since the errors observed using the modified analyzer were much smaller than those observed using the prototype, we feel that the modified analyzer can be used in a wider range of applications than was previously possible.

The results illustrated in Fig.5(a) indicate that the magnitude of the effect due to the coexistence of chlorine is very small, and that the effect of the Cl-KX spectrum is adequately reduced by the filter. Without a filter, or other device for eliminating the Cl-KX spectrum, errors can be very large as seen in Fig.5(b).

Test Results

To examine practical usage of the analyzer, analyses were made on a variety of fuel oils whose characteristics are outlined in Table 1. Sulfur contents for these samples had been previously determined by the quartz tube method(JIS K 2541-1971) in several inter-laboratory tests. The standard samples for calibration were made from white oil plus DBDS. Sulfur contents of these standards were 0, 1.5 and 3.0 wt%. In this series of measurements, three 100 sec integrations were made for each sample, and the results were averaged. The results of the analyses are shown in Fig.6, where the horizontal axis indicates the sulfur content determined by the quartz tube method, and the vertical axis indicates the difference between the sulfur level determined by the x-ray method and that determined by the quartz tube method(in the case of fuels used in inter-laboratory tests) or that certified by NBS or JPI(in the case of standard reference materials).

It can be seen from Fig.6 that the errors are within ± 0.01 wt% for most of the samples analyzed, and within ± 0.02 wt% for all of the samples analyzed(ranging up to 3.3 wt% sulfur contents).

Since the observed errors are so small, we can conclude that standard samples prepared from white oil plus DBDS can be used for calibration without loss of accuracy, in spite of the fact that there are many differences in composition between the standards and the unknowns, such as C/H, quantity of ash, chlorine content, etc.

Conclusion

A non-dispersive x-ray sulfur analyzer which consists of the prototype "Rigaku Sulfur-X" plus additional mechanisms for correcting various matrix effects was developed.

Test results made on a variety of fuel oils indicated that the modified analyzer can accurately measure sulfur contents of fuel oils(within ± 0.01 wt% of the actual value) by using calibration standards prepared from white oil plus di-butyl di-sulfide.

References

- (1) G.Frechette, J.C.Herbert, T.P.Thinh and Y.A.Miron; Hydrocarbon Processing, vol.54, 109 (1975).
- (2) A.Masuko; J. Japan Petrol. Inst., vol.20, 909 (1977), in Japanese.
- (3) G. Andermann and J.W.Kemp; Anal. Chem., vol.30, 1306 (1958).

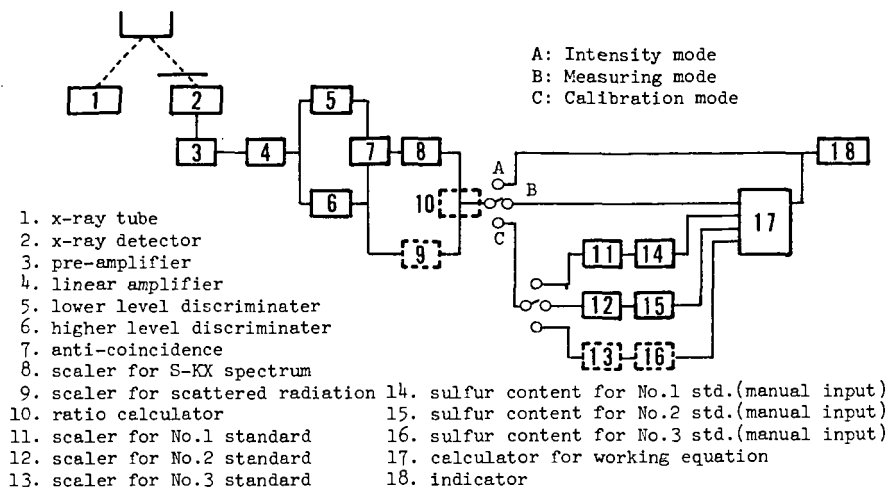


Fig.1 Schematic diagram of the non-dispersive x-ray sulfur analyzer

Note: the blocks surrounded by solid lines are those of the prototype.

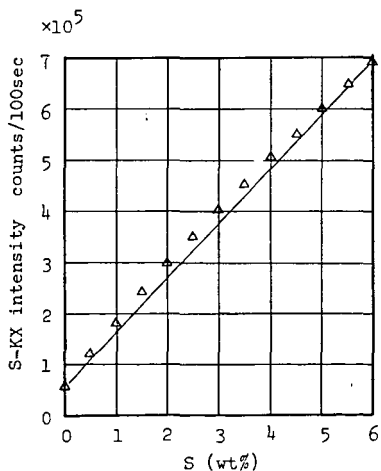


Fig.2 Relation between sulfur content and S-KX intensity

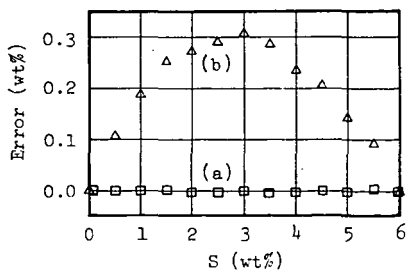


Fig.3 Comparison of linear approximation and quadratic approximation

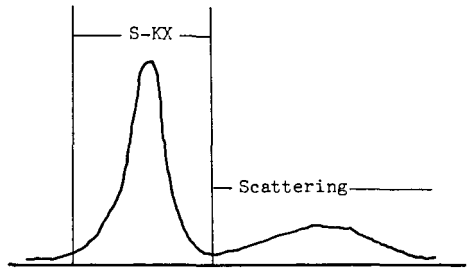
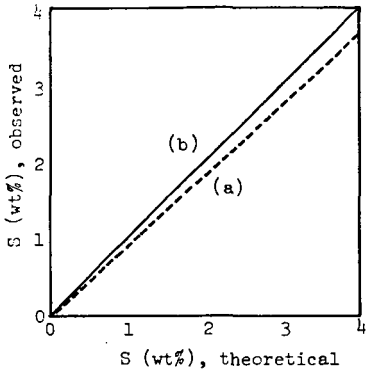


Fig.4 Comparison of absolute method(S-KX intensity) and ratio method(S-KX intensity/scattering intensity)

C/H of the standards: 6.7
C/H of the unknowns :10.0

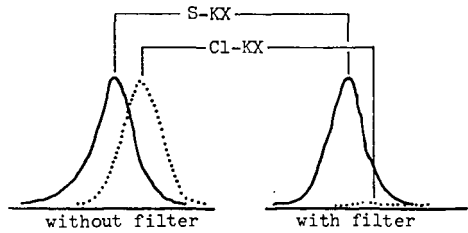
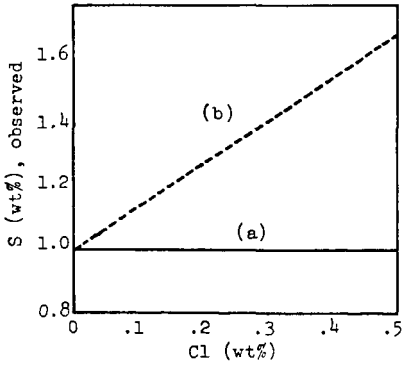


Fig.5 Error due to peak overlapping, and the effect of filtering

Sulfur contents in the samples used in the experiment were 1.0wt%

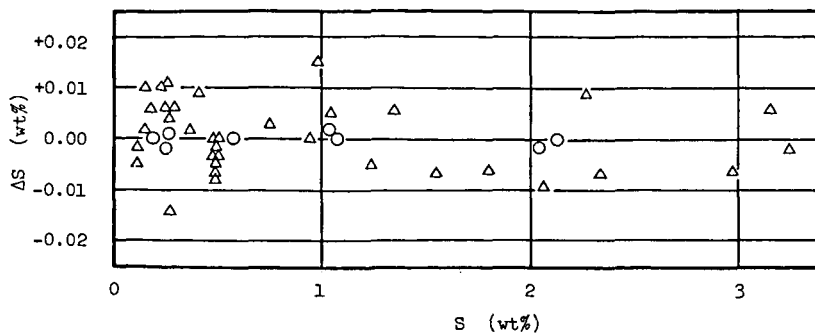


Fig.6 Analytical results for a variety of fuel oils

Δ: Samples which had been used and analyzed in inter-laboratory tests by quartz tube method(JIS K 2541-1971).
 O: Standard reference materials(NBS and JPI).

Horizontal axis: Sulfur content either determined by quartz tube method or certified by NBS or JPI.

Vertical axis : The difference ΔS (wt%) given by following equations,

$$\Delta S = S_{\text{quartz}} - S_{\text{x-ray}}$$

$$\Delta S = S_{\text{SRM}} - S_{\text{x-ray}}$$

Table 1. Characteristics of the sample oils* analyzed

Term	Range
C/H (wt%/wt%)	6.0 - 8.5
Sulfur content (wt%)	0.1 - 3.4
Ash (wt%)	0.01 - 0.2
Pour point (°C)	-10 - +35
Viscosity, @50°C (cSt)	2.5 - 200
Specific gravity (15/4°C)	0.84 - 0.95
Chlorine content**(wt%)	0 - 0.5

* These samples had been analyzed previously in inter-laboratory tests.

** Chlorinated paraffins were added to some of the sample oils for the adjustment of Cl contents.